



The Institute of Oceanology of the Polish Academy of Sciences (IO PAN)

MODELING THE IMPACT OF FARMS, ON THE EXAMPLE OF
THE PUCK COMMUNE, ON SEA WATERS LOCATED IN THE
COASTAL ZONE OF THE BALTIC SEA (PUCK BAY)

Dawid Dybowski

Series of publications constituting the doctoral dissertation

The thesis prepared under
the supervision of Prof. Lidia Dzierzbicka-Głowacka

Sopot 2022



Instytut Oceanologii Polskiej Akademii Nauk

MODELOWANIE WPŁYWU GOSPODARSTW ROLNYCH,
NA PRZYKŁADZIE GMINY PUCK, NA WODY MORSKIE
ZLOKALIZOWANE W STREFIE PRZYBRZEŻNEJ MORZA
BAŁTYCKIEGO (ZATOKA PUCKA)

Dawid Dybowski

Cykl publikacji stanowiący rozprawę doktorską

Praca przygotowana
pod kierunkiem prof. dr hab. Lidii Dzierzbickiej-Głowackiej

Sopot 2022

Contents

1	List of abbreviations	7
2	English abstract	9
2.1	Introduction	9
2.2	Materials and methods	9
2.2.1	EcoPuckBay model	9
2.2.2	Study area	10
2.3	Results and discussion	10
2.3.1	Hydrodynamic part of the EcoPuckBay model	10
2.3.2	Estimation of nitrogen leaching from farmland	11
2.3.3	Biochemical part of the EcoPuckBay model	12
2.3.4	Influence of the Puck Commune catchment on the waters of the Puck Lagoon	12
2.4	Conclusions	13
3	Streszczenie	15
3.1	Wstęp	15
3.2	Materiały i metody badań	16
3.2.1	Model EcoPuckBay	16
3.2.2	Obszar badań	18
3.2.3	Zbiory danych użyte do walidacji modelu	18
3.2.4	Dane ankietowe o praktykach rolniczych na terenie Gminy Puck	19
3.3	Rezultaty i dyskusja	19
3.3.1	Część hydrodynamiczna modelu EcoPuckBay	19
3.3.2	Oszacowanie wielkości wymywania azotu z pól uprawnych	20
3.3.3	Część biochemiczna modelu EcoPuckBay	20
3.3.4	Wpływ zlewni Gminy Puck na wody Zalewu Puckiego	21
3.4	Wnioski	21
	References (Bibliografia)	23
4	Series of publications constituting the PhD thesis	25
4.1	Research paper no. 1	25
4.2	Research paper no. 2	67
4.3	Research paper no. 3	91
5	Attachment	115
6	Authorship statements	135
7	Acknowledgments	155

1 List of abbreviations

Abbreviation	Explanation
3D CEMBS	three-dimensional Coupled Ecosystem Model of the Baltic Sea
AMPA	aminomethylphosphonic acid
BSBD	Baltic Sea Bathymetry Database
CESM	Community Earth System Model
CHL	chlorophyll <i>a</i>
CI TASK	Centre of Informatics Tricity Academic Supercomputer and network
CTD	instrument used to measure the electrical conductivity, temperature, and pressure of seawater
EPB	EcoPuckBay model
HELCOM	Baltic Marine Environment Protection Commission – also known as the Helsinki Commission
HIRLAM	High Resolution Limited Area Model
HIROMB	High Resolution Operational Model for the Baltic Sea
HYPE	Hydrological Predictions for the Environment
ICM UW	Interdisciplinary Centre for Mathematical and Computational Modelling of Warsaw University
IO PAN	Institute of Oceanology of the Polish Academy of Sciences
ITLS	Institute of Technology and Life Sciences - National Research Institute
KPP	k-profile parameterization
ME	mean error
Modflow	modular finite-difference flow model
MODIS	Moderate Resolution Imaging Spectroradiometer
N	nitrogen
NCAR	National Center for Atmospheric Research
NEMO	Nucleus for European Modelling of the Ocean
NEMO-Nordic	model based on NEMO, covers whole Baltic Sea extended to the North Sea area
NEMO-SCOBI	NEMO model coupled with SCOBI model
NO_3^-	nitrate ion
NPZD	nutrient–phytoplankton–zooplankton–detritus
O_2	molecular oxygen
PO_4^{3-}	phosphate ion
POP	Parallel Ocean Program
PSU	Practical Salinity Unit
<i>r</i>	Pearson correlation coefficient
RCO	Rossby Centre Ocean Model
RMSE	root-mean-square-error
SCOBI	Swedish Coastal and Ocean Biogeochemical model
SCS	Soil Conservation Service
SMHI	Swedish Meteorological and Hydrological Institute
STD	standard deviation
SWAT	Soil & Water Assessment Tool
TN	total nitrogen
VIEP	Voivodeship Inspectorate of Environmental Protection in Gdańsk

2 English abstract

2.1 Introduction

The most reliable way to control the condition of the marine environment is to constantly monitor its physicochemical parameters. However, frequent monitoring is extremely costly and provides only limited information, both spatially and temporally. In this context, it is reasonable to supplement the monitoring data with data from numerical simulations. The temporal and spatial resolution of numerical modeling is limited only by the computing capabilities of the computer and the disk space available for data storage. In turn, the development of high-resolution numerical models that are able to effectively and reliably simulate both physical and biogeochemical processes shaping the state of the marine environment is time-consuming and requires extensive knowledge of many processes that take place in the modeled ecosystem. Access to information on direct and indirect forcing factors, such as boundary conditions, river runoff, and atmospheric forces, that affect the dynamics of changes within the model domain, is essential. In order to meet the complexity of this task and increase the efficiency of the implementation process, the Community Earth System Model (CESM) was redesigned and adapted to the research area of the Bay of Puck, allowing the construction of an excellent numerical tool for reanalysis and forecasting of the marine environment in high resolution.

The purpose of the research was to determine the impact of farms, on the example of the Puck Commune, on sea waters located in the coastal zone (the Bay of Puck) using the numerical model.

To achieve the main goal, four specific goals were defined:

1. Characterize the structure and variability of hydrodynamic parameters in the Bay of Puck region.
2. Determine, based on the conducted research (surveys among farmers) and the calculator developed, the leaching of nitrogen from the individual field.
3. Characterize the structure and variability of chemical parameters in the Bay of Puck region.
4. Examine the impact of nutrients deposited with the rivers of the Puck Commune on the waters of the Bay of Puck (with particular emphasis on the waters of the Puck Lagoon).

This doctoral dissertation consists of three scientific articles published in peer-reviewed journals and a manuscript attached at the end of the dissertation, which was submitted to the journal and is a consistent continuation of the research undertaken in the previous three papers. The first article (Dybowski, Jakacki, et al. 2019) focuses on the description and validation of the hydrodynamic part of the EcoPuckBay model. The second article (Dybowski, L. A. Dzierzbicka-Glowacka, et al. 2020) presents an analysis of the size of nitrogen loads applied in the form of fertilizers to farmlands and the estimation of their potential leaching on the scale of a single field. In the third article (Dybowski, Janecki, et al. 2020), the biochemical part of the EcoPuckBay model was presented and validated, and the nutrient spread module was introduced. The fourth manuscript presents an analysis of the spatio-temporal variability of the concentration of nitrates, phosphates, and chlorophyll *a* in the waters of the Puck Lagoon. The study also simulated the impact of small (compared to the Vistula, the largest in the region), that discharge directly into the Puck Lagoon, on algae blooms in this reservoir. The vast majority of the results presented in this dissertation were obtained using data from the EcoPuckBay model; therefore, at the beginning of the next chapter there is a brief description of it, which is intended to enable the reader to become familiar with the tool used and to better understand the results.

2.2 Materials and methods

2.2.1 EcoPuckBay model

The EcoPuckBay model was developed as an adaptation of the Community Earth System Model (CESM), which is a global climate coupled model. CESM consists of five separate components with an additional module to control time, forcing forces, domains, meshes, and information exchange between individual modules. CESM has been scaled down and adapted for the Bay of Puck region for further development at the Institute of Oceanology of the Polish Academy of Sciences.

The ocean module in the EcoPuckBay model is based on the POP code using three-dimensional equations of motion with hydrostatic and Boussinesq approximations. The horizontal resolution of the EcoPuckBay model is equal to $1/960^\circ$, which corresponds to the resolution of the horizontal grid of approx. 115 m. The vertical resolution is 0.4-0.6 m in the upper layers and then gradually increases to a layer thickness of 5 m. The vertical discretization uses a z formulation, and the bathymetry is based on the Baltic Sea Bathymetric Database (BSBD) from the Baltic Sea Hydrographic Commission resources (Baltic Sea Hydrographic Commission 2013). The bathymetric data were interpolated into the model grid using the Kriging method. The ocean model has a time step of 12 seconds.

The biochemical part of the EcoPuckBay model is based on the NPZD approach (Moore et al. 2001). The model determines the concentration of biogenic substances, three types of phytoplankton (diatoms, picophytoplankton/nanophytoplankton and diazotrophs (nitrogen-binding organisms)), chlorophyll a , zooplankton, pelagic detritus, dissolved oxygen and pesticides (glyphosate, diflazachlorate, chlorpyrifos and anthraquinone). Many, but not all, models can be represented in general form as a conjugate set of time-dependent advection diffusion equations with sources.

The EcoPuckBay model is forced by meteorological data from the UM model provided by the Interdisciplinary Center for Mathematical and Computational Modeling of the University of Warsaw (ICM UW). The following external fields are used: air temperature and specific humidity at a height of 2 m, pressure at sea level, atmospheric precipitation, short and long wave radiation, wind speed at a height of 10 m, air density.

The results of the EcoPuckBay 3D model are limited to the Bay of Puck area. However, the entire model mesh covers a wider area. This is to ensure an appropriate simulation of the boundary conditions. Along the northern boundary of the EcoPuckBay model, data from the 2.3 km CEMBS 3D predictive model is delivered to the EcoPuckBay model as boundary conditions. The results provided by the 3D CEMBS model (Dzierzbicka-Głowacka, Jakacki, et al. 2013; Dzierzbicka-Głowacka, Janecki, et al. 2013) are used to provide forcing fields in the EcoPuckBay model by sequential information transfer. The mechanism of this module is based on interpolation of values from 3D CEMBS to the grid of the EcoPuckBay model. Furthermore, at the water-land border, the EcoPuckBay model was connected to the SWAT (surface water runoff) and Modflow (groundwater flow) models.

2.2.2 Study area

The southern part of the Baltic Sea is a popular tourist region, which is also greatly influenced by the anthropogenic activities of the residents and agriculture. As a result, the Bay of Puck is a natural reservoir for the deposition of fertilizer waste and other pollutants entering through groundwater, rivers, surface runoff, and direct deposition.

One of the most important factors influencing the region's unique ecosystem is bathymetry. The average depth of the Bay of Puck is about 15 m, and the maximum depth is 54 m. From the north-east it is surrounded by the Hel Peninsula, which is a natural barrier for mixing with the open waters of the Baltic Sea. The Bay of Puck is also strongly influenced by river influx from the mainland, which reduces salinity, especially in coastal surface waters. The largest river in the region is the Vistula with an average runoff of over $1000 \text{ m}^3 \text{ s}^{-1}$. The average monthly water temperature in the region ranges from about 2°C in February to over 20°C on the surface in the summer period, with a maximum usually in August. In warmer months, in the outer part of the Bay of Puck, water is often stratified, leading to the occurrence of seasonal thermoclines.

2.3 Results and discussion

In this chapter, the most important results of the research are presented, while the individual results and analyzes are presented in the articles that constitute this doctoral dissertation.

2.3.1 Hydrodynamic part of the EcoPuckBay model

To assess the quality of the physical parameters obtained in the hydrodynamic part of the EcoPuckBay model, a set of basic statistical measures (Dybowski, Jakacki, et al. 2019), such as the Pearson correlation coefficient (r), mean square error (RMSE), standard deviation (STD) and ME (mean error) were calculated with available model data (NEMO-Nordic) and *in situ* (VIEP) measurements for temperature and salinity.

Table 1: Statistical comparison between the modeled temperature and the reference data from *in situ* measurements (VIEP and s/y Oceania) and numerical data (NEMO-Nordic).

Reference data	Pearson's r	RMSE [°C]	STD [°C]	ME [°C]
Time series (VIEP)	0.97	1.45	5.67	-0.83
Time series (NEMO-Nordic)	0.98	1.33	6.01	-0.31
Vertical profiles (s/y Oceania)	0.92	2.85	5.29	-1.16

Pearson's correlation coefficient r determined for temperature comparing the EcoPuckBay model data with VIEP monitoring data is 0.97 and 0.92 for data from vertical profiles obtained during s/y Oceania cruises (Tab. 1). Comparison with the results from the NEMO-Nordic model shows an even greater correlation of the results ($r = 0.98$). RMSE for all compared data sets is significantly lower than the STD. On the other hand, the ME, i.e. the difference of the mean values of both sets, is negative in all cases, which means that the temperature in the model was burdened with a statistical error. However, it should be emphasized that at this stage of model validation, the satellite data assimilation module has not been launched yet.

Table 2: Statistical comparison between the salinity modeled and the reference data from *in situ* measurements (VIEP and s/y Oceania) and numerical data (NEMO-Nordic).

Reference data	Pearson's r	RMSE [PSU]	STD [PSU]	ME [PSU]
time series (VIEP)	0.58	0.67	0.60	0.16
time series (NEMO-Nordic)	0.17	0.97	0.70	-0.24
vertical profiles (s/y Oceania)	0.90	0.40	0.84	-0.03

Pearson's correlation coefficient between salinity determined using the EcoPuckBay model and VIEP monitoring data is equal to 0.58 and 0.90 for data from vertical profiles obtained during s/y Oceania cruises (Tab. 2). Comparison with the results from the NEMO-Nordic model shows a very weak correlation of the results (factor r equal to 0.17) due to the difference in model resolution. ME for vertical profiles is near zero, which means a very good representation of the vertical stratification of the water body. It should be noted that the value of the correlation coefficient r differs greatly in individual VIEP stations and takes values from 0.28 to 0.86. However, for vertical profiles, the value of r ranges from 0.78 to 1.00.

2.3.2 Estimation of nitrogen leaching from farmland

The next stage of the research was to determine the intensity of fertilization and to estimate the amount of nitrogen leaching from the soil on the scale of a single farmland in the Puck Commune (Dybowski, L. A. Dzierzbicka-Glowacka, et al. 2020). The average value of the intensity of mineral fertilization in the studied sample (about 110 kg N ha⁻¹) is higher than the average for Poland (80 kg N ha⁻¹), while in other countries of the Baltic Sea region these values are about 30 kg N ha⁻¹ in Sweden and Estonia, over 100 kg N ha⁻¹ in Norway, about 80 kg N ha⁻¹ in Denmark and about 75 kg N ha⁻¹ in Germany (European Environment Agency 2018).

For almost half of all fields (49.8%), additional N leaching is 0 kg N ha⁻¹, which means that for crops grown in these fields the recommended fertilizer dose was not exceeded. However, there are fields (12.4%) where additional N leaching exceeds 7 kg N ha⁻¹ and there is the opportunity for agricultural advisors to take actions to improve the situation.

The mean (field-weighted) basic N leaching resulting from the soil type and rainfall is 18.3 kg N ha⁻¹. While the mean basic N leaching, modified by factors related to the type of crop cultivated in the previous year, plowing time and application of natural fertilizers, is about 17.5 kg N ha⁻¹ which suggests good agricultural practice in the studied farms. However, the weighted mean of total N leaching for the test sample is ca. 20.3 kg N ha⁻¹ (greater than the median of the sample, suggesting slightly higher N leaching from relatively larger fields). The mean total N leaching is about 16% higher than the mean modified basic N leaching from the field and is due to exceeding the recommended mineral fertilizer doses.

The estimated N leaching losses are difficult to compare quantitatively with the results of other studies due to the multitude of natural and anthropogenic factors - often specific to regio. As an example, it is worth mentioning that under conditions somewhat similar to the Puck Commune,

in the south-west of Sweden, the amount of N leached (from sandy loam soil) in a mild winter in the cultivation of wheat and oilseed rape was 35-94 kg N ha⁻¹ and 16-23 kg N ha⁻¹ respectively. In contrast, in the cold winter, the N leaching values were similar for all crops and ranged from 32-58 kg N ha⁻¹ (Engström et al. 2011). These values were higher than the values estimated for the studied fields in the Puck Commune. Mean estimated N leaching from the study area (20.3 kg N ha⁻¹) was in the lower range of the annual N losses from arable land in southern Sweden at the end of the 20th century, which was estimated as 15-45 kg N ha⁻¹ (Stenberg et al. 1999).

2.3.3 Biochemical part of the EcoPuckBay model

In order to assess the quality of the results obtained in the biochemical part of the EcoPuckBay model, a set of basic statistical measures (Dybowski, Janecki, et al. 2020) was calculated, such as the mean, Pearson’s correlation coefficient (r), root-mean-square-error (RMSE) and standard deviation (STD). Concentrations of dissolved oxygen, nitrate, phosphate and chlorophyll a were selected for comparison.

Table 3: Statistical comparison of EcoPuckBay model with Voivodship Inspectorate of Environmental Protection (VIEP) monitoring data.

	VIEP Mean	VIEP STD	EPB Mean	EPB STD	RMSE	r
O ₂ [mmol m ⁻³]	315.30	43.06	337.50	35.97	31.03	0.71
NO ₃ [mmol m ⁻³]	1.74	2.31	2.48	2.87	2.19	0.66
PO ₄ [mmol m ⁻³]	0.35	0.23	0.32	0.21	0.21	0.56
CHL [mg m ⁻³]	4.44	3.14	4.40	3.59	2.89	0.64

Comparing the results of the EcoPuckBay model with the VIEP monitoring data (Tab. 3), we see that the modeled variables are of the same order of magnitude as the environmental data. The highest uncertainty (about 30%) is for nitrates, in other cases the difference in the averages does not exceed 10%. In terms of temporal variability of the modeled variables, the concentration of dissolved oxygen was best represented ($r = 0.71$).

Table 4: Statistical comparison of EcoPuckBay model with NEMO-SCOBİ model data.

	NEMO Mean	NEMO STD	EPB Mean	EPB STD	RMSE	r
O ₂ [mmol m ⁻³]	360.63	43.74	358.90	35.95	29.02	0.75
NO ₃ [mmol m ⁻³]	4.68	5.18	5.70	3.82	4.20	0.60
PO ₄ [mmol m ⁻³]	0.68	0.36	0.21	0.15	0.29	0.59
CHL [mg m ⁻³]	6.37	5.87	3.51	2.40	4.74	0.63

Statistical comparison between biochemical parameters from the EcoPuckBay model and the model results from NEMO-SCOBİ (Tab. 4) shows a satisfactory representation of mean values and standard deviations from the mean. The value of the Pearson correlation coefficient is the highest for the dissolved oxygen concentration ($r = 0.75$), for the remaining modeled variables the value of the correlation coefficient is approximately 0.60. However, it should be emphasized that the EcoPuckBay and NEMO models have very different grid sizes (the horizontal resolution of the NEMO model is ca. 4 km, while the horizontal resolution of the EcoPuckBay model is ca. 115 m).

2.3.4 Influence of the Puck Commune catchment on the waters of the Puck Lagoon

In the last part of the study (Dybowski and L. Dzierzbicka-Glowacka 2022), the influence of nutrients (nitrates and phosphates) on the waters of the Puck Lagoon (Gdańsk Basin, South Baltic) deposited from the land side was analyzed using numerical modeling. Model data was verified by comparison with *in situ* measured data. The spatial and temporal variability of nitrate, phosphate and chlorophyll a concentrations was analyzed. As a result of the conducted research, we have come to the conclusion that the load of phosphates and nitrates deposited from rivers that flow directly into the Puck Lagoon is relatively small compared to the Vistula. However, even when a small load enters a reservoir with very limited water exchange, such as the Puck Lagoon, there are periods when it can significantly affect the functioning of the ecosystem.

The impact of rivers flowing directly into the Puck Lagoon on the algae blooms in its waters was analyzed. For this purpose, the EcoPuckBay model has been configured with the rivers modeled

using the SWAT model being disconnected. The analysis was carried out from the beginning of February to the end of July 2018. In the configuration with the rivers turned on, the size of the diatom bloom was greater by approx. 22% compared to the configuration without rivers, while the bloom of toxic cyanobacteria decreased by 9%. This is because in the configuration without rivers, the lack of nitrogen input in spring limits the blooming of diatoms, which consequently causes an increase in phosphate concentration in spring (phosphates are not consumed). Then, when the temperature reaches a level that triggers summer bloom, this excess load of phosphate is absorbed into cyanobacterial bloom.

2.4 Conclusions

The Puck Bay is an extremely valuable and diverse area, especially its inner part known as the Puck Lagoon (Wesławski et al. 2009). Nevertheless, the frequency of published scientific research on this subject, in my opinion, is not big enough. It is noteworthy that the EcoPuckBay model is the first model to map the physicochemical variables of the Bay of Puck in high resolution, both temporal and spatial. The results of the verification of the model indicate its suitability for forecasting hydrodynamic and biochemical conditions. The satisfactory agreement between the *in situ* measurements and the simulations enables further analyzes to be undertaken and further corrections to the model to be made. Correct mapping of the entire water column mixing, advection, and heat transfer that control the heating and cooling of the aqueous masses is essential in predicting biological processes. Especially in a region such as the Bay of Puck, with its unique ecosystem, different from the conditions in the open sea due to the presence of natural topographic barriers and the strong influence of environmental factors, both natural and induced by human activity.

The EcoPuckBay model was developed as a part of the implementation of the project "Integrated Information and Prediction Service WaterPUCK" financed by NCBiR under Strategic Programs - BIOSTRATEG III. The conducted environmental and numerical studies allowed for the development of numerical models, a model of surface water flow and transport of nutrients and pesticides, a model of groundwater flow and a model of the Puck Bay ecosystem EcoPuckBay, which were made available to the Puck Commune as analysis tools as part of the product preparation for implementation phase, forecasts and decision support. The application of the models will be related to the strategic problem of environmental protection in Poland, which is limiting the inflow of nutrients to the Baltic Sea and limiting its eutrophication. Linking the runoff models of surface and groundwater and sea waters in the Bay of Puck as part of the WaterPuck service is innovative on a global scale and will allow for a more accurate and comprehensive mapping of the processes taking place in the coastal zone. Access to the WaterPuck Website products and a description of their operation is available through the WaterPuck project website <https://waterpuck.pl/en/> in the WATERPUCK PRODUCTS tab or directly on the website <https://waterpuck.pl/en/produkty.html> (L. Dzierzbicka-Glowacka et al. 2022).

3 Streszczenie

3.1 Wstęp

Rosnąca liczba ludności wymusza na rolnictwie coraz wydajniejsze zaspokajania potrzeb żywnościowych. Jednym ze sposobów na osiągnięcie wyższych plonów z hektara gruntów ornych jest zwiększenie ilości stosowanego nawozu. Jednak niesie to ze sobą wysokie ryzyko potencjalnego zanieczyszczenia środowiska i zagrożenia dla zdrowia ludzkiego (Galloway i in. 2008). Praktycznie nie ma obszaru, na który człowiek nie ma wpływu, a duża część (41%) jest silnie dotknięta wieloma czynnikami antropogenicznymi (Halpern i in. 2008). Jednak gdy ekosystem wciąż funkcjonuje (pomimo niewielkiej liczby osobników w gatunku) możliwe jest odwrócenie procesu jego degradacji (Lotze i in. 2006). Jest to szczególnie ważne w kontekście odbudowy zasobów ryb, które przez lata były nadmiernie eksploatowane (Shahidul Islam i Tanaka 2004; Worm i in. 2009). Środowisko wodne jest podatne na zanieczyszczenia niepunktowe pochodzące z rolnictwa, które może intensyfikować proces eutrofizacji w wyniku wzbogacania wodę w składniki pokarmowe. Morza i oceany mają niewątpliwie bezpośredni wpływ na zdrowie człowieka, gospodarkę i zasoby żywnościowe, mają walory rekreacyjne i estetyczne oraz odgrywają ogromną, korzystną rolę w globalnym bilansie tlenu i dwutlenku węgla. Ekosystemy morskie są jednak niezwykle wrażliwe, a ze względu na ogromną czasową i przestrzenną skalę procesów zachodzących w środowisku morskim, znaczące zakłócenia w ich funkcjonowaniu mogą mieć dalekosiężne, a czasem nieodwracalne skutki. Jakość wody zależy od fizycznych, chemicznych i biologicznych właściwości oraz potencjału akwenu do wspierania korzystnych zastosowań dla społeczeństwa. Eutrofizacja to proces, w którym wzrost depozycji składników pokarmowych powoduje nadmierną produkcję pierwotną (wzrost glonów i trawy morskiej). Objawy eutrofizacji obejmują zakwity glonów, zmniejszoną przezroczystość wody i utratę tlenu, co powoduje dodatkowe koszty dla środowiska (Álvarez i in. 2017; Heisler i in. 2008; Howarth 2008). Wyzwania stojące przed współczesną globalną gospodarką związane są głównie ze społeczną odpowiedzialnością i zarządzaniem zasobami zgodnie z zasadami zrównoważonego rozwoju (Badri Ahmadi, Kusi-Sarpong i Rezaei 2017). Wzięcie odpowiedzialności za zanieczyszczenie środowiska jest konieczne nie tylko w przedsiębiorstwach przetwórczych i energetycznych, ale także w turystyce i rolnictwie. Duże rozproszenie emitentów zanieczyszczeń nie sprzyja efektywnemu zarządzaniu środowiskiem w wymiarze regionalnym. Działania mające na celu ograniczenie eutrofizacji Morza Bałtyckiego wiążą się również z innym wyzwaniem, jakim są zmiany klimatyczne. W przyszłości przewidywane są krótsze i bardziej mokre zimy, które spowodują zmniejszenie opadów śniegu i zmniejszoną warstwę pokrywy lodowej oraz intensywniejszy spływ z dorzecza. W związku z tym prognozowany jest wzrost transportu substancji biogenicznych do Bałtyku (Hägg i in. 2014). Podnosi się temperatura wody w Bałtyku, co stwarza korzystniejsze warunki do występowania zakwitów glonów.

Najbardziej wiarygodnym sposobem kontroli stanu środowiska morskiego jest prowadzenie nieustannego monitoringu jego parametrów fizykochemicznych. Taki monitoring jest jednakże niezwykle kosztowny i dostarcza tylko ograniczonej informacji, zarówno przestrzennie, jak i czasowo. W tym kontekście zasadnym jest uzupełnienie danych monitoringowych poprzez dane z symulacji numerycznych, których czasowa i przestrzenna rozdzielczość ograniczona jest wyłącznie możliwościami obliczeniowymi komputera oraz przestrzenią dyskową dostępną do składowania danych. Z kolei opracowanie modeli numerycznych o wysokiej rozdzielczości, które są w stanie skutecznie i wiarygodnie symulować zarówno fizyczne, jak i biogeochemiczne procesy kształtujące stan środowiska morskiego, jest czasochłonne i wymaga szerokiej wiedzy o wielu procesach zachodzących w modelowanym ekosystemie. Niezbędny jest dostęp do informacji o bezpośrednich i pośrednich czynnikach wymuszających, takich jak warunki brzegowe, dopływy rzeczne i wymuszenia atmosferyczne, które wpływają na dynamikę zmian w obrębie domeny modelu. Aby sprostać złożoności tego zadania i zwiększyć wydajność procesu implementacji, zaprojektowany i dostosowany do obszaru badawczego został model Community Earth System Model (CESM), co pozwoliło skonstruować doskonałe narzędzie numeryczne, jakim jest model EcoPuckBay w ramach projektu WaterPUCK (www.waterpuck.pl), służące do reanalizy oraz prognozowania środowiska morskiego Zatoki Puckiej w wysokiej rozdzielczości.

Celem podjętych badań było określenie wpływu gospodarstw rolnych, na przykładzie Gminy Puck, na wody morskie zlokalizowane w strefie przybrzeżnej (Zatoka Pucka) z wykorzystaniem modelu numerycznego. Dla osiągnięcia celu nadrzędnego określono cztery cele szczegółowe:

1. Scharakteryzować strukturę i zmienność parametrów hydrodynamicznych w rejonie Zatoki Puckiej.
2. Określić, na podstawie przeprowadzonych badań (ankiet wśród rolników) i opracowanego kalkulatora, wielkość wymywania azotu w skali pojedynczego pola.
3. Scharakteryzować strukturę i zmienność parametrów biochemicznych w rejonie Zatoki Puckiej.
4. Zbadać wpływ dopływu substancji biogenicznych z rzek Gminy Puck na wody Zatoki Puckiej (ze szczególnym naciskiem na wody Zalewu Puckiego).

Każdy z powyższych celów szczegółowych został omówiony w osobnym artykule naukowym, a ich zestaw jako całość stanowi przedmiot niniejszej rozprawy.

Niniejsza praca doktorska składa się z trzech, opublikowanych w recenzowanych czasopismach, artykułów naukowych oraz manuskryptu, załączonego na końcu rozprawy, który został złożony do czasopisma i jest spójną kontynuacją badań podjętych w poprzednich trzech pracach. Pierwszy artykuł (Dybowski, Jakacki i in. 2019) skupia się na opisie oraz walidacji części hydrodynamicznej modelu EcoPuckBay. Drugi artykuł (Dybowski, L. A. Dzierzbicka-Głowacka i in. 2020) przedstawia analizę wielkości ładunków azotu aplikowanego w postaci nawozów na pola uprawne oraz oszacowanie ich potencjalnego wymywania w skali pojedynczego pola. W trzecim artykule (Dybowski, Janecki i in. 2020) została przedstawiona oraz zwalidowana część biochemiczna modelu EcoPuckBay oraz wprowadzony został moduł rozplywu substancji biogenicznych. Natomiast w czwartym manuskrypcie (Dybowski i L. Dzierzbicka-Głowacka 2022) przedstawiono analizę zmienności przestrzenno-czasowej stężenia azotanów, fosforanów i chlorofilu a w wodach Zalewu Puckiego. W pracy tej przeprowadzono również symulację wpływu małych (w porównaniu do największej w rejonie Wisły) rzek i cieków mających ujście bezpośrednio w Zalewie Puckim na zakwity glonów w tym akwenie. Zdecydowana większość wyników prezentowanych w tej rozprawie została uzyskana przy wykorzystaniu danych pochodzących z modelu EcoPuckBay, dlatego na początku kolejnego rozdziału znajduje się jego krótki opis, który ma na celu umożliwienie czytelnikowi zaznajomienie się z używanym narzędziem oraz lepsze zrozumienie przytoczonych rezultatów.

3.2 Materiały i metody badań

3.2.1 Model EcoPuckBay

Model EcoPuckBay został opracowany na podstawie Community Earth System Model (CESM), który jest globalnym sprzężonym modelem klimatycznym. CESM składa się z pięciu oddzielnych komponentów z dodatkowym modułem kontrolującym czas, siły wymuszające, domeny, siatki i wymianę informacji między poszczególnymi modułami. CESM został przeskalowany i przystosowany dla rejonu Zatoki Puckiej do dalszego rozwoju w Instytucie Oceanologii PAN.

Rozdzielczość pozioma modelu EcoPuckBay jest równa $1/960^\circ$, co odpowiada rozdzielczości poziomej siatki ok. 115 m. Rozdzielczość pionowa jest równa 0,4-0,6 m w górnych warstwach, a następnie stopniowo wzrasta do miąższości warstwy równej 5 m. Dyskretyzacja pionowa wykorzystuje sformułowanie typu z , a topografia dna jest oparta na Baltic Sea Bathymetric Database (BSBD) pochodzącej z zasobów Komisji Hydrograficznej Morza Bałtyckiego (Baltic Sea Hydrographic Commission 2013). Dane batymetryczne interpolowano na siatkę modelu wykorzystując metodę Kriginga. Krok czasowy modelu oceanu wynosi 12 sekund.

Moduł oceanu w modelu EcoPuckBay opiera się na kodzie POP, wykorzystując trójwymiarowe równania ruchu z przybliżeniami hydrostatycznymi i Boussinesqa. Poniżej przedstawiono główne równania hydrodynamiczne w układzie sferycznym, które są zaimplementowane w modelu.

Równania ruchu poziomego:

$$\frac{\partial u}{\partial t} + L(u) - fv = -\frac{1}{\rho_0 a \cos \phi} \frac{\partial p}{\partial \lambda} + \frac{\partial}{\partial z} \left(K_M \frac{\partial u}{\partial z} \right) + B_M \nabla_H^4 u, \quad (1)$$

$$\frac{\partial v}{\partial t} + L(v) - fu = -\frac{1}{\rho_0 a} \frac{\partial p}{\partial \phi} + \frac{\partial}{\partial z} \left(K_M \frac{\partial v}{\partial z} \right) + B_M \nabla_H^4 v. \quad (2)$$

Równanie pędu wzdłuż kierunku pionowego w przybliżeniu hydrostatycznym:

$$\frac{\partial p}{\partial z} = -\rho g. \quad (3)$$

Równanie ciągłości:

$$\frac{1}{a \cos \phi} \frac{\partial u}{\partial \lambda} + \frac{1}{a \cos \phi} \frac{\partial (v \cos \phi)}{\partial \phi} + \frac{\partial w}{\partial z} = 0 \quad (4)$$

Równanie transportu ciepła i soli:

$$\frac{\partial T}{\partial t} + L(T) = \frac{\partial}{\partial z} \left(K_D \frac{\partial T}{\partial z} \right) + B_D \nabla_H^4 T, \quad (5)$$

$$\frac{\partial S}{\partial t} + L(S) = \frac{\partial}{\partial z} \left(K_D \frac{\partial S}{\partial z} \right) + B_D \nabla_H^4 S, \quad (6)$$

Równanie stanu:

$$\rho = \rho(S, T, p). \quad (7)$$

gdzie: u, v składowe poziome prędkości; w składowa pionowa prędkości; g przyspieszenie grawitacyjne; p ciśnienie; T, S temperatura i zasolenie; ρ_0 średnia gęstość wody; λ i ϕ długość i szerokość geograficzna; a efektywny promień Ziemi; t czas; $f = 2\Omega \sin \phi$ parametr Coriolisa (Ω prędkość kątowa Ziemi); L operator adwekcyjny; ∇_H^4 horyzontalny operator biharmoniczny; K_M biharmoniczny pionowy współczynnik turbulentnej lepkości; B_D biharmoniczny horyzontalny współczynnik turbulentnej lepkości. Jako stałe przyjmuje się współczynniki B_D i B_M . Mieszanie pionowe w EcoPuckBay jest określane przez parametryzację KPP (Large, McWilliams i Doney 1994) określoną przez pionowe współczynniki K_D, K_M . Zastosowano ulepszenie schematu KPP z dolną warstwą graniczną (Durski, Glenn i Haidvogel 2004):

$$C_d = \kappa^2 \left(\ln \frac{dz}{z_r} \right)^{-2}, \quad (8)$$

gdzie C_d współczynnik oporu; κ stała von Karmana; dz odległość od dna do punktu siatki; z_r chropowatość określona jako 0,5 cm (wartość dostrojona na podstawie przepływu wody przez Sund w modelu 3D CEMBS). W modelu zastosowano parametryzację równania stanu MWJF (McDugall i in. 2003). POP jest modelem o powierzchni swobodnej, a prędkość pionowa na powierzchni wynosi:

$$w = \frac{\partial \eta}{\partial z}, \quad z = 0, \quad (9)$$

gdzie: η to wolna rzędna powierzchni. Naprężenie przy dnie τ_b jest wyrażone jako:

$$\frac{\tau_b}{\rho} = \frac{C_d \vec{U} |\vec{U}|}{d^2}, \quad (10)$$

gdzie: d grubość warstwy przydennej, C_d współczynnik tarcia przydennej, \vec{U} wektor prędkości wody przy dnie.

Część biochemiczna modelu EcoPuckBay opiera się na podejściu NPZD (Moore i in. 2001). W modelu wyznaczone są stężenia substancji biogenicznych, trzy rodzaje fitoplanktonu (okrzemki, pikofitoplankton/nanofitoplankton i diazotrofy (organizmy wiążące azot)), chlorofil a , zooplankton, detrytus pelagiczny, tlen rozpuszczony oraz pestycydy (glifosat, diflufenikan, metazachlor, chloropiryfos i antrachinon). Wiele modeli, choć nie wszystkie, można przedstawić w ogólnej formie jako sprzężony zestaw zależnych od czasu równań adwekcji-dyfuzji ze źródłami:

$$\frac{\partial S}{\partial t} + (V + w_s) \nabla S - \sum_{i=1}^3 \frac{\partial}{\partial x_i} \left(K_{x_i} \frac{\partial S}{\partial x_i} \right) = F_S, \quad (11)$$

gdzie S oznacza zmienną biochemiczną. Drugi i trzeci wyraz po lewej stronie równania opisują odpowiednio adwekcję i mieszanie, gdzie $V(u, v, w)$ jest wektorem prędkości, w_s jest prędkością opadania szczątków pelagicznych, a K_{x_i} to współczynnik dyfuzji turbulentnej. Wszystkie procesy chemiczne i biologiczne są przedstawione jako jeden wyraz F_S (tzw. źródło) po prawej stronie równania, a szczegółowe równania są wymienione w opisie modelu 3D CEMBS (Dzierzbicka-Głowacka, Janecki i in. 2013).

Model EcoPuckBay jest wymuszany danymi meteorologicznymi z modelu UM dostarczonego przez Interdyscyplinarne Centrum Modelowania Matematycznego i Komputerowego Uniwersytetu

Warszawskiego (ICM UW). Używane są następujące pola zewnętrzne: temperatura powietrza i wilgotność właściwa na wysokości 2 m, ciśnienie na poziomie morza, opady atmosferyczne, promieniowanie krótko- i długofalowe, prędkość wiatru na wysokości 10 m, gęstość powietrza.

Wyniki modelu 3D EcoPuckBay są ograniczone do obszaru Zatoki Puckiej. Jednak cała siatka modelu obejmuje szerszy obszar. Ma to zapewnić odpowiednią symulację warunków brzegowych. Wzdłuż linii północnej granicy modelu EcoPuckBay dane z modelu predykcyjnego 3D CEMBS o długości 2,3 km są przesyłane do modelu EcoPuckBay. Wyniki dostarczane z modelu 3D CEMBS (Dzierzbicka-Głowacka, Jakacki i in. 2013; Dzierzbicka-Głowacka, Janecki i in. 2013) służą do zapewnienia pól wymuszających w modelu EcoPuckBay poprzez sekwencyjny transfer informacji. Mechanizm tego modułu polega na interpolacji wartości z 3D CEMBS do siatek modelu EcoPuckBay. Dodatkowo, na granicy woda-ład, model EcoPuckBay został połączony modelami: SWAT (spływ wód powierzchniowych) i Modflow (dopływ wód gruntowych).

3.2.2 Obszar badań

Południowa część Bałtyku obejmująca Gminę Puck jest popularnym regionem turystycznym, na który duży wpływ ma również antropogeniczna działalność mieszkańców i rolnictwo. W rezultacie Zatoka Pucka jest naturalnym rezerwuarem do składowania odpadów nawozów i innych zanieczyszczeń deponowanych w niej poprzez wody gruntowe, rzeki i spływ powierzchniowy lub bezpośrednie składowanie.

Jednym z najważniejszych czynników wpływających na unikalny ekosystem regionu jest batymetria. Średnia głębokość Zatoki Puckiej wynosi około 15 m, a maksymalna 54 m. Od północnego wschodu otacza go Mierzeja Helska, która stanowi naturalną barierę dla mieszania się z otwartymi wodami Bałtyku. Zatokę Pucką można podzielić na dwie części: Zalew Pucki (zwany też wewnętrzną Zatoką Pucką) oraz zewnętrzną Zatokę Pucką, które są odseparowane Rybitwią Mielizną ograniczającą mieszanie wód pomiędzy nimi. Zatoka Pucka jest również pod silnym wpływem dopływów rzecznych z lądu, co powoduje obniżenie zasolenia, zwłaszcza w przybrzeżnych wodach powierzchniowych.

Największą rzeką regionu jest Wisła, ze średnim odpływem równym ponad $1000 \text{ m}^3 \text{ s}^{-1}$. Średnia miesięczna temperatura wody w regionie waha się od około 2°C w lutym do ponad 20°C na powierzchni w okresie letnim, z maksimum zwykle w sierpniu. W cieplejszych miesiącach, w zewnętrznej części Zatoki Puckiej, często dochodzi do stratyfikacji wody, co prowadzi do występowania sezonowych termoklin.

3.2.3 Zbiory danych użyte do walidacji modelu

Celem walidacji modelu EcoPuckBay wykorzystaliśmy następujące zbiory danych pomiarowych *in situ*: zbiór danych zebranych w trakcie działań monitoringowych Wojewódzkiego Inspektora Ochrony Środowiska (VIEP) w Gdańsku oraz zbiór danych zawierających pionowe profile temperatury i zasolenia zarejestrowane w 2018 roku podczas jednej z kampanii pomiarowych s/y Oceania wzdłuż południowego wybrzeża Bałtyku. Dodatkowo wykorzystano dane modelowe parametrów fizycznych i biochemicznych wyznaczonych z wykorzystaniem modeli NEMO-Nordic i NEMO-SCOBi pochodzących z bazy Marine Copernicus. Poniżej przedstawiono krótki opis wymienionych zbiorów danych.

Największym zbiorem danych *in situ* użytych do walidacji modelu EcoPuckBay, przeprowadzonej w ramach prac składających się na niniejszą rozprawę, są próbki zebrane podczas regularnych pomiarów środowiska morskiego Morza Bałtyckiego prowadzonych przez Wojewódzki Inspektorat Ochrony Środowiska (VIEP) w Gdańsku. Sposób prowadzenia monitoringu oraz sposób oceny stanu Morza Bałtyckiego przez VIEP został określony przepisami ustawy Prawo wodne oraz przyjętym przez Radę Ministrów Programem monitoringu wód morskich, który realizuje wymagania art. 11. Dyrektywy Parlamentu Europejskiego i Rady 2008/56/WE z dnia 17 czerwca 2008 r. ustanawiającej ramy działań Wspólnoty w dziedzinie polityki środowiska morskiego (dyrektywa ramowa w sprawie strategii morskiej).

Źródłem wyników modelowych są dane pobrane z bazy Marine Copernicus. Jest to produkt do reanalizy warunków środowiskowych Morza Bałtyckiego, który zapewnia 25-letnią reanalizę biogeochemiczną Morza Bałtyckiego z wykorzystaniem modelu NEMO-Nordic sprzężonego z modelem biogeochemicznym SCOBi. Rozdzielczość pozioma modeli NEMO-Nordic oraz NEMO-SCOBi jest równa około 4 km. Wszystkie zmienne są dostępne jako średnie dzienne oraz średnie miesięczne

i obejmują temperaturę, zasolenie, stężenia azotanów, fosforanów, rozpuszczonego tlenu oraz chlorofilu *a*. Domeny NEMO-Nordic oraz NEMO-SCOBI obejmują całe Morze Bałtyckie poszerzone o obszar Morza Północnego.

Dane zebrane podczas regularnego rejsu s/y Oceania latem 2018 r. po Zatoce Puckiej obejmowały przekroje pionowe dla 18 stacji pomiarowych, które wykonano przy użyciu sondy Seabird 49 Conductivity Temperature Depth (CTD). Dokładność czujnika CTD wynosiła $0,0003 \text{ mS cm}^{-1}$ dla przewodności, $0,002^\circ\text{C}$ dla temperatury i $0,1\%$ dla ciśnienia. Czujniki temperatury i przewodności systemu CTD były kalibrowane corocznie, po rejsie, przez producentów. Próbkowanie pionowe było wyższe niż rozdzielczość modelu (od 10-40 odczytów na poziom modelu, w zależności od głębokości próbkowania), dlatego dane pomiarowe zostały uśrednione, aby odpowiadały rozdzielczości modelu EcoPuckBay.

3.2.4 Dane ankietowe o praktykach rolniczych na terenie Gminy Puck

W ramach projektu WaterPUCK przeprowadzona została ankietyzacja reprezentatywnej grupy rolników w 31 gospodarstwach na terenie Gminy Puck, co stanowi ok. $3,6\%$ wszystkich gospodarstw zlokalizowanych w tej gminie. Rolnicy przekazali dane dotyczące sposobu nawożenia i uprawy roślin. Na podstawie zebranych danych, określono następnie szacunkową ilość wymywania N z pola, co zostało szczegółowo opisane w drugim artykule składającym się na niniejszą rozprawę doktorską.

3.3 Rezultaty i dyskusja

W tym rozdziale przedstawiam najważniejsze rezultaty przeprowadzonych badań, natomiast po szczegółowe wyniki oraz analizy odsyłam czytelnika do artykułów składających się na niniejszą rozprawę doktorską.

3.3.1 Część hydrodynamiczna modelu EcoPuckBay

W celu oceny poprawności wartości parametrów uzyskiwanych w części hydrodynamicznej modelu EcoPuckBay z okresu od stycznia 2014 r. do grudnia 2018 r. obliczono zestaw podstawowych miar statystycznych (Dybowski, Jakacki i in. 2019), takich jak współczynnik korelacji Pearsona (r), błąd średniokwadratowy (RMSE), odchylenie standardowe (STD) i ME (różnica wartości średnich) w odniesieniu do dostępnych danych modelowych (NEMO-Nordic) oraz pomiarów *in situ* (VIEP) dla temperatury i zasolenia.

Tabela 1: Porównanie statystyczne pomiędzy modelowaną temperaturą a danymi referencyjnymi z pomiarów *in situ* (VIEP i s/y Oceania) oraz danymi modelowymi (NEMO-Nordic).

Dane referencyjne	r	RMSE [$^\circ\text{C}$]	STD [$^\circ\text{C}$]	ME [$^\circ\text{C}$]
seria czasowa (VIEP)	0.97	1.45	5.67	-0.83
seria czasowa (NEMO-Nordic)	0.98	1.33	6.01	-0.31
profil pionowy (s/y Oceania)	0.92	2.85	5.29	-1.16

Współczynnik korelacji Pearsona r temperatury wyznaczonej z użyciem modelu EcoPuckBay z danymi monitoringowymi VIEP jest równy 0,97 oraz 0,92 dla danych z profili pionowych uzyskanych podczas rejsów s/y Oceania (Tab. 1). Porównanie z wynikami z modelu NEMO-Nordic wskazuje na jeszcze większą korelację wyników (współczynnik r równy 0,98). RMSE dla wszystkich porównywanych zbiorów jest istotnie mniejsze niż STD. Natomiast ME, czyli różnica średnich wartości obu zbiorów, jest we wszystkich przypadkach ujemny, co oznacza, że temperatura w modelu była obarczona błędem statystycznym. Należy jednak podkreślić, że na tym etapie walidacji modelu, moduł asymilacji danych satelitarnych nie był jeszcze uruchomiony.

Tabela 2: Porównanie statystyczne pomiędzy modelowanym zasoleniem a danymi referencyjnymi z pomiarów *in situ* (VIEP i s/y Oceania) oraz danymi modelowymi (NEMO-Nordic).

Dane referencyjne	r	RMSE [PSU]	STD [PSU]	ME [PSU]
seria czasowa (VIEP)	0.58	0.67	0.60	0.16
seria czasowa (NEMO-Nordic)	0.17	0.97	0.70	-0.24
profil pionowy (s/y Oceania)	0.90	0.40	0.84	-0.03

Współczynnik korelacji Pearsona r zasolenia wyznaczonego z użyciem modelu EcoPuckBay z danymi monitoringowymi VIEP jest równy 0,58 oraz 0,90 dla danych z profili pionowych uzyskanych podczas rejsów s/y Oceania (Tab. 2). Porównanie z wynikami z modelu NEMO-Nordic wskazuje na bardzo słabą korelację wyników (współczynnik r równy 0,17), jest to spowodowane różnicą rozdzielczości modeli. RMSE dla wszystkich porównywanych zbiorów jest istotnie mniejsze niż STD. Z kolei ME dla profili pionowych jest w okolicach zera, co świadczy o bardzo dobrym odwzorowaniu stratyfikacji pionowej akwenu. Warto dodać, że wartość współczynnika korelacji r bardzo różni się w poszczególnych stacjach VIEP i przyjmuje wartości od 0,28 do 0,86. Natomiast dla profili pionowych wartość r zmienia się w zakresie od 0,78 do 1,00.

3.3.2 Oszacowanie wielkości wymywania azotu z pól uprawnych

Następnym etapem prac badawczych było wyznaczenie intensywności nawożenia oraz oszacowanie wielkości wymywania azotu z gleby w skali pojedynczego pola uprawnego na terenie Gminy Puck (Dybowski, L. A. Dzierzbicka-Głowacka i in. 2020). Średnia wartość intensywności nawożenia mineralnego w badanej próbie (około 110 kg N ha⁻¹) jest wyższa od średniej dla Polski (80 kg N ha⁻¹), podczas gdy w innych krajach regionu Morza Bałtyckiego wartości te wynoszą: w Szwecji i Estonii około 30 kg N ha⁻¹, w Norwegii ponad 100 kg N ha⁻¹, w Danii około 80 kg N ha⁻¹ i około 75 kg N ha⁻¹ w Niemczech (European Environment Agency 2018).

Dla prawie połowy wszystkich pól (49,8%) dodatkowe wymywanie N wynosi 0 kg N ha⁻¹, co oznacza, że dla upraw uprawianych na tych polach zalecana dawka nawozu nie została przekroczona. Istnieją jednak pola (12,4%), na których dodatkowe wymywanie N przekracza 7 kg N ha⁻¹ i tutaj doradcy rolni mają możliwość podjęcia działań w celu poprawy sytuacji poprzez konsultacje z rolnikami uprawiającymi te pola.

Średnia (ważona powierzchnią pól) podstawowego wymywania N dla badanej próbki wynikająca z rodzaju gleby i opadów wynosi 18,3 kg N ha⁻¹. Podczas gdy średnie podstawowe wymywanie N zmodyfikowane czynnikami wynikającymi z rodzaju uprawianej rośliny w poprzednim roku, terminu wykonania orki i stosowania nawozów naturalnych wynosi około 17,5 kg N ha⁻¹ co sugeruje dobre praktyki rolnicze ze względu na wymienione czynniki. Jednak średnia ważona całkowitego wymywania N dla badanej próbki wynosi około 20,3 kg N ha⁻¹ (jest większa niż mediana próbki, co sugeruje nieco wyższe wymywanie N z relatywnie większych pól). W związku z tym średnie całkowite wymywanie N jest o około 16% wyższe niż średnie modyfikowane podstawowe wymywanie z pola i jest spowodowane przekroczeniem zalecanych dawek nawozów mineralnych.

Oszacowane straty wymywania N trudno porównywać ilościowo z wynikami innych badań ze względu na mnogość czynników naturalnych i antropogenicznych – często bardzo specyficznych dla danego obszaru. Jako przykład warto wspomnieć, że w warunkach nieco podobnych do Gminy Puck, w południowo-zachodniej Szwecji, ilość N wymywanego (z gleby piaszczysto-gliniastej) w łagodną zimę przy uprawie pszenicy i rzepaku wynosił odpowiednio 35–94 kg N ha⁻¹ i 16–23 kg N ha⁻¹. Natomiast w mroźną zimę poziomy wymywania N były podobne dla wszystkich upraw i wynosiły 32–58 kg N ha⁻¹ (Engström i in. 2011). Wartości te były wyższe od wielkości oszacowanych dla badanych pól w Gminie Puck. Średni N wypłukany z badanego obszaru (20,3 kg N ha⁻¹) mieścił się w dolnym zakresie rocznych strat azotanów z gruntów ornych w południowej Szwecji pod koniec okresu XX wieku, które ustalono na 15–45 kg N ha⁻¹ (Stenberg i in. 1999).

3.3.3 Część biochemiczna modelu EcoPuckBay

W celu oceny jakości wyników uzyskanych w części biochemicznej modelu EcoPuckBay obliczono zestaw podstawowych miar statystycznych (Dybowski, Janecki i in. 2020), takich jak średnia, współczynnik korelacji Pearsona (r), błąd średniokwadratowy (RMSE) i odchylenie standardowe (STD). Do porównania wybrano rozpuszczone stężenia tlenu, azotanów, fosforanów i chlorofilu a .

Tabela 3: Porównanie statystyczne wyników modelu EcoPuckBay z danymi monitoringowymi Wojewódzkiego Inspektoratu Ochrony Środowiska (VIEP).

	VIEP Mean	VIEP STD	EPB Mean	EPB STD	RMSE	r
O ₂ [mmol m ⁻³]	315.30	43.06	337.50	35.97	31.03	0.71
NO ₃ [mmol m ⁻³]	1.74	2.31	2.48	2.87	2.19	0.66
PO ₄ [mmol m ⁻³]	0.35	0.23	0.32	0.21	0.21	0.56
CHL [mg m ⁻³]	4.44	3.14	4.40	3.59	2.89	0.64

Porównując wyniki modelu EcoPuckBay z danymi monitoringowymi VIEP (Tab. 3), widzimy, że stężenia modelowanych zmiennych są tego samego rzędu wielkości co dane środowiskowe. Najwyższa niepewność (około 30%) dotyczy azotanów, w pozostałych przypadkach różnica w średnich nie przekracza 10%. W przypadku czasowej zmienności modelowanych zmiennych najlepiej odwzorowane zostało stężenie tlenu rozpuszczonego, dla którego współczynnik korelacji Pearsona jest najwyższy ($r = 0,71$).

Tabela 4: Porównanie statystyczne wyników modelu EcoPuckBay z danymi modelowymi z NEMO-SCOBI.

	NEMO Mean	NEMO STD	EPB Mean	EPB STD	RMSE	r
O ₂ [mmol m ⁻³]	360.63	43.74	358.90	35.95	29.02	0.75
NO ₃ [mmol m ⁻³]	4.68	5.18	5.70	3.82	4.20	0.60
PO ₄ [mmol m ⁻³]	0.68	0.36	0.21	0.15	0.29	0.59
CHL [mg m ⁻³]	6.37	5.87	3.51	2.40	4.74	0.63

Porównanie statystyczne parametrów biochemicznych z modelu EcoPuckBay z wynikami modelowymi z NEMO-SCOBI (Tab. 4) wskazuje na zadowalające odwzorowanie wartości średnich oraz odchyłeń standardowych od średniej. Wartość współczynnika korelacji jest największa dla stężenia tlenu rozpuszczonego ($r = 0.75$), dla pozostałych modelowanych zmiennych wartość współczynnika korelacji jest równa około 0.60, należy jednak podkreślić, że modele EcoPuckBay oraz NEMO mają bardzo różne rozmiary siatki (rozdzielczość pozioma modelu NEMO to ok. 4 km, podczas gdy rozdzielczość pozioma modelu EcoPuckBay to ok. 115 m).

3.3.4 Wpływ zlewni Gminy Puck na wody Zalewu Puckiego

W ostatniej części pracy (Dybowski i L. Dzierzbicka-Głowacka 2022) z wykorzystaniem modelowania numerycznego przeanalizowano wpływ składników pokarmowych (azotanów i fosforanów) na wody Zalewu Puckiego (Basen Gdański, Bałtyk Południowy) zasilane od strony lądu. Dane modelowe zweryfikowano przez porównanie z danymi pomiarowymi *in situ*. Przeanalizowano przestrzenną i czasową zmienność stężeń azotanów, fosforanów i chlorofilu *a*. W wyniku przeprowadzonych badań doszliśmy do wniosku, że ładunek fosforanów i azotanów deponowanych z rzek mających ujście bezpośrednio w Zalewie Puckim jest stosunkowo niewielki w porównaniu z Wisłą. Jednak nawet gdy niewielki spływ dostanie się do zbiornika o bardzo ograniczonej wymianie wód, jak Zalew Pucki, zdarzają się okresy, w których ładunek składników pokarmowych rzecznych znacząco wpływa na funkcjonowanie ekosystemu.

Przeprowadzono analizę wpływu rzek mających ujście bezpośrednio do Zalewu Puckiego na zakwit glonów w jej wodach. W tym celu model EcoPuckBay został skonfigurowany w ten sposób, że rzeki modelowane z wykorzystaniem modelu SWAT zostały odłączone. Analizę przeprowadzono od początku lutego do końca lipca 2018 roku. W konfiguracji z włączonymi rzekami wielkość zakwitów okrzemek była większa o ok. 22% w stosunku do konfiguracji bez rzek, z kolei zakwit toksycznych sinic zmniejszył się o 9%. Dzieje się tak dlatego, że w konfiguracji bez rzek brak dopływu związków azotu wiosną ogranicza kwitnienie okrzemek, co w następstwie powoduje podwyższenie stężenia fosforanów wiosną (fosforany nie są zużywane). Następnie, gdy temperatura osiągnie poziom, wywołujący zakwit letni, ten nadmiarowy ładunek fosforanów jest pobierany na zakwit sinic.

3.4 Wnioski

Zatoka Pucka jest obszarem niezwykle cennym i różnorodnym, szczególnie jej wewnętrzna część zwana Zalewem Puckim (Wesławski i in. 2009). Mimo to, częstotliwość publikowanych badań naukowych na jej temat w mojej ocenie jest niewielka. Na uwagę zasługuje fakt, że model EcoPuckBay jest pierwszym modelem, który odwzorowuje zmienne fizykochemiczne Zatoki Puckiej w wysokiej rozdzielczości, zarówno czasowej jak i przestrzennej. Wyniki weryfikacji modelu wskazują na jego przydatność do prognozowania warunków hydrodynamicznych oraz biochemicznych. Zadowalająca zgodność między pomiarami *in situ* a symulacjami umożliwia podejmowanie dalszych analiz i wprowadzania kolejnych poprawek w modelu. Prawidłowe odwzorowanie mieszania w całej kolumnie wody, adwekcji i wymiany ciepła, które kontrolują nagrzewanie i schładzanie mas wodnych, ma istotne znaczenie dla prognozowania procesów biologicznych. Zwłaszcza w regionie

takim jak Zatoka Pucka, z jej unikalnym ekosystemem, odmiennym od warunków na otwartym morzu ze względu na występowanie naturalnych barier topograficznych oraz silny wpływ czynników środowiskowych, zarówno naturalnych, jak i indukowanych działalnością człowieka.

Praca powstała w ramach realizacji projektu „Zintegrowany Serwis informacyjno-predykcijny WaterPUCK” finansowanego przez NCBiR w ramach Programów Strategicznych – BIOSTRATEG III. Przeprowadzone badania środowiskowe i numeryczne pozwoliły na opracowanie numerycznych modeli, modelu przepływu wód powierzchniowych i transportu substancji biogennych oraz pestycydów, modelu przepływu wód podziemnych i modelu ekosystemu Zatoki Puckiej EcoPuckBay, które w ramach fazy przygotowanie produktu do wdrożenia zostały udostępnione Gminie Puck, jako narzędzia analiz, prognoz i wspomagania decyzji. Zastosowanie modeli będzie związane ze strategicznym problemem ochrony środowiska w Polsce, jakim jest ograniczenie dopływu substancji biogennych do Bałtyku i ograniczenie jego eutrofizacji. Powiązanie modeli spływu wód lądowych powierzchniowych i podziemnych oraz wód morskich w Zatoce Puckiej w ramach serwisu WaterPuck ma charakter innowacyjny w skali światowej i pozwoli na dokładniejsze i bardziej kompleksowe odwzorowanie procesów zachodzących w strefie brzegowej. Dostęp do produktów Serwisu WaterPUCK i opis ich działania jest poprzez stronę internetową projektu WaterPuck <https://waterpuck.pl/> w zakładce PRODUKTY WATERPUCK lub bezpośrednio na stronie <https://waterpuck.pl/pl/produkty.html> (L. Dzierzbicka-Głowacka i in. 2022).

References (Bibliografia)

- Álvarez, X. et al. (2017). “Anthropogenic nutrients and eutrophication in multiple land use watersheds: Best management practices and policies for the protection of water resources”. In: *Land Use Policy* 69, pp. 1–11. ISSN: 0264-8377. DOI: <https://doi.org/10.1016/j.landusepol.2017.08.028>.
- Badri Ahmadi, Hadi, Simonov Kusi-Sarpong, and Jafar Rezaei (2017). “Assessing the social sustainability of supply chains using Best Worst Method”. en. In: *Resources, Conservation and Recycling* 126, pp. 99–106. ISSN: 0921-3449. DOI: 10.1016/j.resconrec.2017.07.020.
- Baltic Sea Hydrographic Commission (2013). *Baltic Sea Bathymetry Database Version 0.9.3*. URL: <http://data.bshc.pro/#2/52.8/20.4> (visited on 02/15/2020).
- Durski, Scott M., Scott M. Glenn, and Dale B. Haidvogel (2004). “Vertical mixing schemes in the coastal ocean: Comparison of the level 2.5 Mellor-Yamada scheme with an enhanced version of the K profile parameterization”. en. In: *Journal of Geophysical Research: Oceans* 109.C1. ISSN: 2156-2202. DOI: 10.1029/2002JC001702.
- Dybowski, Dawid and Lidia Dzierzbicka-Głowacka (2022). “Analysis of the Impact of Nutrients Deposited from the Land Side on the Waters of Puck Lagoon (Gdańsk Basin, Southern Baltic)”. In: *submitted to Journal of Hydrology*.
- Dybowski, Dawid, Lidia Anita Dzierzbicka-Głowacka, et al. (2020). “Estimation of nitrogen leaching load from agricultural fields in the Puck Commune with an interactive calculator”. en. In: *PeerJ* 8, e8899. ISSN: 2167-8359. DOI: 10.7717/peerj.8899.
- Dybowski, Dawid, Jaromir Jakacki, et al. (2019). “High-Resolution Ecosystem Model of the Puck Bay (Southern Baltic Sea)—Hydrodynamic Component Evaluation”. en. In: *Water* 11.10, p. 2057. ISSN: 2073-4441. DOI: 10.3390/w11102057.
- Dybowski, Dawid, Maciej Janecki, et al. (2020). “Assessing the Impact of Chemical Loads from Agriculture Holdings on the Puck Bay Environment with the High-Resolution Ecosystem Model of the Puck Bay, Southern Baltic Sea”. en. In: *Water* 12.7, p. 2068. DOI: 10.3390/w12072068.
- Dzierzbicka-Głowacka, Lidia, Jaromir Jakacki, et al. (2013). “Activation of the operational ecohydrodynamic model (3D CEMBS) – the hydrodynamic part *”. In: *Oceanologia* 55.3, pp. 519–541. ISSN: 0078-3234. DOI: 10.5697/oc.55-3.519.
- Dzierzbicka-Głowacka, Lidia, Maciej Janecki, et al. (2013). “Activation of the operational ecohydrodynamic model (3D CEMBS) – the ecosystem module*”. In: *Oceanologia* 55.3, pp. 543–572. ISSN: 0078-3234. DOI: 10.5697/oc.55-3.543.
- Dzierzbicka-Głowacka, Lidia et al. (2022). “Modelling the impact of the agricultural holdings and land-use structure on the quality of inland and coastal waters with an innovative and interdisciplinary toolkit”. en. In: *Agricultural Water Management* 263, p. 107438. ISSN: 0378-3774. DOI: 10.1016/j.agwat.2021.107438.
- Engström, Lena et al. (2011). “Reducing nitrate leaching after winter oilseed rape and peas in mild and cold winters”. en. In: *Agronomy Sust. Developm.* 31.2, pp. 337–347. ISSN: 1773-0155. DOI: 10.1051/agro/2010035.
- European Environment Agency, . (2018). *Agricultural land: nitrogen balance*. en. Briefing. URL: <https://www.eea.europa.eu/airs/2018/natural-capital/agricultural-land-nitrogen-balance> (visited on 10/31/2019).
- Galloway, James N. et al. (2008). “Transformation of the Nitrogen Cycle: Recent Trends, Questions, and Potential Solutions”. en. In: *Science* 320.5878, pp. 889–892. ISSN: 0036-8075, 1095-9203. DOI: 10.1126/science.1136674.
- Hägg, Hanna Eriksson et al. (2014). “Future Nutrient Load Scenarios for the Baltic Sea Due to Climate and Lifestyle Changes”. en. In: *AMBIO* 43.3, pp. 337–351. ISSN: 1654-7209. DOI: 10.1007/s13280-013-0416-4.
- Halpern, Benjamin S. et al. (2008). “A Global Map of Human Impact on Marine Ecosystems”. en. In: *Science* 319.5865, pp. 948–952. ISSN: 0036-8075, 1095-9203. DOI: 10.1126/science.1149345.
- Heisler, J. et al. (2008). “Eutrophication and harmful algal blooms: A scientific consensus”. In: *Harmful Algae* 8.1, pp. 3–13. ISSN: 1568-9883. DOI: <https://doi.org/10.1016/j.hal.2008.08.006>.
- Howarth, Robert W. (2008). “Coastal nitrogen pollution: A review of sources and trends globally and regionally”. In: *Harmful Algae* 8.1, pp. 14–20. ISSN: 1568-9883. DOI: <https://doi.org/10.1016/j.hal.2008.08.015>.

- Large, W. G., J. C. McWilliams, and S. C. Doney (1994). “Oceanic vertical mixing: A review and a model with a nonlocal boundary layer parameterization”. en. In: *Reviews of Geophysics* 32.4, pp. 363–403. ISSN: 1944-9208. DOI: 10.1029/94RG01872.
- Lotze, Heike K. et al. (2006). “Depletion, Degradation, and Recovery Potential of Estuaries and Coastal Seas”. en. In: *Science* 312.5781, pp. 1806–1809. ISSN: 0036-8075, 1095-9203. DOI: 10.1126/science.1128035.
- McDougall, Trevor J. et al. (2003). “Accurate and Computationally Efficient Algorithms for Potential Temperature and Density of Seawater”. In: *Journal of Atmospheric and Oceanic Technology* 20.5. Publisher: American Meteorological Society, pp. 730–741. ISSN: 0739-0572. (Visited on 03/15/2020).
- Moore, J. Keith et al. (2001). “An intermediate complexity marine ecosystem model for the global domain”. en. In: *Deep Sea Research Part II: Topical Studies in Oceanography*. The US JGOFS Synthesis and Modeling Project: Phase 1 49.1, pp. 403–462. ISSN: 0967-0645. DOI: 10.1016/S0967-0645(01)00108-4.
- Shahidul Islam, Md. and Masaru Tanaka (2004). “Impacts of pollution on coastal and marine ecosystems including coastal and marine fisheries and approach for management: a review and synthesis”. en. In: *Marine Pollution Bulletin* 48.7, pp. 624–649. ISSN: 0025-326X. DOI: 10.1016/j.marpolbul.2003.12.004.
- Stenberg, Maria et al. (1999). “Soil mineral nitrogen and nitrate leaching losses in soil tillage systems combined with a catch crop”. en. In: *Soil and Tillage Research* 50.2, pp. 115–125. ISSN: 0167-1987. DOI: 10.1016/S0167-1987(98)00197-4.
- Wesławski, J.M. et al. (2009). “Biological valorization of the southern Baltic Sea (Polish Exclusive Economic Zone)”. English. In: *Oceanologia* 51.3, pp. 415–435. ISSN: 0078-3234. DOI: 10.5697/oc.51-3.415.
- Worm, Boris et al. (2009). “Rebuilding Global Fisheries”. en. In: *Science* 325.5940, pp. 578–585. ISSN: 0036-8075, 1095-9203. DOI: 10.1126/science.1173146.

4 Series of publications constituting the PhD thesis

4.1 Research paper no. 1

Dybowski, D., Jakacki, J., Janecki, M., Nowicki, A., Rak, D., Dzierzbicka-Glowacka, L., 2019. *High-Resolution Ecosystem Model of the Puck Bay (Southern Baltic Sea)—Hydrodynamic Component Evaluation*. *Water* 11, 2057. <https://doi.org/10.3390/w11102057>

(IF¹ = 3.103; MEiN² = 70)

¹Journal Impact Factor (IF) according to the Journal Citation Reports

²Journal score according to the list of the Polish Ministry of Education and Science

Article

High-Resolution Ecosystem Model of the Puck Bay (Southern Baltic Sea)—Hydrodynamic Component Evaluation

Dawid Dybowski ^{1,*}, Jaromir Jakacki ², Maciej Janecki ¹, Artur Nowicki ¹, Daniel Rak ³ and Lidia Dzierzbicka-Glowacka ^{1,*}

¹ Physical Oceanography Department, Ecohydrodynamics Laboratory, Institute of Oceanology Polish Academy of Sciences, Powstańców Warszawy 55, 81-712 Sopot, Poland; mjanecki@iopan.pl (M.J.); anowicki@iopan.pl (A.N.)

² Physical Oceanography Department, Ocean and Atmosphere Numerical Modeling Laboratory, Institute of Oceanology Polish Academy of Sciences, Powstańców Warszawy 55, 81-712 Sopot, Poland; jjakacki@iopan.pl

³ Physical Oceanography Department, Observational Oceanography Laboratory, Institute of Oceanology Polish Academy of Sciences, Powstańców Warszawy 55, 81-712 Sopot, Poland; rak@iopan.pl

* Correspondence: ddybowski@iopan.pl (D.D.); dzierzb@iopan.pl (L.D.-G.); Tel.: +48-587-311-912 (D.D.); +48-587-311-915 (L.D.-G.)

Received: 21 August 2019; Accepted: 26 September 2019; Published: 1 October 2019



Abstract: In recent years, thanks to the enormous computational power of modern supercomputers, modeling has become one of the most highly evolving scientific fields. It is now possible to describe relatively large physical bodies and to study the changes occurring in these bodies with resolution never attainable before. The paper describes the initial implementation of the EcoPuckBay model system and presents the results of the model simulations compared to observations from monitoring stations and other model reanalyses. High correlation between model results and observations has been confirmed both in terms of spatial and temporal approach. Data acquired via simulations of the EcoPuckBay model was deployed in the project archive database. The dedicated service was created, allowing the user to visualize all produced hydrodynamic parameters as raster maps, time series, and/or cross-sections. This functionality is available online via the official WaterPUCK project website in the services web section. In the next stage of the project, this service will be upgraded to an operational state and forecasts will be added.

Keywords: WaterPUCK; Puck Bay; 3D model; hydrodynamic variables

1. Introduction

The Puck Bay is part of the Gdańsk Basin (southern Baltic Sea). It is separated from deep-water areas by the Hel Peninsula. Puck Bay consists of the inner part called Puck Lagoon and the outer part of Puck Bay. The boundary between them runs from the Rybitwia Sandbank to the Cypel Rewski and has two straits within which there is an intensive water exchange between the Puck Lagoon and the outer part of the Puck Bay. The commonly accepted eastern border of the Puck Bay is the line connecting the Hel Peninsula with Kamienna Góra [1].

The Puck Bay is an example of a region that is highly vulnerable to anthropogenic impact. Therefore, it has been included into Natura 2000. As a result, it requires preservation or restoration of “favorable conservation status” of species and habitats by introducing appropriate “protection measures”. The strategic actions and the policy of the authority of the Puck District regarding the environmental protection involve not only the respect of the Natura 2000 legislation but also realization

of European legislation including Water Framework Directive, Marine Strategy Framework Directive, Habitats Directive, Baltic Sea Action Plan and the strategic program of the environment protection for the Puck District. The main aims of the Puck District policy are improvement of the environment, sustainable development, protection from climate change, and protection of the natural resources such as water.

There are several models describing processes occurring in marine environment in use such as: HIROMB (High-Resolution Operational Model for the Baltic Sea), RCO (Rossby Centre Ocean Model), NEMO (Nucleus for European Modeling of the Ocean) and biogeochemical model SCOBI (Swedish Coastal and Ocean Biogeochemical model),HIRLAM (High-Resolution Limited Area Model) or ecosystem model of the Baltic Sea BALTSEM. At the end of 2015, the SatBałtyk System has been initiated in the IO PAN (Institute of Oceanology of the Polish Academy of Sciences). It enables efficient and systematic monitoring of the Baltic Sea Environment state based on innovative satellite techniques backed up with mathematical models of processes occurring in the sea. As part of the grant and continued work a three-dimensional model of the ecosystem 3D CEMBS (3D Coupled Ecosystem Model of the Baltic Sea) was improved and expanded. 3D CEMBS model (<http://www.cembs.pl>) generates 48-h forecast which include currents, temperature, salinity and ice parameters. In addition, the model forecasts ecological parameters i.e., nutrients, dissolved oxygen concentration and biomass of phytoplankton and zooplankton in the entire water column.

The EcoPuckBay model is being developed as part of the WaterPUCK project. The aim of the project is to create an integrated information and predictive service for the Puck District through the development of a computer system providing WaterPUCK service, which will clearly and practically assess the impact of farms and land-use structures on surface waters and groundwater in the Puck District, and consequently on the quality of the waters of the Puck Bay [2,3]. The construction of the service is based on in situ research, environmental data (chemical, physicochemical and hydrological) and numerical modeling. WaterPUCK service is an integrated system consisting of computer models interconnected with each other, operating continuously by supplying it with meteorological data and consists of 4 main modules:

- a comprehensive model of surface water runoff based on SWAT code,
- a numerical model of groundwater flow based on MODFLOW code,
- a three-dimensional numerical model of the Puck Bay ecosystem,
- a calculator of farms in Puck District as an interactive application [4].

2. Materials and Methods

The development of high-resolution numerical models that are able to simulate both physical and biogeochemical processes driving the state of the marine environment is time-consuming and requires broad knowledge of multiple events that occur in the modeled ecosystem. That requires access to information of direct and indirect forcing factors such as border fluxes, deposition from land and inputs that influence the dynamic of changes within the model domain. In order to match the complexity of this task and increase the efficiency of the development process, an existing state-of-the-art Community Earth System Model had been redesigned and adapted to the research area, allowing us to deliver an excellent tool for the purpose of either reanalysis or forecasting. We named it EcoPuckBay which corresponds to ecohydrodynamic model of the Puck Bay.

Here we describe an end-development (version 1.0) hydrodynamic configuration of the EcoPuckBay model. Biogeochemical configuration setup and results will be presented in the nearest future as a separate paper.

2.1. Study Area

The southern part of the Baltic Sea enclosing the Puck District is a tourist popular region that is also heavily influenced by an anthropogenic activity of local residents and farming. This makes the

Puck Bay a natural reservoir for waste deposition of fertilizers and other inputs delivered through soil, groundwater, river or direct deposition. In order to assess the possibility and scale of an eutrophication and water pollution the area of interest and effective domain in the EcoPuckBay model covers the western part of Gulf of Gdańsk (Figure 1). It can be divided further into a shallow part known as Puck Bay and the semi-enclosed Puck Lagoon to the west.

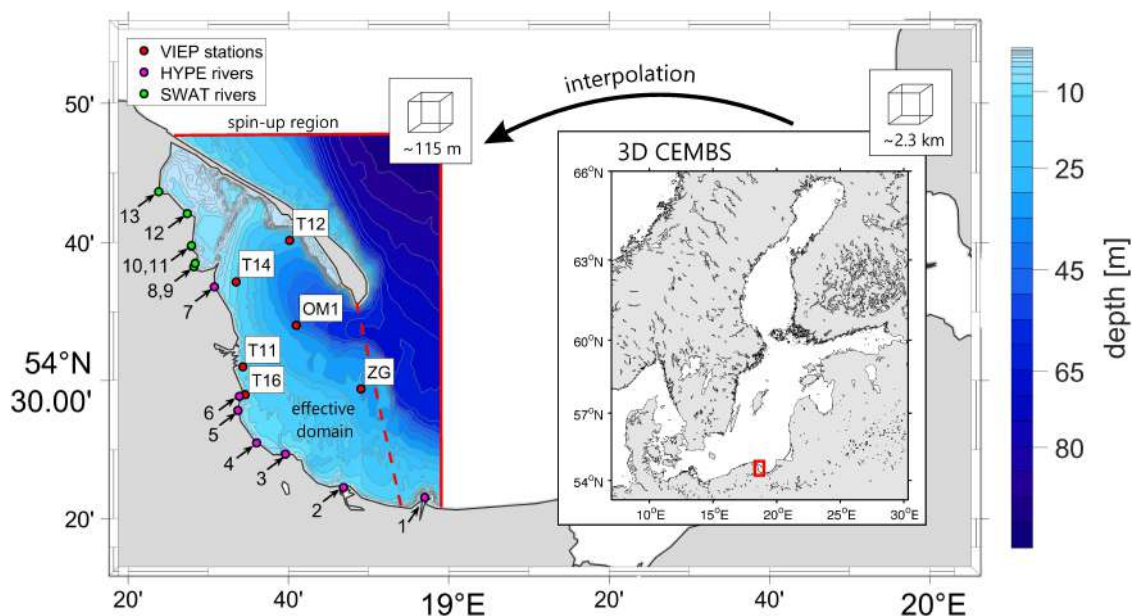


Figure 1. Model effective domain with topography, locations of sampling stations used for evaluation, and locations of mouths of watercourses included in domain. Green dots represent rivers that in the final product will be delivered using SWAT hydrological model.

This region is massively shaped and influenced by a several factors that can pressure the state of physical and biochemical parameters. One of the most important factor influencing region's unique ecosystem is topography. The average depth of the gulf is about 50 m, with the maximum depth (Gdańsk Deep) of 118 m. From the north-east it is surrounded by Hel Peninsula which serves as a natural barrier for mixing with the open waters of the Baltic Sea keeping the salinity ranging mostly within the range of 7–8 PSU with a deviation of around 1 PSU. Puck Bay is also heavily influenced by the river discharge from land resulting in lowered salinity especially in the coastal surface waters. The largest river in the region is Vistula, discharging an average of over $1000 \text{ m}^3 \text{ s}^{-1}$ of fresh water. Water temperature in the region ranges from over $20 \text{ }^\circ\text{C}$ at the surface during summer, with the maximum usually in August, to around $2 \text{ }^\circ\text{C}$ in February. Water stratification is frequent during the warmer months, leading to the occurrence of seasonal thermocline. During the winter seasons thermocline declines and water become well-mixed.

2.2. EcoPuckBay Configuration

EcoPuckBay origins from Community Earth System Model (CESM) coupled global climate model (<http://www.cesm.ucar.edu/models/ccsm4.0>) by NCAR. CESM is a state-of-the-are model system consisting of five separate components with an additional coupler controlling time, exciting forces, domains, grids and information exchange between the models. For the purpose of the WaterPUCK project, CESM was downscaled and adapted for the Puck Bay region for further development at the Institute of Oceanology, Polish Academy of Sciences.

EcoPuckBay's horizontal resolution is $1/960^\circ$ which amounts to a nominal resolution of 115 m. The vertical resolution is 0.4–0.6 m in the upper layers down to 3 m, and then gradually increases to 5 m at depth, with a total of 24 layers (Table 1). The vertical discretization uses the z formulation and the bottom topography is based on Baltic Sea Bathymetric Database (BSBD) from the Baltic Sea

Hydrographic Commission [5]. The bathymetric data were interpolated into the model grid using Kriging method. The ocean model time step is 12 s.

Table 1. EcoPuckBay’s vertical resolution.

Model Level	Thickness (m)	Lower Depth (m)	Mid-Depth (m)
1	0.60	0.60	0.30
2	0.40	1.00	0.80
3	0.40	1.40	1.20
4	0.40	1.80	1.60
5	0.40	2.20	2.00
6	0.50	2.70	2.45
7	0.60	3.30	3.00
8	0.80	4.10	3.70
9	1.00	5.10	4.60
10	1.40	6.50	5.80
11	1.80	8.30	7.40
12	2.50	10.80	9.55
13	4.00	14.80	12.80
14	5.00	19.80	17.30
15	5.00	24.80	22.30
16	5.00	29.80	27.30
17	5.00	34.80	32.30
18	5.00	39.80	37.30
19	5.00	44.80	42.30
20	5.00	49.80	47.30
21	5.00	54.80	52.30
22	5.00	59.80	57.30
23	5.00	64.80	62.30
24	5.00	69.80	67.30

The ocean component in EcoPuckBay is based on POP using three-dimensional equations of motion with hydrostatic and Boussinesq approximations. Main ocean equations in the spherical system are presented below.

Equations of horizontal motion:

$$\frac{\partial u}{\partial t} + L(u) - fv = -\frac{1}{\rho_0 a \cos \phi} \frac{\partial p}{\partial \lambda} + \frac{\partial}{\partial z} \left(K_M \frac{\partial u}{\partial z} \right) + B_M \nabla_H^4 u, \tag{1}$$

$$\frac{\partial v}{\partial t} + L(v) - fu = -\frac{1}{\rho_0 a} \frac{\partial p}{\partial \phi} + \frac{\partial}{\partial z} \left(K_M \frac{\partial v}{\partial z} \right) + B_M \nabla_H^4 v. \tag{2}$$

The momentum equation along the vertical direction within the hydrostatic approximation:

$$\frac{\partial p}{\partial z} = -\rho g. \tag{3}$$

Continuity equation:

$$\frac{1}{a \cos \phi} \frac{\partial u}{\partial \lambda} + \frac{1}{a \cos \phi} \frac{\partial (v \cos \phi)}{\partial \phi} + \frac{\partial w}{\partial z} = 0 \tag{4}$$

The equation of heat and salt transport:

$$\frac{\partial T}{\partial t} + L(T) = \frac{\partial}{\partial z} \left(K_D \frac{\partial T}{\partial z} \right) + B_D \nabla_H^4 T, \tag{5}$$

$$\frac{\partial S}{\partial t} + L(S) = \frac{\partial}{\partial z} \left(K_D \frac{\partial S}{\partial z} \right) + B_D \nabla_H^4 S, \tag{6}$$

The equation of state:

$$\rho = \rho(S, T, p). \quad (7)$$

where: u, v horizontal components of velocity, w vertical component of velocity, g gravitational acceleration, p pressure, T, S temperature and salinity, ρ_0 average water density, λ, ϕ latitude and longitude, a effective Earth radius, t time, $f = 2\Omega \sin \phi$ the Coriolis parameter (Ω the rotation rate of the Earth), L advection operator, ∇_H^4 horizontal biharmonic operator, K_M biharmonic vertical eddy viscosity, B_D biharmonic horizontal eddy viscosity. Horizontal coefficients B_D, B_M are assumed as constants. Vertical mixing in EcoPuckBay is determined by k-profile parameterization (KPP) [6] determining the vertical coefficients K_D, K_M . In the current setup, an enhancement of the KPP Scheme with Bottom Boundary Layer introduced by Durski [7] has been applied:

$$C_d = \kappa^2 \left(\ln \frac{dz}{z_r} \right)^{-2}, \quad (8)$$

where C_d is drag coefficient κ is von Karman's constant, dz is the distance from the bottom to grid point, z_r is a roughness height specified as 0.5 cm (value tuned up based on the water flow through The Sund in 3D CEMBS model). Parametrization of the MWJF state equation, developed by McDougall et al. [8], was applied in the model. The EcoPuckBay chosen parametrization is very similar to the 3D CEMBS model. The model uses preconditioned conjugate gradient solver (PCG) in the barotropic part. Our configuration uses Lax–Wendroff with 1-D flux limiters advection scheme. We also introduced biharmonic (bilaplacian operator) horizontal friction (momentum) as well as biharmonic horizontal mixing for tracers. POP is a model with free surface, and vertical velocity on the surface amounts to:

$$w = \frac{\partial \eta}{\partial z}, \quad z = 0, \quad (9)$$

where: η free surface elevation. Stress at the bottom τ_b is expressed as:

$$\frac{\tau_b}{\rho} = \frac{C_d \vec{U} |\vec{U}|}{d^2}, \quad (10)$$

where: d thickness of the benthic layer, C_d drag coefficient, \vec{U} water velocity vector at the bottom. Ocean in EcoPuckBay is coupled to the sea-ice model based on Community Ice Code (CICE). The main equation solved by CICE is:

$$\frac{\partial k}{\partial t} = -\nabla \cdot (k\mathbf{U}) - \frac{\partial}{\partial h}(ck) + \psi, \quad (11)$$

where: \mathbf{U} is horizontal ice velocity, c the ice growth rate, ψ ridging redistribution, k distribution of ice thickness.

2.3. Open Boundary

EcoPuckBay model results discussed in this paper are limited to an effective area of Puck District surroundings. Whole grid of the model however, covers wider domain reaching to Gdańsk Deep latitudes. This is made to ensure that boundary conditions are simulated properly. Along the line of the EcoPuckBay's northern border an information exchange with 2.3 km prognostic model 3D CEMBS takes place (see Figure 1). Results from 3D CEMBS serve as forcing fields to EcoPuckBay through a sequential information exchange. The algorithm performing the connection ensures mass and energy conservation. Currently exists two approaches that can include tides in the ocean model. First is adding tidal potential in the barotropic equation. The second provides tides in the lateral boundaries (it can be done as a surface variation or Flather lateral boundaries). The first approach does not work properly for small seas. The main reason is that the water mass is small, thus the result of such implementation provide proper period and phase of the tidal constituents, but the amplitude

is usually too low. The second approach is indirectly included in the EcoPuckBay model because lateral boundaries are included in the coarse resolution model in an open boundary area via sea level provided by Goteborg station. Thus, although there is a tacit assumption that the Baltic Sea has no tides, they are being broadcasted via lateral boundaries.

2.4. Atmosphere Forcing

EcoPuckBay model is forced by 48-h meteorological forecasts from the UM model delivered by the Interdisciplinary Centre for Mathematical and Computational Modeling of Warsaw University (ICM UW). Following external fields are used:

- 2 m air temperature and specific humidity,
- sea level pressure,
- precipitation,
- short and long wave radiation,
- 10 m wind speed,
- air density.

2.5. River Discharge

At this stage of the development the volume data of river discharge come from the Hydrological Predictions for the Environment (HYPE) model. It is a semi-distributed, physically based catchment model, which simulates water flow and substances on their way from precipitation through different storage compartments and fluxes to the sea [9–11]. We used historical time series from the period 1980–2010 for the Europe geographical domain available as a daily means. The spatial resolution is given by landscape delineation into catchments, for which HYPE data represents average conditions or the outlets. Six HYPE catchments have been taken into account to resolve 13 discharge locations (rivers, canals and streams) of watercourses with their estuaries running alongside the EcoPuckBay model domain (Table 2). Volumes for the years past 2010 have been calculated as a long-term means from the available 30-year period.

Table 2. Locations of mouths of watercourses included in the EcoPuckBay model domain.

	Watercourse	Longitude	Latitude
1	Vistula	18.95	54.35
2	Bold Vistula	18.78	54.37
3	Still Vistula	18.66	54.41
4	Oliwski Stream	18.60	54.42
5	Kamienny Stream	18.56	54.46
6	Kacza	18.56	54.48
7	Ściekowy Canal	18.51	54.61
8	Zagórska Stream	18.47	54.63
9	Reda	18.47	54.64
10	Mrzezino Canal	18.46	54.66
11	Gizdepka	18.46	54.66
12	Żelistrzewo Canal	18.45	54.70
13	Płutnica	18.39	54.72

At the final stage of the development, the HYPE information about the water volume discharged by rivers with their mouths located within the Puck District (Figure 1, numbers from 8 to 13) will be replaced by the hydrological model SWAT that is being implemented as one of the WaterPUCK project's stages [12–16]. SWAT model includes the preparation of innovative and complex hydrological model including meteorological data (precipitation, wind, temperature, atmospheric pressure). The proposed solution is based upon real time observation (local weather station) and on short-term weather forecasts (the ICM UW web page). The hydrological computations will be performed with SWAT software.

The transformation of precipitation data into surface runoff will be achieved with the SCS (Soil Conservation Service) Curve Number procedure through the accumulated runoff volume and the time of concentration (the time from the beginning of a rainfall event until the entire sub-basin area is contributing to flow at the outlet).

2.6. Simulation Run

To calculate hydrodynamic conditions of the Puck Bay area a simulation run has been performed for the time period January 2011 to December 2018. Since we had no access to reliable long-term and spatially representative in situ database preceding year 2014 that could be used to make a comparison with model results, we treat the starting three years as a spin-up stage, even though it would be enough to use a simulation with a spin-up period of one year or less on a homogeneous domain of this size and resolution.

There is no data assimilation module in the current development version of the model yet; however, it will be introduced in the next stages of the project's workflow.

2.7. Datasets Used for Evaluation

We used several sources of in situ samples to evaluate EcoPuckBay model. That includes measurements taken throughout the monitoring activities of the Voivodship Inspector of Environmental Protection in Gdańsk and vertical profiles of temperature and salinity recorded in 2018 during one of the measurement campaigns of the s/y Oceania along the Southern Baltic coast. In addition, the numerical data of physical parameters calculated with the circulation model system NEMO-Nordic that comes from the Marine Copernicus database was processed too. A brief summary description of each of the databases used in this paper for the evaluation purpose has been presented below.

2.7.1. VIEP

The biggest set of the in situ data used for the EcoPuckBay model evaluation performed in this paper are samples collected during regular measurements of the marine environment of the Baltic Sea conducted by Voivodship Inspectorate of Environmental Protection (VIEP) in Gdańsk. We used data from 6 stations located within the model domain (Figure 1) taken between January 2014 and December 2016. VIEP's scope, methods of monitoring and the manner of assessing the status of the Baltic Sea has been defined by the provisions of the Water Law Act and the monitoring program of marine waters adopted by the Council of Ministers, which implements the requirements of Article 11 of Directive of the European Parliament and of the Council 2008/56/EC of 17 June 2008, establishing a framework for community action in the field of marine environmental policy. Monitoring service performed by VIEP constitute the fulfilment of Poland's obligations arising from the Convention on the protection of the marine environment of the Baltic Sea area, and since 15 July 2014, of Article 11 of Directive 2008/56/EC of the European Parliament and establishing a framework for community action in the field of marine environmental policy.

2.7.2. s/y Oceania

Hydrodynamical data samples analyzed in this paper were collected during the summer 2018 regular cruise of s/y Oceania on the Puck Bay. (data not yet published). Vertical sections for 18 stations (Figure 2) were performed using a Seabird 49 Conductivity Temperature Depth (CTD) probe.

CTD sensor's accuracy was $0.0003 \text{ mS cm}^{-1}$ for Conductivity, $0.002 \text{ }^{\circ}\text{C}$ for Temperature and 0.1% for the pressure. Temperature and conductivity sensors of CTD system were calibrated annually, post-cruise, by the manufacturers. The vertical sampling was higher than model resolution (from 10–40 readings per model level, depending on its depth), therefore ship readings were averaged to match EcoPuckBay resolution.

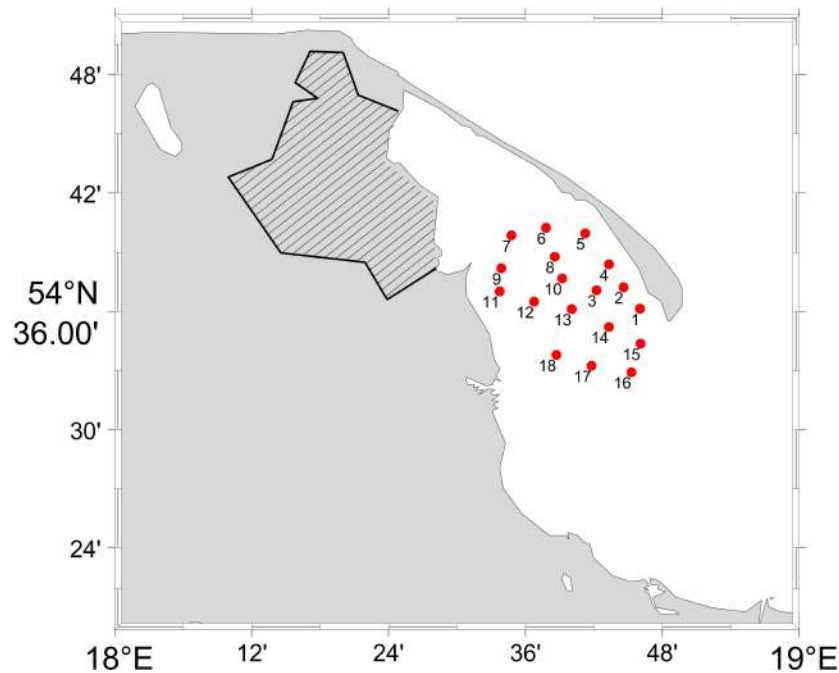


Figure 2. Location of stations for vertical profiles collected from s/y Oceania.

2.7.3. NEMO-Nordic

The source of the numerical results used in the manuscript is the data downloaded from Marine Copernicus (<http://marine.copernicus.eu>) database. This product origin from a Baltic Sea physical reanalysis for the period January 1993 to December 2016 at 3.9 km horizontal resolution and had been produced using the ice-ocean model NEMO-Nordic. Temperature, salinity for surface and bottom layer and currents data were delivered as daily means.

The circulation model NEMO-Nordic is based on NEMO-3.6 model version. It has been the operational ocean and sea-ice forecasting model used at SMHI (the Swedish Meteorological and Hydrological Institute) since 2016 [17,18]. NEMO-Nordic domain covers whole Baltic Sea extended to the North Sea area.

3. Results

3.1. Model Evaluation

To evaluate the quality of the results obtained from the EcoPuckBay model for the period of January 2014 to December 2018, a set of basic statistical measures were calculated, such as Pearson correlation coefficient (r), root-mean-square-error (RMSE), standard deviation (STD) and bias (in terms of means).

The results of comparisons are presented in Sections 3.1.1 and 3.1.2 in graphical and tabular form. The obtained statistical parameters allowed verification of the model in terms of seasonal and spatial variability of simulated water temperature and salinity, which are the most essential physical parameters when describing the state of the marine environment.

3.1.1. Temperature

The quality of the temperature is assessed by comparing the modeled temperature with all available observations from VIEP and s/y Oceania stations. Statistical comparison is presented in form of Taylor diagrams [19] in Figure 3. To present result from time series and vertical profiles on one diagram all the statistics were normalized with standard deviation of reference measurement. Non-normalized values are presented in Table 3. In Figure 4 we present the average vertical water temperature profiles for all stations (Figure 4a) and for one selected station (Figure 4b).

Table 3. Statistical comparison between modeled temperature and reference data from in situ measurements (VIEP and s/y Oceania) and numerical data (NEMO-Nordic).

Reference Data	Pearson's r	RMSE ($^{\circ}\text{C}$)	STD ($^{\circ}\text{C}$)	Bias ($^{\circ}\text{C}$)
Time series (VIEP)	0.97	1.45	5.67	−0.83
Time series (NEMO-Nordic)	0.98	1.33	6.01	−0.31
Vertical profiles (s/y Oceania)	0.92	2.85	5.29	−1.16

Time series for separate VIEP stations can be found in the Appendix A (Figures A1–A6) as well as vertical profiles for separate s/y Oceania stations (Figure A7). The statistics calculated for each station has been summarized in Tables 4 and 5, for VIEP and s/y Oceania stations respectively.

The Pearson correlation coefficient r for all measured values is equal to 0.97 for VIEP stations and 0.92 for s/y Oceania stations. The RMSE from all VIEP stations is equal to 1.45 $^{\circ}\text{C}$ and 2.85 $^{\circ}\text{C}$ from all s/y Oceania stations.

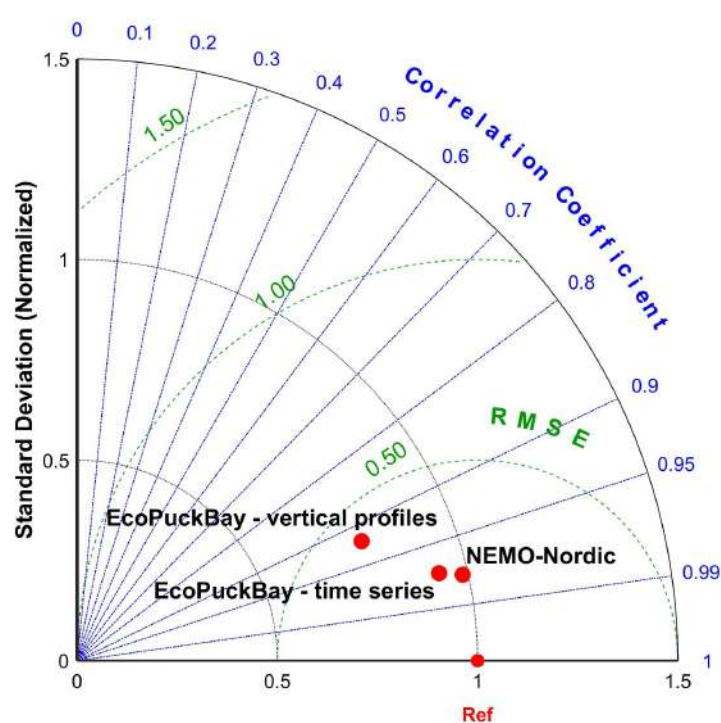


Figure 3. Taylor diagram for temperature.

The Pearson correlation coefficient calculated for the VIEP time series has the minimum value of 0.94 and the maximum value of 0.99. Such results indicate a very good representation of the variability characteristics of the modeled data with the measurement data. RMSE for T11, T14, T16 and OM1 stations does not exceed 1.5 $^{\circ}\text{C}$, while on the other two stations it is around 2 $^{\circ}\text{C}$. A negative bias value indicates that the modeled data for the considered stations have a lower value than the measurement data.

Analyzing the vertical temperature profiles from s/y Oceania, a high correlation between the EcoPuckBay model and the in situ measurements can be observed. At all measurement stations the Pearson correlation coefficient between modeled data and measured values is higher than 0.7. For stations from 12 to 17 the correlation exceeds 0.98, which indicates a perfect correspondence between the profiles and the correct implementation of the vertical mixing in the EcoPuckBay model. The lowest correlations occurred at stations 7, 9, 11 and, as you can see in Figure 2, these are the stations most far to the west, i.e., those on the shallow water and additionally strongly influenced by external forces, e.g., rivers.

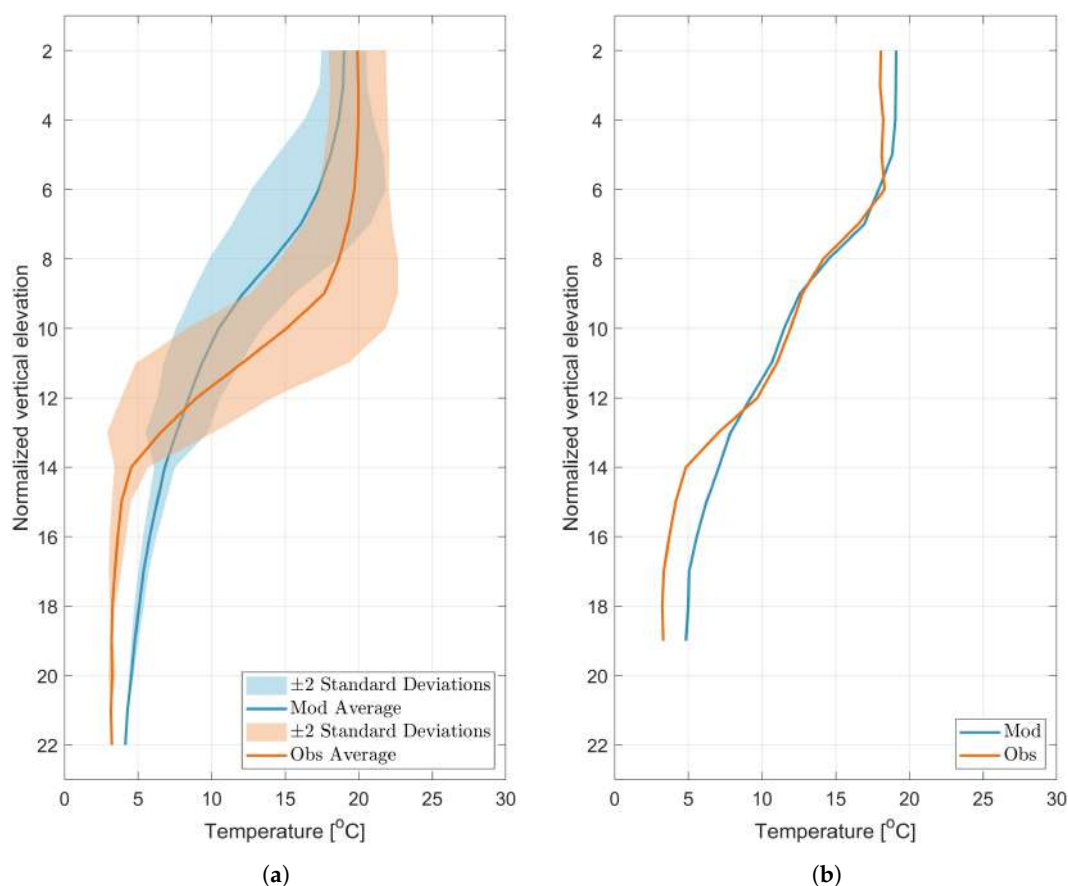


Figure 4. Temperature vertical profiles (a) from all stations (b) at station 13.

Table 4. Statistical comparison between model results and in situ measured water temperature at the surface level (VIEP).

Station	Pearson's r	RMSE (°C)	STD (°C)	Bias (°C)
T11	0.99	1.24	5.48	−0.99
T12	0.94	2.08	5.37	−1.12
T14	0.98	1.41	5.45	−1.24
OM1	0.98	1.16	5.30	−1.32
T16	0.99	1.17	5.47	−0.66
ZG	0.95	1.98	4.87	−1.71

The STD at respective stations varies from the minimum value of 4.05 °C at station 2 to 5.64 °C at station 16. This is the expected result, especially for the day when the cruise took place because at virtually every station you can see a scratching thermocline which is the result of a weak mixing in this period and the formation of stagnant layers of water near the surface with a high temperature reaching from 18 to even more than 20 °C (depending on the profile station) which at the bottom drops to about 10 °C in places where there is a shallow to less than 5 °C for the deepest points in which the ship measured the profile. High STD reproduces this large variation from the surface to the bottom.

A negative bias on 15 of 18 profiles indicates that in the transition section of the thermocline, the model tends to lower the results, but at the bottom it reaches values close to those measured.

Generally, the model reproduces well the temperature in the water column, as demonstrated by high correlations and low RMSE which is formed at a level of about 3 °C.

Table 5. Statistical comparison between model results and in situ measured water temperature in vertical profiles (s/y Oceania).

Station	Pearson's r	RMSE (°C)	STD (°C)	Bias (°C)
1	0.95	3.44	4.68	−0.77
2	0.84	4.23	4.05	−1.96
3	0.95	2.87	5.18	−1.24
4	0.92	3.58	4.30	−1.27
5	0.95	2.31	4.59	−0.45
6	0.91	2.86	4.88	−1.67
7	0.72	3.71	5.03	−3.19
8	0.93	2.70	5.61	−0.71
9	0.77	2.74	4.18	−3.19
10	0.95	2.79	5.61	−0.71
11	0.77	2.66	4.13	−3.88
12	0.99	1.06	5.23	0.24
13	0.99	0.90	5.46	0.81
14	0.98	1.66	5.41	−0.04
15	0.98	2.15	5.21	−0.34
16	0.98	1.60	5.64	−0.38
17	0.98	1.41	5.47	0.22
18	0.93	2.82	5.16	−1.75

3.1.2. Salinity

The quality of the salinity is assessed by comparing the modeled salinity with all available observations from VIEP and s/y Oceania stations. Statistical comparison is presented in form of Taylor diagrams in Figure 5. To present result from time series and vertical profiles on one diagram all the statistics were normalized with standard deviation of reference measurement. Non-normalized values are presented in Table 6. In the Figure 6 we present vertical water temperature profiles for all stations (Figure 6a) and for one selected station (Figure 6b).

Table 6. Statistical comparison between modeled salinity and reference data from in situ measurements (VIEP and s/y Oceania) and numerical data (NEMO-Nordic).

Reference Data	Pearson's r	RMSE [PSU]	STD [PSU]	Bias [PSU]
time series (VIEP)	0.58	0.67	0.60	0.16
time series (NEMO-Nordic)	0.17	0.97	0.70	−0.24
vertical profiles (s/y Oceania)	0.90	0.40	0.84	−0.03

Time series for separate VIEP stations can be found in the Appendix A (Figures A10–A15) as well as vertical profiles for separate s/y Oceania stations (Figure A16). The statistics calculated for each station has been summarized in Tables 7 and 8, for VIEP and s/y Oceania stations respectively.

The correlation coefficient r for all measured values is equal to 0.58 for VIEP stations and 0.90 for s/y Oceania stations. Therefore, it varies from 0.28 to 0.86 for VIEP and from 0.78 to 1.00 for s/y Oceania stations.

Pearson's correlation coefficients for time series from the VIEP salinity measurements ranges from 0.28 to 0.86. Station T11, for which the correlation coefficient reaches the lowest value, is located close to the Port of Gdynia, which may be the cause of such a result. RMSE does not exceed 1 PSU for all stations and is less than 0.5 PSU for half of them. The STD changes from 0.34 to 0.81 PSU depending on the station. The lowest time variability is observed in the T12 and T14 stations that are located nearest to Puck Lagoon. The bias is less than 0.3 PSU and always positive, i.e., the salinity calculated by the model is slightly higher than the salinity measured by the VIEP. This situation can be improved by attaching SWAT model data to the EcoPuckBay model.

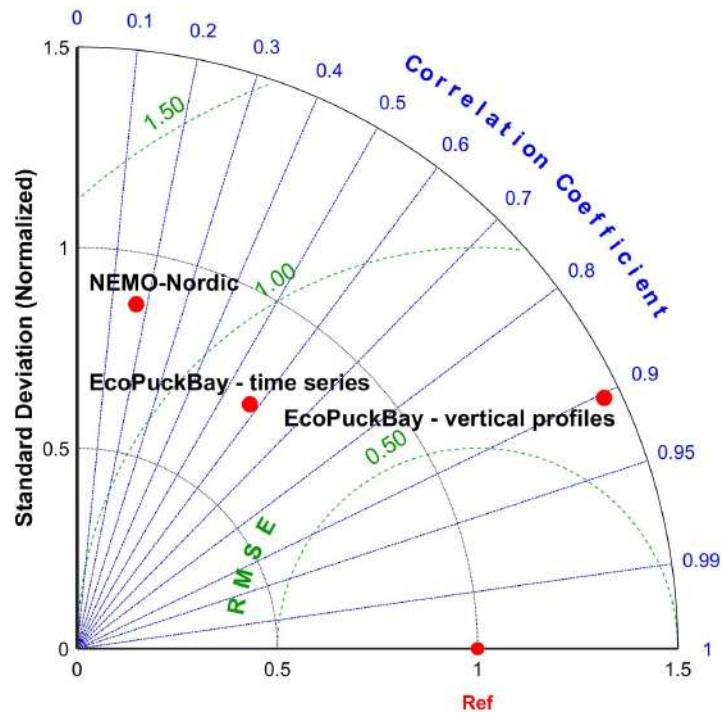


Figure 5. Taylor diagram for salinity.

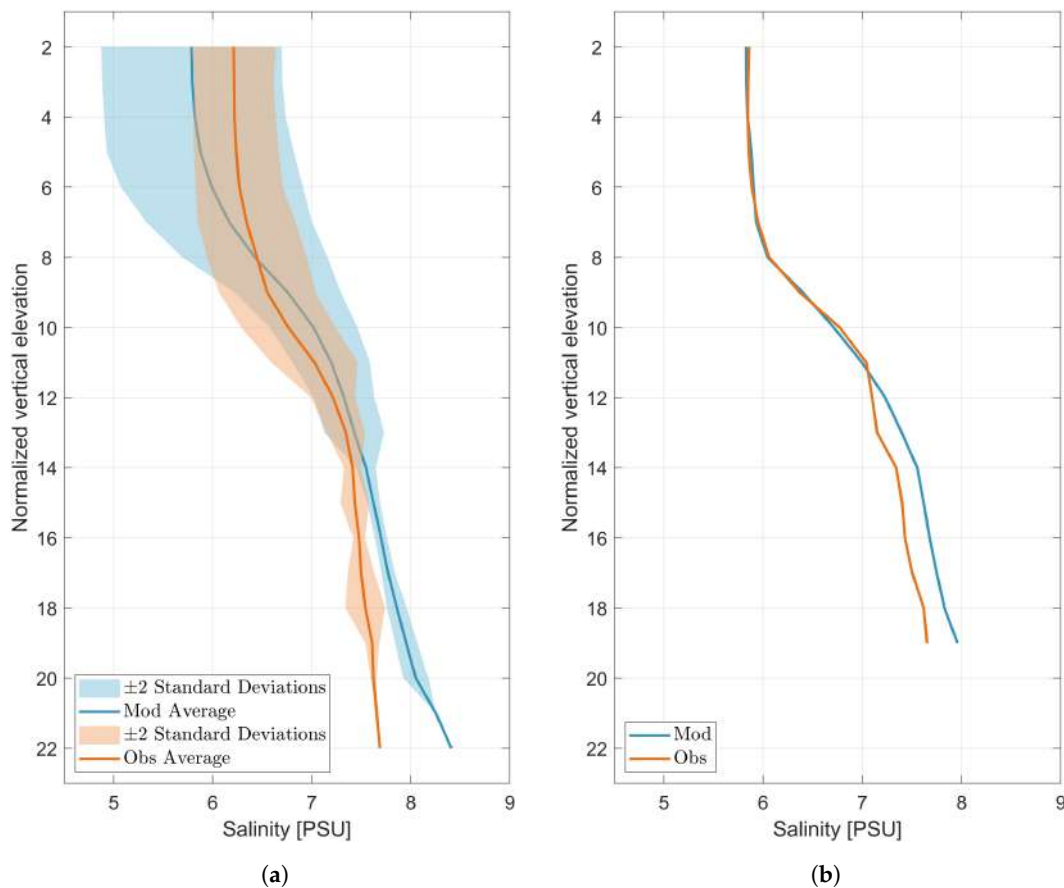


Figure 6. Salinity vertical profiles (a) from all stations (b) at station 16.

Comparing the vertical salinity profiles from the modeled data with the profiles from s/y Oceania measurements, we observe Pearson’s correlation coefficients from 0.78 to 1.00. As with the temperature,

lower correlation coefficients occur at stations 7, 9, 11, which are located near the Rybitwia Sandbank which separates Puck Lagoon from the outer part of the Puck Bay. RMSE does not exceed 0.5 PSU except for the three mentioned stations and station 13.

Table 7. Statistical comparison between model results and in situ measured water salinity at the surface level (VIEP).

Station	Pearson's r	RMSE [PSU]	STD [PSU]	Bias [PSU]
T11	0.28	0.99	0.54	0.21
T12	0.53	0.43	0.37	0.12
T14	0.64	0.35	0.34	0.19
OM1	0.86	0.32	0.51	0.27
T16	0.51	0.81	0.61	0.04
ZG	0.62	0.78	0.81	0.14

3.2. Simulation Results

Below we present spatial distributions of selected physical parameters in the Puck Bay region simulated by the EcoPuckBay model. To avoid exceeding paper size, we limited this section only to the monthly averages of water temperature, salinity, sea level and currents from the 5-year period of 2014–2018. Figures and Tables for the separate years were moved to the Appendix A (Figures A8–A9, A17–A22 and Tables A1–A15).

Table 8. Statistical comparison between model results and in situ measured water salinity in vertical profiles (s/y Oceania).

Station	Pearson's r	RMSE [PSU]	STD [PSU]	Bias [PSU]
1	0.97	0.14	0.58	0.21
2	0.91	0.20	0.47	0.24
3	0.99	0.17	0.72	0.10
4	0.96	0.14	0.49	0.18
5	0.98	0.19	0.53	0.01
6	0.92	0.28	0.58	0.04
7	0.78	0.48	0.72	0.06
8	0.95	0.32	0.77	0.00
9	0.80	0.69	0.92	−0.41
10	0.96	0.31	0.82	0.00
11	0.88	0.64	0.92	−0.36
12	0.96	0.49	0.93	−0.42
13	0.98	0.60	0.99	−0.37
14	0.99	0.32	0.79	−0.01
15	0.98	0.21	0.76	0.19
16	1.00	0.12	0.81	0.10
17	0.98	0.28	0.86	−0.10
18	0.95	0.39	0.95	−0.09

3.2.1. Temperature

The average surface temperature inside domain was 10.3 °C. The lowest monthly mean temperature for specified model cell was in January 2016 with a value of −0.28 °C and the highest in July 2014 with a maximum exceeding 24 °C both inside Puck Lagoon (Figures A8–A9 and Table A1). The standard deviation from the average for whole period from 2014 to 2018 is nearly 6 °C, which indicates high seasonal variability of temperature in the Puck Bay presented in Figure 7 (based on Tables A1–A4).

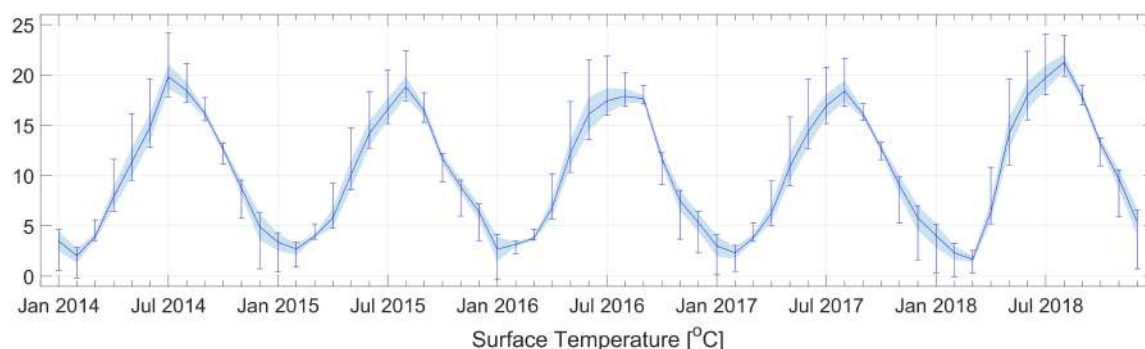


Figure 7. Monthly means of temperature at sea surface level for whole domain. Error bars represent minimum and maximum values. Solid line connects monthly means and shadow area shows standard deviation from the mean values.

Figure 8 shows the average surface temperature for the individual months of the 2014–2018 period. Puck Lagoon is characterized by the highest dynamics of temperature variability due to its geomorphological separation from the rest of the Puck Bay. In summer, the water in Puck Lagoon warms up to higher temperatures, while in winter it reaches lower temperatures than the rest of the Puck Bay (Figures A8 and A9). The highest average monthly water temperature in the surface layer for the whole domain was higher than 21 °C in August 2018. Moreover, from May to August 2018 the average monthly surface temperature for the whole domain was over 1.5 °C higher than the 5-year average for the whole domain (for the years 2014–2018) and for May, June and August, more than 2.2 °C from that average (Table A1). Additionally, in March 2018, monthly average surface temperature was the lowest for the entire modeled period and deviated from the average by nearly 1.8 °C.

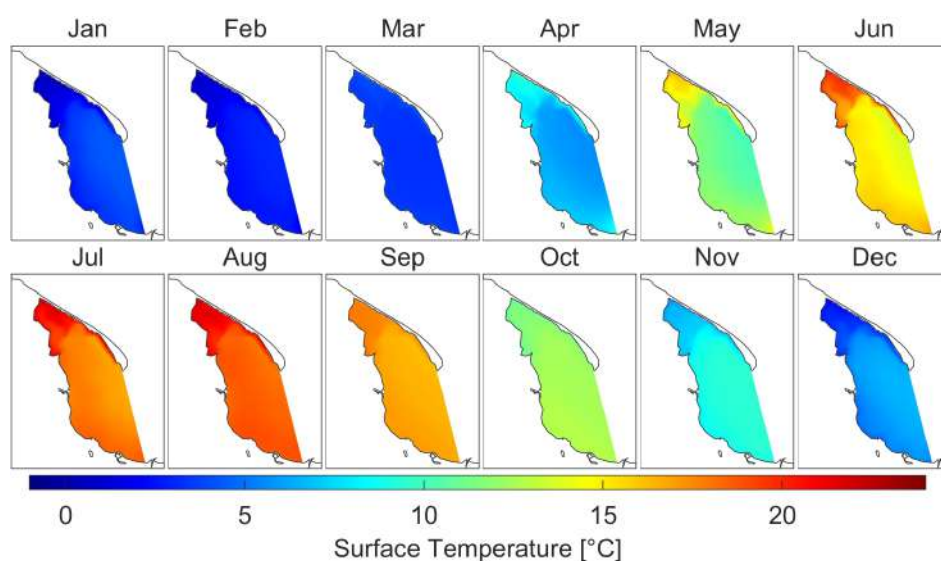


Figure 8. Monthly means of water temperature at sea surface level.

3.2.2. Salinity

The average surface salinity in the domain was 7.05 PSU. The lowest salinity value was calculated near the river mouths with a minimum of 0.18 PSU (March 2014) and the highest value on the eastern border of the region with a maximum of 8.19 PSU (January 2016). The standard deviation for whole modeled period was equal to 0.81 PSU. Figure 9 (based on Tables A5–A8) shows the seasonal variability of the monthly mean surface salinity inside entire domain. Monthly average salinity in the surface layer varies from 5.5 to about 8 PSU. For nearly 50% of the modeled months (28 out of 60) the standard deviation does not exceed 0.5 PSU. The most significant impact on the water salinity in the Puck Bay is the amount of freshwater inflow from rivers (mainly the Vistula river).

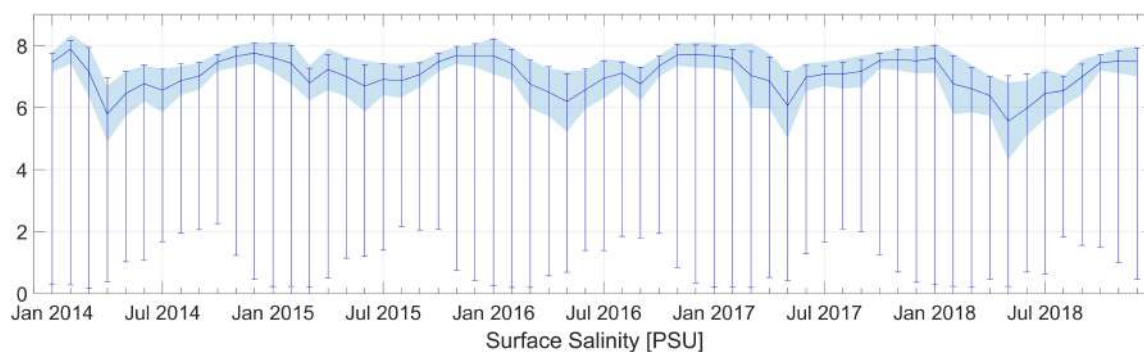


Figure 9. Monthly means of salinity at sea surface level for whole domain. Error bars represent minimum and maximum values. Solid line connects monthly means and shadow area shows standard deviation from the mean values.

Figure 10 presents the monthly averages of surface salinity from years 2014–2018. The lowest values of surface salinity were calculated in the vicinity of river mouths. The biggest influence on salinity of the Puck Bay has the Vistula river. The strong influence of fresh water between March and September is particularly pronounced (Figures A17 and A18). Analyzing the 5-year period (2014–2018), the lowest average salinity in the surface layer of the domain was in May, while the highest in December. From October to January, for all modeled years, the absolute value of the difference between the 5-year average and the monthly average for a given year did not exceed 0.15 PSU (Table A5).

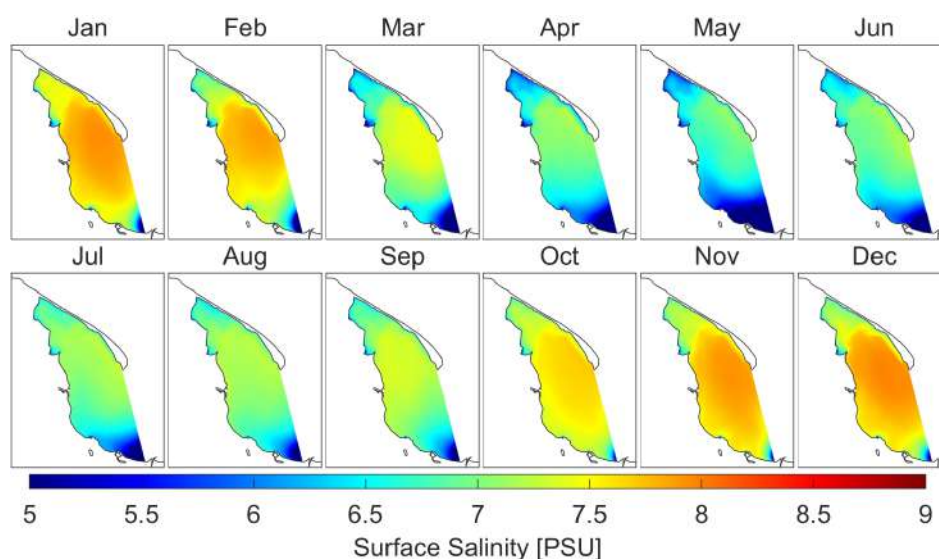


Figure 10. Monthly means of salinity at sea surface level.

3.2.3. Sea Surface Height

The lowest monthly average sea level calculated in the model was -3.35 cm in December 2016 inside Puck Lagoon. The highest monthly average sea level was 2.81 cm in November 2014 also inside Puck Lagoon (Figure 11 based on Tables A9–A12).

The monthly average sea surface height oscillates between a minimum value of about -3.4 cm and a maximum value of 2.8 cm with mean value of -0.18 cm for whole domain. Standard deviation from the mean is equal to 0.6 cm which indicates a small variation in the average sea surface height in the Puck Bay (see Figure 12). As expected, extreme values of sea surface height occurs mainly along the coasts because the monthly average sea surface height is determined by long-term wind forcing (Figures A19 and A20).

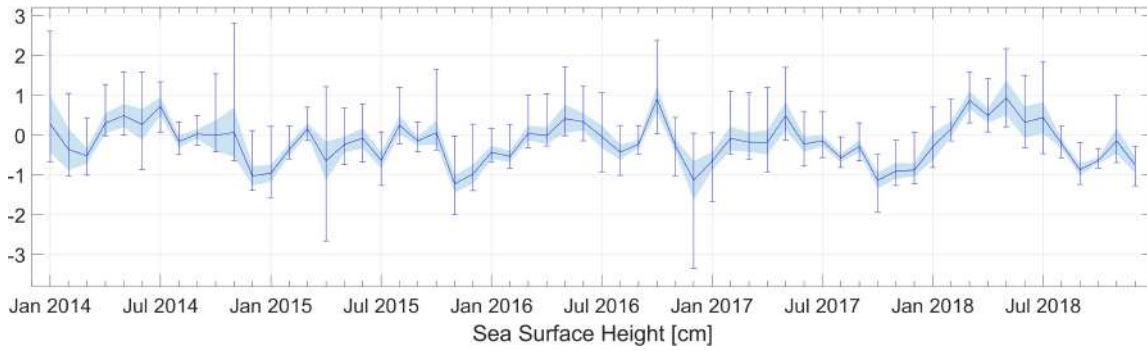


Figure 11. Monthly means of sea surface height for whole domain. Error bars represent minimum and maximum values. Solid line connects monthly means and shadow area shows standard deviation from the mean values.

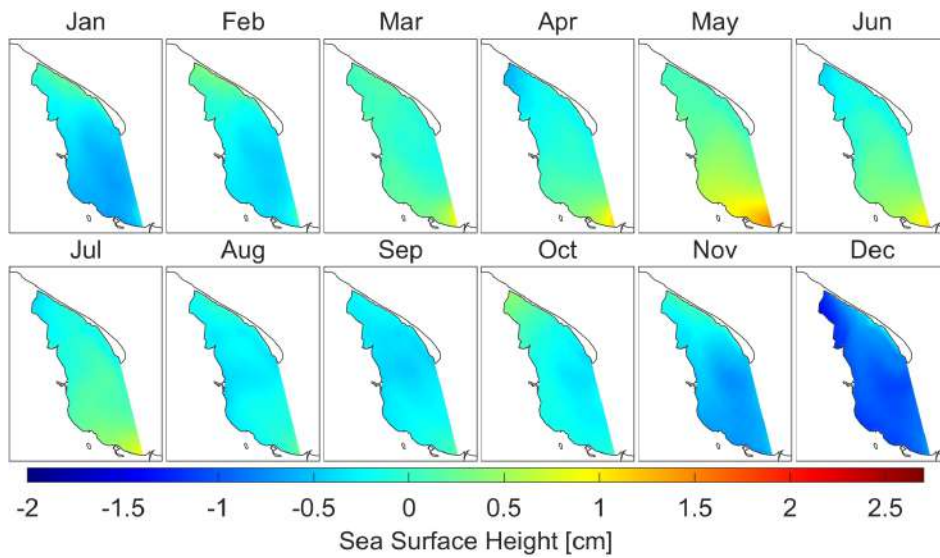


Figure 12. Monthly means of sea surface height.

3.2.4. Currents

The average value of the current for the whole domain in the whole period was equal to $3.36 \text{ cm}\cdot\text{s}^{-1}$ with the standard deviation from the average equal to $2.34 \text{ cm}\cdot\text{s}^{-1}$ (Figure 13 based on Tables A13–A15). The maximum value of the monthly average horizontal velocity was above $27 \text{ cm}\cdot\text{s}^{-1}$ and was calculated on July 2018 near Hel.

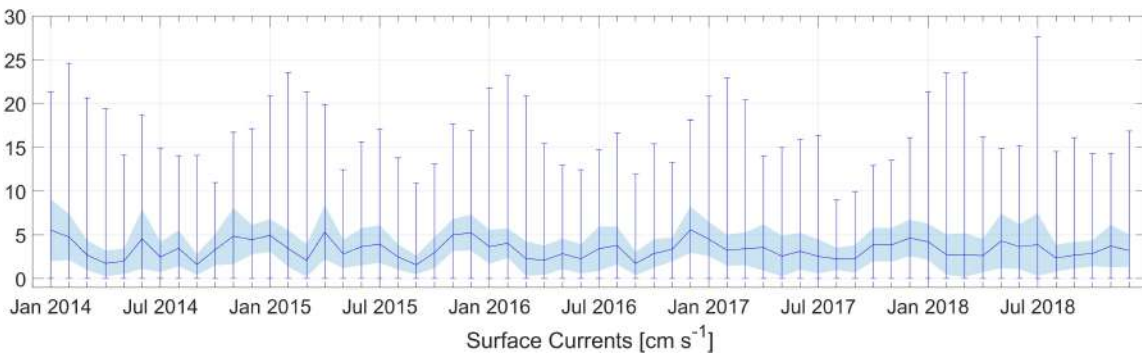


Figure 13. Monthly means of currents at sea surface level for whole domain. Error bars represent minimum and maximum values. Solid line connects monthly means and shadow area shows standard deviation from the mean values.

Figure 14 shows the monthly average spatial distribution of currents over the whole modeled period. In the monthly average, the picture of circulation inside the Puck Bay does not show a vortex character. On the other hand, Figure 15a shows an exemplary image of anticyclonic eddy produced inside the Puck Bay with a temperature cross-section (Figure 15b). According to numerical simulations carried out for the period 1960–1969 by Osiński [20], the vortex size in this area is about 15 km and the average duration about 7 days. Based on our calculations using the EcoPuckBay model developed for WaterPUCK service the diameter of the anticyclonic eddy is about 15–20 km and its duration time is between 7–10 days; in the case shown in Figure 15 it was 10 days (from 21 May to 30 May). Velocities on the east side of the vortex reached $50 \text{ cm}\cdot\text{s}^{-1}$, on the west side up to $40 \text{ cm}\cdot\text{s}^{-1}$ and on the inside up to $20 \text{ cm}\cdot\text{s}^{-1}$.

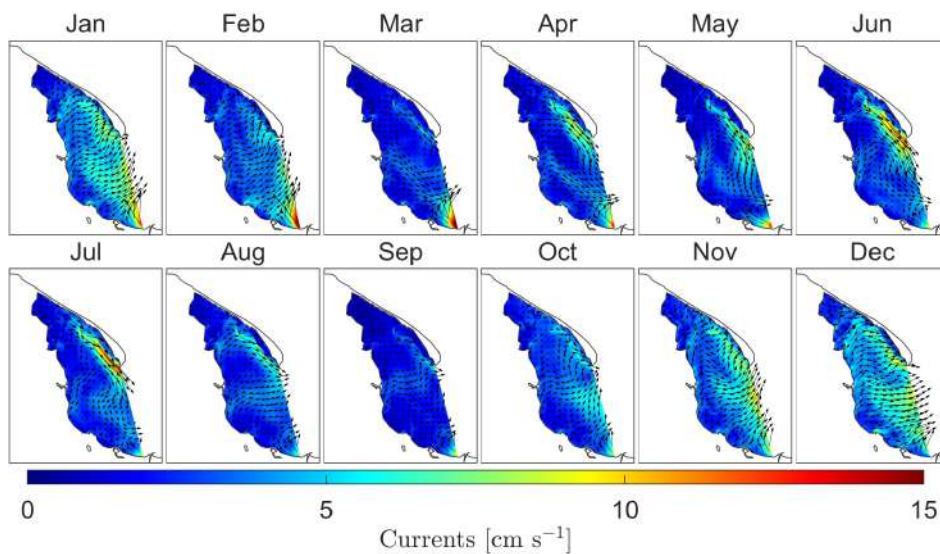


Figure 14. Monthly means of currents at sea surface level.

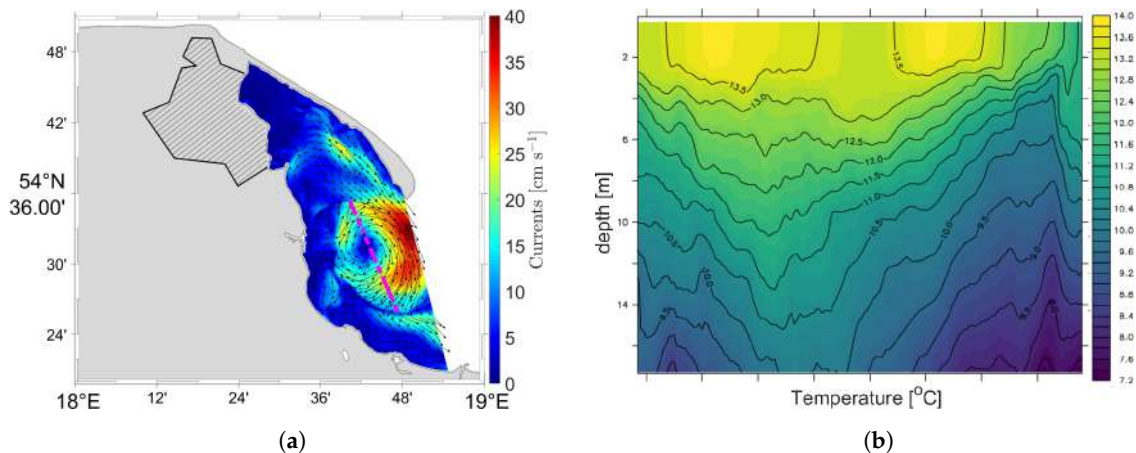


Figure 15. Surface currents distribution of anticyclone on 24 May 2018 (a) with marked (dashed purple) line of vertical cross-section of water temperature (b).

Analyzing the distribution of currents in individual months (see Figures A21 and A22) in relation to sea surface height in those months (see Figures A19 and A20), we can observe some correlations. If the vectors of currents are directed in one direction for most cells in the domain, then the flow of water takes place in the direction indicated by these vectors and there are two possible consequences. The first one when the water is pushed into the bay (i.e., October 2016) and the second when the water is drained from the bay (i.e., December 2016). In the first case, sea surface height on the western side of the domain is higher than on the eastern side. In the second case the sea surface height is relatively lower on the western side of the domain than on the eastern side.

3.3. Web Portal

Presently, quick access to expert knowledge is highly valued, especially in the context of decision-making by the authorities [21]. In order to meet these requirements, the internet service has been developed. This is one of the key services created within the framework of the project, on which the results of all models included in the WaterPUCK Integrated Information and Prediction Service will be made available. This website will operate dynamically in the operational mode allowing for visualization of forecast maps, time series and vertical sections.

In this paper, we present the launch of the website development version, which allows you to generate maps of selected hydrodynamic parameters from the EcoPuckBay model in the area of the Puck Bay and the western part of the Gulf of Gdańsk. Currently, service has a temporal coverage from 2014 to 2018. It is now possible to generate raster maps (Figure 16a) for individual depths, which represent the next vertical level of the model. In addition, it is possible to create time series (Figure 16b) for set periods in the selected location (after prior determination or indication of the desired latitude and longitude) as well as W-E and/or S-N cross-sections, allowing for analysis of the variability of the parameter state in the entire water column (Figure 16c). This service can be accessed from the project website (www.waterpuck.pl) after choosing “Services” from the navigation menu and selecting “EcoPuckBay Hydrodynamical Model of the Puck Bay”.

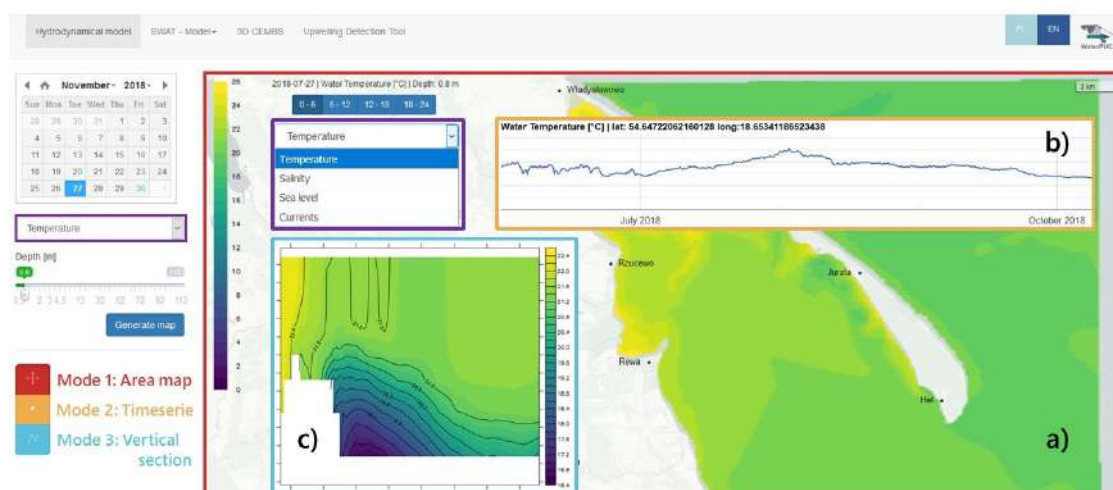


Figure 16. Screenshot of navigation menu and results for the Web Portal service (a) raster map (b) time series (c) vertical cross-section of selected parameter.

The portal operates on the basis of front-end/back-end technology. The mechanisms responsible for displaying (front-end) are separated from the data processing (back-end). This solution allows you to build a portal with high scaling capabilities, i.e., increasing the number of connections supported at one time. In addition, separation of displaying from data processing provides additional server security and allows independent development of both parts. Front-end layer responsible for data visualization was created in Bootstrap technology and adapted to be operated from mobile devices. Back-end responsible for data processing and transferring them to the front-end part was created in the RESTful-API technology. This technology is based on communication between parts of the portal using stateless queries (Figure 17).

The hydrodynamic data comes from the EcoPuckBay model run on the Tryton computing cluster in CI TASK [22] once a day. After completing the calculations, the data is copied to the disk space of the back-end part.

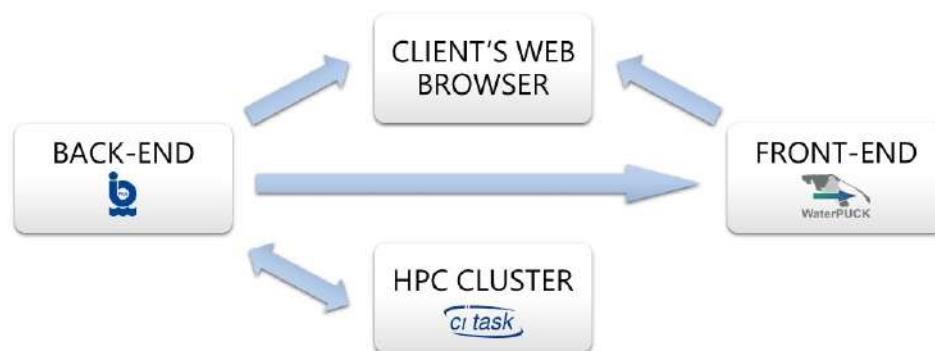


Figure 17. Architecture diagram of the WaterPUCK project's service - the hydrodynamic part of the EcoPuckBay model.

4. Discussion

The paper presents the hydrodynamic part of the three-dimensional ecohydrodynamic model of the Puck Bay EcoPuckBay, which determines the main physical environmental parameters such as water potential temperature, salinity, horizontal velocity components and sea surface height.

The statistical analysis was carried out to confirm that EcoPuckBay model's predictions are similar to field data. The time series from model simulations were compared with in situ samples from several locations across the entire effective domain using VIEP environmental samples database and s/y Oceania vertical profiles conducted during its cruise. For all locations described in the paper, we calculated basic statistics such as RMSE, standard deviations (STD) and Pearson's correlation coefficients for the full period of available measurements in the dataset (Section 3.1).

The comparison of the EcoPuckBay model computations revealed that modeled water temperature results are in very good agreement with experimental samples with lowest correlation of 0.92 for s/y Oceania profiles and 0.97 when tested against time series of VIEP samples (Table 3). To balance our model against another state-of-the-art model, we compared numerical data from NEMO-Nordic to VIEP time series measurements. The Pearson's correlation coefficient between NEMO-Nordic model and VIEP data is equal to 0.98. On the one hand, this comparison shows that the temperature is slightly better reproduced by the NEMO-Nordic model. On the other hand, taking into account the salinity (Table 6) we see a significant advantage of the EcoPuckBay model. This is most likely due to the higher resolution of the EcoPuckBay model compared to the NEMO-Nordic model resolution. It is worth mentioning that the Pearson's correlation coefficients for vertical profiles of salinity are in the range from 0.78 to 1.0, with a value equal to 0.9 for all stations. However, for VIEP time series data we have a correlation coefficient equal to 0.58 for all stations.

It is worth mentioning that the shape of the mixed layer depends on vertical grid resolution as well as on vertical viscosity. Vertical mixing scheme provides the best solutions if the horizontal resolution is not variable. It means if our model will have a constant thickness of the cells, vertical profiles will better fit observation data. Bathymetry of the model has been adapted to the Puck Bay and not for the Gdańsk Bay, therefore from the depth of 4 m the thickness of layers increases up to 5 m, which in turn affects the shape of temperature and salinity profiles. This choice is a consequence of the trade-off between the vertical resolution and computational time. Adopting the same cell thicknesses for the entire domain as for Puck Bay would lead to over 250 layers, which would consequently lengthen the calculations by 8 times. The POP model which is the main core of the hydrodynamic part has been purposed for global simulations. Adopting it for shallow waters required modifying the dependence of vertical viscosity on Richardson's number. Our modification (suggested by Durski et al. [7]) brought the adopted turbulence scheme closer to the parameterization of Mellor-Yamada (level 2.5) which is one of the best for estuaries and shelf seas.

Analyzing the 5-year period (2014–2018), the greatest variability of surface temperature can be observed inside Puck Lagoon. In summer the surface temperature inside Puck Lagoon is about

5 °C higher than in the rest of the Puck Bay and in winter about 3 °C lower (Figures A8 and A9). Such changes are due to the geomorphological separation of Puck Lagoon from the rest of the Puck Bay and to the fact that the area of Puck Lagoon is 30% of the entire Puck Bay and only about 6% of the water volume of the entire Puck Bay is located within Puck Lagoon.

Fresh water inflow from rivers (mainly from the Vistula river) has the greatest influence on the variability of surface salinity values in the Puck Bay. Analyzing the modeled period, we can see that in the summer the surface salinity decreases most strongly in the vicinity of the Vistula river and inside the Puck Lagoon (Figures A17 and A18). The changes in the south part of domain are a consequence of the natural cycle of the Vistula discharges. Within Puck Lagoon, isolation from the rest of the Puck Bay and the discharge of fresh water from rivers 8–13 (mainly from Reda, see Figure 1) has the most impact on the variability of the surface salinity.

The variability of the monthly sea surface height average in the studied period is in line with expectations and its gradient is similar to the wind forcing fields (Figures A19 and A20). Average monthly values of currents, depending on the month, varied from about $2 \text{ cm}\cdot\text{s}^{-1}$ to over $4.5 \text{ cm}\cdot\text{s}^{-1}$ and were higher for winter months in relation to summer months (Table A13).

The analysis show that the dynamics of changes is well reflected in general. Standard deviation was quite low and systematic error was negative in comparison with, which means that model results were usually lower than the results from VIEP database. The analyzed period 2014 to 2018 can be characterized as moderate dynamic in terms of inter-annual variability of parameters. The correspondence between EcoPuckBay model results and observations in terms of both temporal and spatial analysis is encouraging. It is clearly visible that even though the model tends to slightly underestimate water temperature conditions it reacts very well to atmosphere forcing.

In high-resolution Baltic Sea configurations, river runoff is prone to cause numerical problems because the salinity is close to zero in the vicinity of some rivers. This can, at times, due to the dispersive nature inherent to all state-of-the-art advection schemes (other than the outdated upstream scheme), induce negative salinities for which the equation of state is not defined. We solved this problem by distributing the runoff over the 22 grid boxes closest to the actual position of the river mouth. The distribution among the grid cells is determined by weights calculated with a trigonometric decay radius of 2.5 km as a function of the respective cell distance to the location of the Vistula river mouth.

5. Conclusions

The paper describes the initial implementation of the EcoPuckBay model which is the part of the WaterPUCK project. The WaterPUCK project's goal is to provide integrated information and predictive service for the Puck District by developing a system that works in an operational state and providing reliable forecasts of the waters surrounding the region. The evaluation of the quality of the results obtained from the EcoPuckBay model for the period of January 2014 to December 2018 was performed by statistical comparison with in situ measurements and another model reanalysis.

The results of the model verification indicate its suitability for forecasting hydrodynamic conditions within the concerned region. Satisfactory compatibility between in situ measurements and simulations enables reliable physical conditions to be established for future simulations with the active biogeochemical part.

The correct representation of the mixing in the whole water column, advection and heat exchange, which control the heating and cooling of water masses, is of particular importance for the forecasting of biological processes especially in a region such as the Puck Bay, with its unique ecosystem, different from the conditions of the open sea due to the presence of natural topographical barriers as well as the strong influence of environmental factors, both natural and induced by human activity.

The presented results show that the analyzed effective domain model dynamically reacts to the considered forces both in the coastal zone and further southeast towards the Gulf of Gdańsk, which depends on the changes in the open Baltic Sea.

The lower accuracy of the results that can be observed on some of the measuring stations may be due to the fact that some modules of the final product are still under development or testing, as well as the nature of the samples used for model evaluation.

Visible improvement of the EcoPuckBay model results is expected when the satellite and environmental data assimilation module is enabled.

The current configuration also uses forcings, which has been prepared from long-term averages (e.g., fresh water from water courses flowing into the Puck Bay) replacing target methods, which will be characterized by much higher time resolution of the information provided and will have a correctly mapped character and dynamics of individual external forcings. An example of a product that is currently being replaced by climatological averages is the SWAT hydrological model, which will provide information about the volume and temperature of fresh water and the concentrations of deposited inorganic substances entering the Puck Bay together with surface waters.

To study the complexity of hydro-physical and biological processes in the marine environment, and the links between these processes, modern techniques, i.e., mathematical modeling and computer simulations are required. Although the field work provides the most reliable information on these mechanisms and processes, it requires comprehensive and costly in situ observations conducted under a variety of hydrological conditions for long periods of time.

It is also worth mentioning that in situ measurements conducted at the monitoring stations have the highest accuracy of all monitoring method; however readings and the samples collected during the monitoring process are only snapshots of the environment state which in fact is the 1-dimensional 'here and now' information. In addition there is a limited quantity of data for each parameter at selected station with irregular time span between the campaigns.

The development of integrated approaches, such as monitoring measures and modeling, became an important tool not only for understanding the processes taking place in both inland and marine ecosystems but also for evaluating the impact of various land-use and climate scenarios on water quantity and quality at the basin scale. The main objective of this paper, i.e., development of a hydrodynamic (physical) module for the EcoPuckBay model, was achieved in the following steps:

- down-scaling and adapting the 3D CEMBS model for the Puck Bay region;
- advanced model tuning and optimization;
- topography implementation on the model grid;
- production of atmospheric data based on the UM weather model;
- incorporation of rivers from hydrological model SWAT;
- opening the boundary with the Baltic Sea;
- switching to the operational mode

Along with the operational mode that will be introduced in the EcoPuckBay model within upcoming development stages, an assimilation module will be enabled in the final configuration. This module's job is to process all the available environmental and satellite data at the time of the forecast start and force the simulation to produce results that better fit the environment state. This will provide lower model uncertainties and therefore improve overall accuracy.

Satellite-measured sea surface temperature (SST) information for the assimilation module will be taken from the Moderate Resolution Imaging Spectroradiometer (MODIS, Aqua satellite). Environmental packages of in situ data samples collected during VIEP monitoring campaigns will be delivered once per year. On a delivery event EcoPuckBay model will induce the 1-year hindcast parallel simulation that will assimilate those results and after reaching present day updating the archives and switching back to the operational state continuing with forecasts.

Author Contributions: Conceptualization, D.D. and L.D.-G.; Methodology, D.D., J.J., M.J. and L.D.-G.; Software, D.D. and A.N.; Validation, D.D.; Formal analysis, D.D. and L.D.-G.; Investigation, D.D. and J.J.; Resources, D.D. and J.J.; Data curation, D.D., J.J. and D.R.; Writing—original draft preparation, D.D., M.J. and L.D.-G.; Writing—review and editing, D.D., M.J. and L.D.-G.; Visualization, D.D.; Supervision, L.D.-G.; Project administration, L.D.-G.; Funding acquisition, L.D.-G.

Funding: This research was funded by National Centre for Research and Development of Poland within the BIOSTRATEG III program No. BIOSTRATEG3/343927/3/NCBR/2017.

Acknowledgments: This study has been conducted using E.U. Copernicus Marine Service Information. Calculations were carried out at the Academic Computer Centre in Gdańsk.

Conflicts of Interest: The authors declare no conflict of interest.

Appendix A

Main part of the paper was limited to the monthly averages and statistical comparison results. However, detailed Figures and Tables for separate years and measurement stations are presented in the Appendix section.

Appendix A.1. Temperature

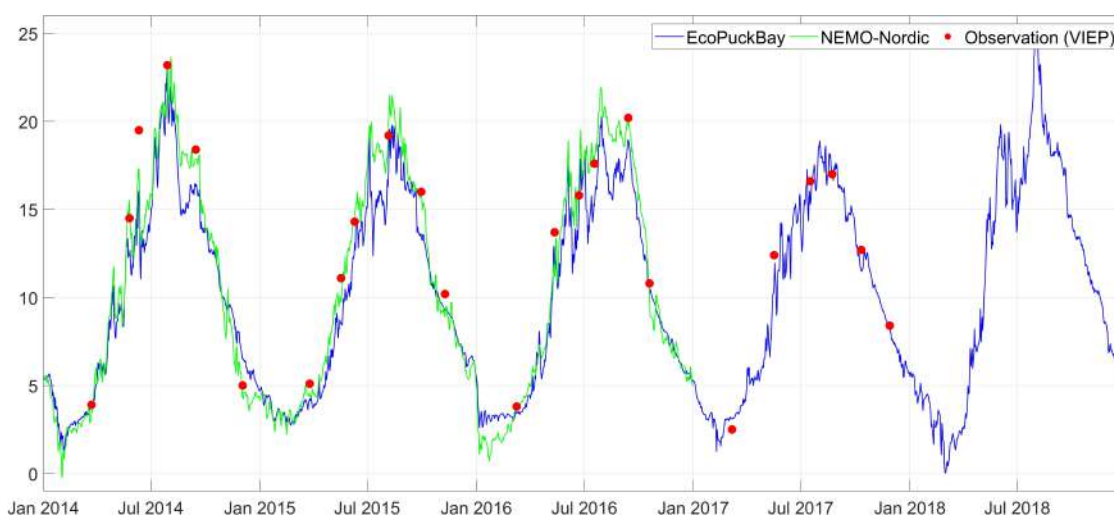


Figure A1. Time series of surface water temperature on station OM1 compared with VIEP observations and NEMO-Nordic model.

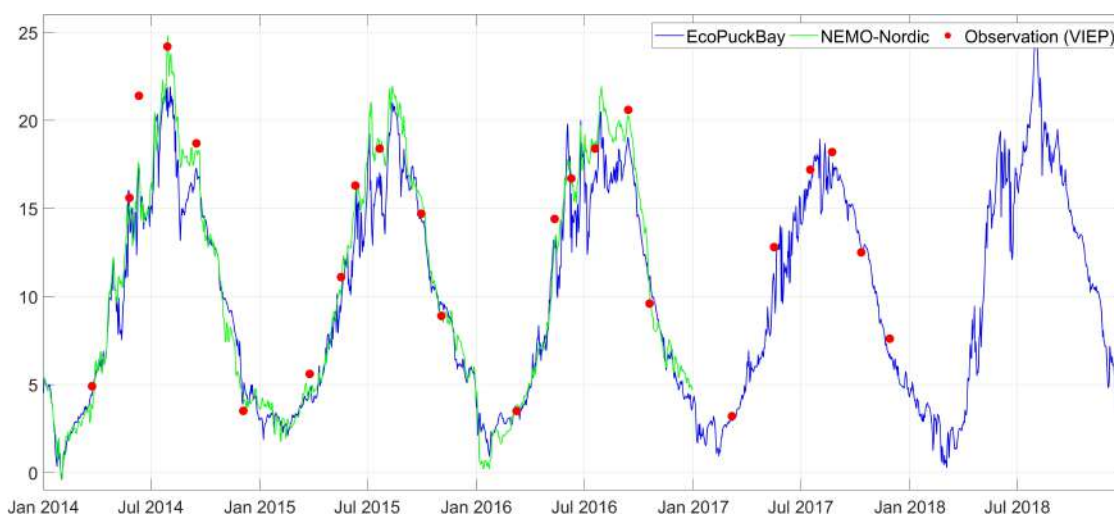


Figure A2. Time series of surface water temperature on station T11 compared with VIEP observations and NEMO-Nordic model.

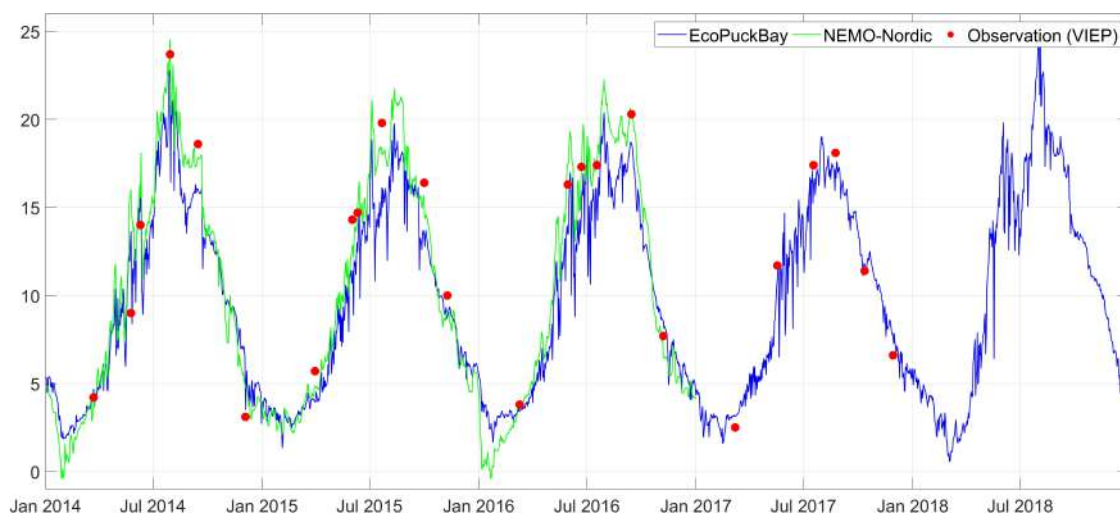


Figure A3. Time series of surface water temperature on station T12 compared with VIEP observations and NEMO-Nordic model.

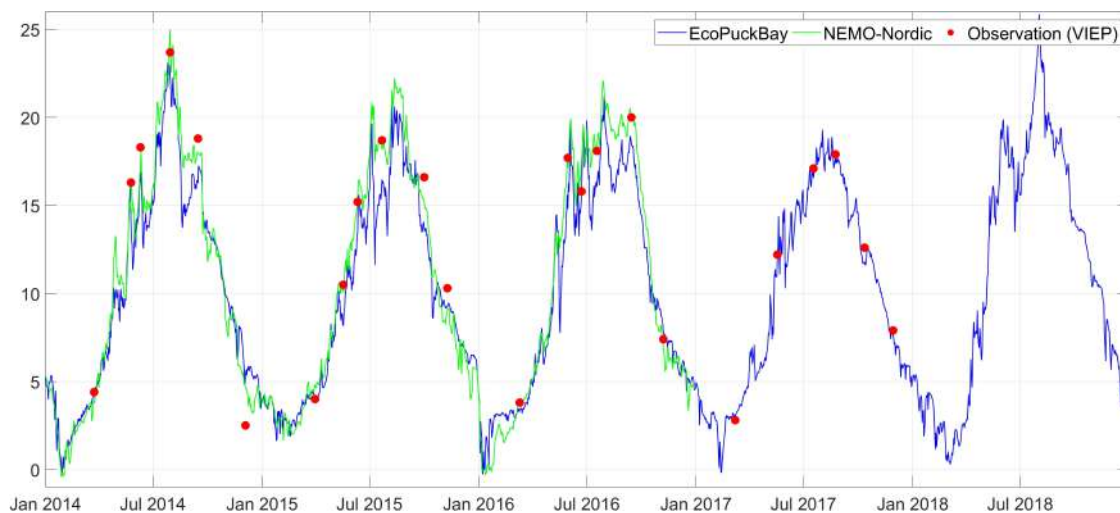


Figure A4. Time series of surface water temperature on station T14 compared with VIEP observations and NEMO-Nordic model.

Table A1. Monthly means for surface temperature for the years 2014–2018.

Year\Month	Jan	Feb	Mar	Apr	May	Jun	Jul	Aug	Sep	Oct	Nov	Dec
2014	3.50	2.03	3.96	7.83	11.34	14.81	19.82	18.44	16.15	12.61	8.77	4.89
2015	3.38	2.70	3.97	5.78	10.13	14.19	16.59	18.82	16.41	11.67	8.89	6.37
2016	2.69	3.16	3.79	6.84	12.25	16.11	17.44	17.89	17.63	11.72	7.49	5.33
2017	3.02	2.32	3.83	6.30	10.87	14.32	16.95	18.40	16.12	12.68	9.04	5.80
2018	4.03	2.34	1.67	6.44	14.23	17.97	19.73	21.25	17.81	13.18	9.67	5.38
mean	3.32	2.51	3.44	6.64	11.76	15.48	18.11	18.96	16.82	12.37	8.77	5.55

Table A2. Monthly minimums for surface temperature for the years 2014–2018.

year\month	Jan	Feb	Mar	Apr	May	Jun	Jul	Aug	Sep	Oct	Nov	Dec
2014	0.59	−0.16	3.54	6.45	9.55	12.83	17.78	17.30	15.45	11.19	5.76	0.74
2015	0.42	0.91	3.69	4.74	8.61	12.72	15.19	17.43	15.30	9.38	6.00	3.51
2016	−0.28	2.23	3.59	5.69	10.33	13.62	16.01	16.93	17.12	9.11	3.70	2.29
2017	0.15	0.47	3.45	4.98	8.96	12.62	15.17	16.88	15.46	11.58	5.27	1.64
2018	0.34	−0.04	0.32	5.20	11.05	15.50	18.02	19.87	16.99	10.97	5.91	0.74

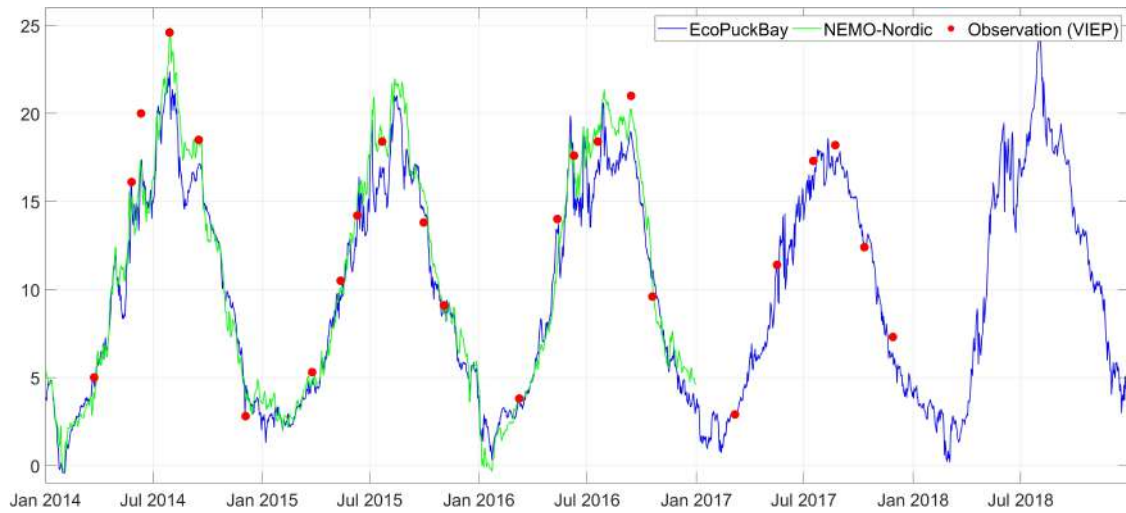


Figure A5. Time series of surface water temperature on station T16 compared with VIEP observations and NEMO-Nordic model.

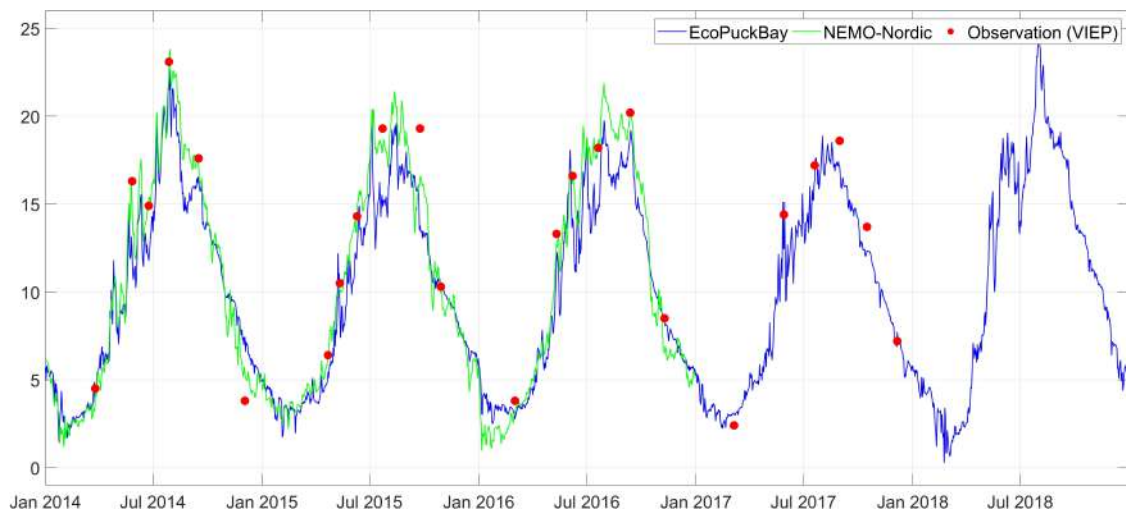
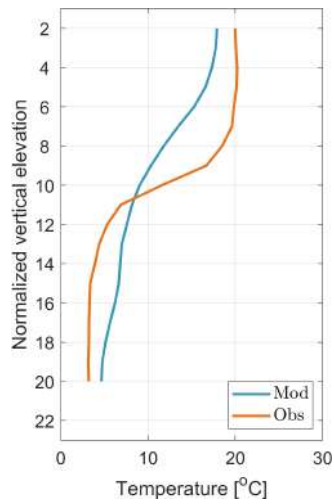
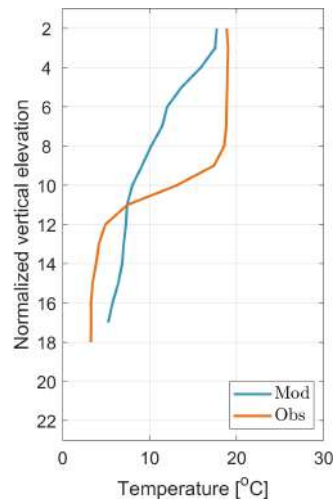


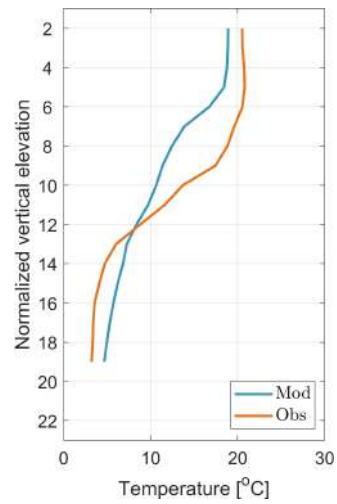
Figure A6. Time series of surface water temperature on station ZG compared with VIEP observations and NEMO-Nordic model.



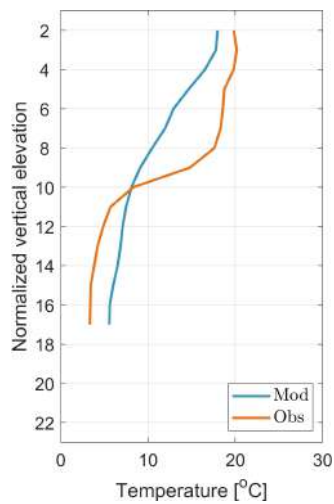
(a) Station 1.



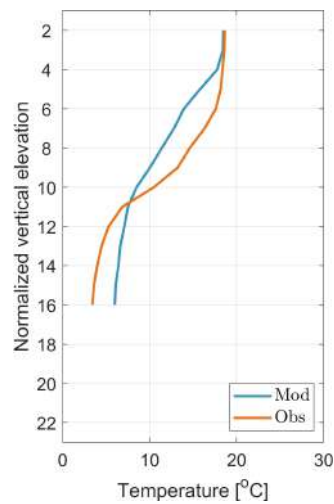
(b) Station 2.



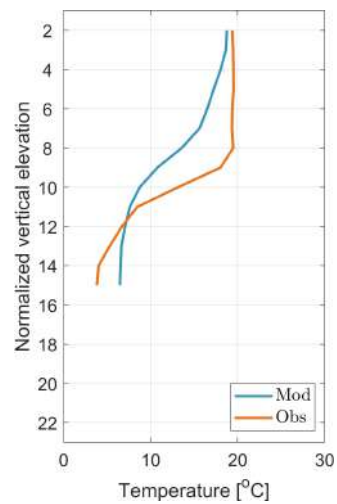
(c) Station 3.



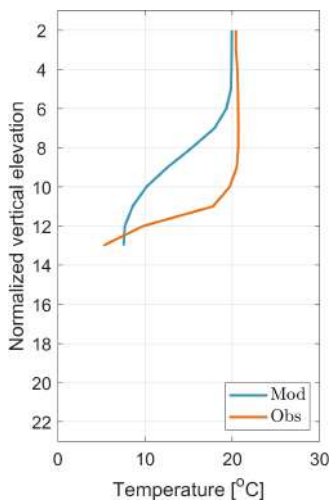
(d) Station 4.



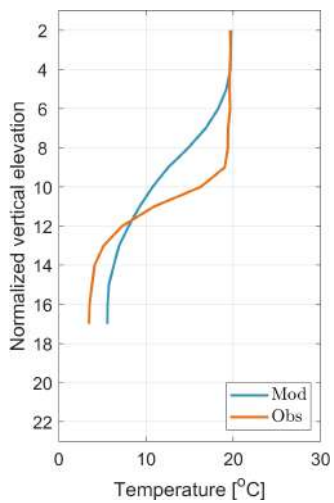
(e) Station 5.



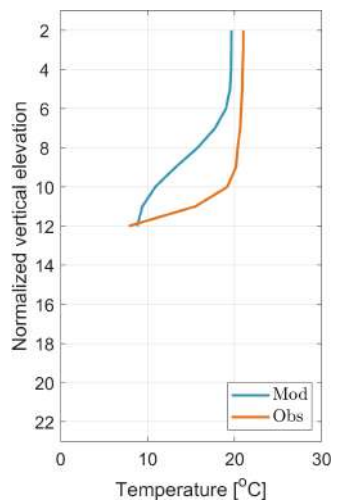
(f) Station 6.



(g) Station 7.



(h) Station 8.



(i) Station 9.

Figure A7. Cont.

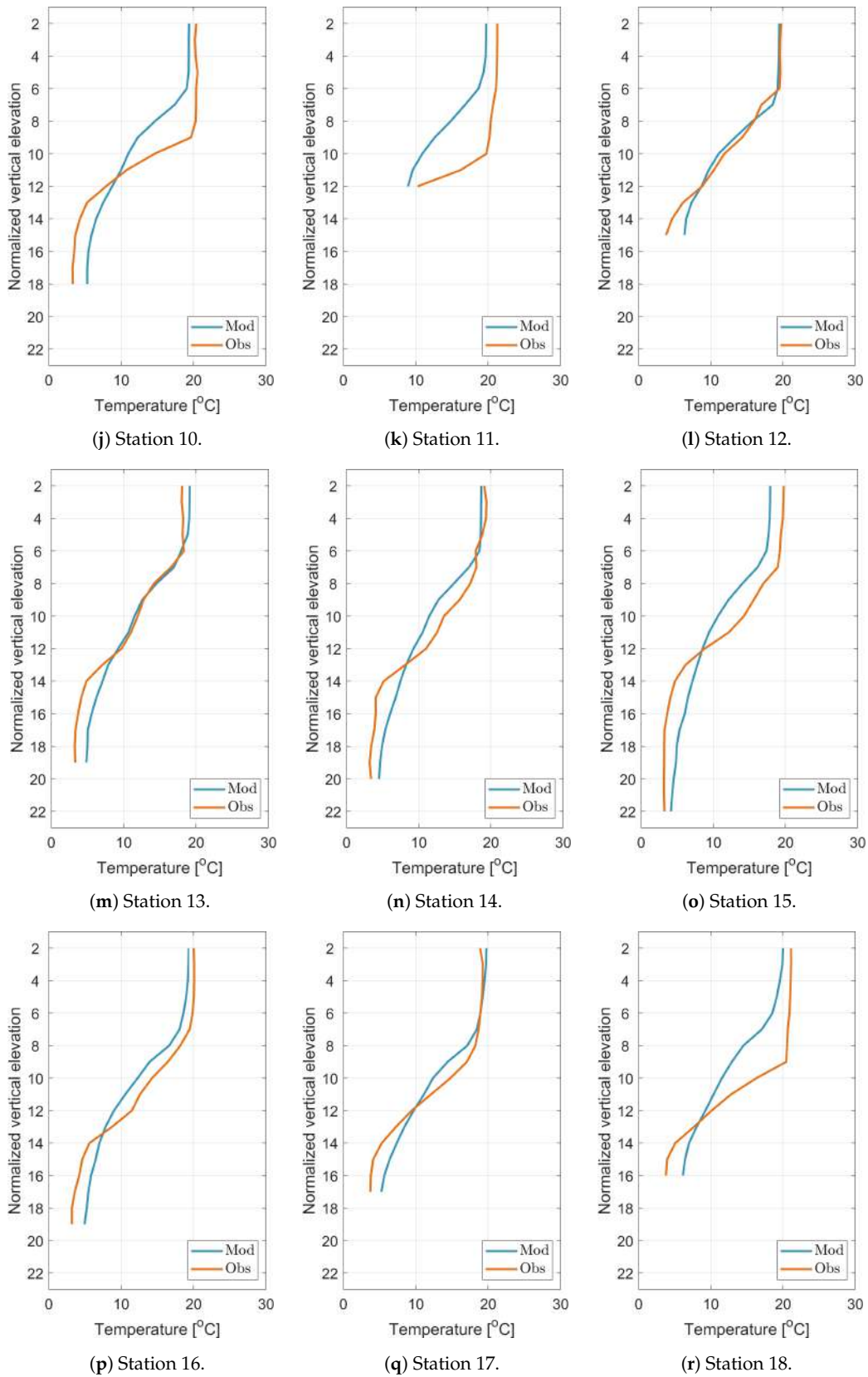


Figure A7. Temperature vertical profiles for all stations compared with s/y Oceania observations.

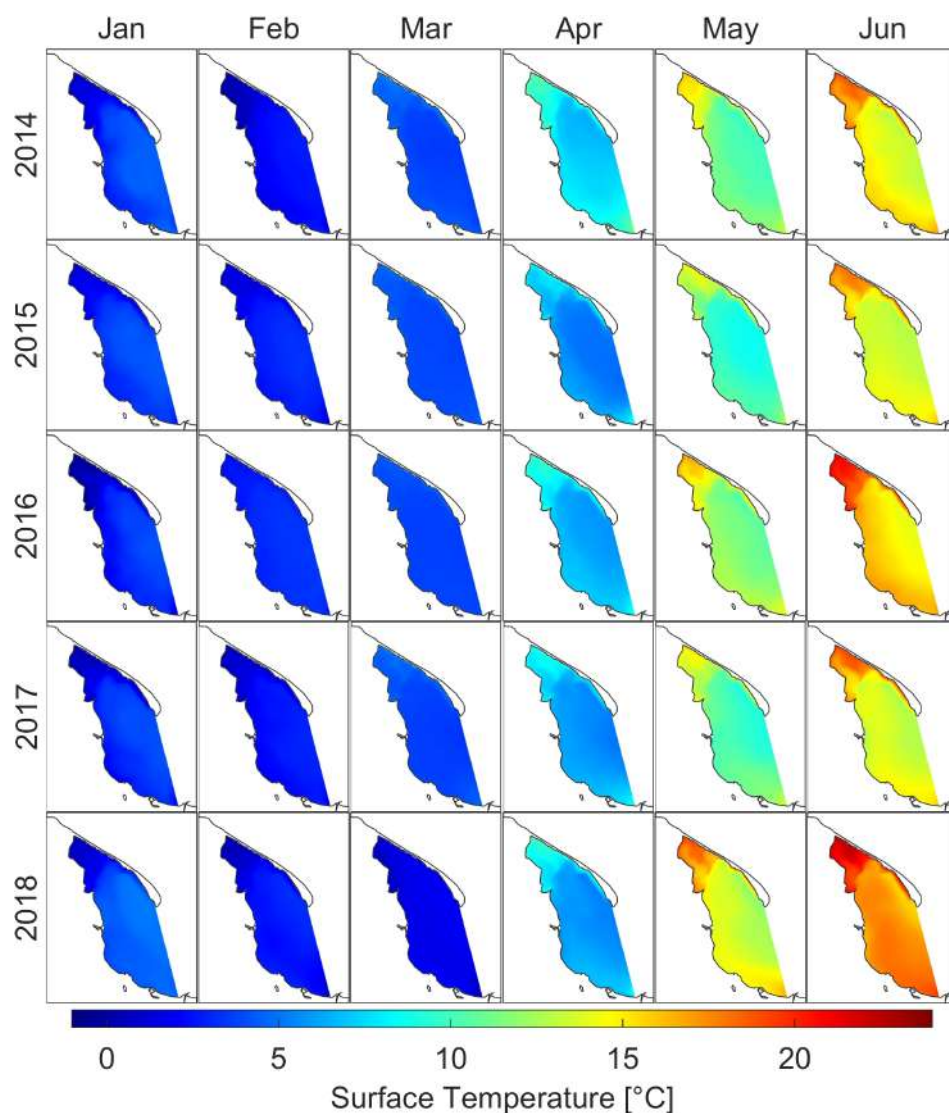


Figure A8. Monthly means of water temperature at sea surface for separated years. January to June.

Table A3. Monthly maximums for surface temperature for the years 2014–2018.

year\month	Jan	Feb	Mar	Apr	May	Jun	Jul	Aug	Sep	Oct	Nov	Dec
2014	4.65	2.85	5.60	11.63	16.13	19.57	24.21	21.14	17.74	13.26	9.56	6.37
2015	4.31	3.39	5.22	9.23	14.76	18.37	20.45	22.39	18.24	12.16	9.57	7.19
2016	4.15	3.50	4.67	10.18	17.34	21.50	21.88	20.24	18.93	12.29	8.53	6.44
2017	4.13	3.07	5.32	9.47	15.83	19.55	20.75	21.64	17.16	13.31	9.84	6.99
2018	5.15	3.25	2.56	10.84	19.56	22.35	24.03	23.89	18.98	13.74	10.58	6.55

Table A4. Monthly standard deviations for surface temperature for the years 2014–2018.

year\month	Jan	Feb	Mar	Apr	May	Jun	Jul	Aug	Sep	Oct	Nov	Dec
2014	1.01	0.71	0.38	1.00	1.42	1.41	1.20	0.86	0.43	0.30	0.79	1.34
2015	0.83	0.58	0.22	0.95	1.43	1.27	1.11	1.02	0.55	0.52	0.71	0.76
2016	1.21	0.27	0.17	0.94	1.36	1.67	1.28	0.74	0.37	0.61	1.07	0.91
2017	1.03	0.60	0.35	0.91	1.37	1.47	1.16	1.06	0.39	0.34	1.02	1.24
2018	1.20	0.69	0.30	1.03	1.55	1.40	1.24	0.86	0.41	0.51	0.97	1.39

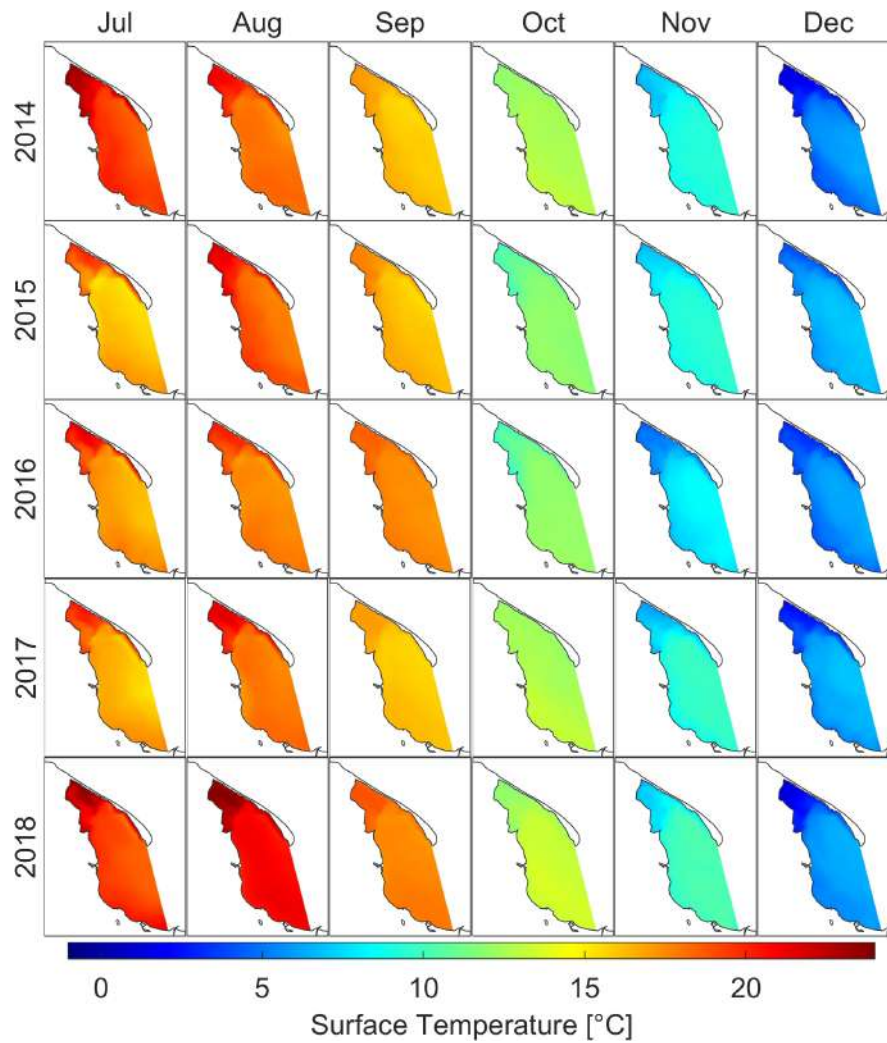


Figure A9. Monthly means of water temperature at sea surface for separated years. July to December.

Appendix A.2. Salinity

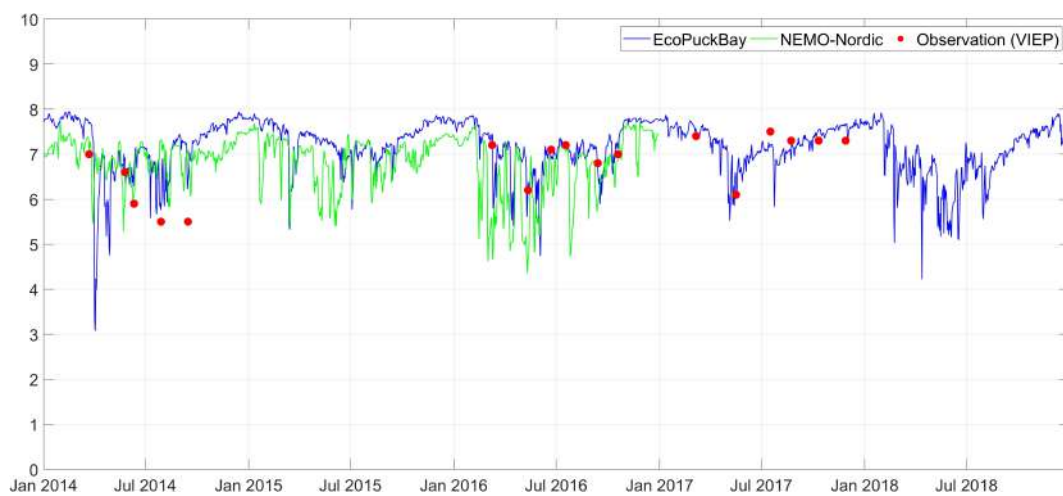


Figure A10. Time series of surface salinity on station OM1 compared with VIEP observations and NEMO-Nordic model.

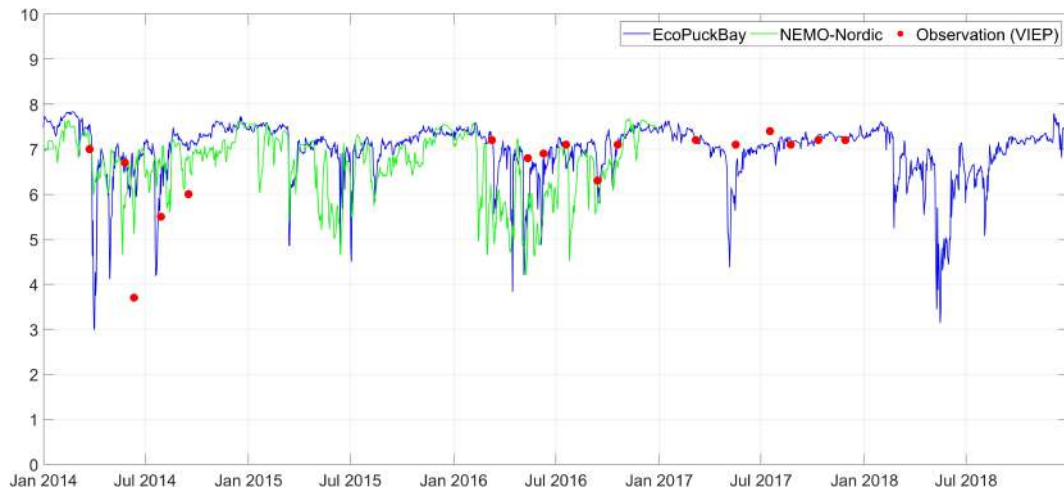


Figure A11. Time series of surface salinity on station T11 compared with VIEP observations and NEMO-Nordic model.

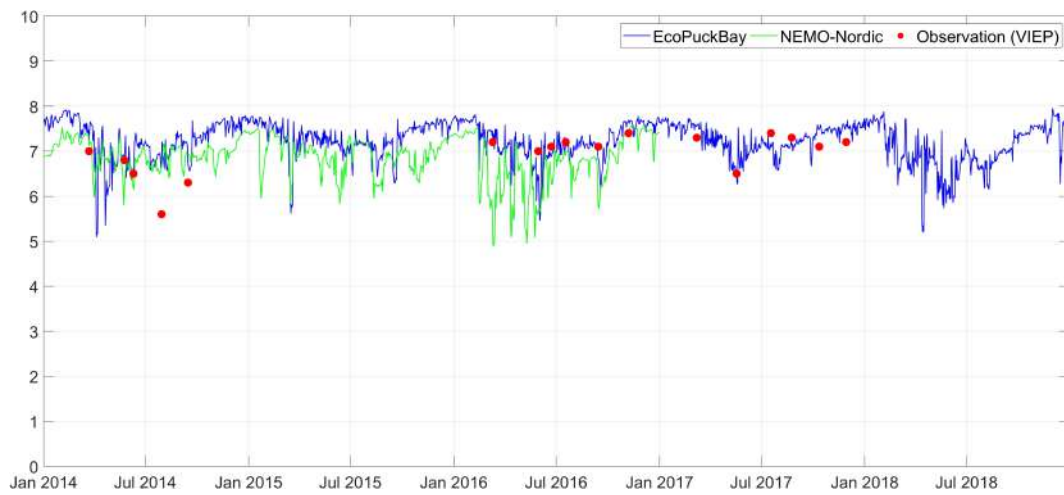


Figure A12. Time series of surface salinity on station T12 compared with VIEP observations and NEMO-Nordic model.

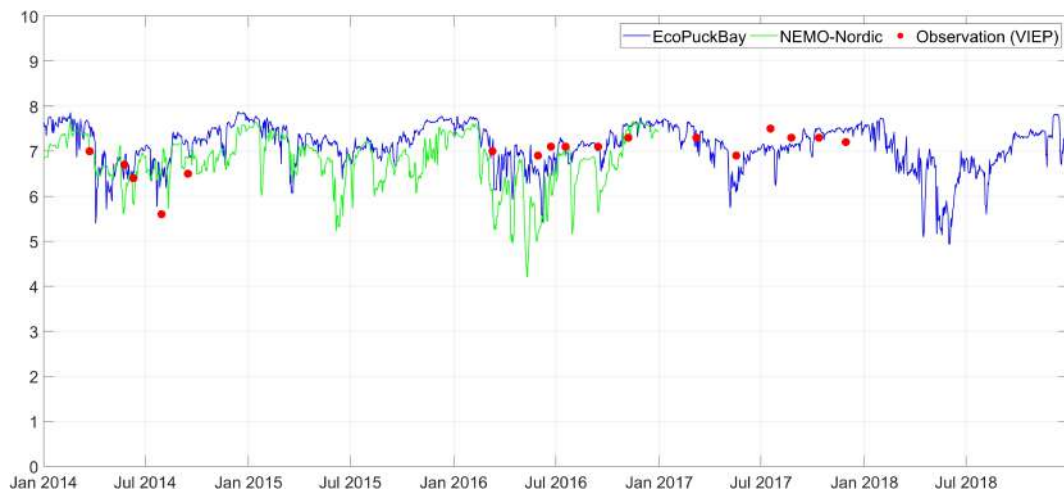


Figure A13. Time series of surface salinity on station T14 compared with VIEP observations and NEMO-Nordic model.

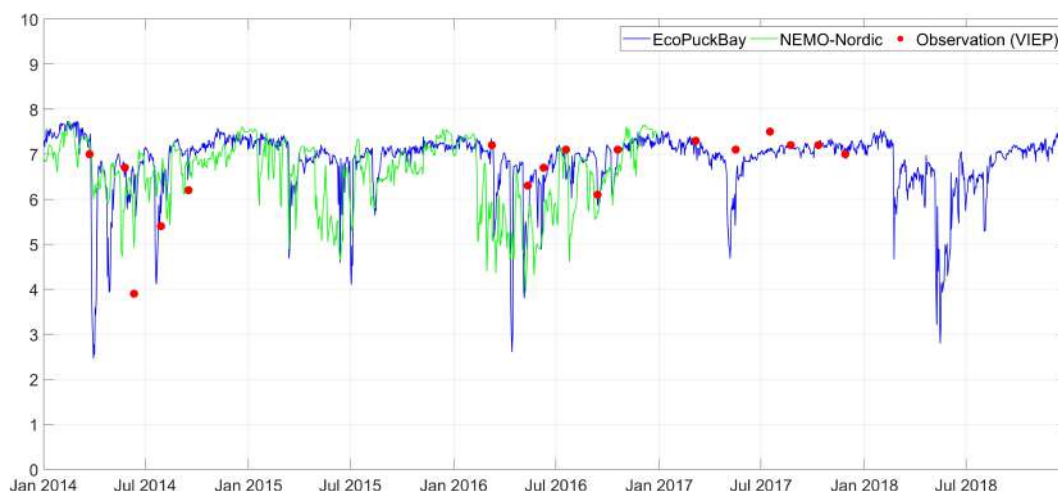


Figure A14. Time series of surface salinity on station T16 compared with VIEP observations and NEMO-Nordic model.

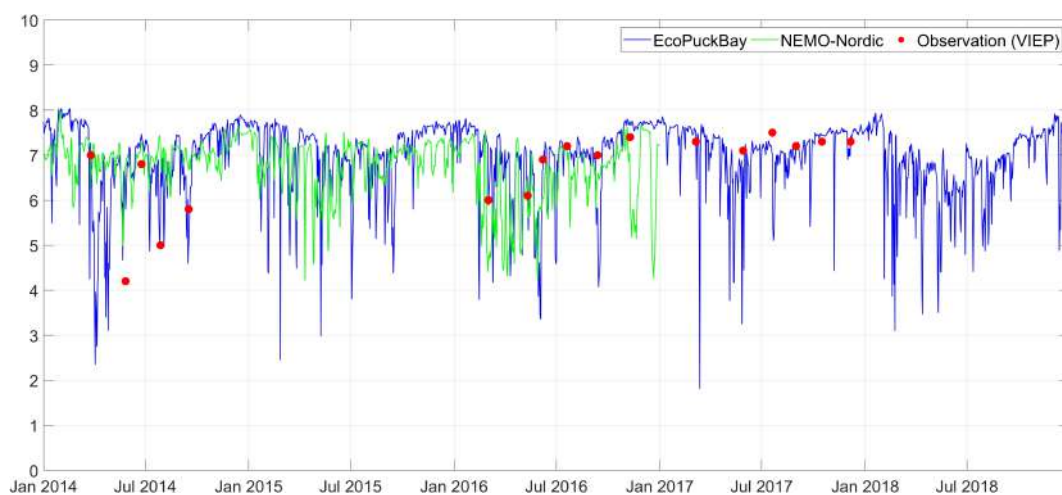


Figure A15. Time series of surface salinity on station ZG compared with VIEP observations and NEMO-Nordic model.

Table A5. Monthly means for surface salinity for the years 2014–2018.

Year\Month	Jan	Feb	Mar	Apr	May	Jun	Jul	Aug	Sep	Oct	Nov	Dec
2014	7.46	7.89	7.15	5.79	6.45	6.77	6.55	6.87	7.01	7.47	7.66	7.76
2015	7.62	7.43	6.79	7.23	7.00	6.69	6.91	6.87	7.07	7.47	7.68	7.67
2016	7.67	7.42	6.75	6.50	6.19	6.57	6.94	7.11	6.76	7.33	7.70	7.70
2017	7.68	7.59	7.03	6.86	6.06	6.97	7.09	7.08	7.17	7.51	7.55	7.51
2018	7.59	6.76	6.61	6.38	5.56	5.97	6.45	6.55	6.98	7.45	7.49	7.50
mean	7.60	7.42	6.87	6.55	6.25	6.59	6.79	6.90	7.00	7.45	7.62	7.63

Table A6. Monthly minimums for surface salinity for the years 2014–2018.

Year\Month	Jan	Feb	Mar	Apr	May	Jun	Jul	Aug	Sep	Oct	Nov	Dec
2014	0.31	0.27	0.18	0.38	1.02	1.08	1.66	1.95	2.05	2.26	1.23	0.46
2015	0.23	0.22	0.20	0.50	1.14	1.19	1.40	2.16	2.04	2.06	0.76	0.41
2016	0.25	0.19	0.19	0.57	0.68	1.38	1.39	1.84	1.79	1.93	0.83	0.31
2017	0.20	0.22	0.19	0.51	0.41	1.28	1.65	2.08	2.00	1.24	0.70	0.36
2018	0.28	0.22	0.22	0.46	0.22	0.69	0.63	1.82	1.55	1.48	0.99	0.46

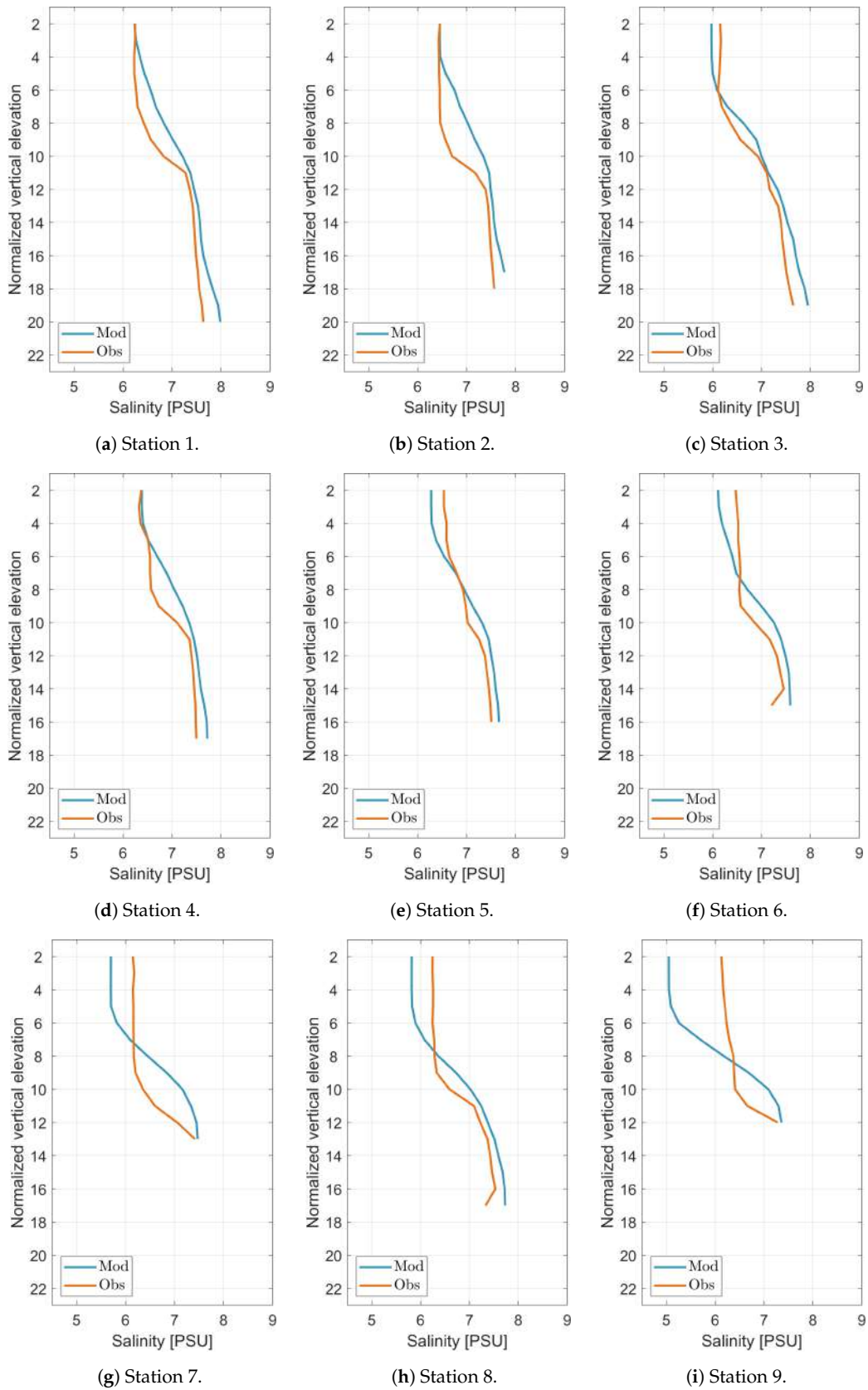


Figure A16. Cont.

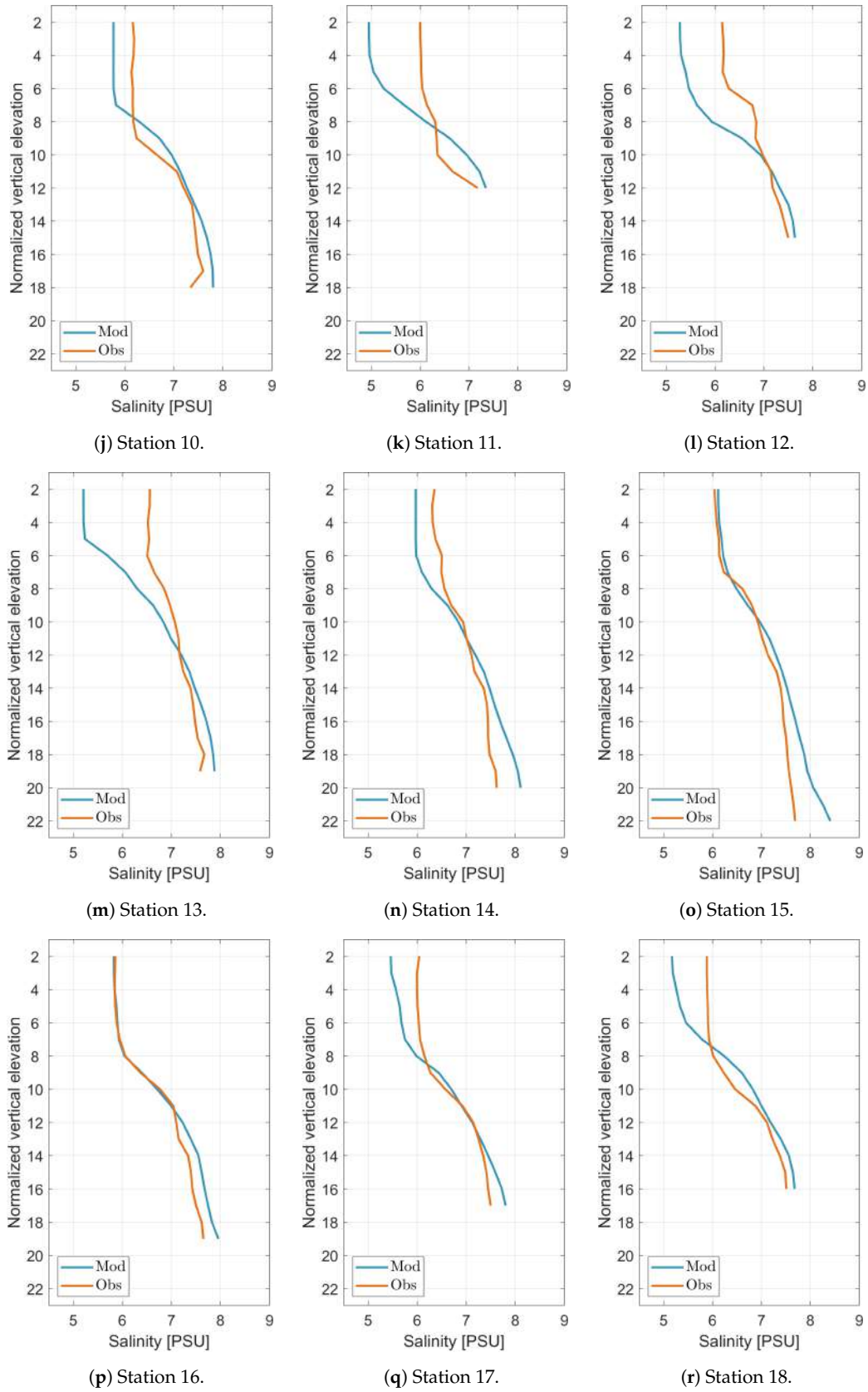


Figure A16. Salinity vertical profiles for all stations compared with s/y Oceania observations.

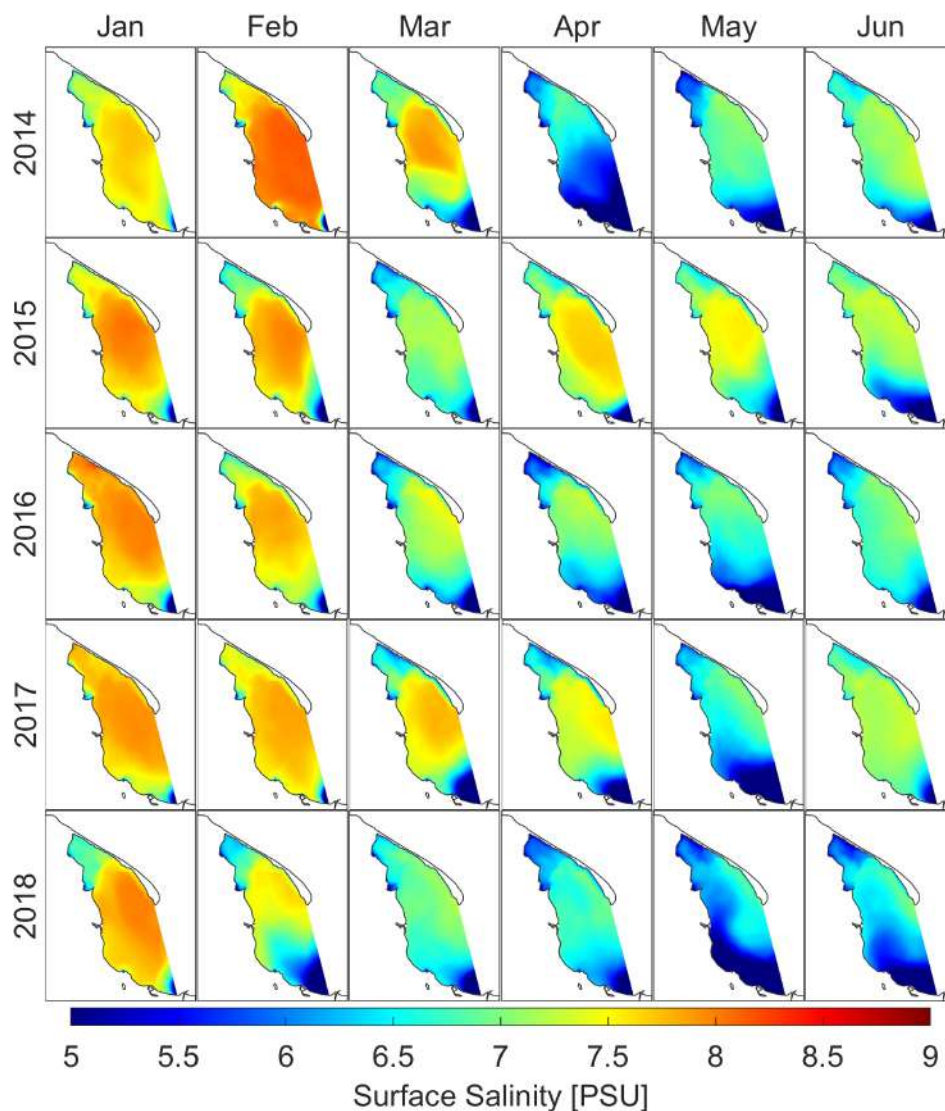


Figure A17. Monthly means of salinity at sea surface for separated years. January to June.

Table A7. Monthly maximums for surface salinity for the years 2014–2018.

Year\Month	Jan	Feb	Mar	Apr	May	Jun	Jul	Aug	Sep	Oct	Nov	Dec
2014	7.75	8.16	7.93	6.95	7.16	7.38	7.24	7.41	7.45	7.72	7.96	8.08
2015	8.07	8.00	7.27	7.71	7.56	7.38	7.41	7.31	7.44	7.74	7.97	8.06
2016	8.19	7.88	7.53	7.31	7.08	7.25	7.49	7.47	7.30	7.67	8.05	8.02
2017	7.98	7.86	7.81	7.63	7.16	7.36	7.35	7.45	7.55	7.75	7.89	7.94
2018	8.00	7.68	7.28	7.01	7.03	7.09	7.13	7.01	7.39	7.70	7.81	7.92

Table A8. Monthly standard deviations for surface salinity for the years 2014–2018.

Year\Month	Jan	Feb	Mar	Apr	May	Jun	Jul	Aug	Sep	Oct	Nov	Dec
2014	0.33	0.47	0.82	0.90	0.72	0.58	0.70	0.46	0.43	0.28	0.36	0.34
2015	0.48	0.68	0.57	0.67	0.65	0.83	0.52	0.55	0.40	0.30	0.27	0.36
2016	0.59	0.53	0.78	0.77	0.98	0.62	0.64	0.39	0.53	0.34	0.35	0.41
2017	0.40	0.43	1.06	0.89	1.05	0.45	0.39	0.47	0.51	0.26	0.34	0.41
2018	0.48	0.98	0.77	0.65	1.25	0.88	0.81	0.50	0.57	0.26	0.39	0.49

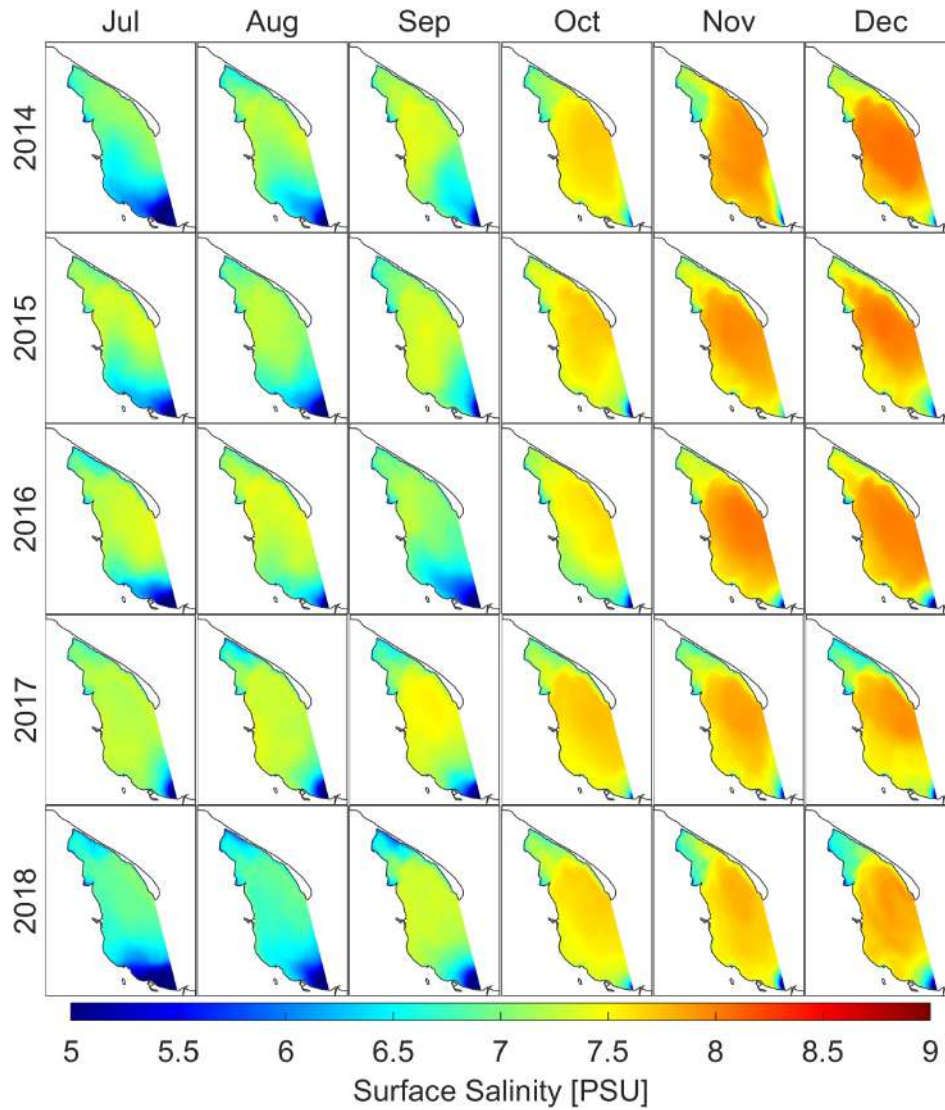


Figure A18. Monthly means of salinity at sea surface for separated years. July to December.

Appendix A.3. Sea Surface Height

Table A9. Monthly means for sea surface height for the years 2014–2018.

Year\Month	Jan	Feb	Mar	Apr	May	Jun	Jul	Aug	Sep	Oct	Nov	Dec
2014	0.28	-0.37	-0.52	0.29	0.49	0.26	0.72	-0.16	0.02	-0.01	0.07	-1.03
2015	-0.96	-0.37	0.15	-0.65	-0.24	-0.08	-0.64	0.25	-0.15	0.06	-1.23	-0.98
2016	-0.43	-0.54	0.04	-0.02	0.41	0.33	-0.04	-0.43	-0.23	0.90	-0.26	-1.14
2017	-0.66	-0.08	-0.18	-0.19	0.48	-0.23	-0.14	-0.57	-0.29	-1.14	-0.90	-0.88
2018	-0.30	0.16	0.87	0.49	0.93	0.32	0.44	-0.22	-0.87	-0.64	-0.15	-0.75
mean	-0.41	-0.24	0.07	-0.02	0.41	0.12	0.07	-0.23	-0.30	-0.17	-0.49	-0.96

Table A10. Monthly minimums for sea surface height for the years 2014–2018.

Year\Month	Jan	Feb	Mar	Apr	May	Jun	Jul	Aug	Sep	Oct	Nov	Dec
2014	-0.67	-1.04	-1.01	-0.01	-0.01	-0.87	0.08	-0.50	-0.25	-0.42	-0.64	-1.39
2015	-1.57	-0.60	-0.14	-2.66	-0.74	-0.68	-1.27	-0.22	-0.42	-0.37	-2.00	-1.40
2016	-0.67	-0.84	-0.32	-0.27	-0.02	-0.15	-0.92	-1.02	-0.48	0.03	-1.03	-3.35
2017	-1.68	-0.48	-0.61	-0.93	-0.12	-0.78	-0.56	-0.82	-0.65	-1.94	-1.27	-1.22
2018	-0.82	-0.15	0.30	0.08	0.21	-0.32	-0.47	-0.57	-1.24	-0.83	-0.69	-1.28

Table A11. Monthly maximums for sea surface height for the years 2014–2018.

Year\Month	Jan	Feb	Mar	Apr	May	Jun	Jul	Aug	Sep	Oct	Nov	Dec
2014	2.60	1.04	0.43	1.27	1.59	1.57	1.34	0.33	0.49	1.53	2.81	0.11
2015	0.21	0.23	0.70	1.21	0.69	0.78	0.08	1.20	0.33	1.65	-0.03	0.27
2016	0.16	0.27	1.01	1.04	1.71	1.23	1.06	0.24	0.24	2.37	0.44	0.05
2017	0.05	1.10	1.06	1.19	1.70	0.60	0.60	-0.05	0.30	-0.49	-0.14	0.06
2018	0.70	0.90	1.57	1.42	2.18	1.50	1.83	0.22	-0.20	-0.34	1.01	-0.29

Table A12. Monthly standard deviations for sea surface height for the years 2014–2018.

Year\Month	Jan	Feb	Mar	Apr	May	Jun	Jul	Aug	Sep	Oct	Nov	Dec
2014	0.73	0.52	0.20	0.26	0.29	0.39	0.23	0.15	0.12	0.39	0.62	0.24
2015	0.21	0.15	0.15	0.49	0.20	0.25	0.20	0.24	0.11	0.31	0.22	0.24
2016	0.17	0.14	0.19	0.21	0.36	0.22	0.29	0.19	0.10	0.34	0.17	0.49
2017	0.23	0.31	0.24	0.31	0.36	0.19	0.14	0.11	0.15	0.20	0.20	0.17
2018	0.35	0.20	0.22	0.17	0.44	0.40	0.40	0.13	0.15	0.07	0.33	0.21

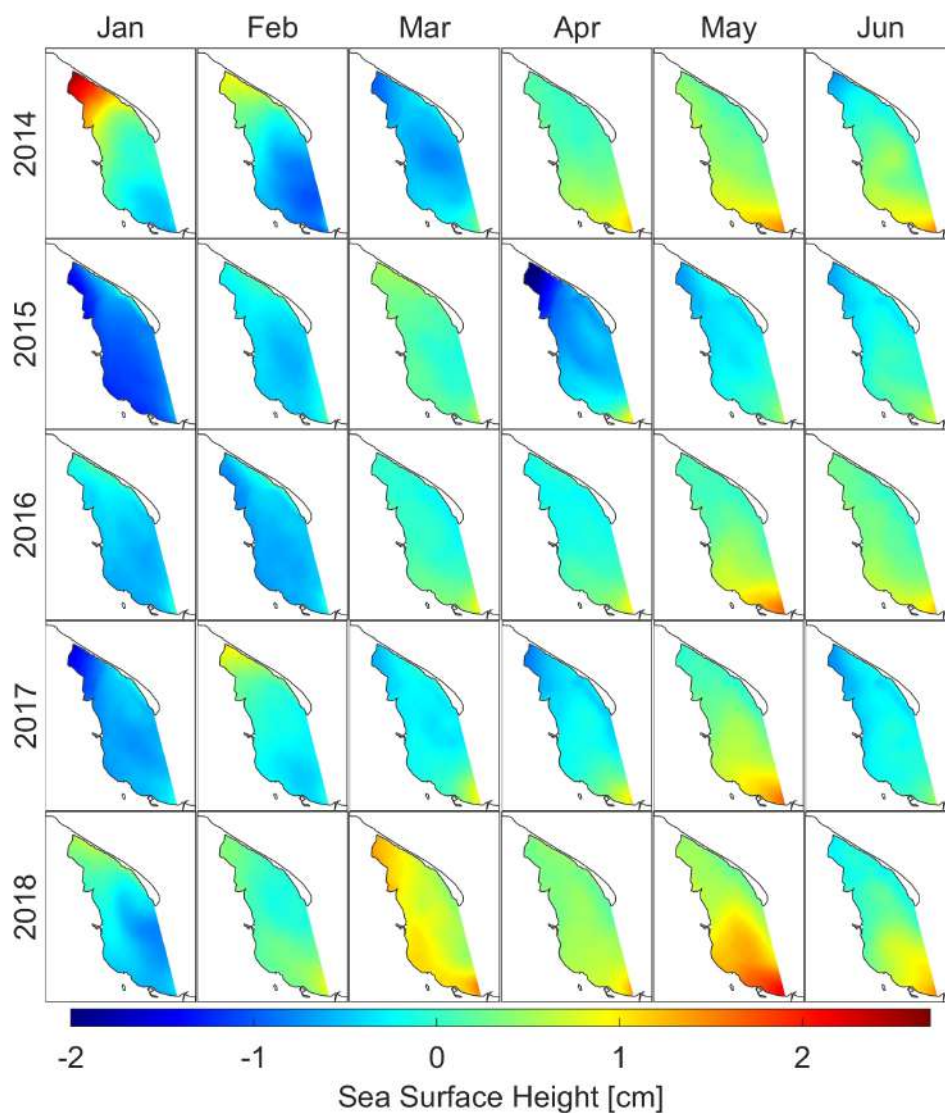


Figure A19. Monthly means of sea surface height for separated years. January to June.

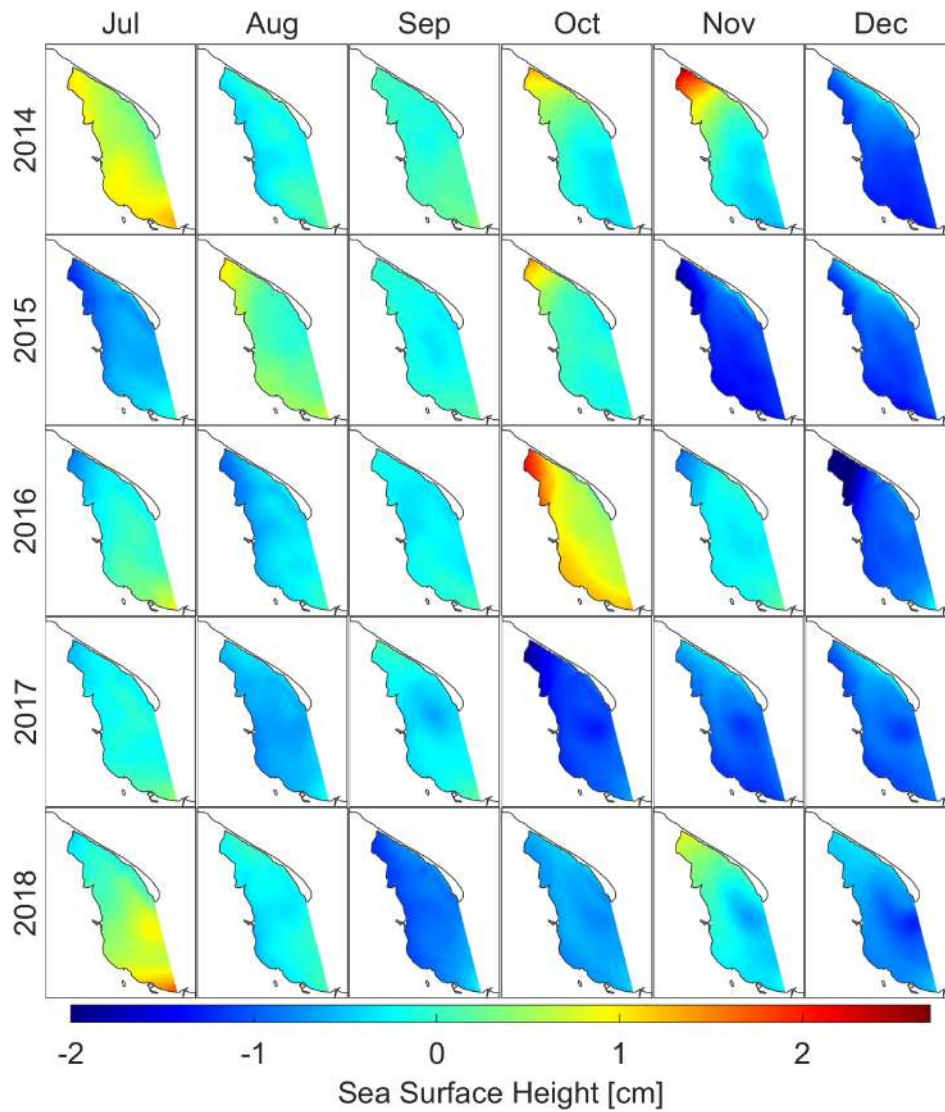


Figure A20. Monthly means of sea surface height for separated years. July to December.

Appendix A.4. Currents

Table A13. Monthly means for currents for the years 2014–2018.

year\month	Jan	Feb	Mar	Apr	May	Jun	Jul	Aug	Sep	Oct	Nov	Dec
2014	5.54	4.76	2.69	1.74	1.97	4.54	2.47	3.47	1.61	3.32	4.85	4.45
2015	4.95	3.43	2.07	5.31	2.81	3.66	3.96	2.48	1.57	2.98	4.98	5.27
2016	3.63	4.06	2.29	2.10	2.84	2.26	3.43	3.79	1.71	2.89	3.33	5.60
2017	4.53	3.24	3.41	3.57	2.57	3.13	2.55	2.25	2.26	3.90	3.85	4.64
2018	4.21	2.75	2.70	2.63	4.31	3.64	3.89	2.34	2.68	2.88	3.73	3.19
mean	4.57	3.65	2.63	3.07	2.90	3.45	3.26	2.87	1.97	3.19	4.15	4.63

Table A14. Monthly maximums for currents for the years 2014–2018.

year\month	Jan	Feb	Mar	Apr	May	Jun	Jul	Aug	Sep	Oct	Nov	Dec
2014	21.33	24.60	20.64	19.41	14.10	18.70	14.92	14.04	14.06	10.99	16.72	17.13
2015	20.94	23.54	21.32	19.88	12.44	15.64	17.05	13.81	10.90	13.08	17.67	16.91
2016	21.79	23.17	20.91	15.51	12.94	12.46	14.71	16.63	11.92	15.40	13.28	18.14
2017	20.89	22.95	20.47	13.98	14.99	15.94	16.33	9.00	9.95	12.92	13.51	16.13
2018	21.33	23.48	23.57	16.17	14.88	15.18	27.59	14.53	16.11	14.30	14.31	16.87

Table A15. Monthly standard deviations for currents for the years 2014–2018.

year\month	Jan	Feb	Mar	Apr	May	Jun	Jul	Aug	Sep	Oct	Nov	Dec
2014	3.55	2.63	1.70	1.47	1.45	3.40	1.73	2.04	1.19	1.79	3.18	1.68
2015	1.87	2.09	1.84	3.09	1.61	2.12	2.16	1.45	1.06	1.77	1.82	2.06
2016	1.96	1.66	1.97	1.67	1.75	1.66	2.55	2.17	1.31	1.63	1.36	2.64
2017	1.96	1.78	1.88	2.64	2.31	2.10	1.94	1.28	1.55	1.90	1.93	2.08
2018	2.08	2.31	2.50	1.89	3.11	2.55	3.59	1.53	1.51	1.48	2.43	1.84

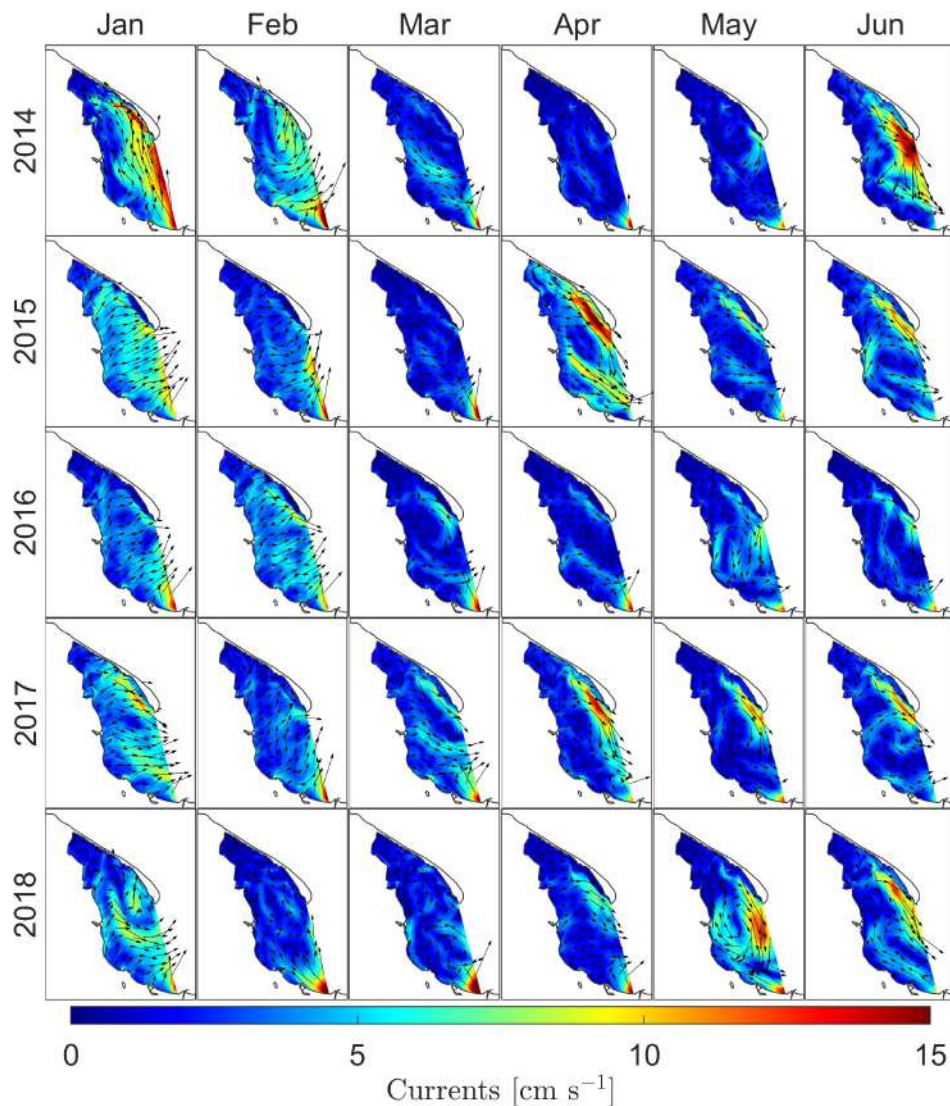


Figure A21. Monthly means of currents at surface level for separated years. January to June.

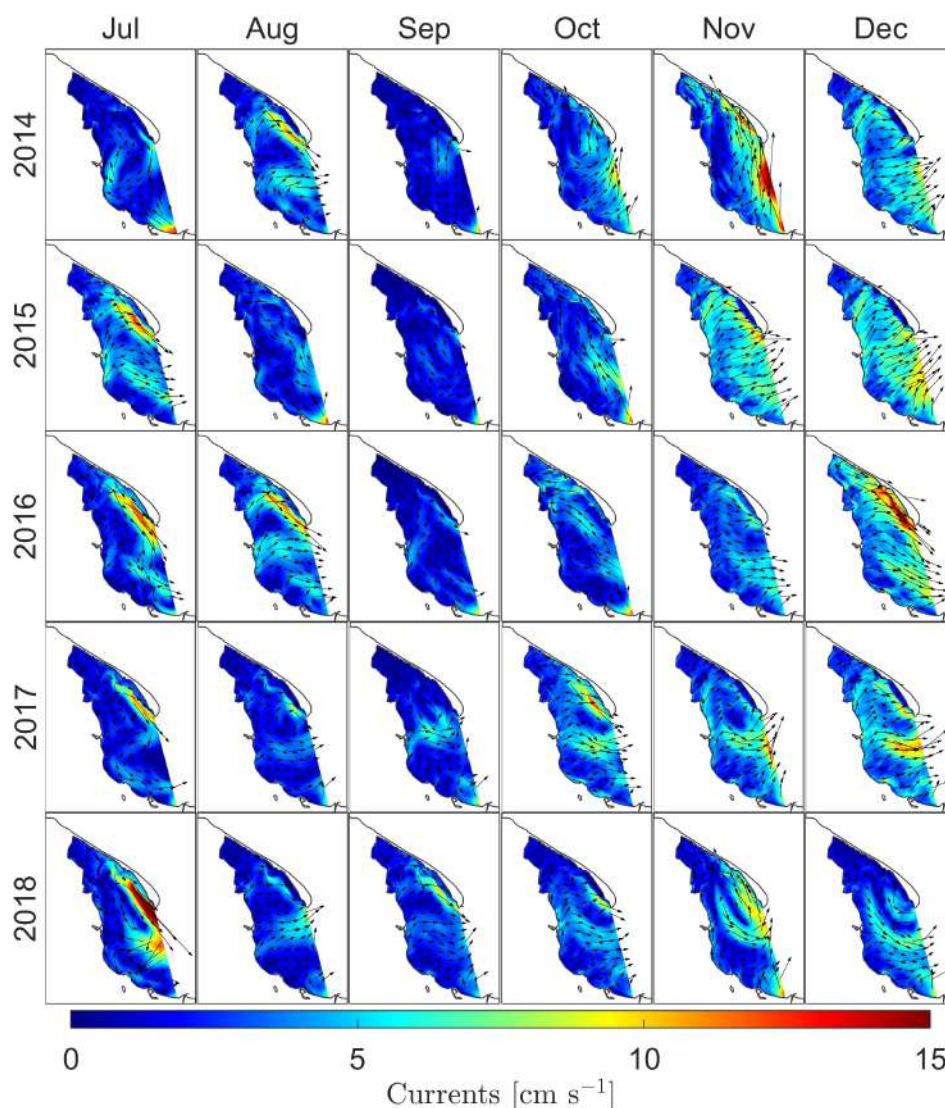


Figure A22. Monthly means of currents at surface level for separated years. July to December.

References

1. Kruk-Dowgiałło, L.; Szaniawska, A. Gulf of Gdańsk and Puck Bay. In *Ecology of the Baltic Coastal Waters*; Schiewer, U., Ed.; Springer: Berlin, Germany, 2010; pp. 154–157.
2. Dzierzbicka-Głowacka, L.; Janecki, M.; Szymczycha, B.; Dybowski, D.; Nowicki, A.; Kłostowska, Ż.; Obarska-Pempkowiak, H.; Zima, P.; Jaworska-Szulc, B.; Jakacki, J.; et al. Integrated information and prediction Web Service WaterPUCK General concept. *MATEC Web Conf.* **2018**, *210*, 02011. [[CrossRef](#)]
3. Dzierzbicka-Głowacka, L.; Janecki, M.; Dybowski, D.; Szymczycha, B.; Obarska-Pempkowiak, H.; Wojciechowska, E.; Zima, P.; Pietrzak, S.; Pazikowska-Sapota, G.; Jaworska-Szulc, B.; et al. A New Approach for Investigating the Impact of Pesticides and Nutrient Flux from Agricultural Holdings and Land-Use Structures on Baltic Sea Coastal Waters. *Pol. J. Environ. Stud.* **2019**, *28*, 2531–2539. [[CrossRef](#)]
4. Dzierzbicka-Głowacka, L.; Pietrzak, S.; Dybowski, D.; Białoskórski, M.; Marcinkowski, T.; Rossa, L.; Urbaniak, M.; Majewska, Z.; Juszowska, D.; Nawalany, P.; et al. Impact of agricultural farms on the environment of the Puck Commune: Integrated agriculture calculator—CalcGosPuck. *PeerJ* **2018**, *7*, e6478. [[CrossRef](#)] [[PubMed](#)]
5. Baltic Sea Bathymetry Database Version 0.9.3. Available online: <http://data.bshc.pro/> (accessed on 8 May 2012).
6. Large, W.G.; McWilliams, J.C.; Doney, S.C. Oceanic vertical mixing: A review and a model with a nonlocal boundary layer parameterization. *Rev. Geophys.* **1994**, *32*, 363–403. [[CrossRef](#)]

7. Durski, S.M.; Glenn, S.M.; Haidvogel, D.B. Vertical mixing schemes in the coastal ocean: Comparison of the level 2.5 Mellor-Yamada scheme with an enhanced version of the K profile parameterization. *J. Geophys. Res.* **2004**, *109*, C01015. [[CrossRef](#)]
8. McDougall, T.J.; Jackett, D.R.; Wright, D.G.; Feistel, R. Accurate and Computationally Efficient Algorithms for Potential Temperature and Density of Seawater. *J. Atmos. Ocean. Technol.* **2003**, *20*, 730–741. [[CrossRef](#)]
9. Arheimer, B.; Dahné, J.; Donnelly, C.; Lindström, G.; Strömqvist, J. Water and Nutrient Simulations Using the HYPE Model for Sweden vs. the Baltic Sea Basin—Influence of Input-Data Quality and Scale. *Hydrol. Res.* **2012**, *43*, 315–329. [[CrossRef](#)]
10. Donnelly, C.; Rosberg, J.; Isberg, K. A Validation of River Routing Networks for Catchment Modelling from Small to Large Scales. *Hydrol. Res.* **2012**, *44*, 917–925. [[CrossRef](#)]
11. Donnelly, C.; Andersson, J.C.M.; Arheimer, B. Using Flow Signatures and Catchment Similarities to Evaluate the E-HYPE Multi-Basin Model across Europe. *Hydrol. Sci. J.* **2016**, *61*, 255–273. [[CrossRef](#)]
12. Zima, P. Modeling of the Two-Dimensional Flow Caused by Sea Conditions and Wind Stresses on the Example of Dead Vistula. *Pol. Marit. Res.* **2018**, *25*, 166–171. [[CrossRef](#)]
13. Szydłowski, M.; Kolerski, T.; Zima, P. Impact of the Artificial Strait in the Vistula Spit on the Hydrodynamics of the Vistula Lagoon (Baltic Sea). *Water* **2019**, *11*, 990. [[CrossRef](#)]
14. Zima, P. Simulation of the Impact of Pollution Discharged by Surface Waters from Agricultural Areas on the Water Quality of Puck Bay, Baltic Sea. *Euro-Mediterr. J. Environ. Integr.* **2019**, *4*, 16. [[CrossRef](#)]
15. Zima, P. Investigations On Water Circulation in Animal Sea-Water Basins—On the Example of Seals’ Breeding Pools. *Pol. Marit. Res.* **2017**, *24*, 224–229. [[CrossRef](#)]
16. Zima, P. Mathematical Modeling of the Impact Range of Sewage Discharge on the Vistula Water Quality in the Region of Włocławek. In *Free Surface Flows and Transport Processes*; Kalinowska, M.B., Mrokowska, M.M., Rowiński, P.M., Eds.; Springer: Basel, Switzerland, 2018; pp. 489–502.
17. Hordoir, R.; Axell, L.; Löptien, U.; Dietze, H.; Kuznetsov, I. Influence of Sea Level Rise on the Dynamics of Salt Inflows in the Baltic Sea. *J. Geophys. Res. Ocean.* **2015**, *120*, 6653–6668. [[CrossRef](#)]
18. Pemberton, P.; Löptien, U.; Hordoir, R.; Höglund, A.; Schimanke, S.; Axell, L.; Haapala, J. Sea-Ice Evaluation of NEMO-Nordic 1.0: A NEMO-LIM3.6-Based Ocean–Sea-Ice Model Setup for the North Sea and Baltic Sea. *Geosci. Model Dev.* **2017**, *10*, 3105–3123. [[CrossRef](#)]
19. Taylor, K.E. Summarizing Multiple Aspects of Model Performance in a Single Diagram. *J. Geophys. Res. Atmos.* **2001**, *106*, 7183–7192. [[CrossRef](#)]
20. Osiński, R. Symulacja Procesów Dynamicznych w Morzu Bałtyckim Zintegrowanym Modelem Ocean Lód. Ph.D. Thesis, Institute of Oceanology Polish Academy of Sciences, Sopot, Poland, 2007; pp. 79–85.
21. Lisi, I.; Feola, A.; Bruschi, A.; Pedroncini, A.; Pasquali, D.; Di Risio, M. Mathematical Modeling Framework of Physical Effects Induced by Sediments Handling Operations in Marine and Coastal Areas. *J. Mar. Sci. Eng.* **2019**, *7*, 149. [[CrossRef](#)]
22. Krawczyk, H.; Nykiel, M.; Proficz, J. Tryton Supercomputer Capabilities for Analysis of Massive Data Streams. *Pol. Marit. Res.* **2015**, *22*, 99–104. [[CrossRef](#)]



© 2019 by the authors. Licensee MDPI, Basel, Switzerland. This article is an open access article distributed under the terms and conditions of the Creative Commons Attribution (CC BY) license (<http://creativecommons.org/licenses/by/4.0/>).

4.2 Research paper no. 2

Dybowski, D., Dzierzbicka-Glowacka, L.A., Pietrzak, S., Juszkowska, D., Puszkarczuk, T., 2020a. *Estimation of nitrogen leaching load from agricultural fields in the Puck Commune with an interactive calculator*. PeerJ 8, e8899. <https://doi.org/10.7717/peerj.8899>

(IF¹ = 2.984; MEiN² = 100)

¹Journal Impact Factor (IF) according to the Journal Citation Reports

²Journal score according to the list of the Polish Ministry of Education and Science

Estimation of nitrogen leaching load from agricultural fields in the Puck Commune with an interactive calculator

Dawid Dybowski¹, Lidia Anita Dzierzbicka-Glowacka¹, Stefan Pietrzak², Dominika Juszkowska² and Tadeusz Puszkarczuk³

¹ Physical Oceanography Department, Ecohydrodynamics Laboratory, Institute of Oceanology Polish Academy of Sciences, Sopot, Poland

² Department of Water Quality, Institute of Technology and Life Sciences in Falenty, Raszyn, Poland

³ Municipality of Puck, Puck, Poland

ABSTRACT

Background: Nutrient leaching from agricultural fields is one of the main causes of pollution and eutrophication of the Baltic Sea. The quantity of nitrogen (N) leached from a particular field can be very different from the amount of N leached from other fields in a given region or even within a single farm. Therefore, it is necessary to estimate the quantity of N leached for each field separately.

Methods: An opinion poll has been conducted on 31 farms within the Puck Commune, which is approximately 3.6% of all farms located in this commune. Farmers provided data on the manner of fertilizing and cultivating crops on all their farms. For each field individually, on the basis of collected data, an estimated amount of the N leaching from the field has been determined.

Results: An interactive calculator to assist farmers in determining the quantity of N leaching from the agricultural field has been developed. The influence of factors shaping the amount of N leaching from a single field has been analyzed, and it has been determined that autumn plowing (specifically its absence) and the type of cultivated soil had the greatest average influence on this value in the studied sample.

Discussion: Due to the possible ways of reducing N leaching from agricultural fields, most of the studied fields were fertilized in an appropriate manner. However, in the studied sample there were fields for which the fertilization intensity significantly exceeded the recommended doses. In this context, a tool in the form of an interactive, easy-to-use N leaching calculator should help farmers to select appropriate doses and optimal fertilization practices.

Submitted 1 November 2019

Accepted 12 March 2020

Published 27 March 2020

Corresponding authors

Dawid Dybowski,

dzybowski@iopan.pl

Lidia Anita Dzierzbicka-Glowacka,

dzierzb@iopan.pl

Academic editor

Maria Luisa Fernandez-Marcos

Additional Information and
Declarations can be found on
page 18

DOI [10.7717/peerj.8899](https://doi.org/10.7717/peerj.8899)

© Copyright

2020 Dybowski et al.

Distributed under

Creative Commons CC-BY 4.0

OPEN ACCESS

Subjects Agricultural Science, Soil Science, Computational Science, Environmental Impacts

Keywords Nitrogen, Leaching, Agriculture, Puck Commune, Puck Bay, Calculator

INTRODUCTION

The aim of agriculture, as well as any human economic activity, is to maximize efficiency. On the one hand, there is an attempt to maximize income (from the sale of plant to animal products). On the other hand, there is an attempt to reduce costs (fertilizers, equipment, activities). Modern large-scale agriculture cannot be imagined without fertilizers and pesticides. Each plant needs a certain amount of nutrients to grow. Increasing fertilizing

intensity may increase the potential yield. However, this yield reaches its maximum at some point and further increases in fertilizing intensity do not increase the yield but cause additional costs. Beside the obvious costs of fertilizer and all fertilizing-related activities of the farmer, there is an additional cost to the environment (*Álvarez et al., 2017; Heisler et al., 2008; Howarth, 2008*). Nutrient leaching from agricultural fields is one of the main causes of pollution and eutrophication of the Baltic Sea (*Elofsson, 2003; Ning et al., 2018; Voss et al., 2011; Savchuk, 2018*). In 2012, approximately 48,600 tonnes of nitrogen (N) (45.2% of total riverine N load from Poland) was delivered to the Baltic Sea as a result of farm activities in Poland (*Sonesten et al., 2018*). In view of the above, it is necessary to take in the measures of farms to reduce N leaching from agricultural soils. Among the possible measures used for this purpose, there should also be tools for quantitative control of nitrate losses due to leaching from agricultural fields. The choice of methods to counteract these losses depends on the recognition of their amount. In this context, it should be emphasized that the risk of N leaching is often considered by the N balance surplus. According to *Kupiec (2015)*, reference levels of N-surplus defining the risk of water hazards are quoted in various sources. Research results indicate that N-surplus can be a good predictor of groundwater nitrate pollution (*Wick, Heumesser & Schmid, 2012; Fraters et al., 2015; Huang, Ju & Yang, 2017*). However, the usefulness of this indicator for determining the risk of surface water nitrate pollution is not obvious when it is defined on the basis of data for the whole farm. Moreover, *Van Beek, Brouwer & Oenema (2003)* claim that estimates of N leaching to surface water based on data obtained for N balance “at the farm gate” level may be biased due to the heterogeneous distribution of N-surpluses on individual fields. Therefore, these authors postulate that N leaching to surface water from each agricultural field can be described as a function of soil surface balance surplus. *Lord, Anthony & Goodlass (2002)* examining the relationship between N balance “at the farm gate” and N leaching found that N-surplus was weakly or even negatively correlated with the concentrations (or loads) of nitrates in river waters. Thus, the use of N-surplus estimated by the “at the farm gate” method to determine the risk of surface water N pollution may not be appropriate.

Surely, the quantity of N leached from a particular agricultural field can be very different from the quantity of N leached from other fields in a given region or even within a single farm. Therefore, it is necessary to estimate the amount of N leaching for each field separately. The factors shaping the magnitude of N leaching are climate, soil type and management system. Each of these factors (except the climate) may vary for different fields within a given region. Main factors related to agriculture influencing the N leaching are:

- cultivation of inter-crops,
- the time of soil tillage,
- application of natural fertilizers, especially in autumn,
- annual doses of natural and mineral fertilizers.

The aim of the research presented in this article is to assess the approximate total N leaching from agricultural fields located in the Puck Commune. In the previous stage of

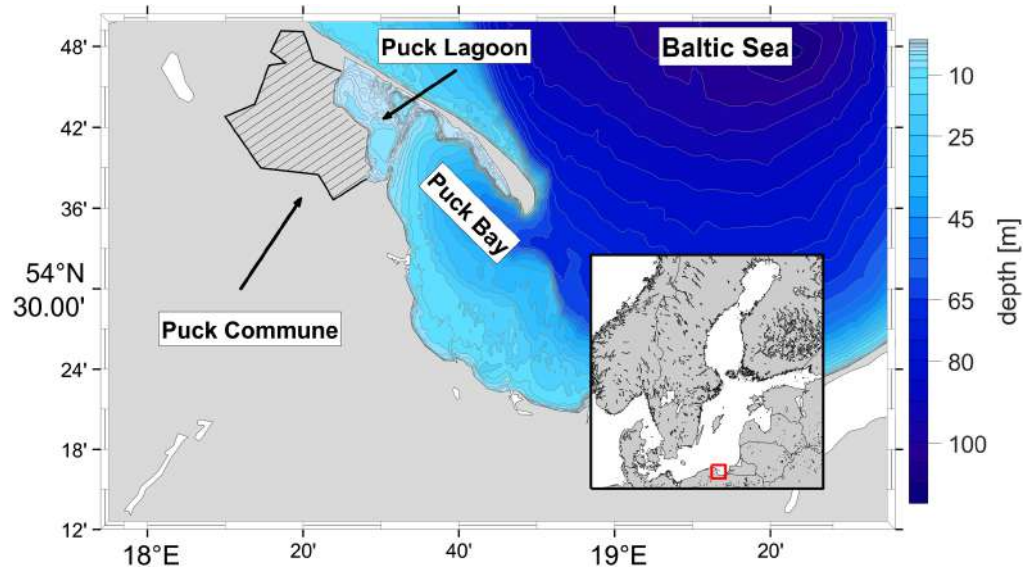


Figure 1 Localization of the Puck Commune and the bathymetry of the Puck Bay as a part of Gdańsk Basin. Full-size [DOI: 10.7717/peerj.8899/fig-1](https://doi.org/10.7717/peerj.8899/fig-1)

work, an integrated agriculture calculator for establishing the balance of nutrients using the “At the farm gate” method was developed (*Dzierzbicka-Głowacka et al., 2019b*). The research was conducted as part of the project on modeling of the impact of the agricultural holdings and land-use structure on the quality of water in the Bay of Puck—Integrated information and forecasting Service “WaterPUCK” (*Dzierzbicka-Głowacka et al., 2019a*).

METHODS

The Puck Commune is located in the north-eastern part of the Pomeranian Voivodeship (northern Poland), on the western shore of the Puck Bay which consists of the inner part called Puck Lagoon and the outer part of Puck Bay (see Fig. 1). The boundary between them runs from the Rybitwia Sandbank to the Cypel Rewski and has two straits within which there is an intensive water exchange between the Puck Lagoon and the outer part of the Puck Bay. Watercourses from Puck Municipality flow directly into the Puck Lagoon. Special attention should be paid to the quality of freshwater entering the Puck Lagoon. This water body is very sensitive to pollution due to geomorphological separation of the Puck Lagoon from the rest of the Puck Bay and its shallowness (the area of the Puck Lagoon is 30% of the entire Puck Bay and only about 6% of the water volume of the entire Puck Bay is located within Puck Lagoon). The ecohydrodynamic model of the Puck Bay called EcoPuckBay, whose hydrodynamic part has been validated (*Dybowski et al., 2019*), is in the final stage of preparation and is the high-resolution model describing the quality of the Puck Bay waters. In terms of climate, the area is located in a coastal region characterized by a high weather variability and, compared with other regions of Poland, colder summers and milder winters. The average temperature in summer is +13.5 °C and in winter +1.8 °C. The average annual precipitation does not exceed 700 mm.

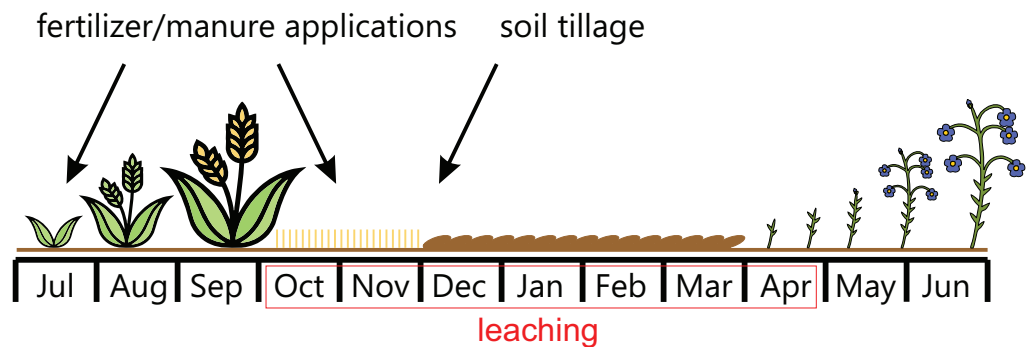



Figure 2 N leaching period.

Full-size  DOI: 10.7717/peerj.8899/fig-2

The prevailing winds are south and south-western. A characteristic phenomenon are breezes, as well as moving low-pressure areas causing strong winds, storms and heavy rainfalls. Snow cover lasts 40–60 days. The length of the growing season reaches 215 days (*Gawlikowska et al., 2009*). The multi-year annual average of solar surface irradiance is about 110 Wm^{-2} , while the multi-year summer average is two times higher (*Klimat w Polsce, 2014*).

The method for estimating the quantity of N leached from the agricultural field used in this article has been adapted to Polish conditions by *Aronsson & Ulén (2013)* from *Aronsson & Torstensson (2004)* and *Hoffmann (1999)* with support from a scientific team from the Institute of Technology and Life Sciences in Falenty.

It has been assumed that the growing season lasts from 1st September of the previous year to 31 August of the current year. N leaching begins at the beginning of autumn, immediately after harvest and continues throughout the winter until the start of the plant growing season (see *Fig. 2*). The amount of leaching is a result of all the activities undertaken in the previous crop season, and the main factors are:

- the type of crop grown in the summer before the start of the current season,
- methods of plant fertilization and soil tillage after harvesting.

Factor A—soil type and the impact of the climate

In soils with high cation-exchange capacity, the nutrients supplied with fertilizers (e.g., ammonium, potassium, magnesium) are not leached into the soil profile and groundwater but are exchanged from the sorption complex during plant development. The sorption capacity is also of key importance for limiting the migration and bioavailability of trace metals. In soils with excessive metal contamination (e.g., cadmium or lead), a high sorption capacity reduces the leaching and transfer of metals to the food chain.

The total N content of the soil is most dependent on humus content, mineralization conditions shaped by water conditions of the soil and climate, the type of bedrock, the direction and degree of advancement of the soil-forming process. In soils used for agricultural purposes, an important factor shaping the N content is the level of organic and mineral fertilization and crop rotation, especially the share of legumes binding free N

Table 1 Basic N leaching ($\text{kg N}\cdot\text{ha}^{-1}$) with different amounts of precipitation and from different soil types. Source: *Aronsson & Ulén (2013)* based on *Aronsson & Torstensson (2004)* and *Hoffmann (1999)*.

Precipitation (mm)	Sandy soil	Loamy soil	Clay soil	Organic soil
500–700	30	20	15	30
700–1,000	40	30	20	40

from the air (*Lityński & Jurkowska, 1982*). The vast majority of the N in the soil is incorporated into the organic part of the solid phase of the soil. N occurs in soil in the form of mineral and organic compounds and as molecular N in soil air. It comes either from fertilization or from microbiological processes—ammonification and nitrification. The average mineral nitrogen content in soils in Poland ranges from about 6 to 11 mg N kg^{-1} depending on the soil type. The most easily available form of N for plants is nitrate nitrogen. It varies considerably during the year depending on the weather conditions, the intensity of uptake by the plants and the amount of fertilizer applied (*Fotyma, Kęsik & Pietruch, 2010*).

The majority of N transformations are determined by the activity of soil microflora. The transformations of N compounds in the soil have a significant influence on the overall natural N cycle. The balance of these transformations determines the conditions of N nutrition of plants and also determines the extent to which they use N fertilization. N mineralization consists of a set of processes leading to the formation of ammonia or ammonium N. This is essential for plants, as ammoniacal N is a form directly absorbed by their root system and is easily converted into nitrates, which are even more easily used by plants. N losses in the soil are caused by crop cultivation, water and wind erosion and denitrification processes. N in nitrate form can be denitrified or leached if it is not taken up by the plants. Because nitrate ions are highly mobile in soil, they move like water, that is, both upward (if evapotranspiration is higher than precipitation) and downward (otherwise). Therefore, a real threat of nitrate leaching occurs only during the winter half-year, because in the summer half-year, that is, when the temperature exceeds 5 °C, evapotranspiration dominates and water moves from deeper layers to the surface. Therefore, in the summer half-year nitrate leaching is recorded only after significant rain event. Nevertheless, with high nitrate content in the soil, there is a risk of eutrophication of surface water (especially the first layer) and therefore rational fertilizer management should be applied in accordance with the guidelines of the Code of Good Agricultural Practices (*Department for Environment, Food & Rural Affairs, 2009*) or the Nitrate Directive (*The Council of the European Communities, 1991*).

The method used in this article defines the concept of so-called basic leaching as the equivalent of N leaching losses in conventional cereal cultivation, under conditions of sustainable mineral fertilization and mid-autumn plowing, but without the use of organic fertilizers (*Aronsson & Ulén, 2013*). When determining the basic leaching value, the soil type and average precipitation in the region have been taken into account (*Table 1*).

Table 2 Factors affecting basic leaching depending on the crop in the previous year. Source: *Aronsson & Ulén (2013)* based on *Aronsson & Torstensson (2004)* and *Hoffmann (1999)*.

Crop in the previous year	Factor
Cereal	1.0
Cereal followed by winter wheat	0.9
Cereal followed by winter oilseed	0.8
Cereal and oilseed with undersown catch crops	0.7
Cereal and oilseed with catch crops sown after	0.9
Cereal with undersown ley (grass and legumes)	0.7
Oilseed	1.2
Oilseed followed by winter wheat	1.1
Oilseed with undersown catch crops	0.7
Oilseed with catch crops sown after	0.9
Finalising ley without plowing	0.6
Ley plowed in early autumn	2.0
Ley plowed in mid-autumn (October–December)	1.9
Potato	1.7
Potato followed by catch crop	1.2
Beet	0.9
Legumes	1.3
Flax	1.3

It should be emphasized that basic leaching does not determine the exact quantity of N leached from a given field, because it does not take into account variations of temperature, amount of precipitation and other quantities influencing N leaching from a specific measurement year. Despite these simplifications, basic leaching calculations can help farmers better understand what factors affect N leaching and what actions they can take to reduce it.

Factor B—type of crop grown in the previous season

The highest N leaching occurs in autumn and winter, that is, at the beginning of each crop year. It is mostly determined by the way in which the field was used in the previous crop year. Thus, crops grown in the previous crop rotation also influence the level of N leaching in the current crop cycle (Table 2).

So if new crops are sown in the autumn, N leaching will decrease, which must be taken into account when estimating the losses. Where temporary grassland is plowed in spring before a new crop is introduced, particular attention should be paid and the relevant coefficient in Table 2 should be multiplied by 1.5. Data from Table 2 cannot be treated only as crop-specific leaching values. For example, N leaching rates in cases such as fodder crops, fallow land, sugar beet and postharvest crops include corrections (adjustments) related to other factors contributing to the reduction of N leaching, for example, late plowing, plow-less tillage.

Table 3 Factor estimating effect of soil tillage on N basic leaching. Source: *Aronsson & Ulén (2013)* based on *Aronsson & Torstensson (2004)* and *Hoffmann (1999)*.

Soil tillage	Factor
In early autumn (August–September)	1.0
Late autumn (October–December)	0.8
No plowing in the autumn	0.7

Factor C—soil tillage

Frequent tillage and the associated soil mixing stimulate the release of nitrate N form from the soil, especially if the tillage is carried out at the beginning of autumn. In case of delay or failure to carry out cultivation operations in autumn, nitrate leaching is reduced. Therefore, a coefficient from [Table 3](#) must be used, taking into account the date of plowing in the previous year. If a perennial crop is grown in the field for fodder, the coefficient from the row “No plowing in the autumn” must be used. In the case of potatoes, beet and root crops, it should be assumed that harvesting means the same as soil tillage in late autumn.

Factor D—application of organic fertilizers

If manure is applied in autumn, some of its N content will be leached. Moreover, with fertilizer, both plant available (mineral) and unavailable (organic) N are introduced into the soil, and the release of mineral N from the latter is not always synchronized with the uptake cycle of the plants. This means that the risk of N leaching increases slightly even after spring application. As shown in [Table 3](#), under the spring application of manure and liquid fertilizers, N leaching is only slightly higher than when only mineral fertilizers in balanced doses are applied. After the application of organic fertilizers in autumn, the leaching is greater than after the application of mineral fertilizers. Slurry (livestock urine with a possible small amount of feces and/or water; contains on average 1–3% of dry matter) consists mainly of plant-available ammonium N, so its fertilizing effect can be compared to that of mineral N fertilizers. Solid manure, on the other hand, contains almost exclusively N in organic form (*Font-Palma, 2019*). Therefore, the release of mineral N from solid manure can be slower than from liquid organic fertilizers (*Antil et al., 2005*). Probably the most favorable way to use manure for N leaching is in spring rather than in autumn. There are discrepancies in the permissible date of application of fertilizers, but the provisions in this respect should be strictly observed (organic fertilizers in liquid and solid form should be applied in the period from 1st March to 30 November, except for fertilizers used in crops under protection, i.e., in greenhouses).

Factor E—excess N leaching

When the field is fertilized with natural or mineral fertilizers at doses appropriate to the nutritional requirements of the crops grown, N leaching may be considered to be low. If too much fertilizer is applied, the leaching will increase, although an overdose of fertilizer is not intentional. Such a situation is possible during the summer drought when small plants cannot fully benefit from the N introduced with the fertilizers in spring

and early summer. When estimating whether, and if so, too much N was applied on the field, it is appropriate to start by estimating the amount of crop-available N that remained from the previous growing season, that is, the total amount of mineral N supplied by mineral and/or natural fertilizers, and to add the amount of predicted additional N leaching losses due to exceeding the optimum fertilizer application rate for average yields on different soils (expressed in $\text{kg N}\cdot\text{ha}^{-1}$). In this way, a sum of leaching is obtained. The amount of N applied should be compared with the recommended N dose needed to obtain planned yield of cultivated plants. A good source of information on nutrient requirements of plants is the Program of measures to reduce pollution of waters with nitrates from agricultural sources and to prevent further pollution (*Ministry of Agriculture & Rural Development of Poland, 2018*).

The N load applied is the sum of the amount of N from mineral fertilizer and the expected (approximately) amount of N contained in the natural fertilizers used for cultivation. If the actual amount of N is greater than the recommended amount, refer to [Table 5](#) for the additional N leaching rate.

Calculations—total N leached from field

The first step in calculating the total N leached from the field (see [Fig. 3](#)) is to determine the extra N leaching from [Table 5](#).

It is necessary to calculate the fertilizer intensity first as:

$$I = \frac{\text{TN}}{A}, \quad \text{TN} = \sum_f m_f \cdot c_f,$$

where I is the fertilizer intensity ($\text{kg N}\cdot\text{ha}^{-1}$), TN is the total N load applied to the field (kg N), A is the area of the field (ha), m_f and c_f are mass of fertilizer (kg) and N content in specific fertilizer respectively, f indexes the fertilizers used in the field. It should be stressed that in the presented method the forms of nitrogen applied with mineral fertilizers are not differentiated and the exact date of application is not taken into account. This means that the method is susceptible to further improvements as the precise determination of the impact of these factors can significantly improve the values of the estimated quantities. In the next step, the excess over the recommended fertilizer intensity should be calculate as:

$$\text{Exc} = I - R \cdot C,$$

where Exc is the excess over the recommended fertilizer intensity ($\text{kg N}\cdot\text{ha}^{-1}$), R is the recommended N load per tonne of product ($\text{kg N}\cdot\text{tonne}^{-1}$), C is the expected crop (tonnes ha^{-1}). Depending on the value of Exc, for a given soil type, the appropriate value of estimated extra N leaching E is now selected from [Table 5](#). Finally, the total N leaching from the field is calculated as:

$$\text{TNL} = A \cdot B \cdot C \cdot D + E,$$

where TNL is the total N leaching from field ($\text{kg N}\cdot\text{ha}^{-1}$), A is basic leaching ($\text{kg N}\cdot\text{ha}^{-1}$) from [Table 1](#), B is the factor affecting basic leaching depending on the crop yield in the

Table 4 Factor for additional N leaching losses compared with basic leaching depending on manure type. Based on an application rate of 20–40 tonnes ha⁻¹. Source: *Aronsson & Ulén (2013)* based on *Aronsson & Torstensson (2004)* and *Hoffmann (1999)*.

Type of manure	Autumn	Spring
Solid manure	1.15	1.10
Slurry	1.30	1.10

Table 5 Estimated extra N leaching (kg N·ha⁻¹) for different soil types and the amount by which the recommended fertilizer doses have been exceeded. Source: *Aronsson & Ulén (2013)* based on *Aronsson & Torstensson (2004)* and *Hoffmann (1999)*.

Excess over the recommended fertilizer intensity (kg N·ha ⁻¹)	Sandy soil	Loamy soil	Clay soil	Organic soil
10–20	3	2	2	3
20–30	6	4	4	6
30–40	10	5	5	10
40–50	16	7	7	16
50–60	22	8	8	22

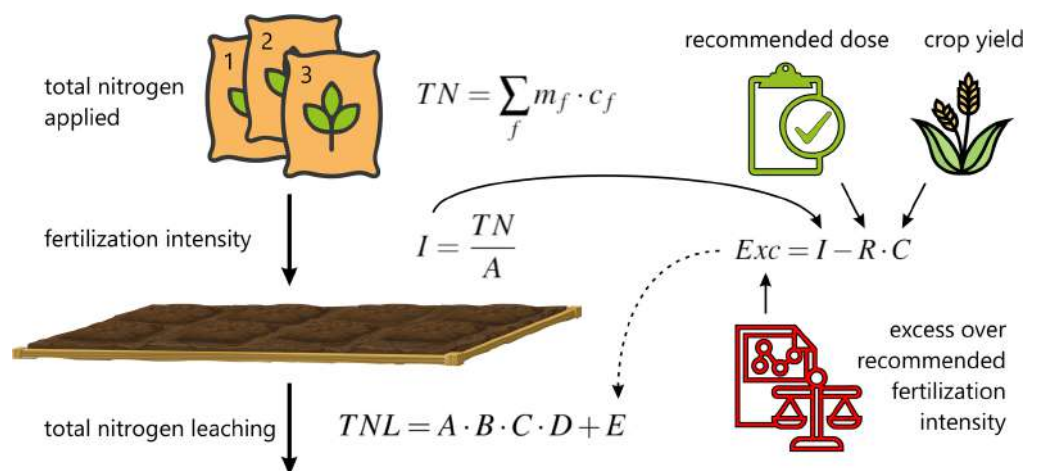


Figure 3 Scheme of total N leaching from the field calculations.

Full-size DOI: 10.7717/peerj.8899/fig-3

previous year from [Table 2](#), *C* is the factor estimating the effect of soil tillage on N basic leaching from [Table 3](#) and *D* is the factor for additional N leaching losses compared with basic leaching depending on manure type from [Table 4](#).

Opinion poll

An opinion poll was conducted on 31 farms within the Puck Commune, which is approximately 3.6% of all farms in this Commune. Field experiments were approved by the

Head of the Puck Commune. Farmers provided the following data for all their fields in the survey:

- soil type (determination of factor A)
- type of crop (determination of factor B)
- date of plowing (determination of factor C)
- information on manure (determination of factor D)
- mass of the product (determination of factor E)
- field area (determination of factor E)
- types and amounts of mineral fertilizers applied on the field (determination of factor E)

RESULTS

N leaching calculator

Within the Water PUCK project, a website in the form of an interactive calculator to assist farmers in determining the quantity of N leaching from the field was developed. Access to the calculator is through the main website of the project www.waterpuck.pl through the “Services” tab.

The method of calculating N leaching from an agricultural field described in this paper has been implemented as a website’s back-end. After entering the correct input data, the result is refreshed immediately.

The user can easily enter the same information as collected in opinion polls into the leaching calculator (see Fig. 4). Entering data is very intuitive and the result is refreshed on the fly. As a result, the farmer, agricultural adviser or other interested parties can quickly and easily obtain information about:

- basic N leaching ($\text{kg N}\cdot\text{ha}^{-1}$),
- total mass of N applied (kg N),
- modified N leaching ($\text{kg N}\cdot\text{ha}^{-1}$),
- crop yield (tonnes ha^{-1}),
- fertilization intensity ($\text{kg N}\cdot\text{ha}^{-1}$),
- extra N leaching ($\text{kg N}\cdot\text{ha}^{-1}$),
- total N leaching ($\text{kg N}\cdot\text{ha}^{-1}$),
- total N leached (kg N).

Using the N leaching calculator described here should help farmers to choose the right dosage of N-containing fertilizers to be applied on the field. In addition, the user of the calculator can check what effect the use of natural fertilizers will have on the N leaching. It also informs which fertilization practices increase the risk of excessive leaching of N.

Surface area of the studied fields

The Puck Commune has the area of 24,266 ha (242.6 km^2), which is 1.33% of the area of Pomeranian Voivodeship. Agricultural land is 61% of the Commune’s area, including

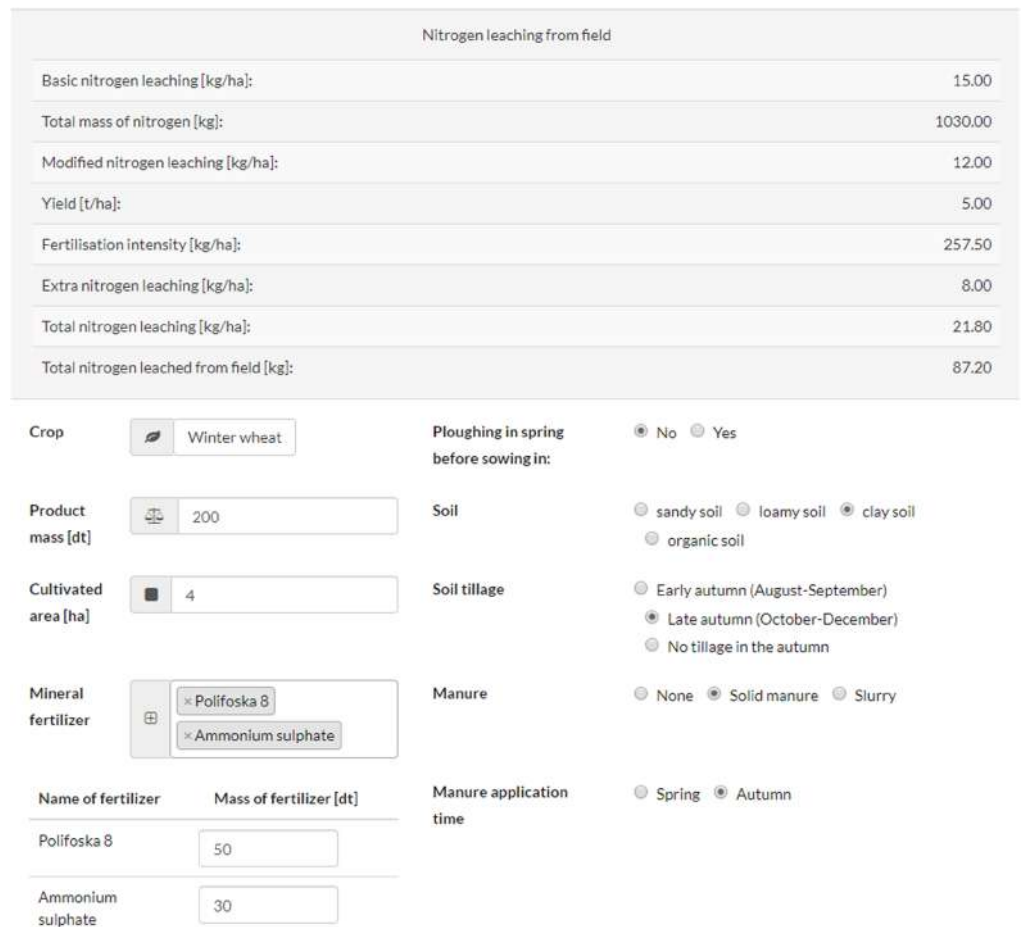


Figure 4 Calculating load of N leaching from cultivated field (website snapshot).

Full-size  DOI: [10.7717/peerj.8899/fig-4](https://doi.org/10.7717/peerj.8899/fig-4)

72.7% of arable land, 19.2% of meadows, 0.2% of orchards and 4.4% of pastures. Forests are 31.2% of the Puck Commune's area. The area of 291 studied fields varies from 0.1 to 25 ha with a median of 2.3 ha. The distribution of the size of the fields according to the type of crop is shown in a box diagram (see Fig. 5). On the vast majority of agricultural fields ($n = 182$) cereals (wheat, rye, oats, barley, triticale, grain mixtures) are grown and a median area of these fields is equal to 2.25 ha. The second crops with the highest number of fields are fodder crops (silage maize, grass mixtures on arable land) ($n = 55$) with a median area equal to 2.50 ha. Oilseeds (colza) are grown on 30 fields with a median area of 2.32 ha, root crops (potatoes) on 19 with a median area of 0.60 ha, legumes (field bean, lupin, field pea) on 4 with a median area of 4.59 ha and textile crops (linum) are grown on only one field of 5.00 ha.

The total area of all studied fields is equal to 956.74 ha which is about 6.5% of total agricultural land of the Puck Commune. Share of individual crops in the total studied area is presented in Fig. 6. Cereals are grown on more than 60% of the studied area, fodder

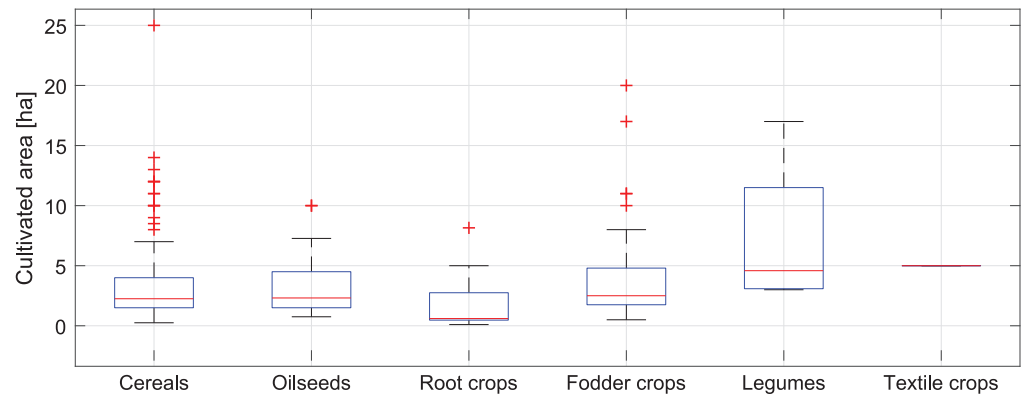


Figure 5 Box plot of the fields' area of cultivated crops on the studied farms in the Puck Commune in 2018. Full-size [DOI: 10.7717/peerj.8899/fig-5](https://doi.org/10.7717/peerj.8899/fig-5)

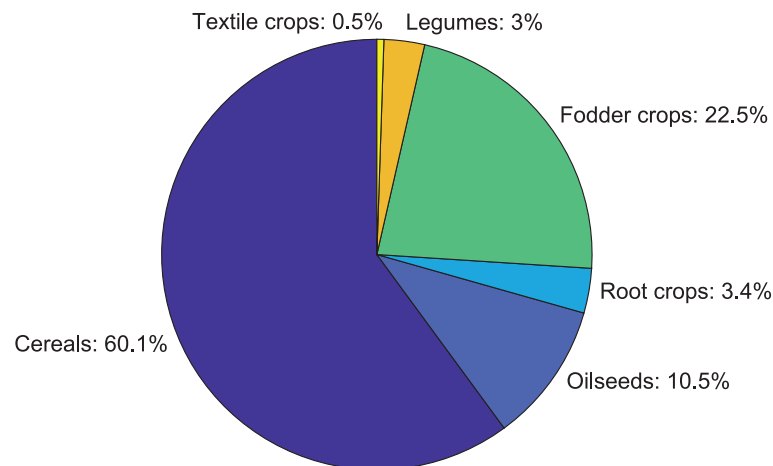


Figure 6 Share of individual crops area in the total cultivated area in 2018. Full-size [DOI: 10.7717/peerj.8899/fig-6](https://doi.org/10.7717/peerj.8899/fig-6)

crops on 22.5%, oilseeds on 10.5%, root crops on 3.4%, legumes on 3% and textile crops on 0.5%.

Basic leaching and its modifications

Clay soils with $15 \text{ kg N}\cdot\text{ha}^{-1}$ of basic leaching (Table 1) are 47.5% ($n = 140$) of the surface area of all studied fields, loamy soils with $20 \text{ kg N}\cdot\text{ha}^{-1}$ of basic leaching are 45.7% ($n = 134$) and sandy together with organic soils ($15 \text{ kg N}\cdot\text{ha}^{-1}$ of basic leaching) are 6.8% ($n = 17$) of the surface area of all studied fields. Table 2 shows that the type of crop cultivated in the previous year may have the greatest influence on the change in basic leaching and its modifications may range from -40% to 100% of the original value. The number of fields with a specific modification of base leaching is presented in Table 6.

Another factor that may influence the basic leaching is the soil tillage time. According to Table 3, the plowing time can change the basic leaching even up to -30% (if no plowing is done at all). Table 7 shows the number of fields depending on the plowing time.

Table 6 Number of fields and their total area with a specific modification of base leaching caused by the type of crop from the previous year.

Basic leaching modification	-30%	-20%	-10%	0%	+10%	+20%	+30%	+70%	+100%
Number of fields	1	25	26	170	23	10	16	15	5
Total area (ha)	2.00	122.72	74.51	552.52	65.37	33.76	60.17	30.39	15.30

Table 7 Number of fields and their total area according to soil tillage time.

Soil tillage (basic leaching modification)	Number of fields	Total area (ha)
Early autumn (0%)	32	120.66
Late autumn (-20%)	98	331.01
No plowing in the autumn (-30%)	161	505.07

Table 8 Number of fields and their total area with specified natural fertilization.

Application time and type of manure (basic leaching modification)	Number of fields	Total area (ha)
No manure application (0%)	182	636.14
Spring—solid manure and slurry (+10%)	63	176.11
Autumn—solid manure (+15%)	43	131.49
Autumn—slurry (+30%)	3	13.00

The third and last factor influencing the basic leaching rate is the application of natural fertilizers. In the case of spring natural fertilizer application, basic leaching is modified by +10% regardless of the type of fertilizer. In the case of natural fertilization in autumn, the use of solid manure increases the basic leaching by 15%, while the use of slurry increases the basic leaching by 30%. The categorization of fields by natural fertilization type is shown in [Table 8](#).

It should be emphasized that the change in basic leaching is the product of all three factors analyzed above. Lack of autumn plowing or late autumn plowing can only reduce the amount of basic leaching. However, both the type of crop cultivated in the previous year and the use of manure can potentially increase this value. Thus, the total change in basic leaching due to these factors can range from -51% to even +160% of its initial value resulting from soil type and average annual precipitation in a given region.

Fertilization intensity

The average value of mineral fertilization intensity calculated as the sum of the total load of N applied to the fields divided by the total area of all fields is equal to 110.94 kg N·ha⁻¹. The mineral fertilization intensity for each type of crop is shown in the box plot (see [Fig. 7](#)). The highest average intensity of mineral fertilization was applied to oilseeds fields (140.87 kg N·ha⁻¹) and the lowest to legumes and textile crops fields (32 and

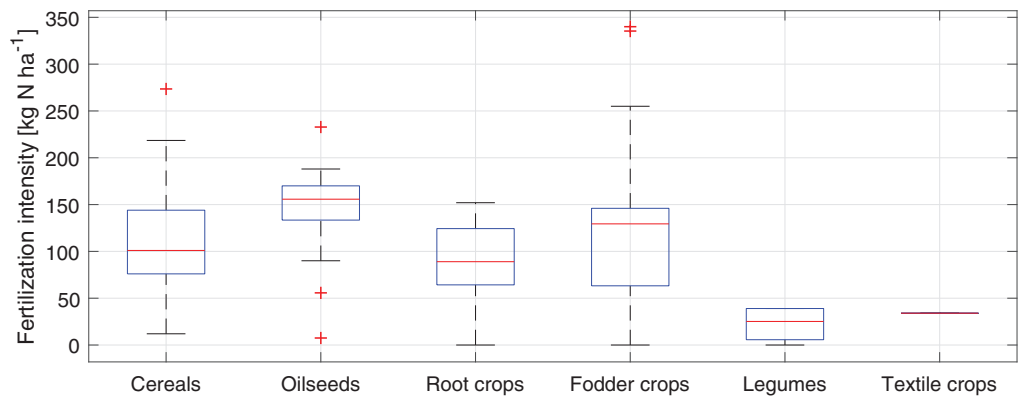


Figure 7 Box plot of the fertilization intensity of studied fields in the Puck Commune in 2018.

Full-size DOI: 10.7717/peerj.8899/fig-7

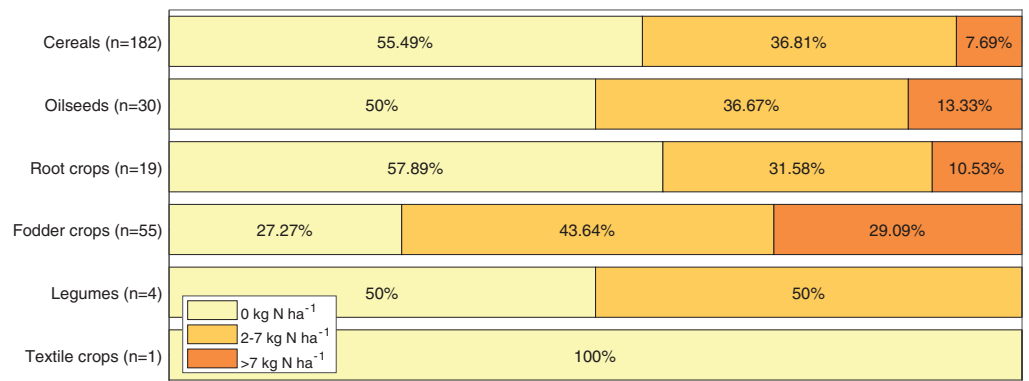


Figure 8 Extra N leaching from studied fields in the Puck Commune in 2018.

Full-size DOI: 10.7717/peerj.8899/fig-8

34 kg N·ha⁻¹ respectively). The most intensively fertilized fields (about 340 kg N·ha⁻¹) were cultivated with fodder crops.

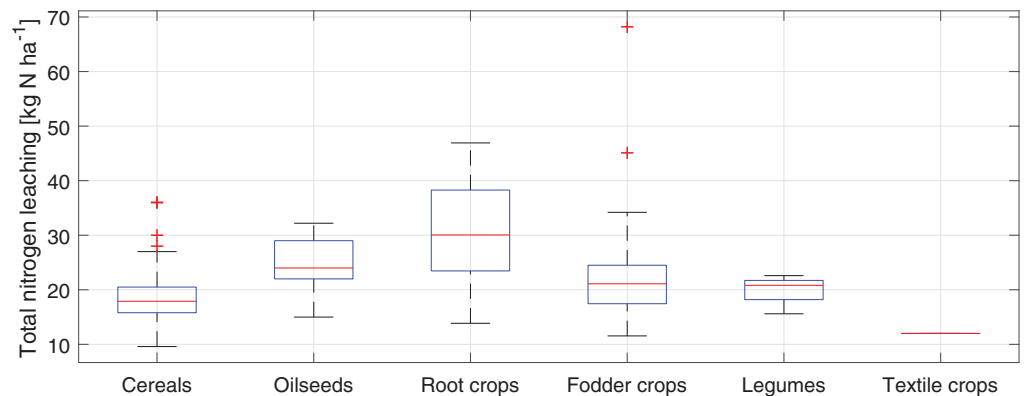
It should be noted that a large variation in the intensity of fertilization within a given type of crop does not necessarily mean that the intensity of fertilization deviates strongly from the recommended dose, but may result from the different N demand of plants included in a particular crop group.

Extra N leaching from field

For all 291 studied fields, on the basis of calculations of exceeding the recommended fertilization intensity and data from Table 4, an estimated value of the extra N leaching was determined. For almost half of all fields (49.8%) the extra N leaching is equal to 0 kg N·ha⁻¹. For 37.8% of the fields, the extra N leaching value is between 2 and 7 kg N·ha⁻¹. In the remaining 12.4% of the fields, the value of the extra N leaching exceeds 7 kg N·ha⁻¹. The amount of extra leaching due to the type of plant was presented as a bar chart (see Fig. 8).

Table 9 Number of fields with specified extra N leaching according to different soil types.

Extra N leaching	Loamy soil	Clay soil	Sandy and organic soils
0 kg N·ha ⁻¹	60	74	11
2–7 kg N·ha ⁻¹	57	49	4
>7 kg N·ha ⁻¹	23	11	2

**Figure 9** Box plot of the total N leaching from study fields in the Puck Commune in 2018.

Full-size DOI: 10.7717/peerj.8899/fig-9

The extra leaching of N depends on the excess over recommended fertilization intensity and the soil type on which the plant is cultivated. The higher the excess of the actual fertilizer intensity over the recommended fertilizer intensity, the greater the extra N leaching from the field is (Table 5). It is also worth comparing how the extra N leaching from the field varies due to the soil type (i.e., whether farmers apply higher than recommended doses on specific soil types). This comparison is presented in Table 9 and shows that such a relationship does not exist (i.e., the distribution of extra N leaching depending on the soil type is similar to the collective distribution for all fields).

Total N leaching from field

The total estimated N leaching from studied fields varies from 4.0 to 68.2 kg N·ha⁻¹ with a median of 19.8 kg N·ha⁻¹. The distribution of the total N leaching from field according to the type of crop is shown in a box diagram (see Fig. 9).

The highest average total leaching of N (weighted by fields' surface areas) is for fields cultivated with root crops (about 33 kg N·ha⁻¹) and the lowest for the field cultivated with textile crop (12 kg N·ha⁻¹).

DISCUSSION

In the examined sample of fields, the highest percentage are fields cultivated with cereals (over 60%) while the lowest percentage are fields cultivated with legumes and textile crops (3% and 0.5% respectively). Taking into account all three factors that influence the basic leaching, that is, the type of crop cultivated in the previous year, the time of soil tillage

and the application of natural fertilizers, we can see that the most dominant factor in the examined sample is the time of soil tillage which decreases basic leaching by 30% for more than half of the studied fields. For nearly 60% of the fields, the basic leaching is not changed by the crop type in the previous year, nor is it changed for more than 60% when it comes to natural fertilizer application. Furthermore, a change of basic leaching due to no plowing or late autumn plowing reduces the average basic leaching of N from the fields by approximately 26% which points to very good agricultural practices on soil tillage in the studied region. The amount of basic leaching increases on average by about 12.5% by applying natural fertilizers and, on average, less than 6% by the type of crop cultivated in the previous year.

The average value of mineral fertilization intensity in the studied sample (about $110 \text{ kg N}\cdot\text{ha}^{-1}$) is higher than Poland's average ($80 \text{ kg N}\cdot\text{ha}^{-1}$) while in other countries of the Baltic Sea region these values are around $30 \text{ kg N}\cdot\text{ha}^{-1}$ in Sweden and Estonia, over $100 \text{ kg N}\cdot\text{ha}^{-1}$ in Norway, c.a. $80 \text{ kg N}\cdot\text{ha}^{-1}$ in Denmark and around $75 \text{ kg N}\cdot\text{ha}^{-1}$ in Germany (*European Environment Agency, 2018*). A recent study conducted by *Wojciechowska et al. (2019)* aimed at examining loads of N and P released into the Puck Bay from three small first-order agricultural watersheds showed that the mean total N concentrations in the analyzed watercourses were similar to other rivers in central Europe with medium-intensive agricultural land use in the catchments. In the mentioned paper correlation was confirmed between precipitation and concentrations of nutrients in watercourses, pointing out the need for measures counteracting nutrient losses through leaching and erosion.

For almost half of all fields (49.8%) the extra N leaching is equal to $0 \text{ kg N}\cdot\text{ha}^{-1}$ which means that for the crops grown on these fields the recommended fertilizer doses have not been exceeded. However, there are fields (12.4%) where the extra N leaching exceeds $7 \text{ kg N}\cdot\text{ha}^{-1}$ and here is a possibility for the agricultural advisers to take action to improve the situation by consulting with the farmers cultivating these fields.

The average (weighted by the surface area of the fields) of the basic leaching of N for the studied sample resulting from the type of soil and precipitation is equal to $18.3 \text{ kg N}\cdot\text{ha}^{-1}$. While the average basic N leaching modified by factors resulting from the type of crop cultivated in the previous year, the time of soil tillage and the application of natural fertilizers is equal to about $17.5 \text{ kg N}\cdot\text{ha}^{-1}$ which suggests good agricultural practices due to mentioned factors. However weighted average of total N leaching for the studied field sample is about $20.3 \text{ kg N}\cdot\text{ha}^{-1}$ (it is greater than the median of the sample, which suggests slightly higher N leaching from relatively larger fields). Therefore, the average total N leaching is about 16% higher than the average modified basic leaching from field and it is caused by exceeding the recommended doses of mineral fertilizers.

Considering the quantity of N leaching from agricultural fields with particular types of crops, it was arranged in the following order: root crops > oilseeds > fodder crops > legumes > cereals > textile crops. Thus, the type of crop, according to what *Simmelsgaard (1998)* stated, is a key factor in shaping nitrate leaching. The largest N losses by leaching were recorded on fields where root crops, especially potatoes were grown. Use of these crops has a high N leaching potential (*Venterea, Hyatt & Rosen, 2011*) which is

related to their relatively shallow root system and high demand for N fertilizers. In literature, there are data showing that N leached from fields where potatoes were grown can reach $143 \text{ kg N}\cdot\text{ha}^{-1}$ (Jégo *et al.*, 2008). At the other end of the spectrum, relatively low quantity of N leaching (apart from N leaching from textile fields which accounts for a small share in the structure of crops) was recorded from fields occupied by cereals. Among them, winter cereals were dominant. To some extent, this state may be explained by the fact that winter cereal species as cover crops have a possibility of capturing N excess and reducing the N leaching by recycling nutrients between autumn and spring seasons (Brandi-Dohrn *et al.*, 1997). Meisinger & Ricigliano (2017) have shown in this area that winter cereal cover can reduce N leaching by 95% in a dry year and by 50% in a wet year compared to N leaching from uncovered crop fields.

It is difficult to compare estimated N leaching losses in quantitative terms with the results of other studies due to the multitude of natural and anthropogenic factors—often very specific for a given area. As an example, it is worth mentioning that in slightly similar conditions to the Puck Commune, in southwest Sweden N leached (from sandy loam soil) in a mild winter under wheat and oilseed rape amounted to $35\text{--}94 \text{ kg N}\cdot\text{ha}^{-1}$ and $16\text{--}23 \text{ kg N}\cdot\text{ha}^{-1}$, respectively. In cold winter, by contrast, N leaching levels were similar for all crops, at $32\text{--}58 \text{ kg N}\cdot\text{ha}^{-1}$ (Engström *et al.*, 2011). These values were higher than the amounts estimated for the tested fields in the Puck Commune. The average N leached from the study area ($203 \text{ kg N}\cdot\text{ha}^{-1}$) was within the lower range of annual losses of nitrates from arable land in southern Sweden at the end of the 20th century which were set at $15\text{--}45 \text{ kg N}\cdot\text{ha}^{-1}$ (Stenberg *et al.*, 1999).

CONCLUSIONS

The interactive N leaching calculator presented at work is a tool that allows farmers to enter data on their agricultural practices in a simple and intuitive way and that displays the results of calculations of the estimated quantity of N leaching in real time. By using a calculator, farmers can also simulate the impact that a change in their current practices will have on N leaching, and thus on soil quality and potentially higher yields in the future. At a time when agriculture is aimed to a massive scale crop cultivation where fertilization and plant protection techniques are extensively used to maximize production efficiency, particular attention should be paid to the risks associated with nutrient leaching. Among these threats, the potential risk of water pollution is particularly important. Further research should be carried out and as simple to implement as possible solutions should be created for farmers, which will ensure a significant reduction in the amount of nutrient leaching from agricultural fields. Forward-looking implementations and perspectives that can improve the quality of surface runoff receivers from fields and prevent erosion include all kinds of Green Infrastructure applications such as constructed wetlands and buffer strips along river beds.

ACKNOWLEDGEMENTS

The authors of this article would like to thank all the farmers who agreed to take part in the research.

ADDITIONAL INFORMATION AND DECLARATIONS

Funding

This work was supported by the National Centre for Research and Development of Poland within the BIOSTRATEG III program No: BIOSTRATEG3/343927/3/NCBR/2017.

The funders had no role in study design, data collection and analysis, decision to publish, or preparation of the manuscript.

Grant Disclosures

The following grant information was disclosed by the authors:

National Centre for Research and Development of Poland: BIOSTRATEG3/343927/3/NCBR/2017.

Competing Interests

The authors declare that they have no competing interests.

Author Contributions

- Dawid Dybowski analyzed the data, prepared figures and/or tables, authored or reviewed drafts of the paper, and approved the final draft.
- Lidia Anita Dzierzbicka-Glowacka conceived and designed the experiments, authored or reviewed drafts of the paper, and approved the final draft.
- Stefan Pietrzak conceived and designed the experiments, authored or reviewed drafts of the paper, and approved the final draft.
- Dominika Juszkowska analyzed the data, authored or reviewed drafts of the paper, and approved the final draft.
- Tadeusz Puzkarczuk performed the experiments, authored or reviewed drafts of the paper, and approved the final draft.

Field Study Permissions

The following information was supplied relating to field study approvals (i.e., approving body and any reference numbers):

Field experiments were approved by the Head of the Puck Commune.

Data Availability

The following information was supplied regarding data availability:

The raw data are available in the [Supplemental Files](#).

Supplemental Information

Supplemental information for this article can be found online at <http://dx.doi.org/10.7717/peerj.8899#supplemental-information>.

REFERENCES

- Álvarez X, Valero E, Santos RMB, Varandas SGP, Fernandes LFS, Pacheco FAL. 2017. Anthropogenic nutrients and eutrophication in multiple land use watersheds: best management

- practices and policies for the protection of water resources. *Land Use Policy* **69**:1–11 DOI [10.1016/j.landusepol.2017.08.028](https://doi.org/10.1016/j.landusepol.2017.08.028).
- Antil RS, Gerzabek MH, Haberhauer G, Eder G. 2005.** Long-term effects of cropped vs. fallow and fertilizer amendments on soil organic matter II Nitrogen. *Journal of Plant Nutrition and Soil Science* **168**(2):212–218 DOI [10.1002/jpln.200421634](https://doi.org/10.1002/jpln.200421634).
- Aronsson H, Torstensson G. 2004.** *Beräkning av olika odlingsåtgärders inverkan på kväveutlakningen*. Uppsala: Swedish University of Agricultural Sciences.
- Aronsson H, Ulén B. 2013.** Estimating nitrogen leaching from individual fields. In: Ulén B, Pietrzak S, Tonderski KS, eds. *Samoocena gospodarstw w zakresie zarz adzania składnikami nawozowymi i oceny warunków środowiskowych*. Falenty: Institute of Technology and Life Sciences in Falenty, 34–41.
- Brandi-Dohrn FM, Hess M, Selker JS, Dick RP, Kauffman SM, Hemphill DD. 1997.** Nitrate leaching under a cereal rye cover crop. *Journal of Environmental Quality* **26**(1):181–188 DOI [10.2134/jeq1997.00472425002600010026x](https://doi.org/10.2134/jeq1997.00472425002600010026x).
- Department for Environment, Food & Rural Affairs. 2009.** *Protecting our water, soil and air: a code of good agricultural practice for farmers, growers and land managers*. Norwich: The Stationery Office.
- Dybowski D, Jakacki J, Janecki M, Nowicki A, Rak D, Dzierzbicka-Głowacka L. 2019.** High-resolution ecosystem model of the Puck Bay (Southern Baltic Sea)—hydrodynamic component evaluation. *Water* **11**(10):2057.
- Dzierzbicka-Głowacka L, Janecki M, Dybowski D, Szymczycha B, Obarska-Pempkowiak H, Wojciechowska E, Zima P, Pietrzak S, Pazikowska-Sapota G, Jaworska-Szulc B, Nowicki A, Klostowska Z, Szymkiewicz A, Galer-Tatarowicz K, Wichorowski M, Białoskórski M, Puszkarczuk T. 2019a.** A new approach for investigating the Impact of pesticides and nutrient flux from agricultural holdings and land-use structures on Baltic Sea coastal waters. *Polish Journal of Environmental Studies* **28**(4):2531–2539.
- Dzierzbicka-Głowacka L, Pietrzak S, Dybowski D, Białoskórski M, Marcinkowski T, Rossa L, Urbaniak M, Majewska Z, Juskowska D, Nawalany P, Pazikowska-Sapota G, Kamińska B, Selke B, Korthals P, Puszkarczuk T. 2019b.** Impact of agricultural farms on the environment of the Puck commune: integrated agriculture calculator—CalcGosPuck. *PeerJ* **7**:e6478.
- Elofsson K. 2003.** Cost-effective reductions of stochastic agricultural loads to the Baltic Sea. *Ecological Economics* **47**(1):13–31 DOI [10.1016/j.ecolecon.2002.10.001](https://doi.org/10.1016/j.ecolecon.2002.10.001).
- Engström L, Stenberg M, Aronsson H, Lindén B. 2011.** Reducing nitrate leaching after winter oilseed rape and peas in mild and cold winters. *Agronomy for Sustainable Development* **31**(2):337–347 DOI [10.1051/agro/2010035](https://doi.org/10.1051/agro/2010035).
- European Environment Agency. 2018.** Agricultural land: nitrogen balance. Available at <https://www.eea.europa.eu/airs/2018/natural-capital/agricultural-land-nitrogen-balance>.
- Font-Palma C. 2019.** Methods for the treatment of cattle manure: a review. *Journal of Carbon Research* **5**(2):27.
- Fotyma M, Kęsik K, Pietruch C. 2010.** Mineral nitrogen in soils of Poland as an indicator of plants nutrient requirements and soil water cleanness. *Fertilizers and Fertilizaton* **38**:5–83.
- Fraters D, Leeuwen Tv, Boumans L, Reijs J. 2015.** Use of long-term monitoring data to derive a relationship between nitrogen surplus and nitrate leaching for grassland and arable land on well-drained sandy soils in the Netherlands. *Acta Agriculturae Scandinavica, Section B—Soil & Plant Science* **65**(Suppl. 2):144–154.

- Gawlikowska E, Seifert K, Pasieczna A, Kwecko P, Tomassi-Morawiec H, Król J. 2009. *Explanation to geoenvironmental (land-use) map of Poland 1: 50 000, sheet PUCK (6) and PUCK N (1071)*. Warsaw: The Polish Geological Institute and Ministry of Environment.
- Heisler J, Glibert PM, Burkholder JM, Anderson DM, Cochlan W, Dennison WC, Dortch Q, Gobler CJ, Heil CA, Humphries E, Lewitus A, Magnien R, Marshall HG, Sellner K, Stockwell DA, Stoecker DK, Suddleson M. 2008. Eutrophication and harmful algal blooms: a scientific consensus. *Harmful Algae* 8(1):3–13 DOI 10.1016/j.hal.2008.08.006.
- Hoffmann M. 1999. *Gårdsmodellen: en empirisk modell för kväveutlakning. Teknisk Rapport—Sveriges Lantbruksuniversitet, Avdelningen för Vattenvårdslära*, 48. Uppsala: Sveriges lantbruksuniv.
- Howarth RW. 2008. Coastal nitrogen pollution: a review of sources and trends globally and regionally. *Harmful Algae* 8(1):14–20 DOI 10.1016/j.hal.2008.08.015.
- Huang T, Ju X, Yang H. 2017. Nitrate leaching in a winter wheat-summer maize rotation on a calcareous soil as affected by nitrogen and straw management. *Scientific Reports* 7(1):1–11 DOI 10.1038/s41598-016-0028-x.
- Jégo G, Martínez M, Antigüedad I, Launay M, Sanchez-Pérez JM, Justes E. 2008. Evaluation of the impact of various agricultural practices on nitrate leaching under the root zone of potato and sugar beet using the STICS soil-crop model. *Science of the Total Environment* 394(2–3):207–221 DOI 10.1016/j.scitotenv.2008.01.021.
- Klimat w Polsce. 2014. Solar condition atlas-Climate IMGW-PiB. Available at <http://klimat.pogodynka.pl/en/solar-atlas/>.
- Kupiec JM. 2015. Przegląd metod bilansowania makroskładników NPK w produkcji rolnej. *Inżynieria i Ochrona Środowiska* 18(3):323–342.
- Lityński T, Jurkowska H. 1982. *Soil fertility and plant nutrition*. Warsaw: PWN.
- Lord EI, Anthony SG, Goodlass G. 2002. Agricultural nitrogen balance and water quality in the UK. *Soil Use and Management* 18(4):363–369 DOI 10.1111/j.1475-2743.2002.tb00253.x.
- Meisinger JJ, Ricigliano KA. 2017. Nitrate leaching from winter cereal cover crops using undisturbed soil-column lysimeters. *Journal of Environmental Quality* 46(3):576–584 DOI 10.2134/jeq2016.09.0372.
- Ministry of Agriculture and Rural Development of Poland. 2018. Ordinance of the Council of Ministers of 5 June 2018 on the adoption of the Programme of measures to reduce pollution of waters with nitrates from agricultural sources and to prevent further pollution. *Journal of Laws*, item 1339, p. 118. Warsaw: Ministry of Agriculture and Rural Development of Poland.
- Ning W, Nielsen AB, Ivarsson LN, Jilbert T, Åkesson CM, Slomp CP, André E, Broström A, Filipsson HL. 2018. Anthropogenic and climatic impacts on a coastal environment in the Baltic Sea over the last 1000 years. *Anthropocene* 21:66–79 DOI 10.1016/j.ancene.2018.02.003.
- Savchuk OP. 2018. Large-scale nutrient dynamics in the Baltic Sea, 1970–2016. *Frontiers in Marine Science* 5:450 DOI 10.3389/fmars.2018.00095.
- Simmelsgaard SE. 1998. The effect of crop, N-level, soil type and drainage on nitrate leaching from Danish soil. *Soil Use and Management* 14(1):30–36 DOI 10.1111/j.1475-2743.1998.tb00607.x.
- Sonesten L, Svendsen LM, Tornbjerg H, Gustafsson B, Frank-Kamenetsky D, Haapaniemi J. 2018. Sources and pathways of nutrients to the Baltic Sea: HELCOM PLC-6. Washington, D.C.: Helsinki Commission.
- Stenberg M, Aronsson H, Lindén B, Rydberg T, Gustafson A. 1999. Soil mineral nitrogen and nitrate leaching losses in soil tillage systems combined with a catch crop. *Soil and Tillage Research* 50(2):115–125 DOI 10.1016/S0167-1987(98)00197-4.

- The Council of the European Communities. 1991.** Council Directive 91/676/EEC of 12 December 1991 concerning the protection of waters against pollution caused by nitrates from agricultural sources. Available at <https://eur-lex.europa.eu/legal-content/EN/ALL/?uri=CELEX%3A31991L0676>.
- Van Beek C, Brouwer L, Oenema O. 2003.** The use of farmgate balances and soil surface balances as estimator for nitrogen leaching to surface water. *Nutrient Cycling in Agroecosystems* **67(3)**:233–244 DOI [10.1023/B:FRES.0000003619.50198.55](https://doi.org/10.1023/B:FRES.0000003619.50198.55).
- Venterea RT, Hyatt CR, Rosen CJ. 2011.** Fertilizer management effects on nitrate leaching and indirect nitrous oxide emissions in irrigated potato production. *Journal of Environmental Quality* **40(4)**:1103–1112 DOI [10.2134/jeq2010.0540](https://doi.org/10.2134/jeq2010.0540).
- Voss M, Dippner JW, Humborg C, Hürdler J, Korth F, Neumann T, Schernewski G, Venohr M. 2011.** History and scenarios of future development of Baltic Sea eutrophication. *Estuarine, Coastal and Shelf Science* **92(3)**:307–322 DOI [10.1016/j.ecss.2010.12.037](https://doi.org/10.1016/j.ecss.2010.12.037).
- Wick K, Heumesser C, Schmid E. 2012.** Groundwater nitrate contamination: factors and indicators. *Journal of Environmental Management* **111**:178–186 DOI [10.1016/j.jenvman.2012.06.030](https://doi.org/10.1016/j.jenvman.2012.06.030).
- Wojciechowska E, Pietrzak S, Matej-Łukowicz K, Nawrot N, Zima P, Kalinowska D, Wielgat P, Obarska-Pempkowiak H, Gajewska M, Dembska G, Jasiński P, Pazikowska-Sapota G, Galer-Tatarowicz K, Dzierzbicka-Głowacka L. 2019.** Nutrient loss from three small-size watersheds in the southern Baltic Sea in relation to agricultural practices and policy. *Journal of Environmental Management* **252**:109637 DOI [10.1016/j.jenvman.2019.109637](https://doi.org/10.1016/j.jenvman.2019.109637).

4.3 Research paper no. 3

Dybowski, D., Janecki, M., Nowicki, A., Dzierzbicka-Glowacka, L.A., 2020b. *Assessing the Impact of Chemical Loads from Agriculture Holdings on the Puck Bay Environment with the High-Resolution Ecosystem Model of the Puck Bay, Southern Baltic Sea*. *Water* 12, 2068. <https://doi.org/10.3390/w12072>

(IF¹ = 3.103; MEiN² = 70)

¹Journal Impact Factor (IF) according to the Journal Citation Reports

²Journal score according to the list of the Polish Ministry of Education and Science

Article

Assessing the Impact of Chemical Loads from Agriculture Holdings on the Puck Bay Environment with the High-Resolution Ecosystem Model of the Puck Bay, Southern Baltic Sea

Dawid Dybowski *, Maciej Janecki , Artur Nowicki  and Lidia Anita Dzierzbicka-Glowacka *

Physical Oceanography Department, Ecohydrodynamics Laboratory, Institute of Oceanology Polish Academy of Sciences, Powstańców Warszawy 55, 81-712 Sopot, Poland; mjanecki@iopan.pl (M.J.); anowicki@iopan.pl (A.N.)

* Correspondence: ddybowski@iopan.pl (D.D.); dzierzb@iopan.pl (L.A.D.-G.); Tel.: +48-587-311-912 (D.D.); +48-587-311-915 (L.A.D.-G.)

Received: 14 June 2020; Accepted: 20 July 2020; Published: 21 July 2020



Abstract: This paper describes the ecohydrodynamic predictive model EcoPuckBay—the ecosystem part—for assessing the state of the Puck Bay coastal environment and its ecosystem. We coupled the EcoPuckBay model with the land water flow models (Soil and Water Assessment Tool (SWAT) for surface water and Modflow for groundwater). To evaluate the quality of the results obtained from the EcoPuckBay model, a set of basic statistical measures for dissolved oxygen, chlorophyll-a, nitrates, and phosphates were calculated, such as mean, Pearson correlation coefficient (r), root-mean-square-error (RMSE), and standard deviation (STD). The analysis presented in this paper shows that the EcoPuckBay model produces reliable results. In addition, we developed a nutrient spread module to show the impact of agricultural activity on the waters of the Puck Bay. The EcoPuckBay model is also available in operational mode where users can access 60-h forecasts via the website of the WaterPUCK Project through the “Products” tab.

Keywords: 3D ecosystem model; nutrients; pesticides; Puck Bay; WaterPUCK

1. Introduction

Puck Bay is an example of a region that is highly vulnerable to anthropogenic impact. Therefore, it has been included in Natura 2000 (<https://ec.europa.eu/environment/nature/natura2000>). As a result, it requires preservation or restoration of the favourable conservation status of species and habitats by introducing appropriate protection measures. The strategic actions and the policy of the authority of the Puck District regarding the environmental protection involve not only the respect of the Natura 2000 legislation but also the execution of European legislation including Water Framework Directive, Marine Strategy Framework Directive, Habitats Directive, Baltic Sea Action Plan, and the strategic program of the environment protection for the Puck Commune. The main aims of the Puck Commune policy are the improvement of the environment, sustainable development, resilience to climate change, and protection of natural resources such as water.

WaterPUCK service, developed as a part of the WaterPUCK project (<https://www.waterpuck.pl/en/>), is a tool to carry out analyses and forecasts and to support key decisions for the management of areas where there is or hypothetically could be agricultural activity. WaterPUCK allows determining the impact of these activities on the surface and underground waters in the area of the analysed municipality and on the coastal waters of the Puck Bay.

The EcoPuckBay model has been developed as part of the WaterPUCK project. The hydrodynamic part of the EcoPuckBay has been described and validated [1]. The aim of the project is to create integrated information and predictive service for the Puck Commune through the development of a computer system providing the WaterPUCK service, which will clearly and practically assess the impact of farms and land use structures on surface waters and groundwater in the Puck Commune and consequently on the quality of the waters of the Puck Bay [2,3]. The construction of the service is based on in situ research, surveys, environmental data (chemical, physicochemical, and hydrological), and numerical modelling. WaterPUCK service is an integrated system consisting of computer models interconnected with each other, operating continuously by supplying it with meteorological data and combines four main modules:

- two calculators for farms in the Puck Commune as an interactive applications [4,5],
- a numerical model of groundwater flow based on Modflow [6],
- a comprehensive model of surface water runoff based on Soil & Water Assessment Tool (SWAT) [7],
- a three-dimensional numerical model of the Puck Bay ecosystem consisting of a hydrodynamic [1] and biochemical part with a nutrient spread module (this paper).

The spatial distributions of major biochemical tracers (e.g., nutrients, dissolved inorganic carbon, and oxygen) are governed by a combination of physics, chemistry, and biology. High-resolution numerical ecosystem models play an important role in deciphering coastal nutrient dynamics, in providing a quantitative framework for assessing the contributions of different processes, and in interpreting field observations. The following sections of the paper present the study area, the configuration of the EcoPuckBay model, its linkage with the surface water flow models and groundwater flow model, statistical analysis of the obtained results compared with both environmental and numerical data, an introduction of the nutrient spread module, and the operational mode of the model with 60-h forecasts.

2. Materials and Methods

2.1. Study Area

The southern part of the Baltic Sea enclosing the Puck Commune is a popular tourist region that is also heavily influenced by an anthropogenic activity of local residents and farming. This makes the Puck Bay a natural reservoir for waste deposition of fertilisers and other inputs delivered through the soil, groundwater, river, or direct deposition.

This region is massively shaped and influenced by several factors that can pressure the state of physical and biochemical parameters. One of the most important factors influencing the region's unique ecosystem is topography. The average depth of the Gulf of Gdańsk is about 50 m, with a maximum depth (Gdańsk Deep) of 118 m. From the northeast, it is surrounded by Hel Peninsula, which serves as a natural barrier for mixing with the open waters of the Baltic Sea, keeping the salinity ranging mostly within the range of 7–8 PSU with a deviation of around 1 PSU. Puck Bay is also heavily influenced by the river discharge from land, resulting in lowered salinity, especially in the coastal surface waters. The largest river in the region is the Vistula (for which the mouth is denoted as a symbol "1" in the left-hand side of Figure 1), discharging an average of over $1000 \text{ m}^3 \text{ s}^{-1}$ of freshwater. Water temperature in the region ranges from over $20 \text{ }^\circ\text{C}$ at the surface during summer, with the maximum usually in August, to around $2 \text{ }^\circ\text{C}$ in February. Water stratification is frequent during the warmer months, leading to occurrence of seasonal thermoclines. During the winter seasons, thermocline declines and the water becomes well mixed.

In order to assess the possibility and scale of eutrophication and water pollution, the area of interest and effective domain (for which size is reduced compared to the previous version [1] to focus mainly on changes occurring closer to the Puck Commune, where the strong influence of the waters flowing with the Vistula River is no longer as great as near its mouth) in the EcoPuckBay model covers

the western part of Gulf of Gdańsk (Figure 1). It can be divided further into a shallow part known as Puck Bay and the semi-enclosed Puck Lagoon to the northwest.

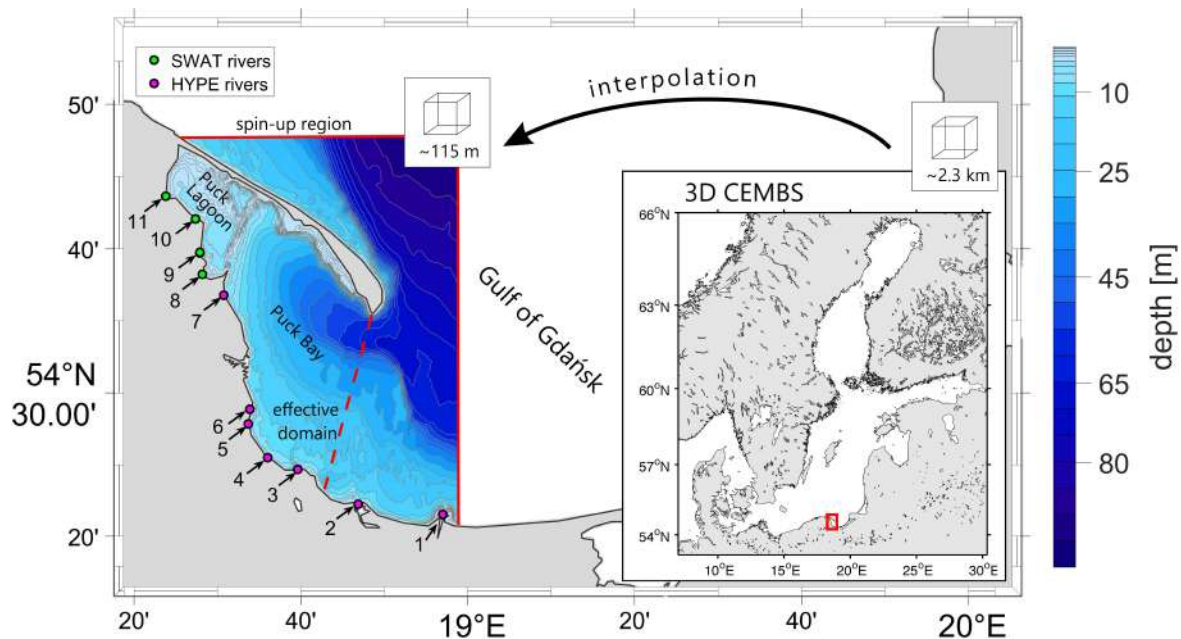


Figure 1. Model of the effective domain with topography and locations of mouths of watercourses included in the domain: Green dots (8–11) represent rivers that are delivered using the Soil & Water Assessment Tool (SWAT) hydrological model. Purple dots (1–7) indicate rivers with flows from the Hydrological Predictions for the Environment (HYPE) model.

2.2. EcoPuckBay Configuration

The EcoPuckBay model originates from Community Earth System Model (CESM)-coupled global climate model by National Center for Atmospheric Research (<http://www.cesm.ucar.edu/models/ccsm4.0>). CESM is a state-of-the-art model system consisting of five separate components with an additional coupler controlling time, exciting forces, domains, grids, and information exchange between the models. For the purpose of the WaterPUCK project, CESM was downscaled and adapted for the Puck Bay region for further development at the Institute of Oceanology, Polish Academy of Sciences.

The EcoPuckBay ecosystem module is based on the nutrient–phytoplankton–zooplankton–detritus (NPZD) approach [8]. The model predicts nutrient distributions (N, Si, and P), three phytoplankton functional types (diatoms, picophytoplankton/nanophytoplankton, and diazotrophs (nitrogen-fixing organisms)), chlorophyll-a as separate variables, zooplankton, pelagic detritus, dissolved oxygen, and pesticides (glyphosate, diflufenican, metazachlor, chlorpyrifos, and antrachinon). Sources of nutrients include atmospheric deposition and sedimentary sources. Sinking particles can be associated with ballast, and the presence of ballast changes the remineralization length scale assumed for the model. Many, though not all, models can be cast in a general form as a coupled set of time-dependent advection, diffusion, reaction equations:

$$\frac{\partial S}{\partial t} + (V + w_s)\nabla S - \sum_{i=1}^3 \frac{\partial}{\partial x_i} \left(K_{x_i} \frac{\partial S}{\partial x_i} \right) = F_S, \quad (1)$$

where S refers to a set of prognostic or predicted biochemical variables. The second and third terms on the left side of the equation describe the advection and mixing, respectively, where $V(u, v, w)$ is the velocity vector, w_s is the sinking velocity of pelagic detritus, and K_{x_i} is a turbulent diffusion coefficient.

All of the chemical and biological interactions are depicted as one term, F_S , on the right-hand side, and the specific equations are listed in the 3D CEMBS model description [9].

2.3. Land–Water Linkage

We coupled the EcoPuckBay model from the land side with two models SWAT (surface water) and Modflow (underground), which we briefly describe below.

2.3.1. Surface Water

Information about the water volume discharged by rivers with their mouths located within the Puck Commune (Figure 1 and Table 1, numbers from 8 to 11) is being provided by the hydrological model SWAT that has been implemented as one of the WaterPUCK project's stages [7]. The SWAT model includes the preparation of the innovative and complex hydrological model coupled with the nutrient concentration module including meteorological data (precipitation, wind, temperature, and atmospheric pressure). The proposed solution is based upon real-time observation (local weather station) and on short-term weather forecasts (the Interdisciplinary Centre for Mathematical and Computational Modelling University of Warsaw (ICM-UW) website). The hydrological computations are performed with SWAT software. The transformation of precipitation data into surface runoff have been achieved with the SCS (Soil Conservation Service) curve number procedure through the accumulated runoff volume and the time of concentration (the time from the beginning of a rainfall event until the entire subbasin area contributes to flow at the outlet) [7].

Table 1. Locations of mouths of watercourses included in the EcoPuckBay model domain.

	Watercourse	Longitude	Latitude
1	Vistula	18.95	54.35
2	Bold Vistula	18.78	54.37
3	Still Vistula	18.66	54.41
4	Oliwski Stream	18.60	54.42
5	Kamienny Stream	18.56	54.46
6	Kacza	18.56	54.48
7	Ściekowy Canal	18.51	54.61
8	Reda	18.47	54.64
9	Gizdepka	18.46	54.66
10	Potok Bładzikowski	18.45	54.70
11	Płutnica	18.39	54.72

Information on the deposition of nutrients from the HYPE model is available in the form of monthly averages. As a result of the HELCOM directives in force, the actual values coming into the Baltic Sea from Polish areas have been strongly reduced over the last 30 years [10]. Therefore, the use of 30-year averages would lead to an overestimation and distortion of the actual runoff. Therefore, the current deposits for the HYPE rivers (numbers 1 to 7, Figure 1) were established on the basis of [10]. On the basis of the abovementioned work, actual concentrations were determined for nitrates (0.9 mg dm^{-3}), ammonia (0.07 mg dm^{-3}), phosphates (0.07 mg dm^{-3}), and silicates contained in the waters of river origin entering the Baltic Sea (1.1 mg dm^{-3}). The concentrations thus established were related to the average daily volumes of freshwater introduced by these rivers, resulting in satisfactory deposition rates close to real ones.

The SWAT model operates in operational mode, producing forcing data for the EcoPuckBay model for the land/water border; however, its area of operation does not cover the entire domain of the EcoPuckBay effective model. SWAT provides information only on the rivers within the Puck Commune, while the EcoPuckBay model also includes the rivers south of the Reda River, i.e., Ściekowy Canal, Kacza, Kamienny Stream, Oliwski Stream, Still Vistula, Bold Vistula, and the Vistula. Therefore, for full information on freshwater streams in the EcoPuckBay model, this data had to be obtained from

another existing hydrological model. For this purpose, numerical values from HYPE model simulations based on historical time series (available: 1980–2010) are used. Its geographical domain covers the whole of Europe, and public data is available in a time resolution analogous to the SWAT model, i.e., as average daily flows in $\text{m}^3 \text{s}^{-1}$. Four subcatchments were separated from the HYPE model—one for each of the Vistula mouths and one for the remaining rivers on the basis of a uniform distribution.

Among the river data obtained from the HYPE model, the Vistula is the most important source of both the volume of freshwater flowing into the Gulf of Gdansk and the deposition of nutrients (Table 2), which has a huge impact on environmental conditions within the effective domain of the model. The order of magnitude of the Vistula's water flow is on average about three orders of magnitude larger than the other freshwater sources in the EcoPuckBay model. The annual cycle of the Vistula has been similar in character for decades, with peaks in the spring months—which is related to snow melt and summer minimum. Thanks to this, the use of historical time series for the Vistula is a good approximation of the actual flow for the last few years.

Table 2. The river runoff into the Baltic Sea in 2016 inside the model domain border.

	Watercourse	Mean Runoff [$\text{m}^3 \text{s}^{-1}$]	Nitrogen [tons year ⁻¹]	Ammonia [tons year ⁻¹]	Phosphorous [tons year ⁻¹]
1	Vistula	1064.20	15,102.32	1174.63	1174.63
2	Bold Vistula	2.06	29.17	2.27	2.27
3	Still Vistula	6.07	86.08	6.69	6.69
4	Oliwski Stream	0.35	4.98	0.39	0.39
5	Kamienny Stream	0.35	4.98	0.39	0.39
6	Kacza	0.35	4.98	0.39	0.39
7	Ściekowy Canal	0.35	4.98	0.39	0.39
8	Reda	0.28	36.33	3.24	0.94
9	Gizdepka	0.49	29.74	1.83	0.72
10	Potok Bładzikowski	0.31	25.17	0.83	0.36
11	Płutnica	1.35	32.62	9.04	3.79

2.3.2. Groundwater

A numerical transport model based on the Modflow code developed at another stage of the project allows determining the nitrate load in the groundwater flowing into the Puck Bay. The MT3DMS numerical code was applied to solve the advection–reaction–dispersion equation [11]. Transient calculations were performed with the third-order total-variational diminishing (TVD) numerical method for the advective term, while for the steady-state solution, the standard finite difference discretization was applied. This model was calibrated based on actual NO_3 concentration values and was joined with the EcoPuckBay model through a coupling module.

2.4. Water–Water Border

The results of the 3D EcoPuckBay model are limited to the effective area of Puck Bay. However, the entire model grid covers a wider area marked in Figure 1. This is to ensure that boundary conditions are properly simulated. Along the line of the northern border of the 3D EcoPuckBay model, data from the 2.3 km 3D CEMBS prediction model are transferred to the EcoPuckBay model (see Figure 1). Results from 3D CEMBS [9,12] are used to provide forcing fields in the EcoPuckBay model through sequential information transfer. The mechanism of this module is to interpolate values from 3D CEMBS to EcoPuckBay model's grids.

2.5. Data Used for Evaluation

To evaluate EcoPuckBay model, we used in situ measurements taken throughout the monitoring activities of the Voivodship Inspector of Environmental Protection in Gdańsk as well as the numerical data of biochemical parameters calculated with the ice–ocean model NEMO-Nordic (Nucleus for

European Modelling of the Ocean) coupled with the biogeochemical model SCOBI (Swedish Coastal and Ocean Biogeochemical model) acquired from the Marine Copernicus database. A brief summary description of the data used for the evaluation in this paper is presented below.

2.5.1. VIEP

The biggest set of the in situ data used for the EcoPuckBay model evaluation performed in this paper is samples collected during regular measurements of the marine environment of the Baltic Sea conducted by Voivodship Inspectorate of Environmental Protection (VIEP) in Gdańsk. We used data from stations located within the model effective domain (Figure 1). VIEP's scope, methods of monitoring, and the manner of assessing the status of the Baltic Sea has been defined by the provisions of the Water Law Act and the monitoring program of marine waters adopted by the Council of Ministers, which implements the requirements of Article 11 of Directive of the European Parliament and of the Council 2008/56/EC of 17 June 2008, establishing a framework for community action in the field of marine environmental policy. Monitoring services performed by VIEP constitute the fulfilment of Poland's obligations arising from the convention on the protection of the marine environment of the Baltic Sea area and, since 15 July 2014, of Article 11 of Directive 2008/56/EC of the European Parliament and establishing a framework for community action in the field of marine environmental policy.

2.5.2. NEMO-SCOBI

The source of the numerical results used in the manuscript is the data downloaded from the Marine Copernicus database (<http://marine.copernicus.eu>). This Baltic Sea biogeochemical reanalysis product provides a 25-year biogeochemical reanalysis for the Baltic Sea (1993–2017) using the ice-ocean model NEMO-Nordic (based on NEMO-3.6, Nucleus for European Modelling of the Ocean) coupled with the biogeochemical model SCOBI (Swedish Coastal and Ocean Biogeochemical model) together with LSEIK (local singular evolutive interpolated Kalman) data assimilation. All variables are available as daily means as well as monthly means and include nitrate, phosphate, ammonium, dissolved oxygen, and chlorophyll-a. The observation types used in the data assimilation are nitrate, phosphate, dissolved oxygen, and chlorophyll-a. The NEMO-SCOBI domain covers the whole Baltic Sea extended to the North Sea area.

2.6. Nutrient Spread Module

In order to model the spread of nutrients, the biochemical model was combined with a hydrological model describing the processes taking place in the Puck Commune's watercourses and rivers in the model domain. For this purpose, we use (Equation (1)) in the Cartesian coordinate system without the source and sink term ($F_S = 0$), where S is the concentration of nutrients and the rate of descent is $w_s = 0$. The nutrient spread module describes the diffusion and advection of nutrients under the influence of sea currents. Data on the flow and concentration of nutrients are provided once a day at the land–water border from the SWAT model. The module consists of two partial second-order differential equations for concentrations of nutrients, e.g., phosphates and sum of nitrates and nitrites.

2.7. Pesticide Distribution

Models of pesticide distribution in surface waters have been reviewed with particular attention to the marine environment. As a result of the literature review, SWAT and FANTOM [13] models were selected as the basis for the development of the pesticide distribution module in the EcoPuckBay model. We developed a computational algorithm including the basic processes taking place in the sea. Sedimentation and degradation processes of pesticides have been introduced through a function of sources and sink $F_s = Q_p$ in the passive substance transport of Equation (1):

$$Q_p = w_s \frac{K_d C_s}{1 + K_d C_s} \frac{\partial C_p}{\partial z} - k_{p,aq} C_p, \quad (2)$$

where C_p is the concentration of pesticide and where empirical model parameters such as degradation factor $k_{p,aq}$ and adsorption factor K_d have been calibrated in the SWAT hydrological model for surface water in watercourses. The concentration of the suspended matter C_s plays a very important role in the adsorption of pesticides and was estimated on the basis of dead and live organic matter described in the biochemical model by appropriate state variables (describing plankton, detritus, etc.). Due to the large number of compounds considered as pesticides, the list of pesticides that are modelled in the Puck Bay area was narrowed down. The list includes pesticides currently used in agriculture. For selected compounds, surface water inflows of selected pesticides to the computational domain simulated with the use of SWAT hydrological model were estimated.

Pesticides are also taken from water by living organisms and accumulated in their bodies. However, since bioaccumulation has a small effect on the concentration of pollutants in water; it can be omitted in the first approximation when modelling pesticide transport in seawater.

2.8. Operational Mode

The hydrodynamic and biochemical parts of the EcoPuckBay model work in the operational version and are available on the website. Every 6 h, a 48-h forecast is generated based on the atmospheric forcing data provided by the UM-ICM weather model and data for the model domain's borders. In addition, the model produces a forecast when new data is released from sources providing data for assimilation, e.g., SWAT, Modflow, 3D CEMBS, and satellite data (see Figure 2).

To connect with EcoPuckBay model data sets from various sources (characterised by very different data formats, spatial grid, and time coverage), scripts were created mainly in Python. They ensure autonomous and automatic operation of the WaterPUCK website with the ability to monitor the correctness of its operation by the administrator.

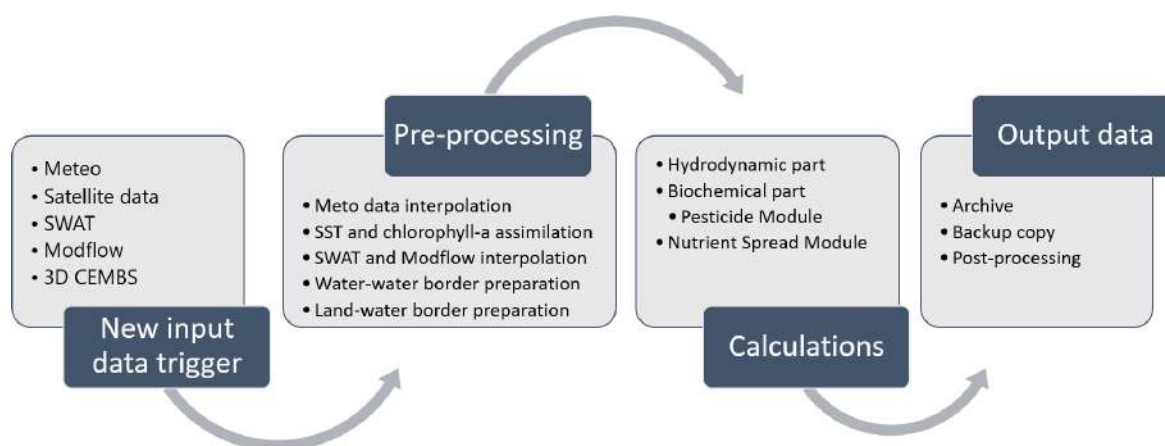


Figure 2. The EcoPuckBay production cycle starts every time new input data (meteo, assimilation, or from SWAT and/or Modflow models) appears.

It is possible to create forecast maps of the Puck Bay for the following hydrodynamic parameters: temperature, salinity, currents, sea surface height, as well as biogeochemical parameters—chlorophyll-a concentration, nutrient concentrations (NO_3 , NH_4 , PO_4 , and SiO_3), dissolved oxygen concentration, and active ingredients of pesticides. It is also possible to create graphs of temporal changes of these parameters at a given point as well as vertical cross sections. The results of simulations for a 48-h forecast are presented for the model with a vertical resolution of 115 m. The possibility of using the WaterPUCK service in operational mode can be helpful for authorities and policymakers to have access to scientific knowledge based on real environmental data as quickly as possible. In addition, prognostic information can be very useful for both shipping and broadly understood tourism sectors.

3. Results

This section gives some of the results obtained from the EcoPuckBay model and presents the Puck Bay's coastal ecosystem functioning. The results presented below demonstrate that the model is operating correctly.

3.1. Statistical Comparison of EcoPuckBay Model With VIEP Monitoring Data and NEMO-SCOBI Model Results

To evaluate the quality of the results obtained from the EcoPuckBay model, a set of basic statistical measures were calculated, such as mean, Pearson correlation coefficient (r), root-mean-square-error (RMSE), and standard deviation (STD). The statistical comparison is presented below in the form of tables and modified Taylor diagrams [14]. Dissolved oxygen, nitrates, phosphates, and chlorophyll-a were selected for comparison.

3.1.1. VIEP Monitoring Data

By comparing the results of the EcoPuckBay model with the VIEP monitoring data, we see that the modelled variables concentrations are of the same order of magnitude as the environmental data. The highest uncertainty (about 30 per cent) is for nitrates; in other cases, the difference in averages does not exceed 10 per cent. In the case of temporal variability of the modelled variables, dissolved oxygen is best determined for which Pearson's correlation coefficient is the highest ($r = 0.71$). In Table 3, we present the results of statistical analysis of the EcoPuckBay model in the context of VIEP environmental data.

Table 3. Statistical comparison of EcoPuckBay model with Voivodship Inspectorate of Environmental Protection (VIEP) monitoring data.

	VIEP Mean	VIEP STD	EPB Mean	EPB STD	RMSE	r
O ₂ [mmol m ⁻³]	315.30	43.06	337.50	35.97	31.03	0.71
NO ₃ [mmol m ⁻³]	1.74	2.31	2.48	2.87	2.19	0.66
PO ₄ [mmol m ⁻³]	0.35	0.23	0.32	0.21	0.21	0.56
CHL [mg m ⁻³]	4.44	3.14	4.40	3.59	2.89	0.64

Figure 3 presents in a graphical form information from Table 3 as a Taylor diagram (modified to show variables with different ranges of variation in one picture). As a rule, in the Taylor diagram, the closer the model point is to the reference point ($r = 1$, $STD = 1$, and $RMSE = 0$), the more accurately the model reproduces measurement data. From the diagram, it can be inferred that the model results of nitrates and chlorophyll-a are characterised by slightly greater inertia (greater range of variation) compared to environmental data while nitrates and dissolved oxygen vary less in the model than the measurement data. Root-mean-square-error (modified by dividing by the reference STD to compare all variables at one time) is less than 1.0 for all modelled variables.

3.1.2. NEMO-SCOBI Model Results

It should be noted that the EcoPuckBay and NEMO-SCOBI models have very different grid sizes. For this reason, for calculations, a sufficiently large number of EcoPuckBay cells were taken to cover the volume of a single NEMO-SCOBI cell. Analysing the statistical comparison of the EcoPuckBay model with the NEMO-SCOBI model, a high correlation for dissolved oxygen ($r = 0.75$) can be observed, while the other variables have a Pearson correlation coefficient of about 0.6 (Table 4).

A graphical representation of the comparison of both models is shown in Figure 4. The Taylor diagram was made in such a way that the reference point ($r = 1$, $STD = 1$, and $RMSE = 0$) corresponds to the NEMO-SCOBI model data. The RMSE is smaller than the reference data STD for all modelled variables (normalised RMSE in the diagram is smaller than 1.0). All presented variables have a smaller range of variations in the EcoPuckBay model compared to the NEMO-SCOBI model.

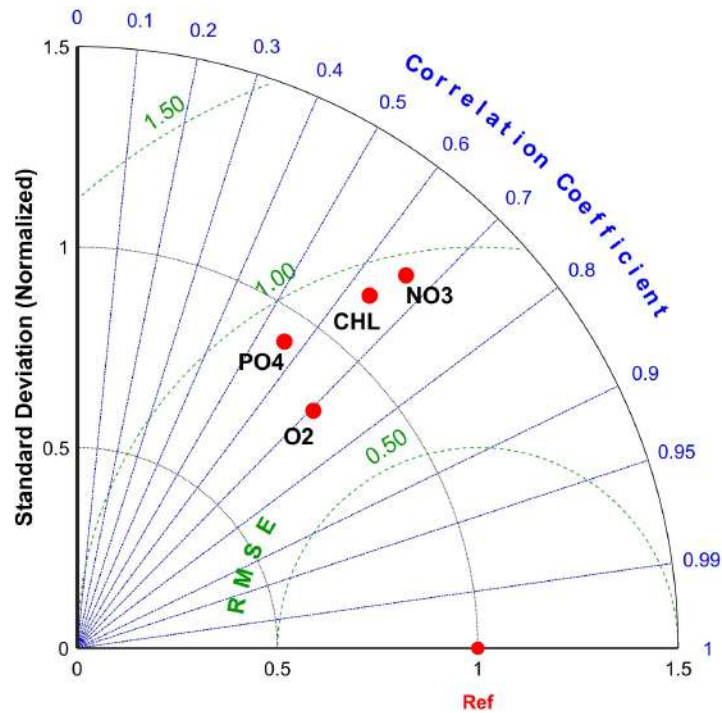


Figure 3. Taylor diagram where the reference point indicate VIEP measurements.

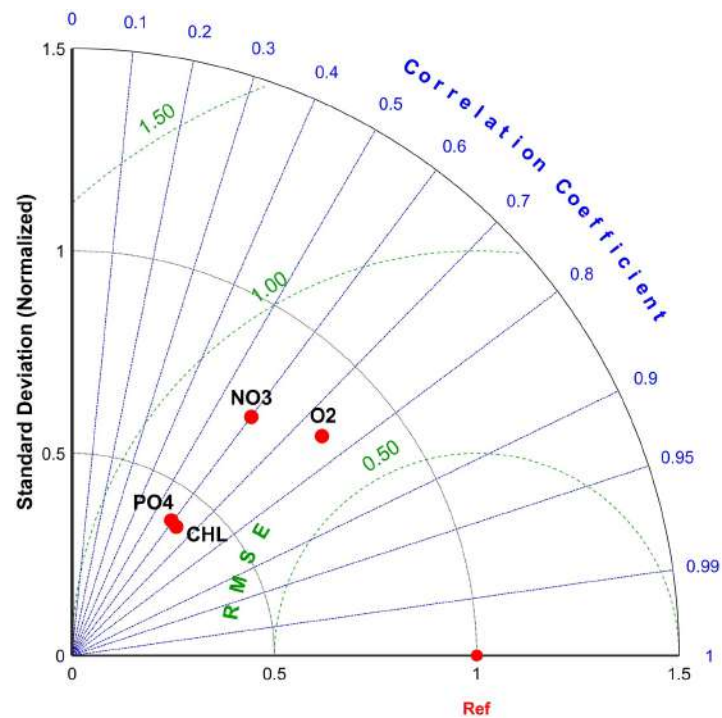


Figure 4. Taylor diagram where the reference point indicate NEMO-SCOBI model data.

Table 4. Statistical comparison of EcoPuckBay model with NEMO-SCOBI (Nucleus for European Modelling of the Ocean coupled with Swedish Coastal and Ocean Biogeochemical model) model data.

	NEMO Mean	NEMO STD	EPB Mean	EPB STD	RMSE	<i>r</i>
O ₂ [mmol m ⁻³]	360.63	43.74	358.90	35.95	29.02	0.75
NO ₃ [mmol m ⁻³]	4.68	5.18	5.70	3.82	4.20	0.60
PO ₄ [mmol m ⁻³]	0.68	0.36	0.21	0.15	0.29	0.59
CHL [mg m ⁻³]	6.37	5.87	3.51	2.40	4.74	0.63

3.2. Land–Water Linkage

We coupled the EcoPuckBay model from the shore side with both the surface water runoff model based on SWAT and the groundwater flow model based on Modflow.

3.2.1. River Runoff

Figures 5 and 6 present the average daily concentrations of nitrates and mineral phosphorus in 2016 for the waters of Reda, Gizdepka, Potok Bładzikowski, and Płutnica. The concentrations of the presented nutrients were determined using the coupling module with data provided by the SWAT hydrological model during 2016 and, as it can be observed in the following plots, varied greatly depending on the river.

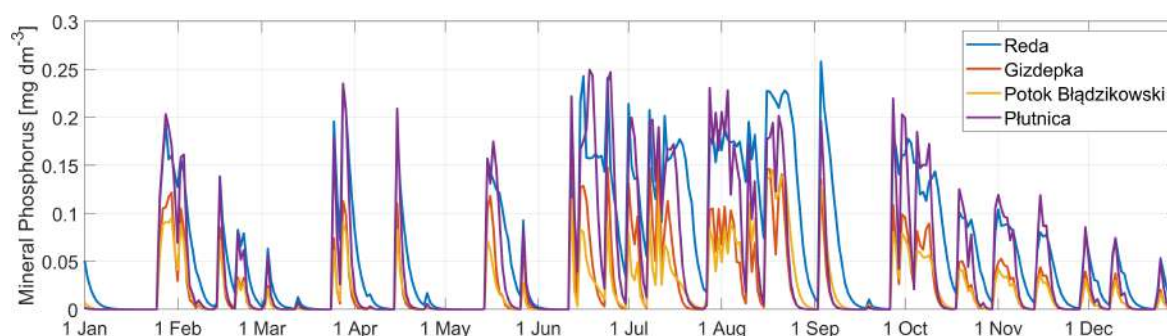


Figure 5. Average concentration of mineral phosphorus in rivers entering the Puck Bay provided by SWAT (mg dm^{-3}).

The concentration of mineral phosphorus was highest in the waters of Reda and Płutnica, reaching up to $0.20\text{--}0.25 \text{ mg dm}^{-3}$, while Gizdepka and Potok Bładzikowski carried waters with a mineral phosphorus concentration of about twice as low as $0.1\text{--}0.15 \text{ mg dm}^{-3}$ (Figure 5). In addition, in the summer, it can be observed that higher concentrations are more frequent than in the other periods of 2016 and that this period has a much higher daily variability (peaks).

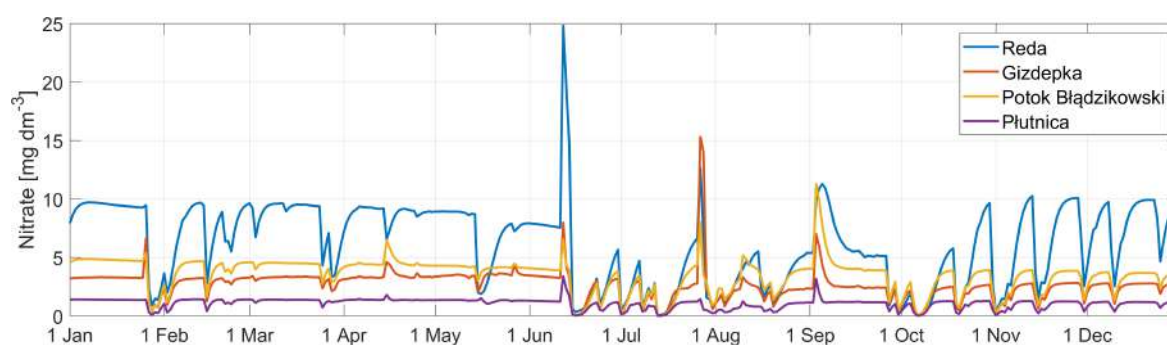


Figure 6. Average concentration of nitrates in rivers entering the Puck Bay provided by SWAT (mg dm^{-3}).

The time variability of the average modelled nitrates concentration is presented in Figure 6 and is qualitatively different for phosphates. In the first half of the year, concentrations remain fairly constant (with several clear dips for the Reda River). However, in the second part of the year, more dynamic changes dominate. The range of variability of mean concentrations for the modelled watercourses is in the range of $0\text{--}25 \text{ mg dm}^{-3}$, the highest mean concentrations were found for the Reda River, and the lowest were found for the Płutnica River.

3.2.2. Groundwater Discharge

Modflow computations indicate that the rate of discharge of groundwater to Puck Bay (averaged monthly) varies from 1000 to ca. $1600 \text{ m}^3 \text{ h}^{-1}$ (i.e., 7.3×10^5 to $11.7 \times 10^5 \text{ m}^3 \text{ month}^{-1}$). These results are consistent with previous studies on groundwater flow in the area [15]. The associated load of nitrate varies in the range of 452 to $1276 \text{ kg month}^{-1}$. The results quoted here refer to the current conditions of land use and agricultural practices as obtained from the survey of Puck area. Modelling studies showed that changes in land use and agricultural practices have considerable influence on groundwater flow rates and nitrate loads at the land-sea interface [6].

3.3. Prognostic Model Parameters

We present the results for 2016 as a representative year for the last 5 years (differences in individual years do not exceed 10 per cent).

3.3.1. Dissolved Oxygen

Seasonal changes in water oxygenation are influenced by both climatic factors and the dynamics of primary production. The nature of these changes is typically seasonal (Figure 7). The maximum oxygen solubility occurs in winter when the water temperature is at its minimum. The highest monthly average of dissolved oxygen concentration occurred in February and was equal to $412.64 \text{ mmol dm}^{-3}$.

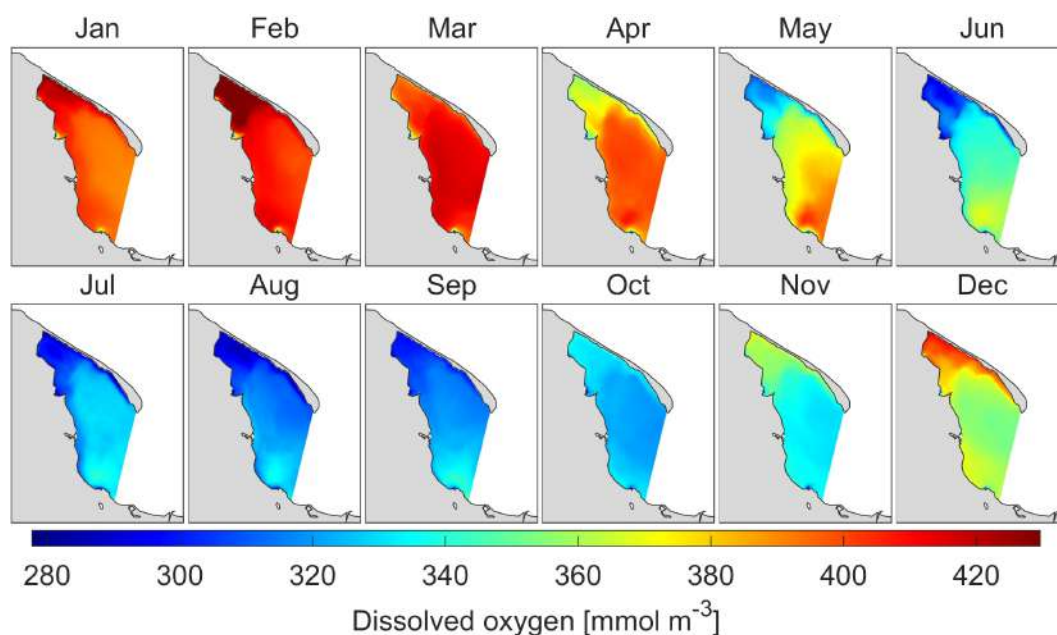


Figure 7. Monthly means of dissolved oxygen concentration at sea surface.

Then, as the temperature increases, the solubility decreases, but in places where there is intensive primary production, increased levels of concentration are noticeable locally. The minimum concentration of dissolved oxygen in water occurs during the summer (specifically in August with a mean value of $313.37 \text{ mmol m}^{-3}$) because of the lowest solubility due to the temperature maximum. The average annual dissolved oxygen concentration for the study area is about $358.06 \text{ mmol m}^{-3}$, with a standard deviation of $37.96 \text{ mmol m}^{-3}$.

3.3.2. Chlorophyll-a

The main source of energy for life on Earth is the Sun, the water environment is no exception. The scattering and reflective properties of organisms and molecules contained in the water column affect the depth of the euphotic layer, for which high values indicate the possibility of a primary

production process in deeper parts of the sea. The rate of phytoplankton primary production in the growing season is usually very high. Owing to the short life span of these microscopic plants and the high productivity of the euphotic layer, phytoplankton is the main source of energy for other ecosystem elements. Some phytoplankton is consumed directly by herbivorous zooplankton, but a large part of the phytoplankton sinks to the bottom. Three phytoplankton abundance peaks are characteristic of the entire Puck Bay; they are determined by the phenologies of the various groups of algae, which are associated with the environmental requirements of these plants. Cyanobacterial blooms appear mostly in July, August, and September. The highest concentrations of chlorophyll-a are observed relatively close to the shore, where access to nutrients is greatest. Initially, no elevated chlorophyll-a concentration is observed in Puck Lagoon until June due to the geomorphological separation from the rest of the basin (Figure 8).

The annual average concentration of chlorophyll-a was 3.76 mg m^{-3} , with a standard deviation of 2.82 mg m^{-3} . The lowest monthly mean concentration of chlorophyll-a in the surface layer of the study area was determined in January and was equal to 0.44 mg m^{-3} , while the highest monthly mean concentration of chlorophyll-a occurred in August and was equal to 8.39 mg m^{-3} .

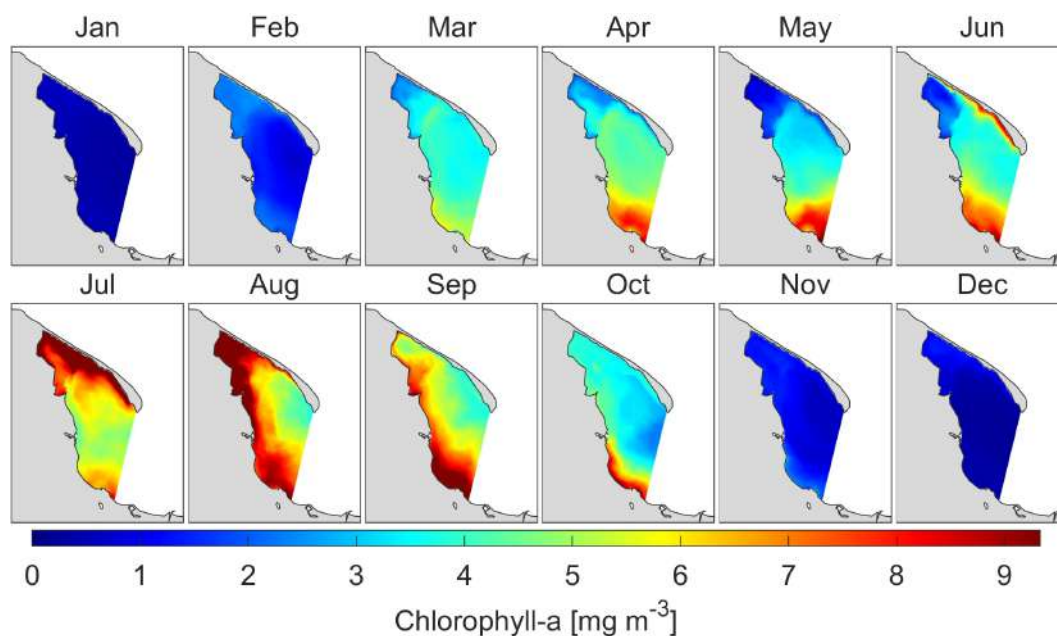


Figure 8. Monthly means of chlorophyll-a concentration at sea surface.

3.3.3. Nutrients

Nutrients such as nitrogen and phosphorus, besides atmospheric deposition, can enter the marine environment from two types of sources: point and nonpoint sources. Point sources are usually municipal wastewater treatment plants, while nonpoint sources include surface runoff from agricultural fields. Therefore, nitrogen and phosphorus are the main limiting factors of biological production and, therefore, it is important to know both the ratio of these two elements and its variability over time. The nutrient concentration in the Puck Bay shows seasonal variability. The maximum concentrations are usually recorded in winter and early spring, before the start of the vegetation period, which starts immediately after the ice has descended. Knowledge of concentration and nutrient load is essential for assessing water quality and for understanding ecosystem functioning. The total nutrient load entering the Bay of Puck is more important than their concentration in watercourses due to advection and diffusion. The load discharged by the examined streams depends on their outflow, which varies significantly throughout the year.

Nitrates

The highest concentrations of nitrate–nitrogen were found in winter and early spring before the beginning of the growing season, and the lowest was found in the middle of the growing season (Figure 9).

The average annual nitrate concentration in the surface layer was 5.06 mmol m^{-3} , with a standard deviation of 3.90 mmol m^{-3} . The highest average monthly nitrate concentration was determined in January ($11.04 \text{ mmol m}^{-3}$), while the lowest nitrate concentration occurred in August (1.29 mmol m^{-3}).

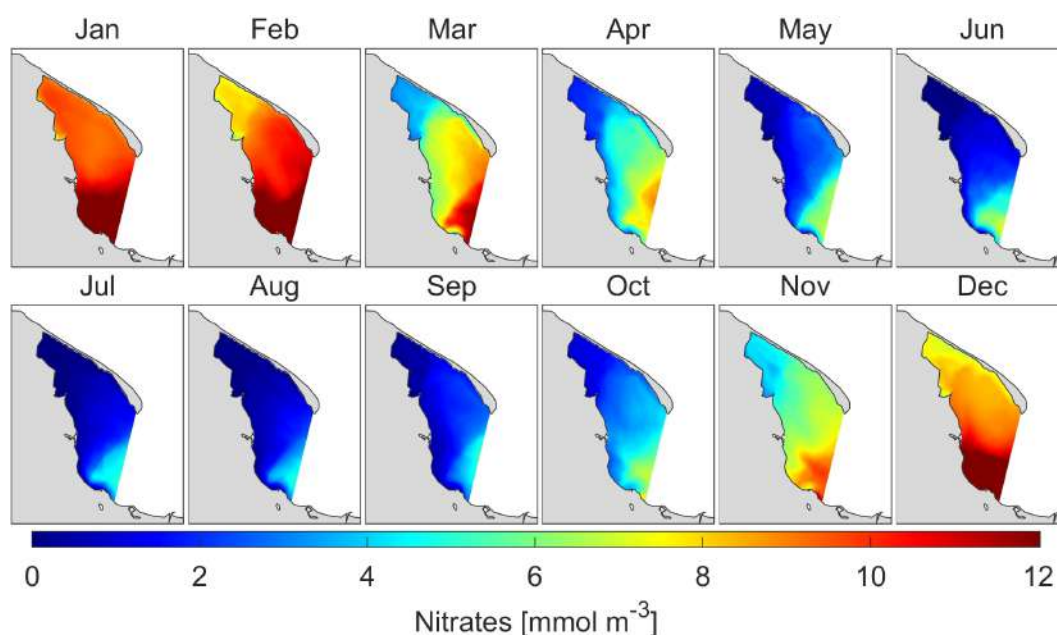


Figure 9. Monthly means of ammonia concentration at sea surface.

Phosphates

Phosphate concentrations in the Puck Bay waters also show seasonal variability, related to the size of loads supplied by surface waters and the depletion of these compounds during the vegetation period as a result of phytoplankton consumption. A clear decrease in the concentration of nitrogen compounds was observed in the summer months, and in early autumn, it increased again (Figure 10).

The annual mean concentration of phosphates in the surface layer was 0.21 mmol m^{-3} , with a standard deviation of 0.14 mmol m^{-3} . The highest monthly average phosphate concentration occurred in December (0.51 mmol m^{-3}), while the lowest phosphate concentration occurred in August (0.04 mmol m^{-3}).

3.4. Nutrient Spread

Figure 11 shows the intensity and character of the spread of nutrients and pollutants supplied to the Baltic Sea waters by rivers flowing within the model domain. Due to the relatively even but dense distribution of rivers along the west coast of the domain (from Gdańsk-Vistula to Puck/Władysławowo, where Płutnica flows), there is a high probability that, after just 1–2 days, the pollution entering the rivers as a result of mixing and currents will be spilt along the whole west coast. On day 3, nutrients can be transported to the coast of Hel Peninsula and will spill along its coastline in the following days. At the same time, with the rapid transport of the pollutants along (and in close proximity) to the shore, they spill over into the central areas of the Puck Lagoon, although it usually takes at least 3–4 days for the pollutants to reach the areas of the Puck Bay lying at an equal distance between the west coast and the Hel Peninsula, although this is not very likely to be the case. After 5 days, there is a nonzero probability that a nutrient or other pollutant that has entered the sea from rivers in the domain will

reach any part of the Puck Bay. From day 6, it is visible that, in the central part of the bay, there is an increased probability of nutrients appearing up to 50–60 per cent in the central part of the bay and over 90 per cent in all waters in close proximity to the coastline. There is also a strong expansion of nutrients coming from the Vistula as a result of the amount of water pumped by the Vistula and the sometimes favourable physical conditions (currents causing water to be pumped inside the Puck Bay).

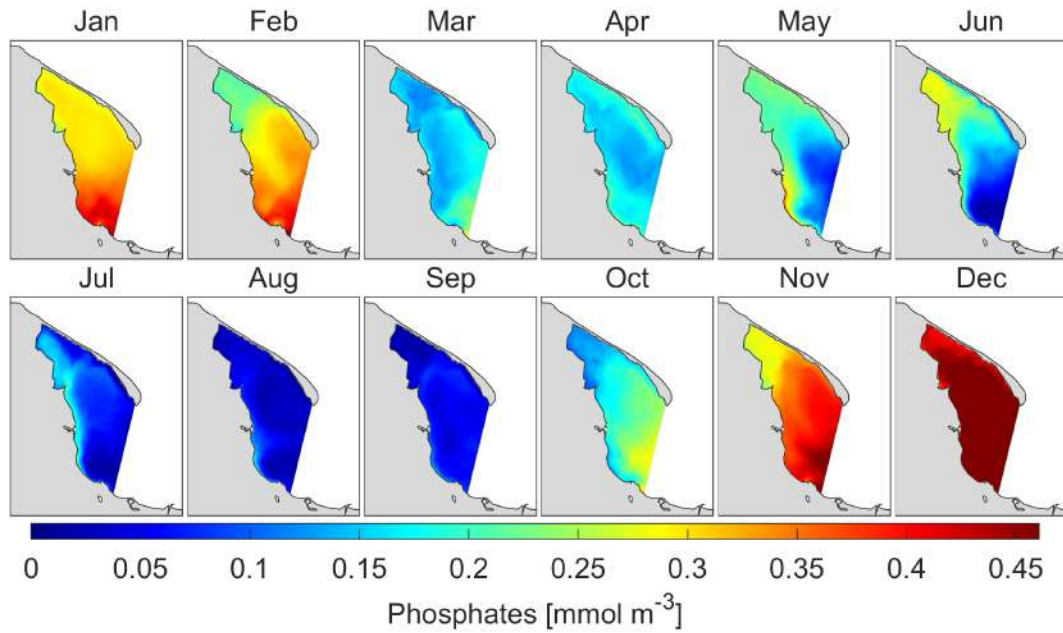


Figure 10. Monthly means of phosphates concentration at sea surface.

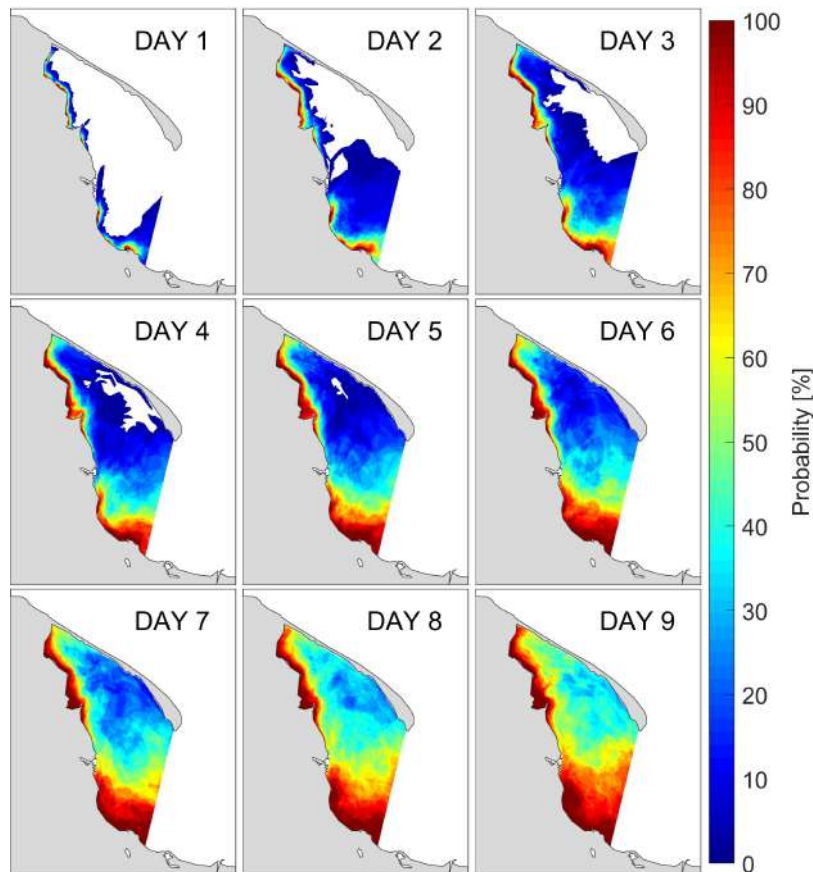


Figure 11. Probability of nutrients reaching location after $n = \{1, \dots, 9\}$ days.

Analysing the distribution of currents in individual months of the year 2016 (see Figure 12), we can observe two possible scenarios: the first one when the water is pushed into the bay (i.e., October) and the second when the water is drained from the bay (i.e., August and December). In the first case, sea surface height on the western side of the domain is higher than on the eastern side (see [1]). In the second case, the sea surface height is relatively lower on the western side of the domain than on the eastern side.

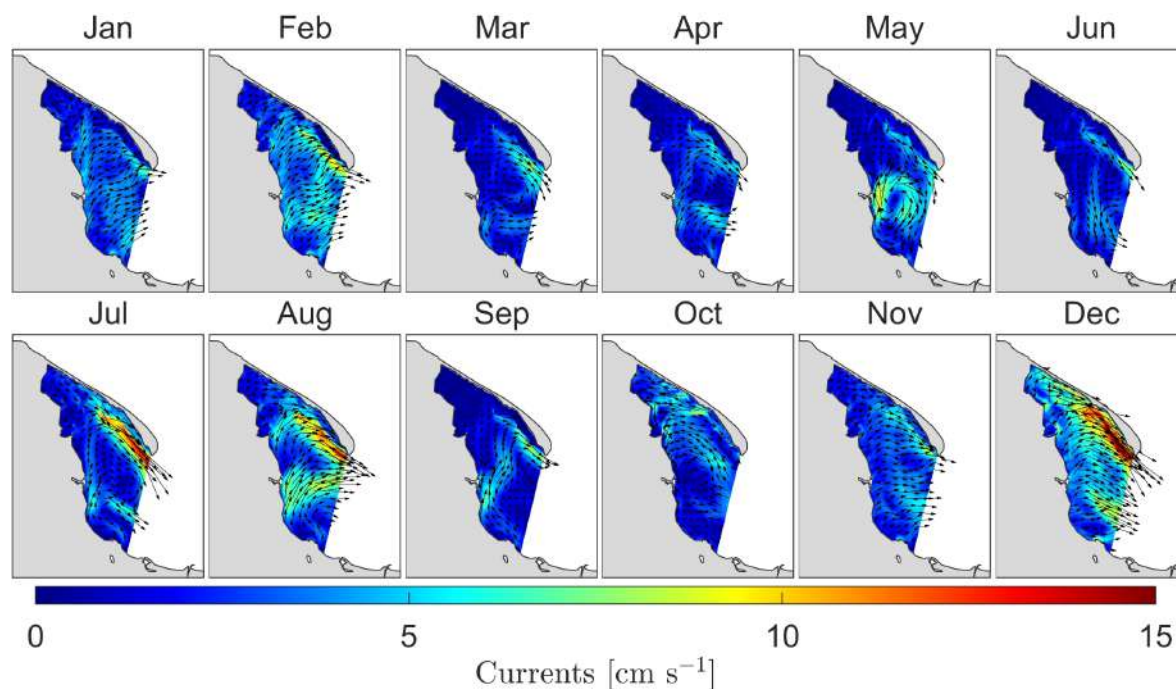


Figure 12. Monthly means of currents at sea surface level.

The north direction of the currents along the west border of the domain is noticeable. The consequences of this state are visible on nutrient distribution maps. Namely, biogenic substances flowing with river waters into the Baltic Sea are often transported along the coast to the north and, only after some time, they spread into the central waters of the Puck Bay. Pollutants, therefore, tend to spread rapidly in the close coastal zone and to expand more slowly into deeper waters far from the coast. One can also see a great influence of biogenic substances coming from the Vistula, which together with the currents according to the scenario when water is pumped into the bay are transferred in the northern and northwestern direction, thus feeding the Puck Lagoon with pollutants and biogenic substances not coming from the rivers directly entering the Puck Lagoon.

Figure 13 presents how many days must elapse from the beginning of the distribution to the moment when a nutrient with a given probability or more will appear at a specific point in the domain. For example, “ $p > 10\%$ ” shows a situation in which, with a probability of 10 per cent or more (i.e., at least once in ten cases), the nutrient from rivers reaches a given point on the bay. Results show that 9 days is enough to reach every place (even the inner part) in the bay with a probability higher than 10 per cent. The increased probability thresholds are intended to show the regions along the west coast of the domain where polluted waters are most likely to reach after only a few days due to northward currents. Spread of pollutants into the central parts of the bay occurs either after a long time or less frequently—i.e., as can be seen in the case “ $p > 50\%$ ”, there are places (marked in white) where the nutrient from the rivers did not appear even after 9 days in half the cases.

It should be emphasised that biological processes are not taken into account in the nutrient spread module (expression $F_5 = 0$ in Equation (1)). Such an approach results in the maximum possible contamination, as the compound could be found to be decomposed and undetectable under real conditions (e.g., in the middle of the bay).

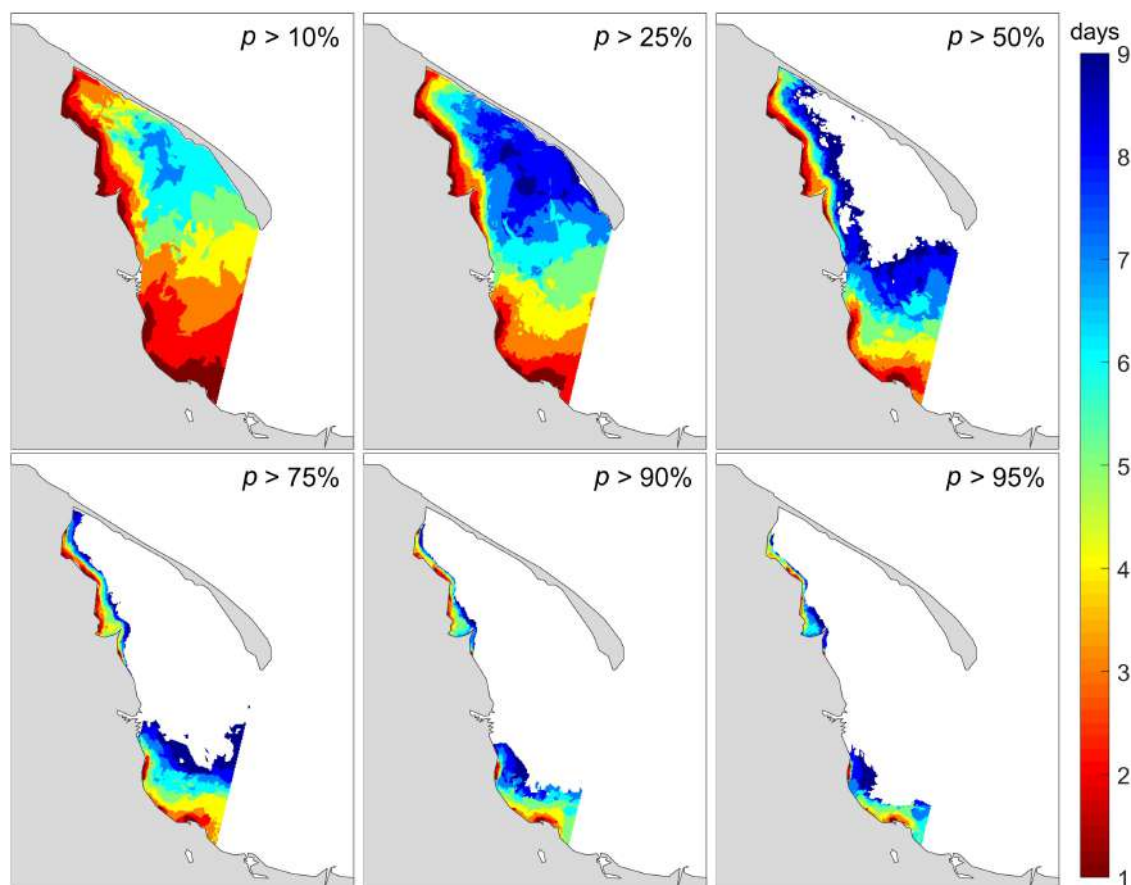


Figure 13. The number of days it takes for pollutants to occur at a location with a probability of more than $p > \{10\%, 25\%, 50\%, 75\%, 90\%, \text{ and } 95\%\}$.

3.5. Pesticides

The concentrations of detected pesticides in soil samples (chlorpyrifos-ethyl, antrachinon, glyphosate, and AMPA (aminomethylphosphonic acid)), measured within the other stage of the WaterPUCK project, ranged from 0.05 to 0.35 mg kg⁻¹. The highest concentrations were obtained in August in water from drainage ditches for metazachlor (2.0 mg dm⁻³), glyphosate (4.7 mg dm⁻³), and AMPA (2.0 mg dm⁻³). In the surface water samples and sediment samples taken from the Puck Bay, none of the 309 substances from the pesticides group were found [16]. However, 5 pesticides of agricultural origin, which are glyphosate, diflufenican, metazachlor, chlorpyrifos, and antrachinon, are modelled in the EcoPuckBay model. In the online portal, it is possible to display spatiotemporal distributions for the concentration of glyphosate, which is the most commonly used pesticide in the studied area. The distributions of other modelled pesticides are very similar, which is why we present only one example on the webpage.

Figure 14 shows a screenshot of the web portal showing the spatial distribution map for the active substance of the pesticide being modelled. It can be seen that the concentrations are so low that it is not possible to detect this compound in the waters of the Gulf of Puck by easily accessible methods.

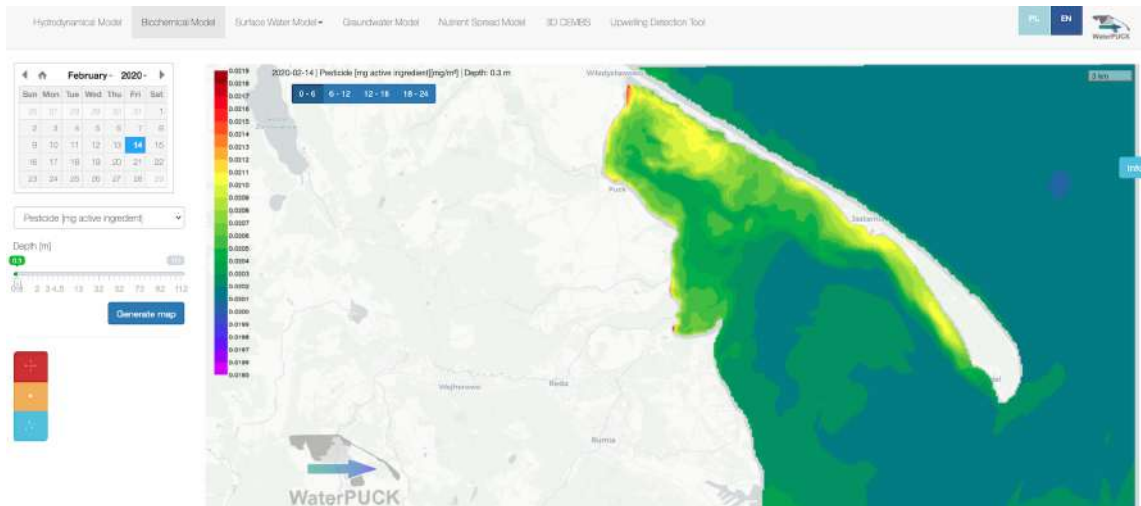


Figure 14. Concentration of the active ingredient of modelled pesticides.

3.6. Web Portal

Nowadays, quick access to expert knowledge is highly valued, especially in the context of decision-making by the authorities. In order to meet these requirements, we developed this internet service. This is one of the key services created within the framework of the project on which the results of all models included in the WaterPUCK Integrated Information and Prediction Service are available. This website operates dynamically in the operational mode, allowing for visualisation of forecast maps, time series, and vertical sections.

In this paper, we present the website which allows to generate maps of selected biochemical parameters from the EcoPuckBay model in the area of the Puck Bay and the western part of the Gulf of Gdańsk. It is now possible to generate raster maps (Figure 15a) for individual depths, which represent the next vertical level of the model. In addition, it is possible to create a time series (Figure 15b) for the set periods in the selected location (after prior determination or indication of the desired latitude and longitude) as well as W-E and/or S-N cross sections, allowing for analysis of the variability of the parameter state in the entire water column (Figure 15c).

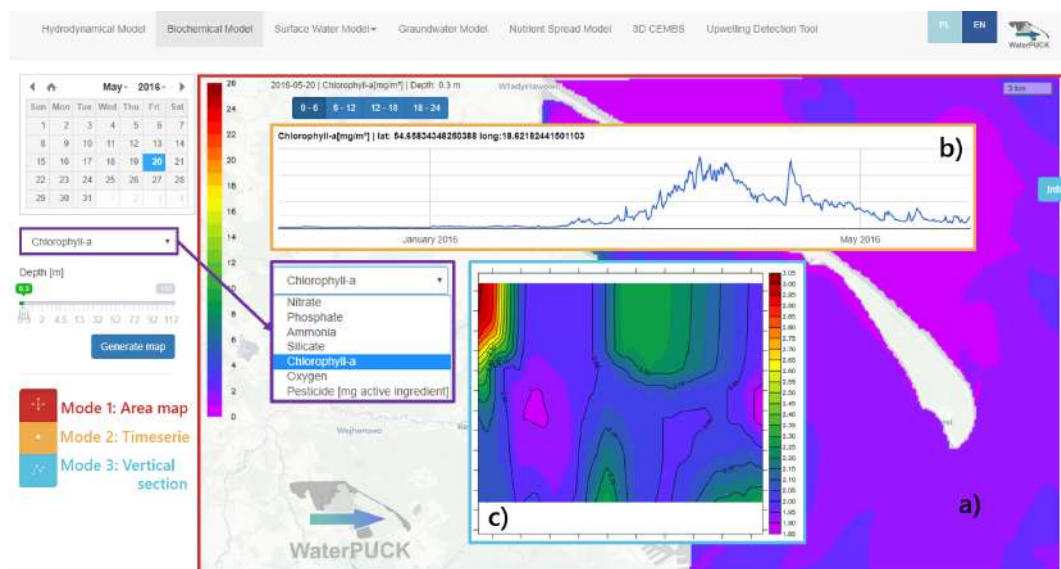


Figure 15. Screenshot of navigation menu and results for the Web Portal service: (a) raster map, (b) time series, and (c) vertical cross section of selected parameters.

An important advantage of the portal is relatively fast access to archival model data and 48-h forecasting data. Using the calendar, any date from the modelled period is selected in an intuitive way. This service can be accessed from the project website (www.waterpuck.pl) after choosing “Products” from the navigation menu and by selecting “EcoPuckBay Biochemical Model of the Puck Bay”.

4. Discussion

4.1. Prognostic Model Parameters

The Puck Bay, and especially its inner part—the Puck Lagoon—is a very dynamic area with relatively low inertia. Evaluation of the hydrodynamic part of the model [1] showed that, in this part, the annual differences in salinity and temperature are the highest. There are several models describing processes occurring in the marine environment in use such as HIROMB (High-Resolution Operational Model for the Baltic Sea), RCO (Rossby Centre Ocean Model), NEMO (Nucleus for European Modeling of the Ocean) and biogeochemical model SCOBI (Swedish Coastal and Ocean Biogeochemical model), HIRLAM (High-Resolution Limited Area Model), or the ecosystem model of the Baltic Sea BALTSEM. At the end of 2015, the SatBałtyk System has been initiated in the IO PAN (Institute of Oceanology of the Polish Academy of Sciences). It should be noted that, for this area, this is the first model with such high resolution that also is combined with terrestrial water flow models (such as the SWAT and Modflow). Also, earlier studies conducted by [17] show that the studied area is extremely difficult to model due to the complexity and intensity of processes occurring in its ecosystem.

The annual averages are of the same order of magnitude for all data sets (Table 5). For dissolved oxygen, the average of the EcoPuckBay model is between the value determined from the NEMO-SCOBI model and from the VIEP measurement data. For nitrates, the average of the EcoPuckBay model is higher than that of the NEMO-SCOBI and the VIEP measurements. For phosphates and chlorophyll-a, on the other hand, the EcoPuckBay model has a lower average compared to the averages determined from the NEMO-SCOBI model and VIEP environmental data. It should be noted that the data from the NEMO-SCOBI model as well as the VIEP measurement data have a much lower spatial and temporal coverage than the data from the EcoPuckBay model.

Table 5. Annual means of the selected variables.

	O ₂ [mmol m ⁻³]	NO ₃ [mmol m ⁻³]	PO ₄ [mmol m ⁻³]	CHL [mg m ⁻³]
EPB mean	358.06	5.06	0.21	3.76
NEMO mean	360.63	4.68	0.68	6.37
VIEP mean	315.30	1.74	0.35	4.44

A very characteristic picture for the spatial and temporal changes for all the examined variables in the surface layer is the very strong separation of the outer part of Puck Bay from the Puck Lagoon. This division is most visible when nutrients from the Vistula River runoff move with the strong eastern winds deeper into the Puck Bay. In such a situation, there is a significant (visible on maps) difference between the concentrations of nutrients in Puck Lagoon and those in the outer Puck Bay in a short time.

The vertical distributions of modelled variables are mainly determined by hydrodynamic processes occurring in the Puck Bay. As a rule, heated and less salty water on the surface is characterised by a high concentration of chlorophyll-a and a lower concentration of nutrients (which were used for primary production). Furthermore, during the growing season, this condition intensifies and the surface waters are clearly separated from the bottom waters rich in nutrients, where decomposition and mineralisation occur.

From the results obtained, it can be concluded that the overall level of impact of farms from the Puck Commune on the environment, including the quality of the waters of the Puck Bay, is relatively low. It should be noted, however, that among the studied farms, there were some for which the environmental pressure due to surveys can possibly have an unusually huge impact.

4.2. Nutrient Spread and Pesticides Distribution

The methodology used in the “EcoPuckBay—Nutrient spread module” assumes visualisation of the distribution of biogenic substances. In real environmental conditions, the presented results of the probability distribution may be different due to the fact that the biogenic substances carried by sea waters may be used by phytoplankton for growth in the primary production process and that, at the same time, their concentrations may increase as a result of the processes of water masses and chemical processes, i.e., remineralization in the water column resuspension from bottom sediments and secretion by zooplankton. The model shows the potential maximum range to which nutrients can spread and their concentrations if no consumption or growth were to occur as a result of appropriate environmental conditions.

As a result of the conducted studies, we come to the conclusion that active substances contained in pesticides used in the agricultural sector in the Puck Commune are present in the marine environment of the Puck Bay in concentrations so small that they are undetectable. Moreover, we come to the same conclusions by conducting numerical research.

4.3. Web Portal

The WaterPUCK’s web portal is an excellent tool that allows to intuitively track changes in both archival and forecasting of selected biochemical variables. In particular, it allows the presentation of data in specific depth layers and vertical sections (see Figures 16–18).

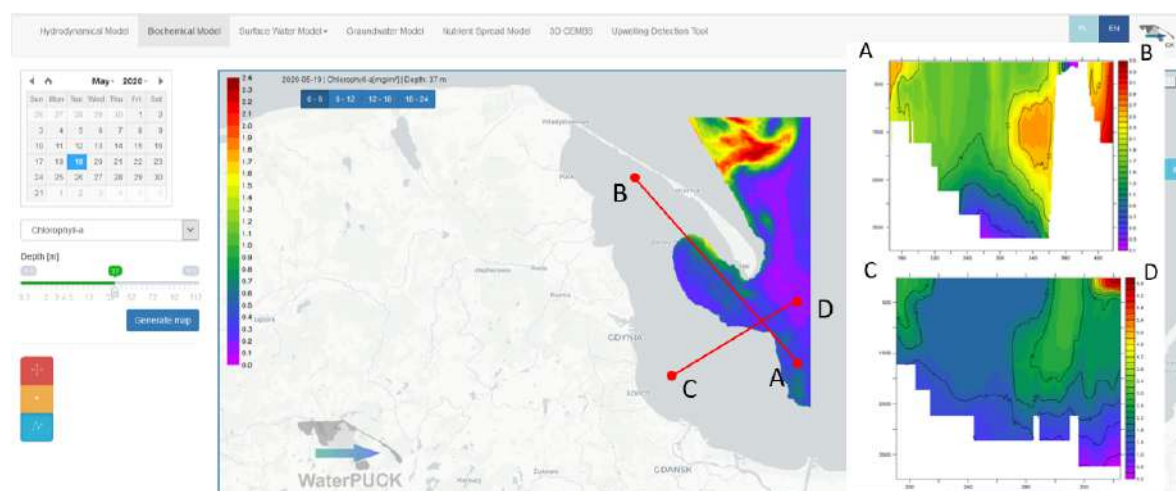


Figure 16. Screenshot of spatial distribution of chlorophyll-a concentration and sample cross sections (AB—end points of the cross-section along the Hel Peninsula, CD—end points of the cross-section perpendicular to the Hel Peninsula).

Using the data presentation tools provided as part of the WaterPUCK service, it is possible to check the status of the waters of the Puck Bay. For example, in Figure 16, we see how the concentration of chlorophyll-a decreases with depth, while in Figure 17, we see a higher concentration of nitrates at the bottom. Such a picture reflects the structure of the primary production process taking place, during which nitrates are consumed in the euphotic layer.

Furthermore, it is possible to study the spread and accumulation of pesticides in various parts of the Puck Bay (Figure 18).

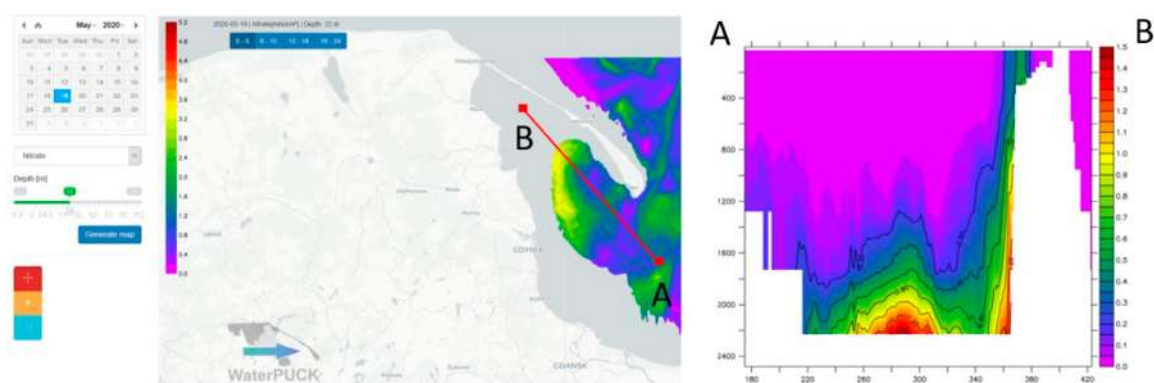


Figure 17. Screenshot of spatial distribution of nitrates concentration and sample cross section (AB - end points of the cross-section along the Hel Peninsula).

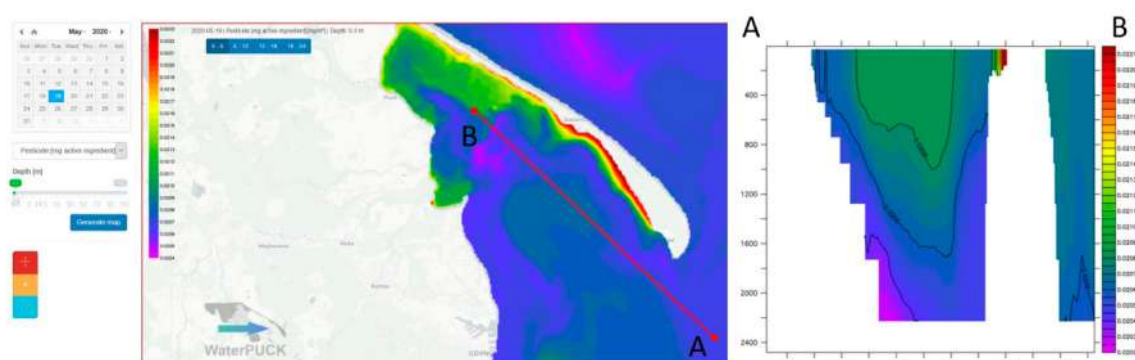


Figure 18. Screenshot of spatial distribution of pesticide concentration and sample cross section (AB - end points of the cross-section along the Hel Peninsula).

5. Conclusions

High-resolution mapping of the state of the marine environment and its ecosystem was, is, and will probably be the object of interest not only for researchers but also for policymakers and authorities. The development of the WaterPUCK service meets these requirements and offers a product that makes it possible to monitor and forecast the state of the marine environment of the Puck Bay in a resolution that has not been offered by any other models so far. The key features of the WaterPUCK system are the use of data from land water models (surface water (SWAT) and groundwater (Modflow)) fed with data from farmers' surveys and environmental measurements. This approach to modelling, especially in the context of modelling coastal waters, is very desirable because, in such a small and dynamically changing water body, correct mapping is only possible taking into account the vast majority of inputs and processes occurring.

The EcoPuckBay model is a useful tool allowing to control the state of the environment of the Puck Bay in terms of hydrodynamic and biochemical parameters, including pollution with nutrients and pesticides based on numerical studies and indirectly through the assimilation of satellite data. It allows tracking changes occurring in the studied area to improve the condition and protection of the ecosystem as well as predicting its response to threats arising from natural causes, independent of human activity as well as threats caused by human activities.

This article presents the validation of the three-dimensional ecohydrodynamic model of the Puck Bay named EcoPuckBay (specifically its ecosystem part). It is possible, via the website www.waterpuck.pl, to access archival and forecast data. The biochemical part presents the results for seven variables (nitrate, phosphate, ammonia, silicate, chlorophyll-a, dissolved oxygen, and active ingredient of pesticide). Presentation of spatial distributions for any depth, time variability for a

selected point, and a vertical cross section between any two points within the domain set by the user is possible. Comparison of the results of the EcoPuckBay model with real measurement data as well as with the NEMO-SCOBI model data indicate the correct parametrization of the EcoPuckBay model.

The model contains a nutrient spread module with which it is possible to track the fate of agricultural nutrients in the coastal environment of the Puck Bay. The presented approach to the description of pollution distribution may be of particular importance in anticipation of events resulting in the occurrence of high-risk states or even ecological disasters by selecting potentially dangerous areas or by selecting safe areas.

The EcoPuckBay model can certainly be further improved. The element that is probably most likely to improve the quality of model performance is to introduce the Vistula River into the model based on actual hydrological conditions, as the studies have shown that its impact on the water environment of the Puck Bay is the greatest.

Author Contributions: Conceptualization, D.D. and L.A.D.-G.; methodology, D.D., M.J., and L.A.D.-G.; software, D.D. and A.N.; validation, D.D.; formal analysis, D.D. and L.A.D.-G.; investigation, D.D. and M.J.; resources, D.D. and M.J.; data curation, D.D. and M.J.; writing—original draft preparation, D.D., M.J., and L.A.D.-G.; writing—review and editing, D.D., M.J., and L.A.D.-G.; visualization, D.D.; supervision, L.A.D.-G.; project administration, L.A.D.-G.; funding acquisition, L.A.D.-G. All authors have read and agreed to the published version of the manuscript.

Funding: This research was funded by National Centre for Research and Development of Poland within the BIOSTRATEG III program No. BIOSTRATEG3/343927/3/NCBR/2017. This work was supported by the National Science Centre and the Polish Ministry of Science and Higher Education under Sonata Bis (2019/34/E/ST10/00217).

Acknowledgments: This study has been conducted using E.U. Copernicus Marine Service Information. Calculations were carried out at the Academic Computer Centre in Gdańsk. We would like to thank Dominika Kalinowska for sharing data from the SWAT model, Adam Szymkiewicz for sharing data from the Modflow model, and Grażyna Pazikowska-Sapota for sharing pesticide concentration measurement data.

Conflicts of Interest: The authors declare no conflict of interest.

References

1. Dybowski, D.; Jakacki, J.; Janecki, M.; Nowicki, A.; Rak, D.; Dzierzbicka-Głowacka, L. High-Resolution Ecosystem Model of the Puck Bay (Southern Baltic Sea)—Hydrodynamic Component Evaluation. *Water* **2019**, *11*, 2057. [[CrossRef](#)]
2. Dzierzbicka-Głowacka, L.; Janecki, M.; Szymczycha, B.; Dybowski, D.; Nowicki, A.; Kłostowska, Z.; Obarska-Pempkowiak, H.; Zima, P.; Jaworska-Szulc, B.; Jakacki, J.; et al. Integrated information and prediction Web Service WaterPUCK General concept. *MATEC Web Conf.* **2018**, *210*, 02011. [[CrossRef](#)]
3. Dzierzbicka-Głowacka, L.; Janecki, M.; Dybowski, D.; Szymczycha, B.; Obarska-Pempkowiak, H.; Wojciechowska, E.; Zima, P.; Pietrzak, S.; Pazikowska-Sapota, G.; Jaworska-Szulc, B.; et al. A New Approach for Investigating the Impact of Pesticides and Nutrient Flux from Agricultural Holdings and Land-Use Structures on Baltic Sea Coastal Waters. *Pol. J. Environ. Stud.* **2019**, *28*, 2531–2539. [[CrossRef](#)]
4. Dzierzbicka-Głowacka, L.; Pietrzak, S.; Dybowski, D.; Białoskórski, M.; Marcinkowski, T.; Rossa, L.; Urbaniak, M.; Majewska, Z.; Juskowska, D.; Nawalany, P.; et al. Impact of agricultural farms on the environment of the Puck Commune: Integrated agriculture calculator—CalcGosPuck. *PeerJ* **2019**, *7*, e6478. [[CrossRef](#)] [[PubMed](#)]
5. Dybowski, D.; Dzierzbicka-Głowacka, L.A.; Pietrzak, S.; Juskowska, D.; Puskarczyk, T. Estimation of nitrogen leaching load from agricultural fields in the Puck Commune with an interactive calculator. *PeerJ* **2020**, *8*, e8899. [[CrossRef](#)] [[PubMed](#)]
6. Szymkiewicz, A.; Potrykus, D.; Jaworska-Szulc, B.; Gumuła-Kawęcka, A.; Pruszkowska-Caceres, M.; Dzierzbicka-Głowacka, L. Evaluation of the Influence of Farming Practices and Land Use on Groundwater Resources in a Coastal Multi-Aquifer System in Puck Region (Northern Poland). *Water* **2020**, *12*, 1042. [[CrossRef](#)]
7. Kalinowska, D.; Wielgat, P.; Kolarski, T.; Zima, P. Model of Nutrient and Pesticide Outflow with Surface Water to Puck Bay (Southern Baltic Sea). *Water* **2020**, *12*, 809. [[CrossRef](#)]

8. Moore, J.K.; Doney, S.C.; Kleypas, J.A.; Glover, D.M.; Fung, I.Y. An intermediate complexity marine ecosystem model for the global domain. *Deep Sea Res. Part II Top. Stud. Oceanogr.* **2001**, *49*, 403–462. [[CrossRef](#)]
9. Dzierzbicka-Głowacka, L.; Janecki, M.; Nowicki, A.; Jakacki, J. Activation of the operational ecohydrodynamic model (3D CEMBS)—The ecosystem module. *Oceanologia* **2013**, *55*, 543–572. [[CrossRef](#)]
10. Pastuszek, M.; Bryhn, A.C.; Håkanson, L.; Stålnacke, P.; Zalewski, M.; Wodzinowski, T. Reduction of nutrient emission from Polish territory into the Baltic Sea (1988–2014) confronted with real environmental needs and international requirements. *Oceanol. Hydrobiol. Stud.* **2018**, *47*, 140–166. [[CrossRef](#)]
11. Zheng, C.; Wang, P.P. *MT3DMS: A Modular Three-Dimensional Multispecies Transport Model for Simulation of Advection, Dispersion, and Chemical Reactions of Contaminants in Groundwater Systems; Documentation and User's Guide; Contract Report SERDP-99-1; U.S. Army Corps of Engineers: Washington, DC, USA, 1999.*
12. Dzierzbicka-Głowacka, L.; Jakacki, J.; Janecki, M.; Nowicki, A. Activation of the operational ecohydrodynamic model (3D CEMBS)—The hydrodynamic part. *Oceanologia* **2013**, *55*, 519–541. [[CrossRef](#)]
13. Thieulot, C. FANTOM: Two- and three-dimensional numerical modelling of creeping flows for the solution of geological problems. *Phys. Earth Planet. Inter.* **2011**, *188*, 47–68. [[CrossRef](#)]
14. Taylor, K.E. Summarizing multiple aspects of model performance in a single diagram. *J. Geophys. Res. Atmos.* **2001**, *106*, 7183–7192. Available online: <https://agupubs.onlinelibrary.wiley.com/doi/pdf/10.1029/2000JD900719> (accessed on 12 December 2019). [[CrossRef](#)]
15. Jaworska-Szulc, B. Groundwater flow modelling of multi-aquifer systems for regional resources evaluation: The Gdansk hydrogeological system, Poland. *Hydrogeol. J.* **2009**, *17*, 1521–1542. [[CrossRef](#)]
16. Pazikowska-Sapota, G.; Galer-Tatarowicz, K.; Dembska, G.; Wojtkiewicz, M.; Duljas, E.; Pietrzak, S.; Dzierzbicka-Głowacka, L.A. The impact of pesticides used at the agricultural land of the Puck commune on the environment of the Puck Bay. *PeerJ* **2020**, *8*, e8789. [[CrossRef](#)] [[PubMed](#)]
17. Węśławski, J.M.; Kryła-Straszewska, L.; Piwowarczyk, J.; Urbański, J.; Warzocha, J.; Kotwicki, L.; Włodarska-Kowalczyk, M.; Wiktor, J. Habitat modelling limitations – Puck Bay, Baltic Sea—A case study. *Oceanologia* **2013**, *55*, 167–183. [[CrossRef](#)]



© 2020 by the authors. Licensee MDPI, Basel, Switzerland. This article is an open access article distributed under the terms and conditions of the Creative Commons Attribution (CC BY) license (<http://creativecommons.org/licenses/by/4.0/>).

5 Attachment

Dybowski, D., Dzierzbicka-Glowacka, L.A., 2022. *Analysis of the Impact of Nutrients Deposited from the Land Side on the Waters of Puck Lagoon (Gdańsk Basin, Southern Baltic)*. Manuscript submitted to the Journal of Hydrology

(IF¹ = 5.722; MEiN² = 140)

¹Journal Impact Factor (IF) according to the Journal Citation Reports

²Journal score according to the list of the Polish Ministry of Education and Science

Analysis of the Impact of Nutrients Deposited from the Land Side on the Waters of Puck Lagoon (Gdańsk Basin, Southern Baltic)

Dawid Dybowski^{a,*}, Lidia Dzierzbicka-Glowacka^a

^a*Physical Oceanography Department, Institute of Oceanology Polish Academy of Sciences, Sopot, Poland*

Abstract

The article analyzes the impact of nutrients (nitrate and phosphate) on the waters of the Puck Lagoon (Gdańsk Basin, southern Baltic) supplied from the land side using numerical modeling. The model data was verified by comparison with the in situ measurement data. The spatial and temporal variability of the concentrations of nitrate, phosphate, chlorophyll *a* were analyzed. As a result of the research conducted, we came to the conclusion that the load of nutrients deposited from the land side to the waters of the Puck Lagoon is relatively small compared to the Vistula river. However, even when a little runoff enters the reservoir with a very limited water exchange, like the Puck Lagoon, there are periods when riverine nutrients load significantly affects the functioning of the ecosystem.

Keywords: coastal zone, agricultural impact, water quality, eutrophication, nutrients

1. Introduction

The growing human population forces agriculture to meet food needs more and more efficiently. One way to achieve higher yields per hectare of arable land is to increase the amount of fertilizer applied. However, this carries a high risk of potential environmental pollution and human health risks (Galloway et al., 2008). There is no area that is unaffected by human influence and a large fraction (41%) is strongly affected by multiple drivers (Halpern et al., 2008). However, when the ecosystem is still functioning (despite the small number of individuals in the species), it is still possible to reverse its degradation (Lotze et al., 2006). This is especially important in the recovery's context of the fisheries that have been overexploited for years (Shahidul Islam and Tanaka, 2004; Worm et al., 2009). The aquatic environment is prone to non-point source pollution from agriculture, which intensifies a process of eutrophication due to nutrients enrichment. The seas and oceans have an unquestionable direct impact on human health, economy and food resources, have recreational and aesthetic qualities and play a huge, beneficial role in the global balance of oxygen and carbon dioxide. However, marine ecosystems are extremely fragile and, because of the enormous temporal and spatial scale of the processes taking place in the marine environment, significant disturbances in their functioning can have far-reaching and sometimes irreversible effects. Eutrophication is a process in which an increase in nutrient deposition causes excessive biological production (growth of algae and seagrass). Eutrophication

*ddybowski@iopan.pl

symptoms include algal blooms, reduced water transparency, and oxygen loss, which brings an additional cost to the environment (Álvarez et al., 2017; Heisler et al., 2008; Howarth, 2008). The challenges facing the modern global economy are mainly related to social responsibility and resource management according to the principles of sustainable development (Badri Ahmadi et al., 2017). The challenges faced by the contemporary global economy are mainly related to social responsibility and resource management according to the principles of sustainable development (Badri Ahmadi et al., 2017). Taking responsibility for environmental pollution is necessary not only in processing and energy enterprises but also in tourism and agricultural businesses. The large dispersion of pollutant emitters is not conducive to the efficient management of the environment in the regional dimension. Actions to reduce the eutrophication of the Baltic Sea are also associated with another challenge, namely climate change. In the future, shorter and wetter winters are projected, which will result in less snowfall and a reduced layer of ice cover and more intensive runoff from the basin. Therefore, an increase in the transport of nutrients to the Baltic Sea is expected (Hägg et al., 2014). The water temperature in the Baltic Sea is rising, creating more favorable conditions for the occurrence of algae blooms. In this paper, we will attempt to estimate the extent to which pollution from a relatively small catchment area (covering the area of the Puck Commune) affects the intensification of eutrophication.

2. Study area

The study area of this work is the inner part of the Bay of Puck (known as the Puck Lagoon), which is geographically part of the Gdańsk Basin (Southern Baltic Sea). The study area is a popular tourist destination that is subject to anthropogenic pressure, also from local agriculture. This makes the Puck Lagoon a direct reservoir in which waste fertilizers and other pollutants supplied by surface runoff, groundwater, and rivers are deposited.

The area of the Puck Lagoon is 103 km², the mean depth is 3.13 m, and the water volume is 0.32 km³. The maximum natural depth is 9.4 m, while the depth of artificial pits is up to 14 m (Gic-Grusza et al., 2009). One of the most important factors that makes the ecosystem of the region unique is the topography (see Figure 1). From the north-east, it is surrounded by the Hel Peninsula, which is a natural barrier to mixing with the open waters of the Baltic Sea, keeping the salinity in the range of 7-8 with a deviation of about 1 under the strong influence of river tributaries from the land, resulting in reduced salinity, especially in coastal surface waters. The temperature of the water in the region ranges from about 2° C in February to more than 20° C on the surface during summer, with a maximum usually occurring in August. In the warmer months, the water is often stratified, leading to a seasonal thermocline. In winter, the thermocline descends and the water is well mixed.

The largest river in the region (but located outside of the study area) is the Vistula, which drains an average of more than 1000 m³ s⁻¹ of fresh water. In turn, there are seven water-courses in the area of interest, i.e. Płutnica, which has a common mouth with Darżlubie Stream, Bładzikowski Stream, Gizdepka, Mrzezino Canal, Reda and Zagórski Stream. The aforementioned rivers, the estuaries of which are within the limits of the Puck Lagoon, deposit three orders of magnitude less nutrients than the Vistula. Therefore, it is worth explaining at the outset why we are trying to assess the impact of these much smaller rivers in terms of the deposition of rivers on the Puck Lagoon. There are two reasons; the first is that the rivers flowing into the Puck Lagoon are simulated using the SWAT model, which allows us to accurately examine their actual impact. The second argument is that the Puck Lagoon is geomorphologically separated

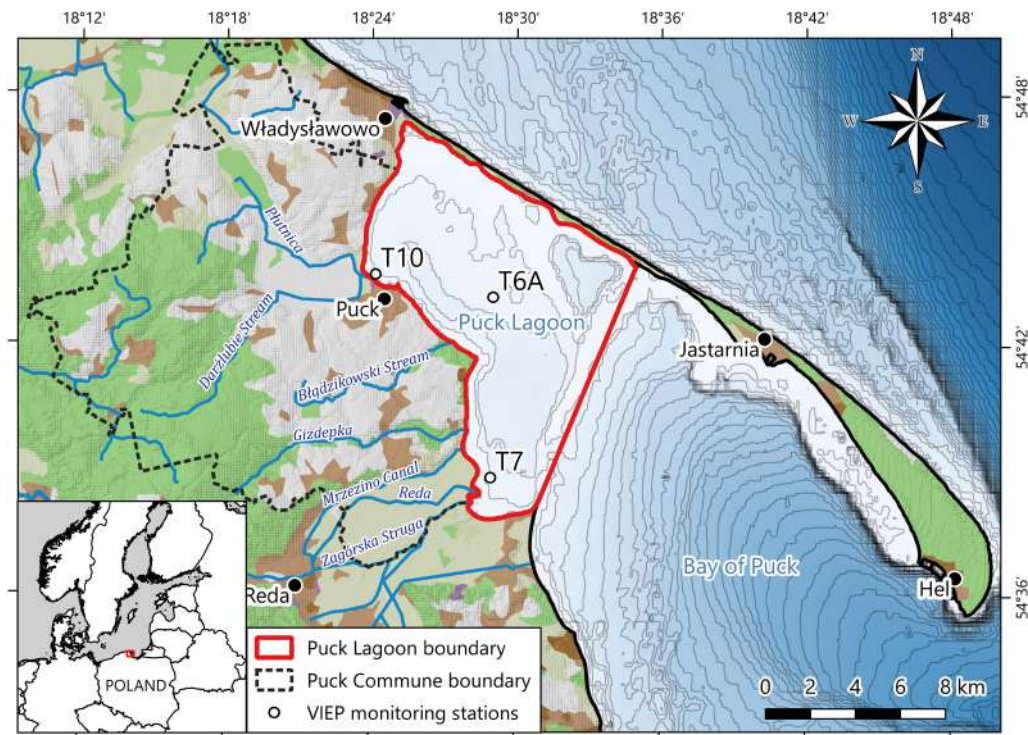


Figure 1: Study area. The red line marks the borders of the Puck Lagoon, the black dashed line marks the border of the Puck Commune, black circles mark the places where the environmental monitoring of coastal areas is carried out by the Provincial Environmental Protection Inspectorate in Gdańsk.

from the rest of the Bay of Puck by the Tern Shoal, which is a natural barrier that significantly limits the water mixing between the Puck Lagoon and the Outer Bay of Puck.

Historically, the waters of the Puck Lagoon, due to the shallow depth, the penetration of sunlight, and the relatively higher temperature than in open waters, were inhabited to a large extent with underwater meadows, providing favorable conditions for the existence of invertebrates. Unfortunately, in the 20th century, municipal and industrial wastewater, runoff from intensively fertilized fields, melioration of coastal meadows, and physical intervention in the seabed caused a lack of oxygen, the area of underwater meadows decreased, rare native species disappeared, and instead new ones appeared, for which it was easier to adapt to less favorable living conditions.

3. Methodology

The work uses monitoring *in situ* data from the Voivodeship Inspectorate for Environmental Protection in Gdańsk (VIEP) and numerical model data from two interconnected models. The Soil & Water Assessment Tool (SWAT) model was used to map the deposition of surface runoff in the Puck Lagoon's waters, while the three-dimensional ecohydrodynamic model of the Puck Bay, called EcoPuckBay (EPB), which is part of a larger set of tools resulting from the Water-PUCK project (Dzierzbicka-Głowacka et al., 2018, 2022), was used to simulate the state of the ecosystem of the Puck Lagoon.

3.1. *EcoPuckBay model*

The EPB model is an adaptation of the Community Earth System Model (CESM) to simulate the marine environment in high resolution in the Bay of Puck region, which is part of the Gdańsk Basin (South Baltic Sea). The ocean component is based on the Parallel Ocean Program (POP) model code, which uses three-dimensional equations of motion with hydrostatic and Boussinesq approximations. The bathymetry of the EPB model is based on the Baltic Sea Bathymetric Database (BSBD) of the Baltic Sea Hydrographic Commission Baltic Sea Hydrographic Commission (2013). The bathymetric data were interpolated into the model mesh using the Kriging method. The model is a model of the z-type, the horizontal resolution of which is equal to $1/96^\circ$ (which corresponds to approximately 115 m), and the vertical thicknesses for the surface layers are 0.4-0.6 m and increase closer to the bottom to 5 m in total 33 layers. To ensure numerical stability and a sufficiently fast simulation time, the time step was set at 12 s. The model has previously been validated and works correctly in operating mode (Dybowski et al., 2019, 2020). This article analyzes the results of numerical simulations for the period from January 2016 to December 2020.

3.2. *SWAT model data*

The SWAT model is a tool for a comprehensive analysis of the agricultural catchment area. Based on weather and spatial data such as digital elevation model, land use, and soil maps, the SWAT model calculates the catchment's hydrological response and water balance. In addition, it calculates the yields and chemical quality of water and soil based on information about plants, the cultivation method, the doses and types of fertilizers and pesticides. Depending on the sources of meteorological information, this model can be used for real-time calculations, forecasting, or simulation of archival events. The SWAT model in the WaterPUCK project configuration uses data from the stations of the Institute of Meteorology and Water Management in Żelistrzewo (start-up period 2000-2010 needed to stabilize soil and water conditions) and the Interdisciplinary Center for Mathematical and Computer Forecasting at the University of Warsaw (ICM) (2011-2019). The weather station that operated in 2018-19 allowed us to verify the data needed to establish the forecast model (Kalinowska et al., 2020). The model was parameterized with 17 catchments and 353 units of hydrological response, that is, areas with the same land use, slope, and soil profile (Wielgat et al., 2021). The four largest rivers that flow directly to the Puck Lagoon are Płutnica, Bładzikowski Stream, Gizdepka, and Reda.

3.3. *VIEP data*

To verify the correctness of the simulations carried out with the use of the EPB model, for a shallow and limited body of water such as the Puck Lagoon, we used data provided by the Voivodeship Inspectorate for Environmental Protection in Gdańsk. VIEP monitoring was carried out at stations T10, T6A, and T7 shown in Figure 1. The VIEP data set that we used covers data from 2016-2018 and has 226 records. In this study, we used data for temperature, salinity, and concentrations of nitrate, phosphate, and chlorophyll *a* measured at a depth of 1 m below the water surface.

4. Results and discussion

4.1. *Comparison of model data with VIEP environmental measurements*

For the available VIEP measurement data, we compare five physicochemical parameters (temperature, salinity, and concentrations of phosphate, nitrate, and chlorophyll *a*) with data

from the EPB model. Box plots were used to investigate whether the ranges of the measured variables and the model results coincide. The best precision for mapping measurement data by model data is for temperature, where the mean error is $0.36\text{ }^{\circ}\text{C}$, and the highest for chlorophyll a , for which the mean error is 10.92 mg m^{-3} .

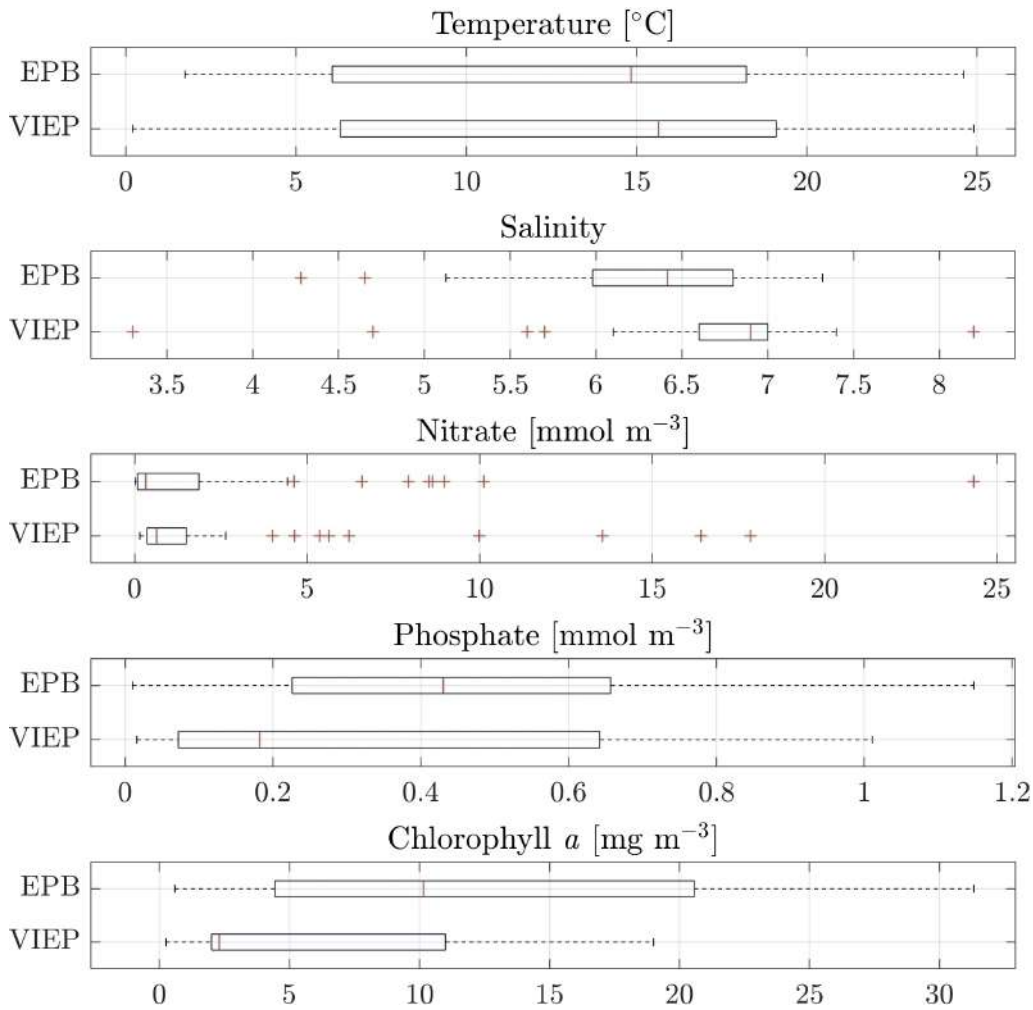


Figure 2: Box plot of physicochemical parameters at the measuring stations of the Voivodeship Inspectorate for Environmental Protection in Gdańsk (VIEP) and the corresponding simulation results from the EPB model.

Comparing the standard deviations from the mean, we find that for NO_3^- , EPB data differs from VIEP data by less than 1%, for temperature the difference is about 5%, for salinity and PO_4^{3-} it is around 10%, and for chlorophyll a the difference is less than 15%. At the same time, it should be remembered that the measurements performed during the monitoring were here and now snapshots, both spatially and temporally, while the corresponding simulation results from the EPB model were 6-hour averages and corresponded to the entire model cell with an area of the square base with a side length of about 115m.

4.2. The load of nutrients deposited into the waters of the Puck Lagoon

We analyze the amounts of nutrients that are deposited in the waters of the Puck Lagoon from the land side. In Figure 3 we present the graph of the average daily loads of NO_3^- and PO_4^{3-} to the Puck Lagoon, which were simulated using the SWAT model for years 2016-2020. It can be observed that NO_3^- and PO_4^{3-} deposition is characterized by a significant number of peaks during the year.

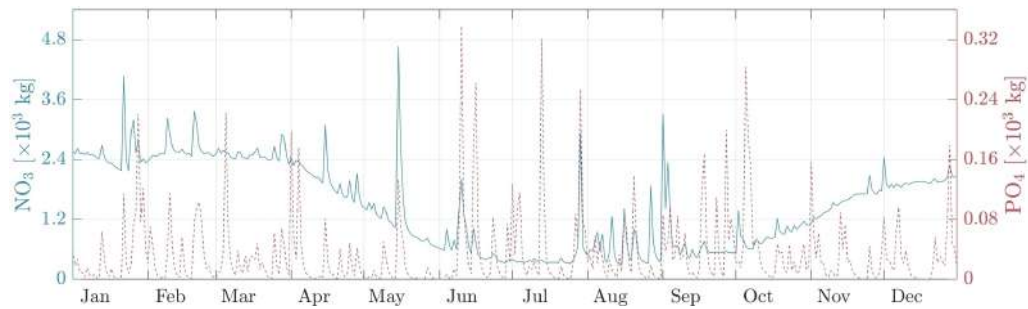


Figure 3: The load of nutrients (nitrate and phosphate) delivered by surface runoff directly to the Puck Lagoon (model values from the SWAT model - average for 2016-2020).

Figure 4 shows the rainfall (ICM data) and the corresponding river runoff (SWAT model data), for which the Pearson correlation coefficient is equal to 0.56. Most of the significant peaks overlap, which results from the relatively small catchment area and the catchment's short response time for precipitation forcing.

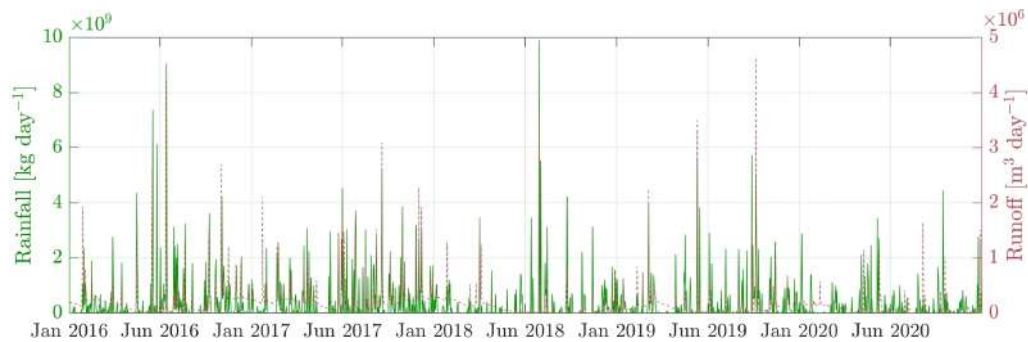


Figure 4: Plot of precipitation (solid green line, left axis; data from ICM) in the area of the Puck Commune and plot of the river runoff into the waters of the Puck Lagoon (red dotted line, right axis; data from the SWAT model) for the years 2016-2020.

Then we present in detail the total mass of NO_3^- and PO_4^{3-} for the entire 5-year simulation period (left axis of Figure 5) along with the daily loads of NO_3^- and PO_4^{3-} deposited directly into the Puck Lagoon (right axis of Figure 5). Such a combination of graphs allows us to check which of the nutrients in the studied reservoir is the factor that limits primary production.

The plots of the total mass of NO_3^- and PO_4^{3-} presented in Figure 5 can be compared with the plot of the total mass of chlorophyll *a* presented in Figure 6. We conclude that phosphorus limits algal blooms, as the total PO_4^{3-} mass shows a much stronger negative correlation with

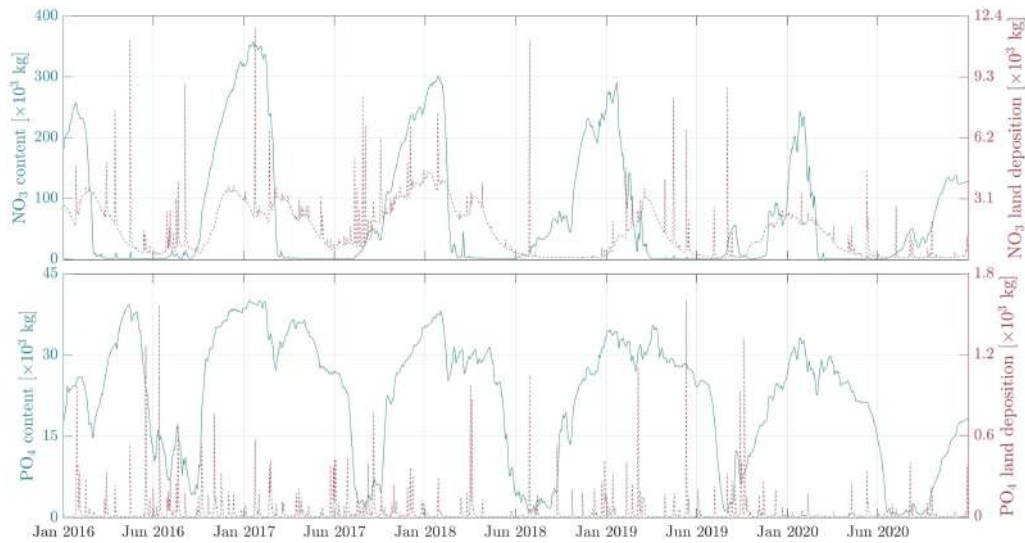


Figure 5: Plots of the total content of NO_3^- and PO_4^{3-} inside the Puck Lagoon (left axis, blue solid lines) and the riverine load of NO_3^- and PO_4^{3-} simulated in the SWAT model (right axis, red dotted lines).

the chlorophyll *a* mass (Pearson's correlation coefficient is -0.72), while the correlation of the total NO_3^- mass with the total chlorophyll *a* mass is significantly lower (Pearson's correlation coefficient -0.32). The plot of the total mass of chlorophyll *a* also gives us information on the intensity and duration of the primary production. The summer of 2018 in the studied area was much warmer than the others, which can also be seen in the graph of the chlorophyll *a* mass.

We have made an attempt to assess the N:P ratio in rivers; however, due to the low values of the mass of PO_4^{3-} supplied with river runoff, such an analysis does not provide a meaningful answer. We would have to set an *ad hoc* threshold for which we accept the amount of PO_4^{3-} load. Then the maximum of N:P ratio would depend solely on the threshold we set. Therefore, there is a recent study conducted by Wojciechowska et al. (2018), where the N:P ratio, for Płutnica, Bładzikowski Stream, and Reda, ranges from 3:1 to 47:1 (calculated from *in situ* measurements).

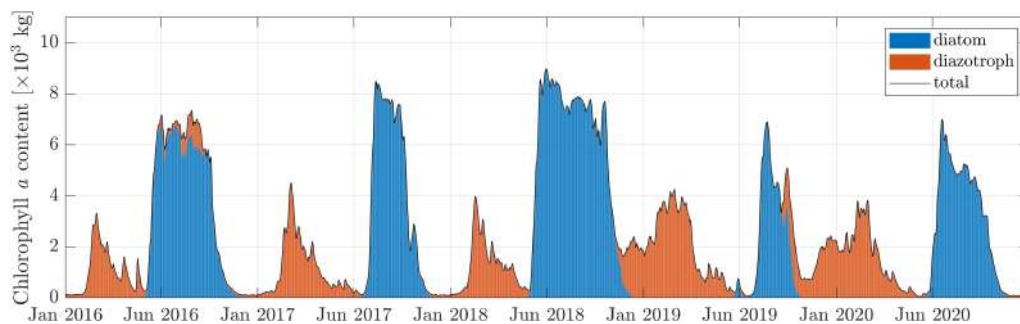


Figure 6: Plot of the total content of chlorophyll *a* inside the Puck Lagoon (solid black line) and the bar chart of the share of individual groups, i.e., diazotrophs, diatoms, and small phytoplankton.

In Figure 6 we also included information on the share of particular algae groups in the total mass of chlorophyll *a*. We observe that diatoms bloom in spring, while in summer, mainly diazotrophs bloom.

4.3. Average annual inflow of nutrients to the Puck Lagoon

We analyze how much nutrients are delivered to the Puck Lagoon with surface runoff per year on average. The average annual deposition of nutrients from the four main rivers that flow into the Puck Lagoon is in total at the level of 433.98×10^3 kg NO_3^- and 11.80×10^3 kg PO_4^{3-} . These values can be compared with the average content of NO_3^- and PO_4^{3-} in the waters of the Puck Lagoon, which are equal to 75.28×10^3 kg NO_3^- and 22.15×10^3 kg PO_4^{3-} . We can see that the mass of NO_3^- delivered by rivers is almost six times larger than the average mass of NO_3^- present in the waters of the Puck Lagoon. The average annual PO_4^{3-} load is approximately 50% of the average PO_4^{3-} mass present in the waters of the Puck Lagoon. There is a study by Bolalek et al. (1993), which estimated annual load from the Reda River as 293.31×10^3 kg NO_3^- and 21.46×10^3 kg PO_4^{3-} , but these data refer to 1989.

4.4. Comparison with model's run without riverine deposition

In the next step, we prepared a model's run in which we disconnected the rivers. Our intention was to compare the main model's run with the scenario in which the rivers stop delivering nutrients to the Puck Lagoon. Due to time constraints and computational power, the additional model's run was calculated for the 6 months of 2018 (from the beginning of February to the end of July), for which the environmental conditions were most favorable to spot intense algae blooms.

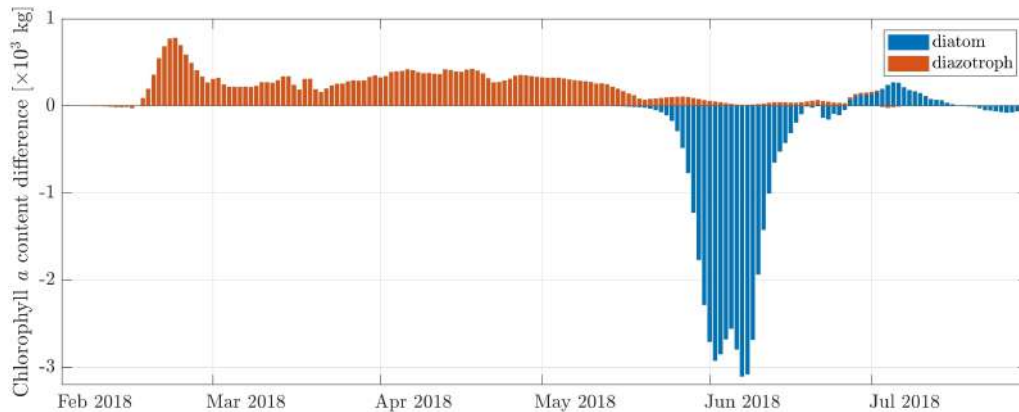


Figure 7: Bar chart of the difference of chlorophyll *a* mass inside the Puck Lagoon for individual algae groups, i.e., diazotrophs, diatoms, and small phytoplankton. The values represent the difference between a model's run with rivers and a run without rivers.

Figure 7 presents the difference in chlorophyll *a* mass inside the waters of the Puck Lagoon split into individual groups of algae. The values calculated in the model's run with rivers were subtracted from the values obtained in the model's run without rivers. We observe a situation in which in spring more diatoms flower in the model's run, in which nutrients are supplied with rivers from the Puck commune, and in summer the initial bloom of diazotrophs is much smaller in running, in which rivers deliver nutrients to the Puck Lagoon.

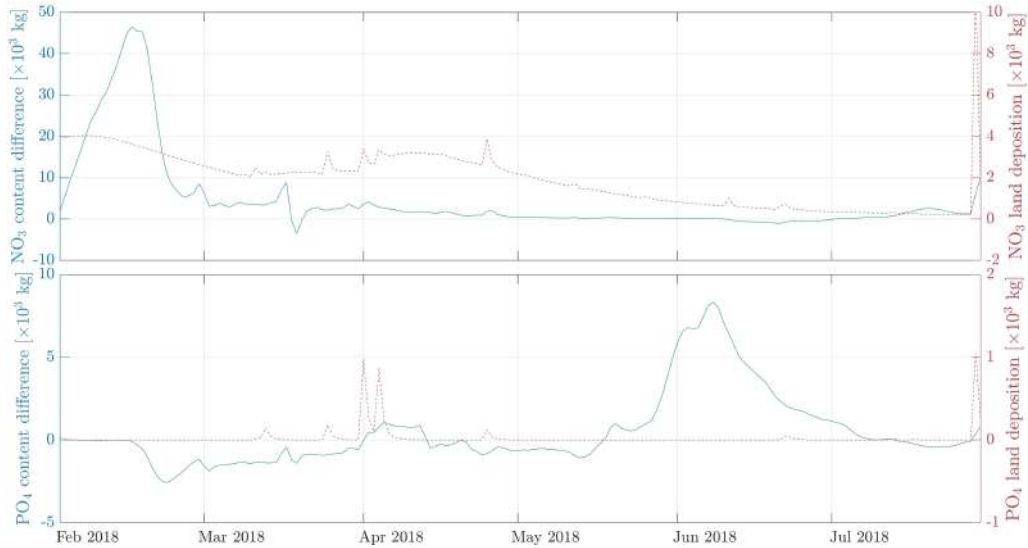


Figure 8: Plots of the difference between a model's run with rivers and a run without rivers of total mass of NO_3^- and PO_4^{3-} inside the Puck Lagoon (left axis, blue solid lines) and the riverine load of NO_3^- and PO_4^{3-} simulated in the SWAT model (right axis, red dotted lines).

Figure 8 shows the difference in the mass of NO_3^- and PO_4^{3-} in the waters of the Puck Lagoon between runs with and without riverine deposition. Initially, the PO_4^{3-} mass remains the same for both runs, but during the diatom blooming period, the PO_4^{3-} mass is lower in the run where the riverine deposition is turned on. We conclude that in this part of the year, the primary production limiting factor is nitrogen, whose shortage (in the model's run without rivers) prevents the flowering of diatoms. This is in line with Howarth and Marino (2006) conclusions. At the same time, we observe that PO_4^{3-} (that have not been depleted in spring) intensify the summer bloom of diazotrophs. The amount of nutrients taken up by the diatom bloom in spring has, in the studied region, a key influence on the intensity of the cyanobacteria bloom in summer.

In other words, without enough nitrogen in spring, phosphorus is not used for primary production, and as a consequence, more intense cyanobacterial blooms can occur. Of course, this does not mean that the nitrogen supply should be increased in the spring, such a conclusion would be quite naive, but it rather shows the great complexity of processes taking place in the ecosystem and the need to be extremely careful in drawing conclusions.

4.5. Concentration of nutrients and chlorophyll *a* in vertical sections

In the next step, we explore the distribution of nutrients concentration in vertical sections that begin from the mouths of the rivers and end inside the Puck Lagoon. For this purpose, we draw four lines, for each river, i.e., Płutnica, Bładzikowski Stream, Gizdepka, and Reda, which are marked as red lines in Figure 9.

The sections were drawn so that they included 20 model cells perpendicular to the coast. The lower depth of the last model cell in the cross sections shown corresponds to a depth of 5.1 m below the water surface. The cross sections present the averages from all five simulated years and are expressed as monthly averages to show the seasonal variation over the year. It should

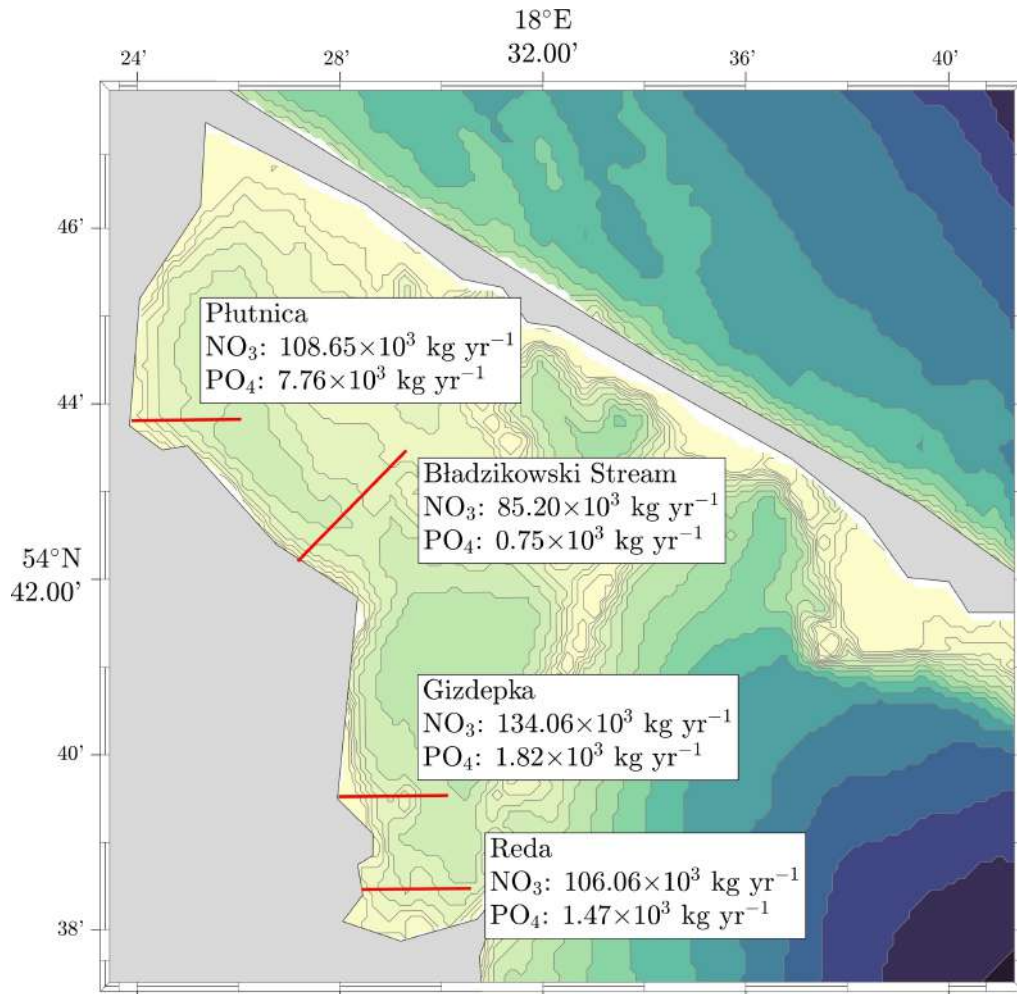


Figure 9: Map of selected locations of vertical sections for the 4 largest (in terms of nutrient deposition) rivers with a mouth within the Puck Lagoon. The values of NO₃⁻ and PO₄³⁻ represent the average annual nutrient deposition for a given watercourse.

be emphasized that such a presentation of averages strongly flattens the dispersion of data for individual years and is mainly aimed at showing the distribution of concentrations in the vicinity of river mouths.

4.5.1. Nitrate

The NO₃⁻ concentration values in the vertical sections of all rivers are very similar. Qualitatively, we can divide the year into two periods in which the NO₃⁻ concentration is high for the former and low for the latter (Figure 10).

We observe high NO₃⁻ concentrations for November, December, January, and February and low NO₃⁻ concentrations for the remaining months of the year. It should be noted that throughout the year, the NO₃⁻ concentration close to river mouths is significantly higher than for the rest

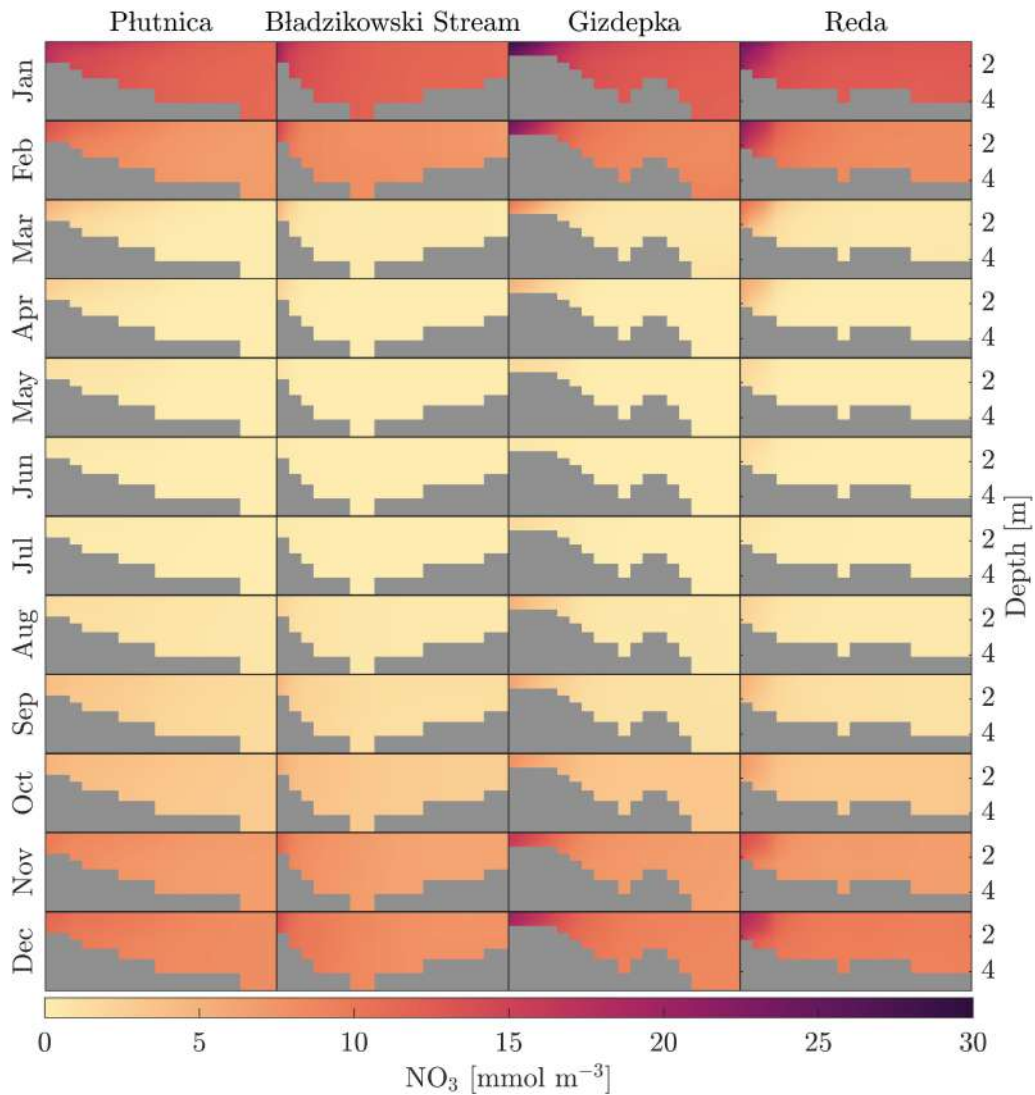


Figure 10: Vertical cross-sections of mean monthly concentrations of NO_3^- for 4 analyzed rivers (Płutnica, Bładzikowski Stream, Gizdepka, Reda). Average of the model data for 2016-2020.

of the presented cross sections. This is due to the fact that nitrogen riverine deposition is not negligible (see Section 4.2).

4.5.2. Phosphate

The characteristics of PO_4^{3-} concentration variability over the year are similar to those of NO_3^- , i.e., we can also observe two periods qualitatively, one with high values of PO_4^{3-} concentrations and the other with relatively lower values of concentrations. Lower concentrations are maintained on average for two months of the year, that is, in August and September, intermediate

values also occur in July and October, while higher values are maintained for the rest of the year (Figure 11).

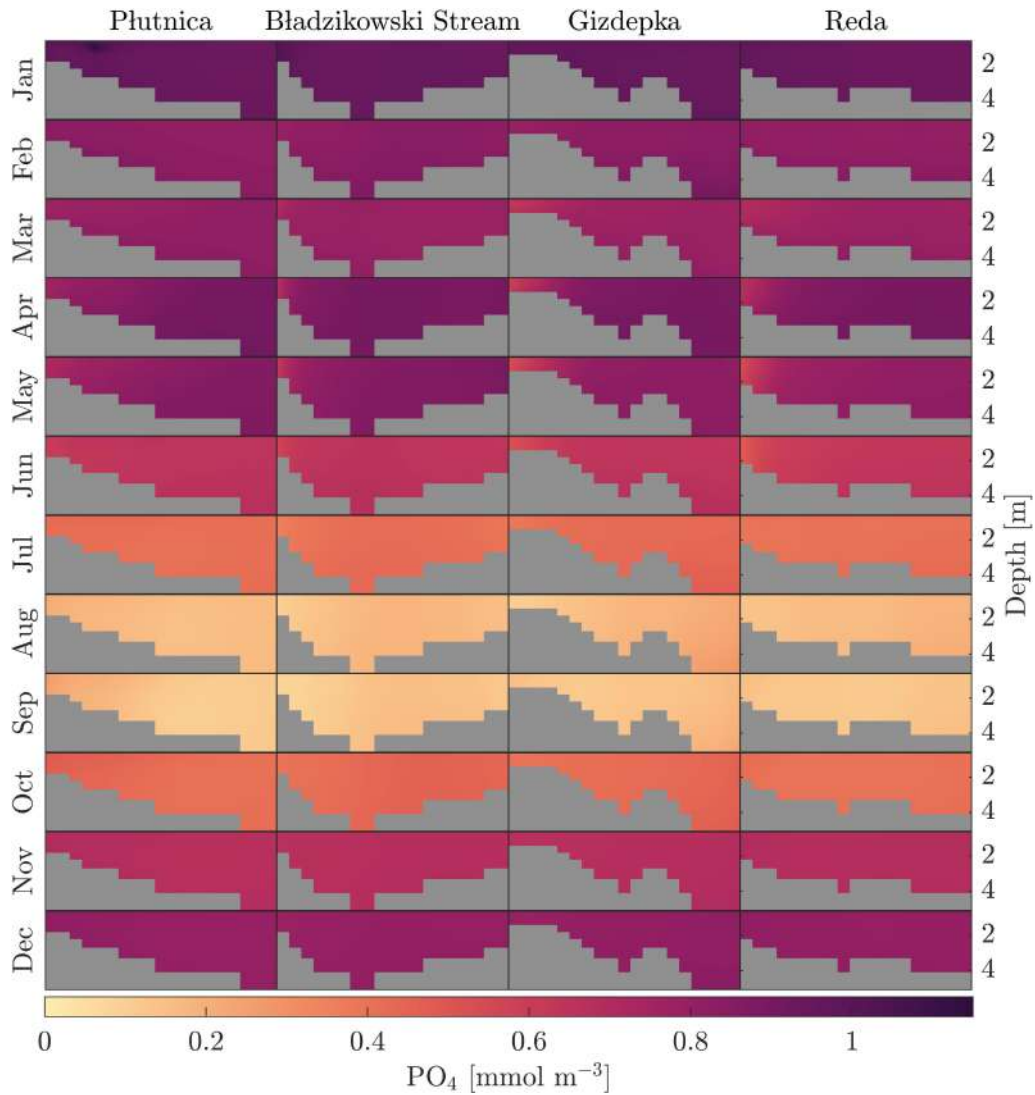


Figure 11: Vertical cross-sections of mean monthly concentrations of PO_4^{3-} for 4 analyzed rivers (Płutnica, Bładzikowski Stream, Gizdepka, Reda). Average of the model data for 2016-2020.

We observe that the water in the immediate vicinity of the river mouths is characterized by PO_4^{3-} concentration lower than that in the rest of the cross section. This is due to the fact that a relatively small amount of phosphorus enters the Puck Lagoon with river runoff compared to nitrogen, which we described in Section 4.2.

4.5.3. Chlorophyll *a*

The concentration of chlorophyll *a* in vertical sections originating in river mouths corresponds to the diagram of the total mass of chlorophyll *a* for the entire Puck Lagoon presented earlier in Figure 6.

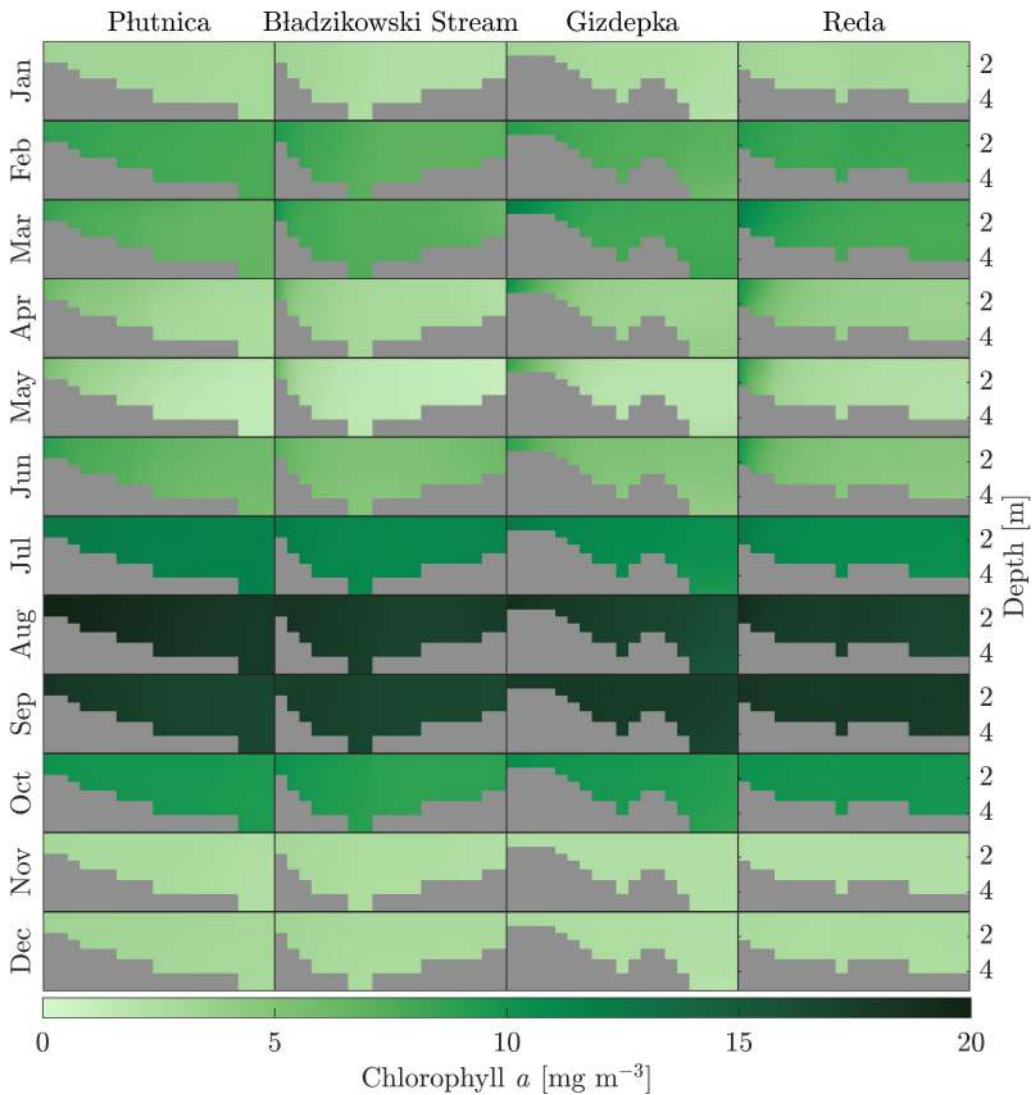


Figure 12: Vertical cross-sections of mean monthly concentrations of chlorophyll *a* for 4 analyzed rivers (Płutnica, Bładzikowski Stream, Gizdepka, Reda). Average of the model data for 2016-2020.

Taking into account chlorophyll *a* concentrations, the year can be divided into three periods. The first, corresponding to the less abundant spring bloom, occurs on average in February and March. The second, corresponding to the intensive summer bloom, occurs in the months of August and September, together with the intermediate months (July and October), where the

concentrations are comparable to those occurring during the spring bloom. The third period, on the other hand, is the time of relatively low chlorophyll *a* concentrations and occurs between two bursts (Figure 12). It should be noted that the highest concentrations are observed in August and September, which is highly correlated with the minimum PO_4^{3-} concentration in the water column and indicates that phosphorus limits summer diazotroph bloom.

4.6. Spatial distributions of nutrients and chlorophyll *a* concentrations in the surface layer

In the next step of the analysis, we examine the distribution of the concentration of nutrients in the surface layer of the Puck Lagoon waters and compare them with the distribution of the chlorophyll *a* concentration. For this purpose, we made maps of the monthly mean concentrations of NO_3^- , PO_4^{3-} , and chlorophyll *a*.

4.6.1. Nitrate

The average annual NO_3^- concentration in the surface water layer of the Puck Lagoon ranges from 0.01 to 43.60 mmol m^{-3} with mean of 3.39 mmol m^{-3} . Miętus et al. (2009) reports that the mean surface NO_3^- concentration in 2009 was 2.18 mmol m^{-3} , while the decade average (1999-2008) was only 0.5 mmol m^{-3} . The annual variability in the surface layer is similar to that observed in the cross sections, i.e., between November and February we observe significantly higher NO_3^- concentration, and in the rest of the year relatively lower (Figure 13).

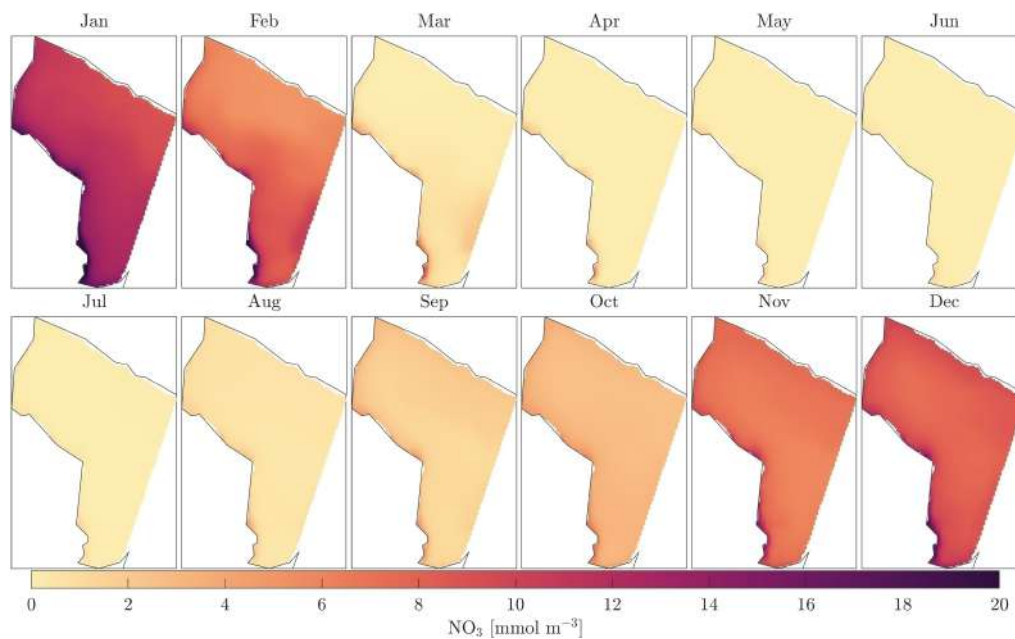


Figure 13: Average monthly distributions of NO_3^- concentration in the surface layer. Results from the EPB model, average for 2016-2020.

It should be noted that along the western border of the reservoir, where the rivers enter the Puck Lagoon, the NO_3^- concentration is higher than in the rest of the Puck Lagoon and this situation persists throughout the year. It is also interesting that after the spring diatom bloom, the low level of NO_3^- concentration persists until autumn.

4.6.2. Phosphate

The average PO_4^{3-} concentration during the year in the surface water layer of the Puck Lagoon ranges from 0.01 to 2.23 mmol m^{-3} with mean of 0.63 mmol m^{-3} (Figure 14). Miętus et al. (2009) reports that the mean surface PO_4^{3-} concentration in 2009 was 0.22 mmol m^{-3} , while the decade average (1999-2008) was 0.23 mmol m^{-3} .

The annual variability of PO_4^{3-} in the surface layer is similar to that observed in the cross sections, i.e. it has relatively lower values in the months of intensive summer algae bloom (August and September).

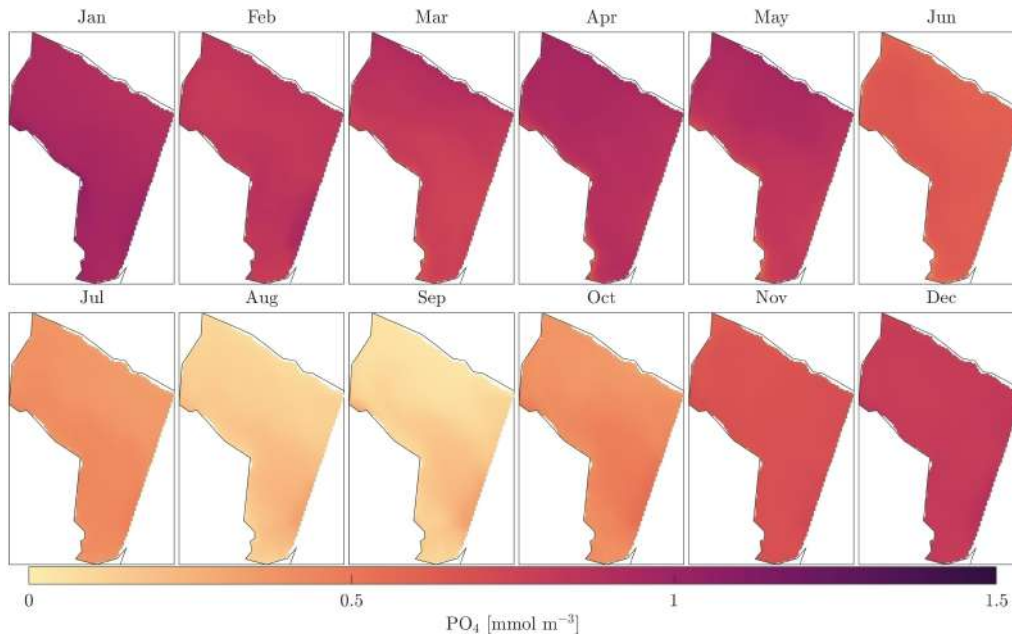


Figure 14: Average monthly distribution of PO_4^{3-} concentrations in the surface layer. Results from the EPB model, average for 2016-2020.

Interestingly, the spring bloom of diatoms does not drain the reservoir of phosphorus, and the real drops in this nutrient are recorded at the turn of June and July, when cyanobacteria begin to bloom. It should be noted that the reduced nitrogen inflow to the Puck Lagoon (see Section 4.4) limited the flowering of diatoms and the additional phosphorus accumulated in spring.

4.6.3. Chlorophyll *a*

The average chlorophyll *a* concentration in the surface layer of the Puck Lagoon varies from 0.21 to 30.20 mg m^{-3} with mean of 7.31 mg m^{-3} . There are several studies reporting chlorophyll *a* concentration in the Puck Lagoon (Miętus et al., 2009, 2012; Osowiecki et al., 2012; Zalewska and Jakusik, 2020) where annual mean varies from 2 to c.a. 17 mg m^{-3} . The most recent study (Zalewska and Jakusik, 2020) gives mean chlorophyll *a* concentration of 4 mg m^{-3} .

Once again, we observe two flowering periods, the first in February and March, and the second, much more intense, which begins in June and ends in October (Figure 15). A higher concentration of chlorophyll *a* (compared to the rest of the basin) is observed along the western border of the domain.

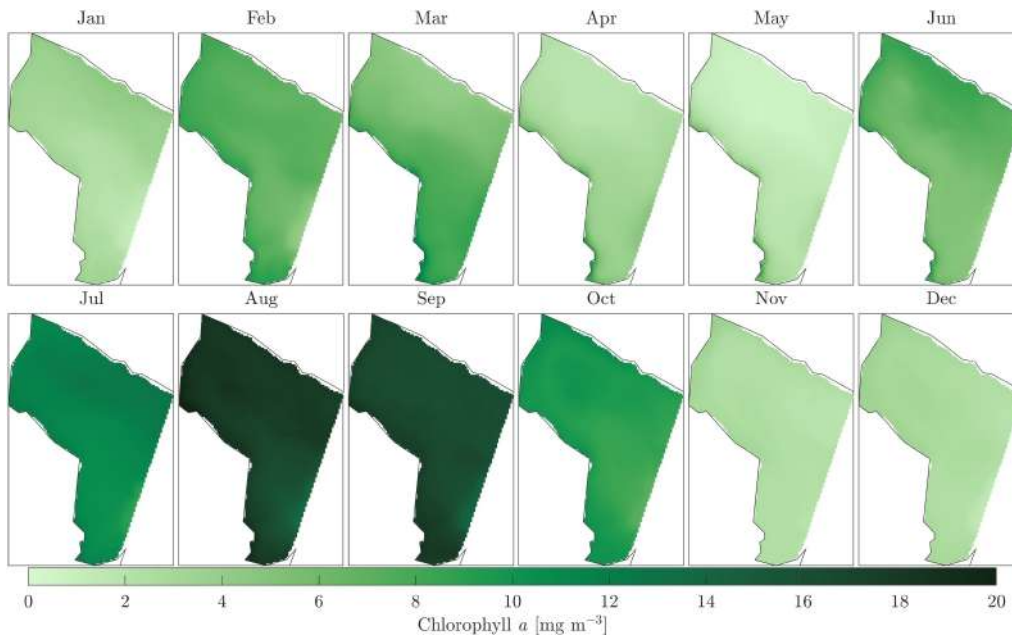


Figure 15: Average monthly distributions of chlorophyll *a* concentration in the surface layer. Results from the EPB model, average for 2016-2020.

5. Conclusions

The Puck Lagoon is an estuary with very limited water exchange with the open sea and considerable anthropogenic pressure. The aim of the study was to investigate the impact of nutrient loads from small rivers with relatively low runoff (compared to the region's largest river, i.e., Vistula) on the water quality of the Puck Lagoon. The study revealed that nutrient inflow from small rivers can significantly affect algal blooms in analyzed area.

It turns out that the study of the bloom intensity with the use of model tools may answer the question of which direction should we aim in limiting the nutrient inflow to the Puck Lagoon. In this context, it is crucial to understand the complexity of the interconnected processes. We have shown that it is extremely important to study the intensity of the spring bloom of diatoms, as its size has a great influence on the subsequent summer bloom of cyanobacteria.

It is worth noting that in the context of planning remedial measures on a regional scale, interesting studies have been carried out on the removal of nitrogen and phosphorus from water reservoirs using a free water surface wetland system where the wetland total nitrogen mass removal was 89% and the total phosphorus mass removal was 98% (Waara and Wojciechowska, 2019).

Funding

This research was funded by National Centre for Research and Development of Poland within the BIOSTRATEG III program No. BIOSTRATEG3/343927/3/NCBR/2017.

Acknowledgements

Calculations were carried out at the Academic Computer Centre in Gdańsk.

References

- Álvarez, X., Valero, E., Santos, R.M.B., Varandas, S.G.P., Fernandes, L.F.S., Pacheco, F.A.L., 2017. Anthropogenic nutrients and eutrophication in multiple land use watersheds: Best management practices and policies for the protection of water resources. *Land Use Policy* 69, 1 – 11. <https://doi.org/https://doi.org/10.1016/j.landusepol.2017.08.028>.
- Badri Ahmadi, H., Kusi-Sarpong, S., Rezaei, J., 2017. Assessing the social sustainability of supply chains using Best Worst Method. *Resources, Conservation and Recycling* 126, 99–106. <https://doi.org/10.1016/j.resconrec.2017.07.020>.
- Baltic Sea Hydrographic Commission, 2013. Baltic Sea Bathymetry Database Version 0.9.3. URL: <http://data.bshc.pro/#2/52.8/20.4>.
- Bolałek, J., Falkowska, L., Korzeniewski, K., 1993. Hydrochemia Zatoki, in: *Zatoka Pucka*. Instytut Oceanografii Uniwersytetu Gdańskiego, Gdańsk, p. 532.
- Dybowski, D., Jakacki, J., Janecki, M., Nowicki, A., Rak, D., Dzierzbicka-Głowacka, L., 2019. High-Resolution Ecosystem Model of the Puck Bay (Southern Baltic Sea)—Hydrodynamic Component Evaluation. *Water* 11, 2057. <https://doi.org/10.3390/w11102057>.
- Dybowski, D., Janecki, M., Nowicki, A., Dzierzbicka-Głowacka, L.A., 2020. Assessing the Impact of Chemical Loads from Agriculture Holdings on the Puck Bay Environment with the High-Resolution Ecosystem Model of the Puck Bay, Southern Baltic Sea. *Water* 12, 2068. <https://doi.org/10.3390/w12072068>.
- Dzierzbicka-Głowacka, L., Dybowski, D., Janecki, M., Wojciechowska, E., Szymczycha, B., Potrykus, D., Nowicki, A., Szymkiewicz, A., Zima, P., Jaworska-Szulc, B., Pietrzak, S., Pazikowska-Sapota, G., Kalinowska, D., Nawrot, N., Wielgat, P., Dembska, G., Matej-Lukowicz, K., Szczepańska, K., Puzkarczuk, T., 2022. Modelling the impact of the agricultural holdings and land-use structure on the quality of inland and coastal waters with an innovative and interdisciplinary toolkit. *Agricultural Water Management* 263, 107438. URL: <https://www.sciencedirect.com/science/article/pii/S0378377421007150>, <https://doi.org/10.1016/j.agwat.2021.107438>.
- Dzierzbicka-Głowacka, L., Janecki, M., Szymczycha, B., Dybowski, D., Nowicki, A., Kłostowska, Ż., Obarska-Pempkowiak, H., Zima, P., Jaworska-Szulc, B., Jakacki, J., Szymkiewicz, A., Pietrzak, S., Pazikowska-Sapota, G., Wojciechowska, E., Dembska, G., Wichorowski, M., Białoskórski, M., Puzkarczuk, T., 2018. Integrated information and prediction Web Service WaterPUCK General concept. *MATEC Web Conf.* 210, 02011. <https://doi.org/10.1051/mateconf/201821002011>.
- Galloway, J.N., Townsend, A.R., Erisman, J.W., Bekunda, M., Cai, Z., Freney, J.R., Martinelli, L.A., Seitzinger, S.P., Sutton, M.A., 2008. Transformation of the Nitrogen Cycle: Recent Trends, Questions, and Potential Solutions. *Science* 320, 889–892. <https://doi.org/10.1126/science.1136674>.
- Gic-Grusza, G., Kryla-Straszewska, L., Urbański, J., Warzocha, J., Weslawski, J., 2009. Atlas of Polish marine area bottom habitats: Environmental valorization of marine habitats.
- Hägg, H.E., Lyon, S.W., Wällstedt, T., Mörth, C.M., Claremar, B., Humborg, C., 2014. Future Nutrient Load Scenarios for the Baltic Sea Due to Climate and Lifestyle Changes. *AMBIO* 43, 337–351. URL: <https://doi.org/10.1007/s13280-013-0416-4>, <https://doi.org/10.1007/s13280-013-0416-4>.
- Halpern, B.S., Walbridge, S., Selkoe, K.A., Kappel, C.V., Micheli, F., D'Agrosa, C., Bruno, J.F., Casey, K.S., Ebert, C., Fox, H.E., Fujita, R., Heinemann, D., Lenihan, H.S., Madin, E.M.P., Perry, M.T., Selig, E.R., Spalding, M., Steneck, R., Watson, R., 2008. A Global Map of Human Impact on Marine Ecosystems. *Science* 319, 948–952. <https://doi.org/10.1126/science.1149345>.
- Heisler, J., Glibert, P.M., Burkholder, J.M., Anderson, D.M., Cochlan, W., Dennison, W.C., Dortch, Q., Gobler, C.J., Heil, C.A., Humphries, E., Lewitus, A., Magnien, R., Marshall, H.G., Sellner, K., Stockwell, D.A., Stoecker, D.K., Suddleson, M., 2008. Eutrophication and harmful algal blooms: A scientific consensus. *Harmful Algae* 8, 3 – 13. <https://doi.org/https://doi.org/10.1016/j.hal.2008.08.006>.
- Howarth, R.W., 2008. Coastal nitrogen pollution: A review of sources and trends globally and regionally. *Harmful Algae* 8, 14 – 20. <https://doi.org/https://doi.org/10.1016/j.hal.2008.08.015>.
- Howarth, R.W., Marino, R., 2006. Nitrogen as the limiting nutrient for eutrophication in coastal marine ecosystems: Evolving views over three decades. *Limnology and Oceanography* 51, 364–376. https://doi.org/10.4319/lo.2006.51.1_part_2.0364.
- Kalinowska, D., Wielgat, P., Kolerski, T., Zima, P., 2020. Model of Nutrient and Pesticide Outflow with Surface Water to Puck Bay (Southern Baltic Sea). *Water* 12, 809. <https://doi.org/10.3390/w12030809>.

- Lotze, H.K., Lenihan, H.S., Bourque, B.J., Bradbury, R.H., Cooke, R.G., Kay, M.C., Kidwell, S.M., Kirby, M.X., Peterson, C.H., Jackson, J.B.C., 2006. Depletion, Degradation, and Recovery Potential of Estuaries and Coastal Seas. *Science* 312, 1806–1809. <https://doi.org/10.1126/science.1128035>.
- Miętus, M., Lysiak-Pastuszek, E., Krzywiński, W., 2009. Bałtyk Południowy w roku 2002. Charakterystyka wybranych elementów środowiska. IMGW, Warszawa.
- Miętus, M., Lysiak-Pastuszek, E., Zalewska, T., Krzywiński, W., 2012. Bałtyk Południowy w roku 2009. Charakterystyka wybranych elementów środowiska. IMGW, Warszawa.
- Oswiecki, A., Lysiak-Pastuszek, E., Kruk-Dowgiałło, L., Błęńska, M., Brzeska, P., Kraśniewski, W., Lewandowski, Ł., Krzywiński, W., 2012. Development of tools for ecological quality assessment in the Polish marine areas according to the Water Framework Directive. Part IV — preliminary assessment. *Oceanological and Hydrobiological Studies* 41, 1–10. <https://doi.org/10.2478/s13545-012-0022-2>.
- Shahidul Islam, M., Tanaka, M., 2004. Impacts of pollution on coastal and marine ecosystems including coastal and marine fisheries and approach for management: a review and synthesis. *Marine Pollution Bulletin* 48, 624–649. <https://doi.org/10.1016/j.marpolbul.2003.12.004>.
- Waara, S., Wojciechowska, E., 2019. Treatment of landfill leachate in a constructed free water surface wetland system over a decade – Identification of disturbance in process behaviour and removal of eutrophying substances and organic material. *Journal of Environmental Management* 249, 109319. <https://doi.org/10.1016/j.jenvman.2019.109319>.
- Wielgat, P., Kalinowska, D., Szymkiewicz, A., Zima, P., Jaworska-Szulc, B., Wojciechowska, E., Nawrot, N., Matej-Lukowicz, K., Dzierzbicka-Głowacka, L.A., 2021. Towards a multi-basin SWAT model for the migration of nutrients and pesticides to Puck Bay (Southern Baltic Sea). *PeerJ* 9, e10938. <https://doi.org/10.7717/peerj.10938>.
- Wojciechowska, E., Nawrot, N., Matej-Lukowicz, K., Gajewska, M., Obarska-Pempkowiak, H., 2018. Seasonal changes of the concentrations of mineral forms of nitrogen and phosphorus in watercourses in the agricultural catchment area (Bay of Puck, Baltic Sea, Poland). *Water Supply* 19, 986–994. URL: <https://doi.org/10.2166/ws.2018.190>.
- Worm, B., Hilborn, R., Baum, J.K., Branch, T.A., Collie, J.S., Costello, C., Fogarty, M.J., Fulton, E.A., Hutchings, J.A., Jennings, S., Jensen, O.P., Lotze, H.K., Mace, P.M., McClanahan, T.R., Minto, C., Palumbi, S.R., Parma, A.M., Ricard, D., Rosenberg, A.A., Watson, R., Zeller, D., 2009. Rebuilding Global Fisheries. *Science* 325, 578–585. <https://doi.org/10.1126/science.1173146>.
- Zalewska, T., Jakusik, E., 2020. Warunki meteorologiczne i hydrologiczne oraz charakterystyka elementów fizycznych, chemicznych i biologicznych południowego Bałtyku w 2018 roku. IMGW, Warszawa. URL: https://www.imgw.pl/sites/default/files/2020-08/imgw-baltyk-monografia_final.pdf.

6 Authorship statements

Dawid Dybowski

Institute of Oceanology of the Polish Academy of Sciences
Powstańców Warszawy 55
81-712 Sopot
Poland

Sopot, 1 June 2022

AUTHORSHIP STATEMENTS OF CO-AUTHOR OF THE ARTICLE

I confirm that I am co-author of the articles:

1. Dybowski, D., Jakacki, J., Janecki, M., Nowicki, A., Rak, D., Dzierzbicka-Glowacka, L., 2019. *High-Resolution Ecosystem Model of the Puck Bay (Southern Baltic Sea)—Hydrodynamic Component Evaluation*. Water 11, 2057. <https://doi.org/10.3390/w11102057>
2. Dybowski, D., Dzierzbicka-Glowacka, L.A., Pietrzak, S., Juszowska, D., Puskarczyk, T., 2020a. *Estimation of nitrogen leaching load from agricultural fields in the Puck Commune with an interactive calculator*. PeerJ 8, e8899. <https://doi.org/10.7717/peerj.8899>
3. Dybowski, D., Janecki, M., Nowicki, A., Dzierzbicka-Glowacka, L.A., 2020b. *Assessing the Impact of Chemical Loads from Agriculture Holdings on the Puck Bay Environment with the High-Resolution Ecosystem Model of the Puck Bay, Southern Baltic Sea*. Water 12, 2068. <https://doi.org/10.3390/w12072068>
4. Dybowski, D., Dzierzbicka-Glowacka, L., 2022. *Analysis of the Impact of Nutrients Deposited from the Land Side on the Waters of Puck Lagoon (Gdańsk Basin, Southern Baltic)*. submitted to the Journal of Hydrology.

I declare that my contribution of 70% to article No.1, 75% to article No. 2, 80% to article No. 3, and 85% to article No. 4 included:

- studies conception
- data preparation and analysis
- interpretation of the results
- writing and revising manuscripts.

Dawid Dybowski

Prof. Lidia Dzierzbicka-Głowacka
Institute of Oceanology of the Polish Academy of Sciences
Powstańców Warszawy 55
81-712 Sopot
Poland

Sopot, 1 June 2022

AUTHORSHIP STATEMENTS OF CO-AUTHOR OF THE ARTICLE

I confirm that I am co-author of the articles:

1. Dybowski, D., Jakacki, J., Janecki, M., Nowicki, A., Rak, D., Dzierzbicka-Głowacka, L., 2019. *High-Resolution Ecosystem Model of the Puck Bay (Southern Baltic Sea)—Hydrodynamic Component Evaluation*. *Water* 11, 2057. <https://doi.org/10.3390/w11102057>
2. Dybowski, D., Dzierzbicka-Głowacka, L.A., Pietrzak, S., Juskowska, D., Puszkarczuk, T., 2020a. *Estimation of nitrogen leaching load from agricultural fields in the Puck Commune with an interactive calculator*. *PeerJ* 8, e8899. <https://doi.org/10.7717/peerj.8899>
3. Dybowski, D., Janecki, M., Nowicki, A., Dzierzbicka-Głowacka, L.A., 2020b. *Assessing the Impact of Chemical Loads from Agriculture Holdings on the Puck Bay Environment with the High-Resolution Ecosystem Model of the Puck Bay, Southern Baltic Sea*. *Water* 12, 2068. <https://doi.org/10.3390/w12072068>
4. Dybowski, D., Dzierzbicka-Głowacka, L., 2022. *Analysis of the Impact of Nutrients Deposited from the Land Side on the Waters of Puck Lagoon (Gdańsk Basin, Southern Baltic)*. submitted to the *Journal of Hydrology*.

I declare that my contribution of 10% to article No.1, 10% to article No. 2, 10% to article No. 3, and 15% to article No. 4 included:

- studies conception
- interpretation of the results
- writing and revising manuscripts.

Lidia Dzierzbicka-Głowacka.

Maciej Janecki

Sopot, 1 June 2022

Institute of Oceanology of the Polish Academy of Sciences
Powstańców Warszawy 55
81-712 Sopot
Poland

AUTHORSHIP STATEMENTS OF CO-AUTHOR OF THE ARTICLE

I confirm that I am co-author of the articles:

1. Dybowski, D., Jakacki, J., Janecki, M., Nowicki, A., Rak, D., Dzierzbicka-Glowacka, L., 2019. *High-Resolution Ecosystem Model of the Puck Bay (Southern Baltic Sea)—Hydrodynamic Component Evaluation*. *Water* 11, 2057. <https://doi.org/10.3390/w11102057>
2. Dybowski, D., Janecki, M., Nowicki, A., Dzierzbicka-Glowacka, L.A., 2020b. *Assessing the Impact of Chemical Loads from Agriculture Holdings on the Puck Bay Environment with the High-Resolution Ecosystem Model of the Puck Bay, Southern Baltic Sea*. *Water* 12, 2068. <https://doi.org/10.3390/w12072068>

I declare that my contribution of 5% to article No.1, 5% to article No. 2 included:

- studies conception
- interpretation of the results
- writing and revising manuscripts.

Maciej Janecki

Dr. Artur Nowicki
Institute of Oceanology of the Polish Academy of Sciences
Powstańców Warszawy 55
81-712 Sopot
Poland

Sopot, 1 June 2022

AUTHORSHIP STATEMENTS OF CO-AUTHOR OF THE ARTICLE

I confirm that I am co-author of the articles:

1. Dybowski, D., Jakacki, J., Janecki, M., Nowicki, A., Rak, D., Dzierzbicka-Glowacka, L., 2019. *High-Resolution Ecosystem Model of the Puck Bay (Southern Baltic Sea)—Hydrodynamic Component Evaluation*. *Water* 11, 2057. <https://doi.org/10.3390/w11102057>
2. Dybowski, D., Janecki, M., Nowicki, A., Dzierzbicka-Glowacka, L.A., 2020b. *Assessing the Impact of Chemical Loads from Agriculture Holdings on the Puck Bay Environment with the High-Resolution Ecosystem Model of the Puck Bay, Southern Baltic Sea*. *Water* 12, 2068. <https://doi.org/10.3390/w12072068>

I declare that my contribution of 5% to article No.1, 5% to article No. 2 included:

- studies conception
- interpretation of the results
- writing and revising manuscripts.



Jaromir Jakacki

Sopot, 1 June 2022

Research Associate Professor

Institute of Oceanology of the Polish Academy of Sciences

Powstańców Warszawy 55

81-712 Sopot

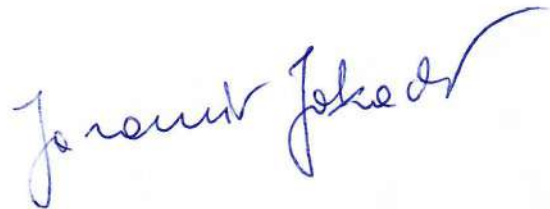
Poland

AUTHORSHIP STATEMENTS OF CO-AUTHOR OF THE ARTICLE

I confirm that I am co-author of the article:

Dybowski, D., Jakacki, J., Janecki, M., Nowicki, A., Rak, D., Dzierzbicka-Glowacka, L., 2019. *High-Resolution Ecosystem Model of the Puck Bay (Southern Baltic Sea)—Hydrodynamic Component Evaluation*. *Water* 11, 2057. <https://doi.org/10.3390/w11102057>

I declare that my contribution to this article is 5%.



Dr. Daniel Rak

Institute of Oceanology of the Polish Academy of Sciences
Powstańców Warszawy 55
81-712 Sopot
Poland

Sopot, 1 June 2022

AUTHORSHIP STATEMENTS OF CO-AUTHOR OF THE ARTICLE

I confirm that I am co-author of the article:

Dybowski, D., Jakacki, J., Janecki, M., Nowicki, A., Rak, D., Dzierzbicka-Głowacka, L., 2019. *High-Resolution Ecosystem Model of the Puck Bay (Southern Baltic Sea)—Hydrodynamic Component Evaluation*. *Water* 11, 2057. <https://doi.org/10.3390/w11102057>

I declare that my contribution (5%) to this article included participation in:

- data acquisition and analysis
- interpretation of the results
- writing and revising manuscripts.



Prof. Stefan Pietrzak

Institute of Technology and Life Sciences - National Research Institute

Aleja Hrabaska 3

05-090 Falenty

Poland

Sopot, 1 June 2022

AUTHORSHIP STATEMENTS OF CO-AUTHOR OF THE ARTICLE

I confirm that I am co-author of the article:

Dybowski, D., Dzierzbicka-Glowacka, L.A., Pietrzak, S., Juskowska, D., Puskarczyk, T., 2020a. *Estimation of nitrogen leaching load from agricultural fields in the Puck Commune with an interactive calculator*. PeerJ 8, e8899. <https://doi.org/10.7717/peerj.8899>

I declare that my contribution (5%) to this article included participation in:

- interpretation of the results
- writing and revising manuscripts.

Pietrzak

Dr. Dominika Juskowska

Institute of Technology and Life Sciences - National Research Institute
aleja Hrabka 3
05-090 Falenty
Poland

Sopot, 1 June 2022

AUTHORSHIP STATEMENTS OF CO-AUTHOR OF THE ARTICLE

I confirm that I am co-author of the article:

Dybowski, D., Dzierzbicka-Glowacka, L.A., Pietrzak, S., Juskowska, D., Puzkarczuk, T., 2020a. *Estimation of nitrogen leaching load from agricultural fields in the Puck Commune with an interactive calculator*. PeerJ 8, e8899. <https://doi.org/10.7717/peerj.8899>

I declare that my contribution (5%) to this article included participation in:

- interpretation of the results
- writing and revising manuscripts.

Dominika Juskowska

Tadeusz Puszkarczuk
Puck Commune Office
10 Lutego 29
84-100 Puck
Poland

Sopot, 1 June 2022

AUTHORSHIP STATEMENTS OF CO-AUTHOR OF THE ARTICLE

I confirm that I am co-author of the article:

Dybowski, D., Dzierzbicka-Glowacka, L.A., Pietrzak, S., Juskowska, D., Puszkarczuk, T., 2020a. *Estimation of nitrogen leaching load from agricultural fields in the Puck Commune with an interactive calculator*. PeerJ 8, e8899. <https://doi.org/10.7717/peerj.8899>

I declare that my contribution (5%) to this article included participation in:

- data acquisition.


WÓJT GMINY PUCK
Tadeusz Puszkarczuk

7 Acknowledgments

Presented studies were carried out in Physical Oceanography Department of the Institute of Oceanology of the Polish Academy of Sciences in Sopot, Poland.

This study was supported by the IOPAN statutory task no. II.1 and project: “Modelling of the impact of the agricultural holdings and land-use structure on the quality of inland and coastal waters of the Baltic Sea set up on the example of the Municipality of Puck region - Integrated info-prediction Web Service WaterPUCK” funded by the National Centre for Research and Development within BIOSTRATEG III Programme "Natural environment, agriculture and forestry" devoted to the Problem Area I "Rational management of natural resources with special regard to water management" (grant no. BIOSTRATEG3/343927/3/NCBR/2017).

First and foremost I am grateful to my supervisor Prof. Lidia Dzierzbicka-Głowacka for her guidance and support during this very interesting research that laid the foundation for this dissertation.

Special thanks are dedicated to the Colleagues, Teachers from Doctoral studies, and Organizations: IO PAN - Maciej Janecki, Artur Nowicki, Jaromir Jakacki, Daniel Rak, Jacek Piskozub, Małgorzata Merchel, Marta Cegłowska, Beata Szymczycha, Monika Lengier, Jan Andrzejewski; ITLS – Stefan Pietrzak, Dominika Juskowska; GUT - Ewa Wojciechowska, Dawid Potrykus, Paweł Wielgat, Dominika Kalinowska; CI TASK - Michał Białoskórski, Bogusław Śmiech.

This journey would not have been possible without the dedicated support of my parents.

Last but not least, I would like to express my deepest gratitude to my beloved wife Dominika for her constant support and belief.